ISSN 2663-1407
Volume 9, Isuue 2, September 2019

Libyan Journal of Science & Technology

An online refereed scientific journal issued by Faculty of Science, University of Benghazi

Benghazi, Libya

Editorial Board

 ISSN 2663-1407; National Library of Libya, Legal number: 390/2018

Libyan Journal of Science and Technology

Contents

Volume 9, Number 2, September 2019

Libyan Journal of Science & Technology 9:2 (2019) 122–128

Faculty of Science - University of Benghazi

Libyan Journal of Science & Technology

journal home page: www.sc.uob.edu.ly/pages/page/77

Performance assessment of the vortex panel method

Khalid M. Sultan*, Anas M. Elshabli, Mohammed A. Kashbour, Seraj A. Ben.Ateiga

Department of Mechanical Engineering, Faculty of Engineering, University of Benghazi, Benghazi,. Libya.

Highlights

- **The vortex panel method has its strength and weakness points.**
- **The method is computationally cheap and relatively easy to program.**
- **The method is capable of solving the incompressible flow past thin airfoils at small angle of attack.**
- **The method can not capture shock waves even if they are weak.**
- **Friction is completely ignored by the method.**

ARTICLE INFO

Article history:
Received 06 August 2018
Revised 10 December 2018
Accepted 17 December 2018
Available online 15 June 2019

Keywords:
Vortex panel method; Potential flow solutions; Kutta condition; CFX; Matlab.

* Corresponding author:
E-mail address: dr-Khalid-Sultan@hotmail.de
K. M. Sultan

ABSTRACT

The vortex panel method is a very simple and computationally effective method to solve the incompressible and inviscid flow past thin airfoils. This work tries to provide a complete and detailed presentation of the mathematical derivation of this method. It also highlights the points of strength and weakness of this method as compared with more advanced yet expensive computational methods. The results obtained from this work have shown that the method is capable of solving the flow past thin airfoils with good precision for subsonic and laminar flow. For transonic and turbulent flows and as the angle of attack of the flow is increased, the method lacks the precision, especially near the leading and trailing edges.

1. Introduction

Numerical methods are nowadays very essential in the aerospace industry. A Simple method such as the vortex panel method is still used in large companies that produce commercial aircraft, especially in the preliminary design stage. The vortex panel method offers a faster and easier alternative as compared to more time consuming both Navier–Stokes and Euler flow solvers due to the fact that the vortex panel method does not require the process of computational grid generation.

2. Mathematical model

The basic equations of fluid motion are called alternatively as the "conservation laws" because they are basically a representation of the three concepts: conservation of mass, conservation of linear momentum, alternatively called Newton's second law of motion, and conservation of energy. In this section, the first two conservation laws will be reviewed in details whereas the third law will be excluded. The panel method, which is the main subject of this study, is based on mass conservation and linear momentum conservation, and it has nothing to do with energy conservation. That is why the conservation of energy is considered as an "out of the scope" subject.

$$\vec{\nabla}.\vec{V} = 0 \tag{1}$$

$$\rho\left[\frac{\partial \vec{V}}{\partial t} - \vec{V}\times\left(\vec{\nabla}\times\vec{V}\right) + \vec{\nabla}\left(\frac{\vec{V}^2}{2}\right)\right] = \rho\vec{g} - \vec{\nabla}P \tag{2}$$

$$u = \frac{\partial \psi}{\partial y}, \qquad v = -\frac{\partial \psi}{\partial x} \tag{3}$$

$$u = \frac{\partial \phi}{\partial x}; \qquad v = \frac{\partial \phi}{\partial y}; \qquad w = \frac{\partial \phi}{\partial z} \tag{4}$$

In this study, the fluid is assumed to be steady, incompressible, irrotational, inviscid, and two-dimensional. Applying the above - mentioned assumptions, and recalling that the continuity equation can be represented by an equivalent total velocity potential function equation in the case of potential flow, Eqs. 1 and 2 are reduced to the following equations:

$$\phi_T = \phi_{v1} + \phi_{v2} = \phi_1 + \phi_2 = \frac{\Gamma_1}{2\pi}\theta_1 + \frac{\Gamma_2}{2\pi}\theta_2 \tag{5}$$

$$P + \frac{1}{2}\rho V^2 + \rho g(Z - Z_o) = P_o \tag{6}$$

In the case of panel codes, the direct implementation of the wall boundary condition would be to mathematically state that the velocity normal to the surface is zero, see (White, 2003).

$$\vec{V}.\vec{n} = 0 \tag{7}$$

The Kutta condition states that in order to obtain a lift from the airfoil, the fluid flow at the trailing edge must satisfy the following condition:

$$V_{upper}(at\ trailing\ edge) = V_{lower}(at\ trailing\ edge) \tag{8}$$

A computer program written by (Kireny, 2002) was employed in this paper. This program implements the variable vortex panel method explained by (Kuethe and Chow, 2009). Although the original computer program, which was introduced by (Kuethe and Chow, 2009) has been written in FORTRAN, the program of (Kireny, 2002) is written in MATLAB. MATLAB is considered a fourth–generation programing language, which has the advantage

 ISSN 2663-1407; National Library of Libya, Legal number: 390/2018

of containing many embedded libraries. Those libraries were developed, tested, and tweaked to provide the most exact solution for several mathematical problems without sacrificing the speed of computation. Moreover, MATLAB has a built-in plotter, which enables the user to see and investigate the results after the computation.

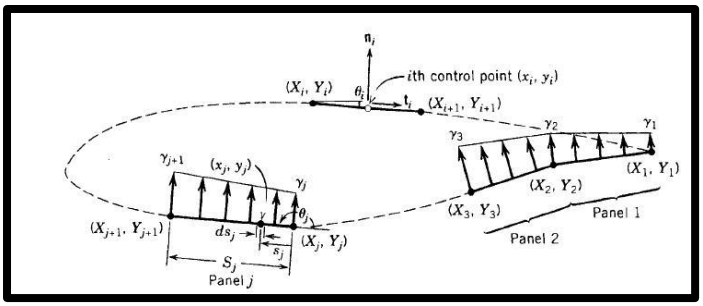

Fig.1. Control Point at Mid Panel (Kuethe and Chow, 2009).

The main idea behind the panel method is in employing the velocity potential instead of the velocity components (u, v) to represent each elementary flow component incorporated in the complex flow at hand. The complex flow at hand in this situation is constructed of a free stream having a velocity of V_∞ at an angle of attack $(\propto)$ and a set of vortex panels (m vortex panels), see Fig. 1. Employing the superposition method to write the equation of the total velocity potential for panel i yields:

$$\emptyset_{(x_i,y_i)} = V_\infty(x_i cos \propto + y_i sin \propto) + \sum_{j=1}^{m} \int_{panel\ j} \frac{-\gamma(s_j)}{2\pi} \tan^{-1}\left[\frac{y_i - y_j}{x_i - x_j}\right] . ds_j \quad (9)$$

It is possible to obtain two equations for the normal and tangential velocity components on panel i as:

$$V_{n_i} = V_\infty(cos\alpha\hat{\imath} + sin\alpha\hat{\jmath}).\vec{n} + \sum_{j=1}^{m} \gamma'_j \int_0^{s_j} f1_n(s_j).ds_j + \gamma'_{j+1} \int_0^{s_j} f2_n(s_j).ds_j \quad (10)$$

$$V_{t_i} = V_\infty(cos\alpha\hat{\imath} + sin\alpha\hat{\jmath}).\vec{t} + \sum_{j=1}^{m} \gamma'_j \int_0^{s_j} f1_t(s_j).ds_j + \gamma'_{j+1} \int_0^{s_j} f2_t(s_j).ds_j \quad (11)$$

Eq. 11 will be dealt with later*. Now concentrating on Eq. 10, the estimation of the two integrals is lengthy and tedious algebraic task. The result is directly given below as:

$$\int_0^{s_j} f1_n(s_j).ds_j = Cn1_{ij} \quad (12-a)$$

$$\int_0^{s_j} f2_n(s_j).ds_j = Cn2_{ij} \quad (12-b)$$

$Cn1_{ij}$ and $Cn2_{ij}$ are coefficients expressed by:

$$Cn1_{ij} = 0.5DF + CG - Cn2_{ij} \quad (13)$$

$$Cn2_{ij} = D + 0.5\frac{QF}{S_j} - \frac{(AC + DE)G}{S_j} \quad (14)$$

The intermediate constants appearing on the right -hand sides of Eqs 13 and 14 and some later expressions are defined as:

$$A = -(x_i - X_j)cos\theta_j - (y_i - Y_j)sin\theta_j$$

$$B = (x_i - X_j)^2 + (y_i - Y_j)^2$$

$$C = sin(\theta_i - \theta_j)$$

$$D = cos(\theta_i - \theta_j)$$

$$E = (x_i - X_j)\, sin\theta_j - (y_i - Y_j)cos\theta_j$$

$$F = \ln\left[1 + \frac{S_j{}^2 + 2AS_j}{B}\right]$$

$$G = \tan^{-1}\left[\frac{ES_j}{B + AS_j}\right]$$

$$P = (x_i - X_j)\sin(\theta_i - 2\theta_j) + (y_i - Y_j)cos(\theta_i - 2\theta_j)$$

$$Q = (x_i - X_j)\cos(\theta_i - 2\theta_j) - (y_i - Y_j)sin(\theta_i - 2\theta_j)$$

Note that these constants are functions of the coordinates of the i^{th} control points, those of the boundary points of the j^{th} vortex panel, and the orientation angles of both i^{th} and j^{th} panels. They can be computed for all possible values of i and j once the panel geometry is specified. Eq. 10 will be employed to write a set of equations for the induced velocity at panel i from all of the remaining panels including the induced velocity from the variable vortex on panel i itself. In addition to this set of equations, the Kutta condition in form of the following equation is added:

$$\gamma'_1 + \gamma'_{m+1} = 0 \quad (15)$$

This will construct a system of (m+1) simultaneous algebraic equations as:

$$\begin{bmatrix} A_{n_{1,1}} & A_{n_{1,2}} & \cdots & A_{n_{1,m}} & A_{n_{1,m+1}} \\ A_{n_{2,1}} & A_{n_{2,2}} & \cdots & A_{n_{2,m}} & A_{n_{2,m+1}} \\ \vdots & \vdots & \cdots & \vdots & \vdots \\ A_{n_{m-1,1}} & A_{n_{m-1,2}} & \cdots & A_{n_{m-1,m}} & A_{n_{m-1,m+1}} \\ A_{n_{m,1}} & A_{n_{m,2}} & \cdots & A_{n_{m,m}} & A_{n_{m,m+1}} \\ 1 & 0 & 0\cdots & 0 & 1 \end{bmatrix} \begin{bmatrix} \gamma'_1 \\ \gamma'_2 \\ \vdots \\ \gamma'_{m-1} \\ \gamma'_m \\ \gamma'_{m+1} \end{bmatrix} = \begin{bmatrix} RHS_1 \\ RHS_2 \\ \vdots \\ RHS_{m-1} \\ RHS_m \\ 0 \end{bmatrix} \quad (16)$$

where:

$$RHS_i = sin(\theta_i - \alpha) \qquad i = 1,2, \ldots\ldots\ldots m+1$$

$A_{n_{ij}}$ is known as the influence coefficient for the normal velocity.

In which, for $\underline{i \neq m+1}$

$$if \quad j = 1 \qquad A_{n_{i1}} = Cn1_{i1}$$

$$if \quad j = 2,3, \ldots\ldots m \qquad A_{n_{ij}} = Cn1_{ij} + Cn2_{ij}$$

$$if \quad j = m+1 \qquad A_{n_{im+1}} = Cn2_{im+1}$$

$$RHS_i = sin(\theta_i - \alpha)$$

And for $\underline{i = m+1}$

$$if \quad j = 1\ and\ j = m+1 \qquad A_{n_{i1}} = A_{n_{im+1}} = 1$$

$$if \quad j = 2,3, \ldots\ldots\ldots\ldots m \qquad A_{n_{ij}} = 0$$

$$RHS_i = 0$$

This system of linear algebraic equations lends itself to solution by the Gauss elimination method to obtain the (m+1) unknowns of γ'_js. Having γ'_js at hand will enable the calculation of the tangential velocity and hence the pressure at the control points. This task will be accomplished by recalling Eq. 11 and substituting for the values of γ'_js in it. The only unknown in Eq. 11 will be the tangential velocities at each panel. Here again, the two integrals on the right-hand side of Eq. 11 will undergo to a lengthy mathematical manipulation and the result is directly given below as:

$$\int_0^{s_j} f1_t(s_j).ds_j = Ct1_{ij} \quad (17-a)$$

$$\int_0^{s_j} f2_t(s_j).ds_j = Ct2_{ij} \quad (17-b)$$

Where:

*The normal velocity component is dealt with firstly because of the boundary condition, which states that this component is equal to zero.

$$Ct1_{ij} = 0.5CF - DG - Ct2_{ij} \quad (18)$$

$$Ct2_{ij} = C + \frac{0.5PF}{S_j} + \frac{(AD - CE)G}{S_j} \quad (19)$$

The constants appearing in Eqs. 18 and 19 are the same constants that appeared when $Cn1_{ij}$ and $Cn2_{ij}$, were calculated. A special case arise when $i = j$, the coefficients have the simplified values:

$$Ct1_{ij} = Ct2_{ij} = \frac{\pi}{2}$$

The local *dimensionless velocity* defined as $V_i = \left[{V_{t_i}}/{V_\infty}\right]$ can be computed as:

$$V_i = \cos(\theta_i - \alpha) + \sum_{j=1}^{m+1} A_{t_{ij}} \cdot \gamma'_j \quad (20)$$

Where $i = 1,2,\dots,m$ and $A_{t_{ij}}$ is known as the influence coefficient for the tangential velocity.

$A_{t_{ij}}$ can be obtained as follows:

$$if \quad j = 1 \qquad A_{t_{i1}} = Ct1_{i1}$$

$$if \quad j = 2,3,\dots\dots\dots m \qquad A_{t_{ij}} = Ct1_{ij} + Ct2_{ij}$$

$$if \quad j = m+1 \qquad A_{t_{i,m+1}} = Ct2_{i,m+1}$$

The γ'_j is already known and the only unknown now is V_i at each control point.

We can determine V_i for each panel by:

$$[V_i] = [\cos(\theta_i - \alpha)] + \left[A_{t_{ij}}\right]\left[\gamma'_j\right] \quad (21)$$

After solving Eq. 21 for each panel, the values of the dimensionless velocity at each control point can be obtained. We can calculate the pressure coefficient at each control point by Bernoulli's law and using dimensionless velocity V_i at each control point, that is:

$$C_{p_i} = 1 - {V_i}^2 \quad (22)$$

3. Results and discussions

3.1 Determination of the Optimum Panel Count

The effect of airfoil thickness on the panel count can be investigated by examination of Figs. 2 to 6. In each figure, six solutions are shown. These solutions are obtained using twenty, forty, eighty, one hundred and twenty, one hundred and sixty, and two hundred panels. As seen in these figures the solutions obtained by using both twenty and forty panels deviate considerably from the other solutions. These deviations occur especially at the regions of high gradients, namely; near the leading and the trailing edges. Another important notice here is that all the remaining obtained solutions are coincident. This means that increasing the panel count above eighty is superfluous and will not lead to any improvement in the accuracy.

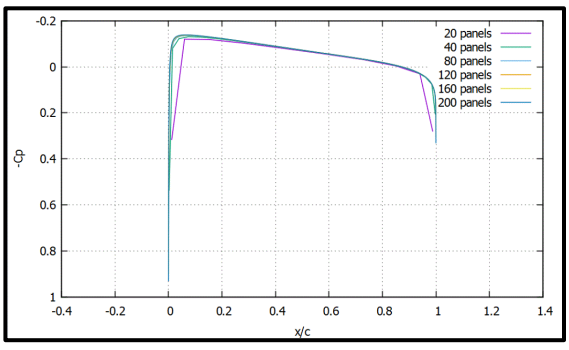

Fig. 2. Effect of Number of Panels on C_P Distribution for NACA0004 at AOA=zero.

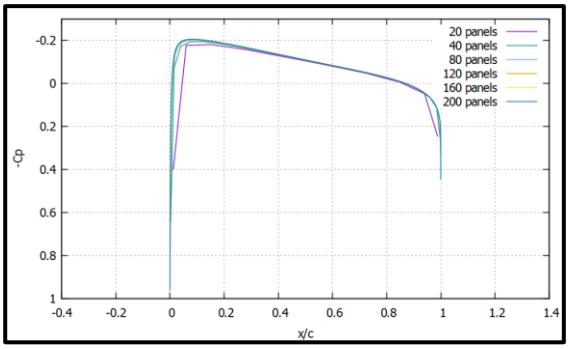

Fig. 3. Effect of Number of Panels on C_P Distribution for NACA0006 at AOA=zero.

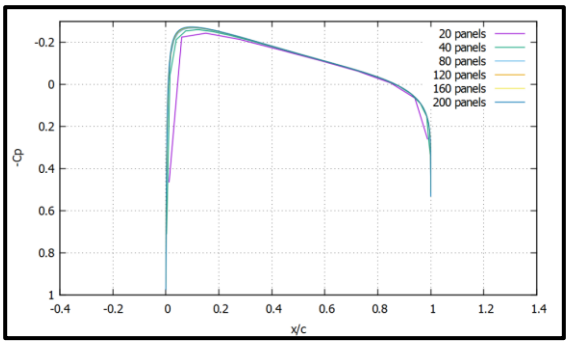

Fig. 4. Effect of Number of Panels on C_P Distribution for NACA0008 at AOA=zero.

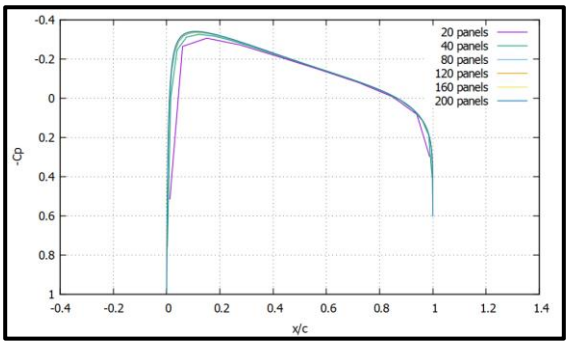

Fig. 5. Effect of Number of Panels on C_P Distribution for NACA0010 at AOA=zero.

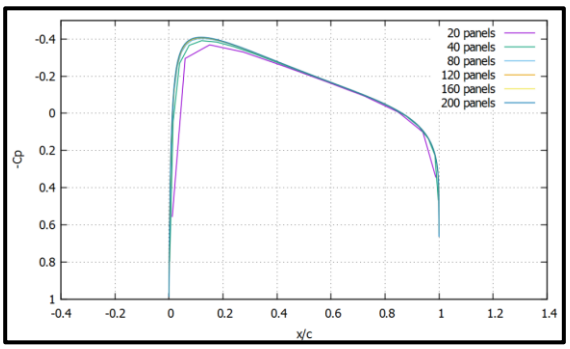

Fig. 6. Effect of Number of Panels on C_P Distribution for NACA0012 at AOA=zero.

The effect of the flow angle of attack on the panel count can be studied by examination of Figs. 7 to 10 a similar observation is made here: Both the solutions obtained by using twenty and forty panels have considerable deviations from the other obtained solutions in the vicinity of the leading as well as the trailing edge. Starting from eighty panels and increasing the panel count to two hundred has not led to any noticeable increase in the accuracy of the obtained solution.

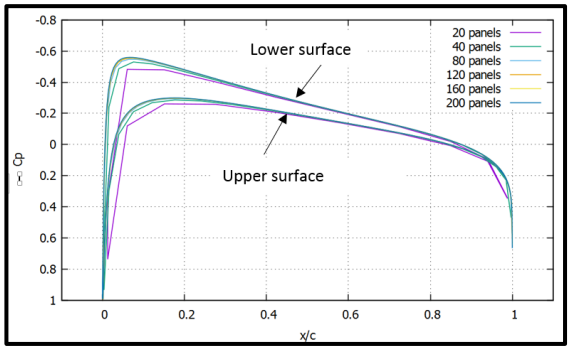

Fig. 7. Effect of Number of Panels on C_P Distribution at AOA=1° for NACA 0012.

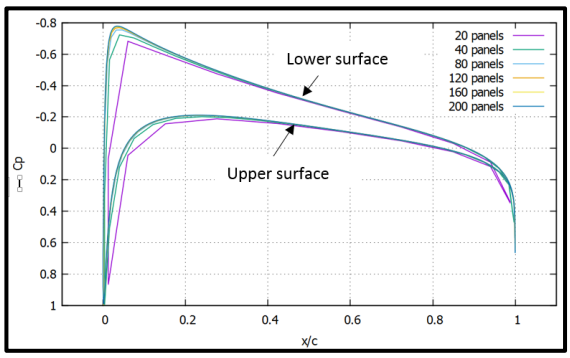

Fig. 8. Effect of Number of Panels on C_P Distribution at AOA=2° for NACA 0012.

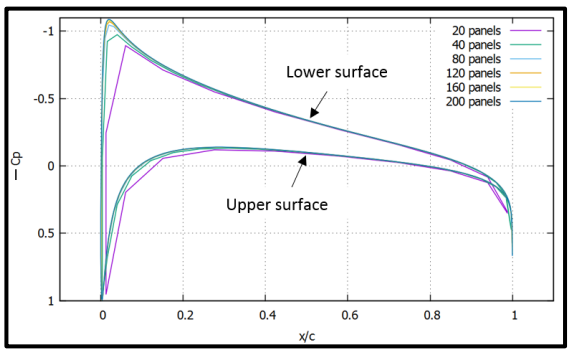

Fig. 9. Effect of Number of Panels on C_P Distribution at AOA =3° for NACA 0012.

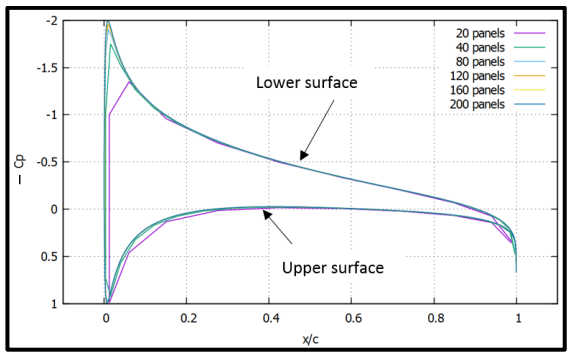

Fig. 10. Effect of Number of Panels on C_P Distribution at AOA=5° for NACA 0012.

3.2 Comparison of the Vortex Panel Method with the CFX

When it comes to choosing the test case, a special care must be taken. In other words, the test case must be chosen such that it lies within the field of application of the vortex panel method. It is well documented in the literature that vortex panel method is developed from the vortex sheet method, that is; it is originally formulated for a sheet or flat plate, and hence it can be extended to airfoils as long as the airfoils are thin.

Another aspect which should be considered when employing the vortex panel method is that it ignores the induced normal velocities on the surface of the airfoil and they are set equal to zero during the solution. This assumption is valid as long as the angle of attack is less than six degree; see (White, 2003). Accordingly, the test cases were chosen to be the flow around the NACA0012 at angles of attack of zero, one, two, three, four, five, and six degrees. Figs. 11 to 17 show the distribution of the coefficient of pressure versus the relative distance measured from the leading edge as obtained by the vortex panel method and by the CFX commercial program.

It should be noted here that the CFX was run based on input flow with a Mach number of 0.3 (incompressible flow) and selecting the laminar flow option. Examination of these six figures leads to two important observations: For angles of attack between zero and three degrees, the panel method solution is in good agreement with the CFX solution except at about 95% of the chord near the trailing edge. Slight deviations for ($0 < \propto < 3$) near the leading edge are also noticed that are related to the presence of the strong gradients near the stagnation point. The solution scheme of the CFX is strongly dependent on the values of these gradients. In contrast, the panel method does not depend on them.

The difference between the two solutions at the trailing edge is explained by the fact that the panel method employs the Kutta condition at the trailing edge whereas the CFX solves the laminar viscous flow past the airfoil. The second observation is that as the angle of attack is increased above three degrees, the solution of the panel method starts slightly to deviate (overestimate) the pressure on the higher-pressure side of the airfoil. This deviation occurs in the vicinity of the leading edge where the flow accelerates very fast from the stagnation point. In doing, so the flow will also pass the point at which the airfoil has the maximum thickness. Here it should be recalled that the panel method has the constraint of being limited to thin air foils and that the NACA0012 is a relatively thick airfoil. Increasing the angle of attack above three degrees will have an effect equivalent to increasing the airfoil thickness, see Fig. 18.

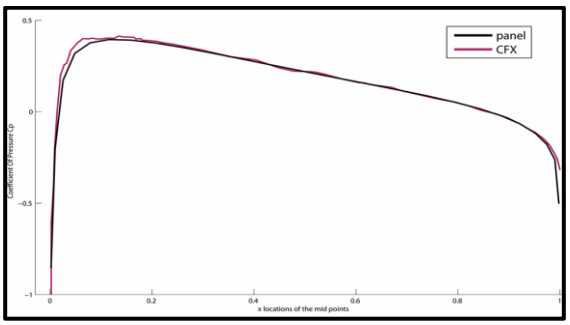

Fig. 11. C_P Distribution versus Distance from the Leading Edge for an AOA=zero.

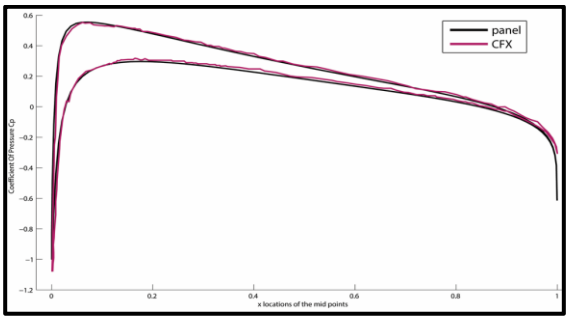

Fig. 12. C_P Distribution versus Distance from the Leading Edge for an AOA=1°.

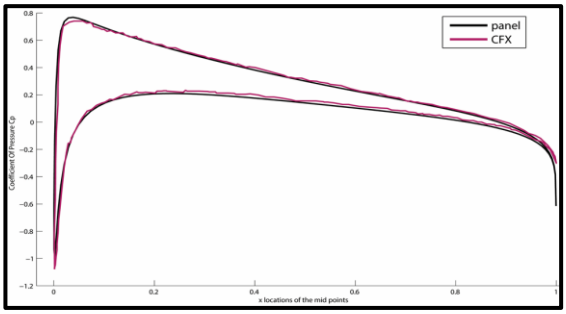

Fig. 13. C_P Distribution versus Distance from the Leading Edge for an AOA=2°.

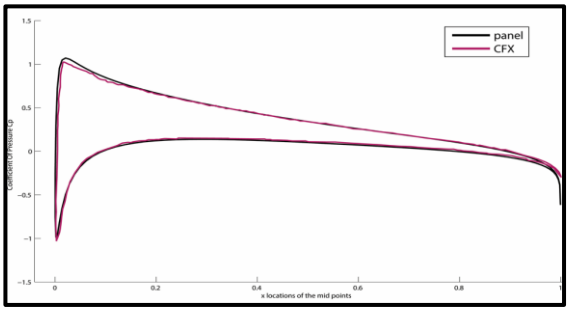

Fig. 14. C_P Distribution versus Distance from the Leading Edge for an AOA=3°.

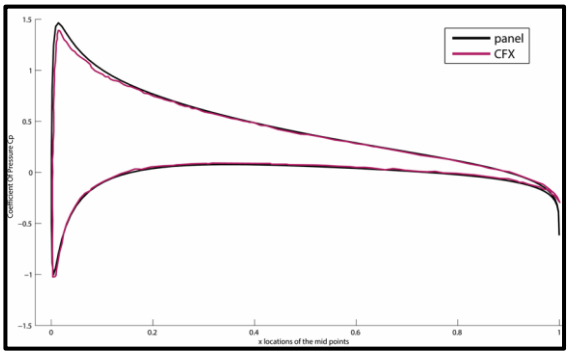

Fig. 15. C_P Distribution versus Distance from the Leading Edge for an AOA=4°.

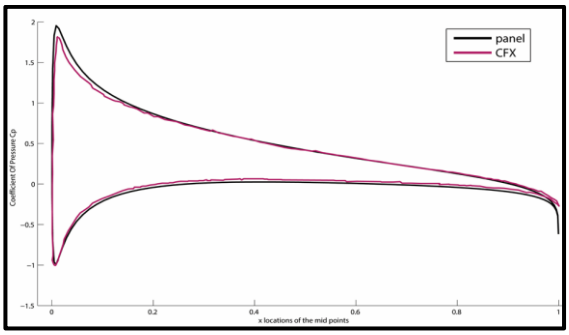

Fig. 16. C_P Distribution versus Distance from the Leading Edge for an AOA=5°.

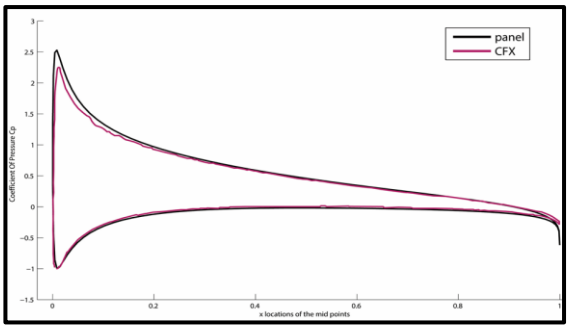

Fig. 17. C_P Distribution versus Distance from the Leading Edge for an AOA=6°.

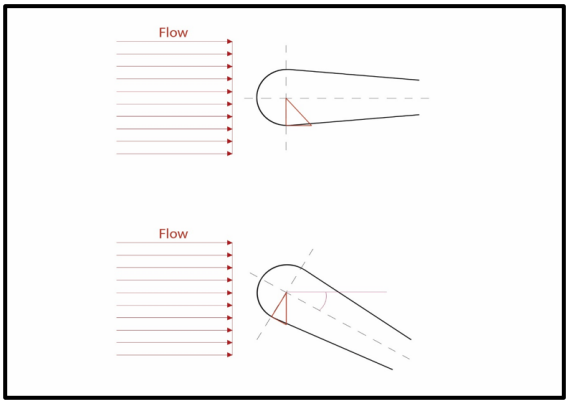

Fig. 18. Airfoil Thickness Change on the Lower Side due to the Increase in AOA.

3.3 Comparison of Panel Method Results with Results from Publications

In order to beef up the assessment process for the performance of the panel method, it was decided to compare its results with results published in the literature for the same test case. This has put a constraint on the selection of the test case. In other words, the authors of this paper were obliged to stick to that special test case which was selected by the authors of that published work. Moreover, most of the recent publications solve the full Navier−Stokes equations taking into account both compressibility and viscous effects. Nevertheless, this is one of the main reasons for this study, that is; to compare the result obtained by the panel method with that obtained by another more advanced yet sophisticated and time-consuming scheme. (Sengupta *et al.*, 2013) presented two different solutions for the flow past NACA0012 airfoil: The first solution is obtained for a compressible flow with a Mach number of 0.6 and an angle of attack of −0.14 degrees. The second solution is obtained for a near –transonic flow with Mach number of 0.758 and an angle of attack of −0.14 degrees. It should be noted that these two solutions were obtained for turbulent flow with Reynolds number of 3×10^6.

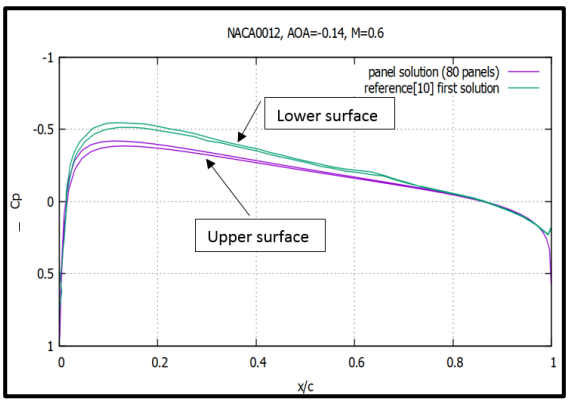

Fig. 19. Comparison of Panel Solution with the First Solution Given by (Sengupta *et al.*, 2013).

Fig. 19 shows a comparison of the first solution of (Sengupta *et al.*, 2013) with that obtained by the vortex panel method. It is very clear that the vortex panel method has performed well as compared to the numerically expensive other solution. Another comparison is shown in Fig. 20 where this time the second solution of (Sengupta *et al.*, 2013) is compared with that of the panel method.

Careful investigation of Fig. 20 delivers two important remarks: The first is that the vortex panel method solution deviates considerably from the solution of (Sengupta *et al.*, 2013). The second remark is that the vortex panel method solution has failed to capture the very weak shock waves that appear on both the lower and the upper surface of the airfoil. This behaviour of the vortex panel

method is pretty expected since this method was developed for incompressible flows that is; for flows with Mach number less than 0.3. As the Mach number is increased, the compressibility of the fluid is increased and accordingly the validity of the panel method will deteriorate. In the transonic flow range Mach number (0.8-1.2), weak shock waves will start to appear in the flow field. Shock waves are thin layers in the flow field through which steep gradients of the flow properties exist.

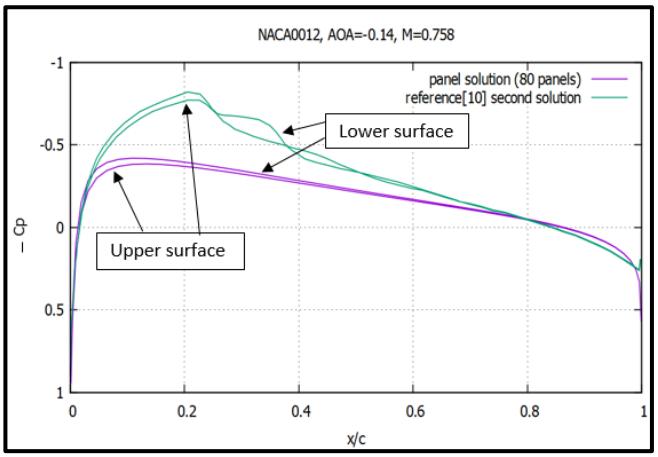

Fig. 20. Comparison of Panel Solution with Second Solution Given in (Sengupta *et al.*, 2013).

Special techniques* are usually incorporated in advanced flow solvers, like the one used by (Sengupta *et al.*, 2013) in order to enable the flow solver to detect the shock wave. Swanson and Lingers (2016) provide a solution for the flow past NACA0012 at Mach number of 0.5 and an angle of attack of zero. This solution was obtained by solving the complete Navier –Stokes equations for laminar flow at Reynolds number of 5000.

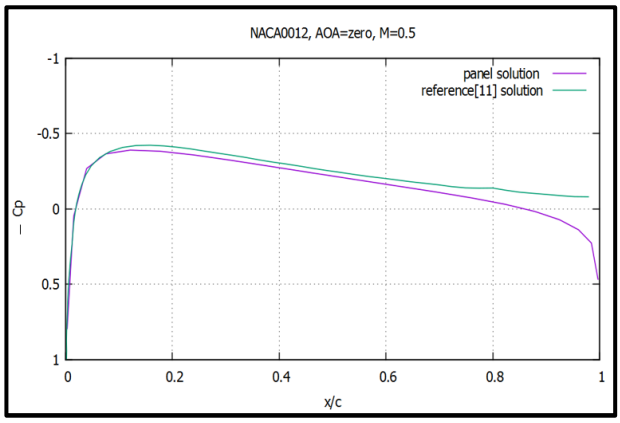

Fig. 21. Comparison of Panel Solution with Solution Given by (Swanson and Lingers, 2016).

Fig. 21 shows a comparison between the solution of the vortex panel method and the aforementioned solution from Swanson and Lingers (2016). As seen in this figure, the panel solution is in good agreement with the solution of Swanson and Lingers (2016) except at the trailing edge of the airfoil. This is again an expected behaviour from the panel method since it employs the Kutta condition (Eq. 8) in its derivation. At about 88% of the chord and before the trailing edge, (Swanson and Lingers, 2016) state that a flow separation will occur and a blow-up of streamline pattern can be clearly observed. Fig. 22 is taken from (Swanson and Lingers, 2016) and is presented here to clarify this phenomenon, which appears as a result of the viscous effect.

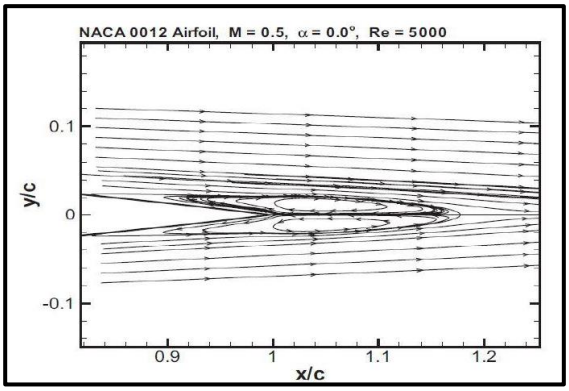

Fig. 22. Blow up of Streamline Pattern in the Airfoil Trailing Edge Region, from (Swanson and Lingers, 2016).

4. Conclusion

The vortex panel method is one of the first mathematical techniques that was used to solve the incompressible inviscid flow past thin airfoils. Since this method was developed originally for flat plate, the extension of its application to airfoils is limited to thin airfoils. The simplicity and compactness of the method have made it a very popular tool in hands of airplanes designers especially for making initial calculations at the early design stage. Another advantage of the vortex panel method is its low computational cost as compared to the computational cost of other more advanced compressible and viscous flow solvers. The results presented and discussed in this paper have shown that this method performs pretty well for thin airfoils and angle of attack of not more than four degrees provided that the flow is subsonic. If the flow is transonic, the vortex panel method was incapable of predicting and capturing even weak shock waves. One last conclusion that was drawn from the results is that the heavy dependence of the vortex panel method on the Kutta condition in its derivation has rendered it disable of capturing the flow separations and streamline's pattern blowups that appear at the trailing edge especially in turbulent flows.

This work can be further extended in a future study by studying the effect of camber and/or changing to another airfoil family, e.g. the NACA five or six-digits family.

Acknowledgments

The authors of this paper would like to thank Mr. Chris Kireney for his wonderful work on the vortex panel method, which is provided for public free of charge at: http://by.genie.uottawa.ca/~mcg4345/CompAssignments/vortexpanel-method.m

References

Anderson, J. D. (2010) Fundamentals of Aerodynamic, McGraw Hill Inc., Fifth Edition, 2010.

Josef Ballman, Richard Eppler, and Wolfgang Hackbush Hrsg. (1987) "Panel Method in Fluid Mechanics with Emphasis on Aerodynamics", Proceedings of Third GAMM Seminar-Kiel, January 16 to 18, 1987.

Chattot and Hafez, 2013) J. J. Chattot and M. M. Hafez "Theoretical and Applied Aerodynamics", Springer, Dordrecht, Heidelberg, and New York, 2013.

Daniel O. Dommasch, Sydney S. Sherby, and Thomas Connolly (1967) "Airplane Aerodynamics", Fourth Edition.

Gary A. Flandro, Howard M. McMahon, and Robert L. Roach (2012) "Basic Aerodynamic: Incompressible Flow", Cambridge University Press.

Katz J., and Plotkin A. (1991) "Low Speed Aerodynamics", McGraw Hill Inc. Series in Aeronautical and Aerospace Engineering, International Edition.

Kireny (2002) A Matlab Code by Chris Kireney Available Online at [http://by.genie.uottawa.ca/~mcg4345/CompAssignments/vortexpanelmethod.m].

Arnold M. Kuethe, and Chuen -Yen Chow (2009) "Foundations of Aerodynamics: Basic of Aerodynamic Design", Wiley India Inc., Fifth Edition.

Sengupta T. K., Bhole A., Sreejith N. A. (2013) 'Direct Numerical Simulation of 2D Transonic Flows around Airfoils', *Journal of Computers and Fluids*, 88, p.p. 19-37.

Swanson R.C., Lingers A. (2016) 'Steady -State Laminar Flow Solutions for NACA0012 Airfoil', *Journal of Computers and Fluids*, 126, p.p. 102-128.

Frank W. (2003) 'Fluid Mechanics'. McGraw Hill Series in Mechanical Engineering, Fifth Edition.

NOMENCLATURES

Latins:

A	Intermediate constant.
AOA	Angle of Attack.
$A_{n_{ij}}$	Influence coefficient for normal velocity.
$A_{t_{ij}}$	Influence coefficient for tangential velocity.
B	Intermediate constant.
C	Intermediate constant.
$C_{n1_{ij}}$, $C_{n2_{ij}}$	Coefficient for normal velocity.
$C_{t1_{ij}}$, $C_{t2_{ij}}$	Coefficient for tangential velocity.
C_p	Coefficient of pressure.
C_{p_i}	Pressure coefficient at control point.
D	Intermediate constant.
$\overrightarrow{d_s}$	Elemental vector.
E	Intermediate constant.
F	Intermediate constant.
G	Intermediate constant.
$\overrightarrow{n}$	Normal vector.
P	Intermediate constant.
Q	Intermediate constant.
Re	Reynolds number based on airfoil chord.
S_j	Length of the panel.
s_j	Distance measured from the leading edge.
t	Time.
$\overrightarrow{t}$	Tangential vector.
u	Velocity in x-coordinate.
$\vec{V}$	Vector velocity.
V_∞	Uniform velocity.
V_{n_i}	Normal velocity at control point.
V_{t_i}	Tangential velocity at control point.
V_i	Dimensionless velocity at control point.
v	Velocity in y-coordinate.
X_i	X-coordination at start point panel $\hat{\imath}^{th}$.
X_j	X-coordination at start point panel $\hat{\jmath}^{th}$.
x	X-coordinate.
x_i	X-coordination at mid-point panel $\hat{\imath}^{th}$.
Y_i	Y-coordination at start point panel $\hat{\imath}^{th}$.
Y_j	Y-coordination at start point panel $\hat{\jmath}^{th}$.
y	Y-coordinate.
y_i	Y-coordination at mid-point panel $\hat{\imath}^{th}$.
z	Z-coordinate.

Greeks:

θ_i	The orientation angle of the $\hat{\imath}^{th}$ panel.
θ_j	The orientation angle of the $\hat{\jmath}^{th}$ panel.
α	Angle of attack.
Γ	Circulation.
γ	Strength of the vortex
γ_j	Strength of the vortex at the start point
$\grave{\gamma}$	Dimensionless strength
ϕ	Velocity potential
ω	Velocity in z-coordinate
ρ	Density.
τ	Viscous stress.
ψ	Stream function.

Libyan Journal of Science & Technology 9:2 (2019) 129–141

Faculty of Science - University of Benghazi

Libyan Journal of Science & Technology

journal home page: www.sc.uob.edu.ly/pages/page/77

Characterization and identification of Libyan olive diversity using microsatellite markers

Salem Abdul Sadeg[*,a], Gayle Volk[c], Christopher Richards[c], and Harrison Hughes[b]

[a]*Biology Department Elmergib University, Masallatah, Libya,*

[b]*Horticulture & Landscape Architecture, Colorado State University, Fort Collins, Colorado*

[c]*National center for genetic resource preservation, Fort Collins, Colorado.*

Highlights

- **Combination of morphological traits and molecular data were highly useful to separate closely related genotypes within Libyan olive landraces.**
- **The denominations of homonyms and synonyms or mislabeling were more frequently within landraces than other cultivated and wild types.**
- **The wild types were more closely related to the introduced genotypes than Libyan olive landraces.**

ARTICLE INFO

Article history:
Received 10 June 2017
Revised 03 March 2019
Accepted 10 March 2019
Available online 16 June 2019

Keywords:
SSR Markers, Olive tree, Microsatellite markers, and Genetic diversity.

* Corresponding author:
E-mail address: salem.elleaga@yahoo.com
S. Abdul

ABSTRACT

Ten microsatellite markers were used to differentiate and evaluate the relationships among a total of 91 olive genotypes (39 local cultivated, 36 introduced cultivars and 16 wild types) collected in Libya. A total of 109 alleles were identified, with the number of alleles per locus ranging from 4 to 20 alleles. Three loci (UDO43, DCA16 and GAPU101) had the most alleles across all loci with 20, 18 and 16, respectively. The wild types and introduced cultivars had greater numbers of alleles than the local cultivars. Six cases of duplicated genotypes, two cases of synonymy, and thirteen homonyms that were genetically distinct were observed in the Libyan collection. UPGMA clustering classified the accessions into two main distinct groups. The first group consisted of local genotypes and the second group included introduced and wild type accessions. Admixture analysis also clearly distinguished between local ancient landraces and wild genotypes. In general, using molecular data enables to separate the Libyan olive accessions based on their origin but not fruit use.

1. Introduction

Libyan olives (*Olea europaea* subsp. *europaea* var. *sativa* or *sylvestris*) have traditionally been evaluated by leaf, fruit, and seed morphological as well as phonological characteristics. It has been difficult to properly manage and conserve olive germplasm because of the problems associated with clearly distinguishing among cultivars. Further complicating identification of cultivars is the observation that wild populations have likely introgressed with locally adapted cultivars. There are more than 100 named olive cultivars are grown along the coastal region of Libya. Some of these cultivars are likely to be identical due to the historical renaming of material. This has led to the perception that numerous cultivars exist when in fact, they are actually synonyms or homonyms Morphological differences associated with specific environmental effects have also lead to a mistaken identification of the cultivars. The level of knowledge about cultivar origin, selection and molecular variability is limited because the identification of Libyan olive accessions has previously been based on phenotypic traits. Recently, morphological descriptions have improved, and are now considered to be complementary tools to molecular marker, aiding in olive cultivar identification. Using both morphological and molecular descriptors of genotypes within other crops (Corrado *et al*., 2009). This combination of techniques leads to more robust results (Leon *et al*., 2005). To date, SSR markers have not been used in combination with morphological data to evaluate and improve the collection of Libyan olive accessions as a genetic resource. In this work, SSR markers were used to differentiate and classify Libyan olive accessions.

2. Materials and methods

2.1 Collection sites and plant materials

Accessions were classified into three categories: 42 local cultivated varieties, 41 introduced cultivars of *Olea europaea* and 16 wild *Olea europaea var. sylvestris*. Leaf tissue was collected in 2009 and 2012. Most of the local cultivars (Libyan landraces) were collected from orchards of Masallatah city while the introduced cultivars were collected from Tharouna and Gharian government collections as well as from farmers in the Zaltin and Tripoli regions. The wild type accessions were collected from four different sites (S1, S2, S3 and S4) in the Green Mountain region (Fig. 1). Leaf samples were collected then immediately stored in containers with dry ice to prevent DNA degradation. They were then transferred to the National Medical Research Center in Tripoli–where they were washed with double distilled water and freeze-dried. Samples were then transported to the Horticulture Laboratory at Colorado State University in Fort Collins, CO. USA where they were stored at –80°C until DNA use.

2.2 Processing samples

Total genomic DNA was extracted from 100-200 mg lyophilized of tissue using the method of large-scale CTAB extraction was performed according to (Mace *et al*., 2003). This protocol was a modification of the CTAB procedure for obtaining purified genomic DNA. Twelve sets of primer pairs were selected (Table 1) because of their high resolution in discriminating polymorphism previous use in the identification of olive genotypes (Ercisli *et al*., 2011; Ercisli *et al*., 2012; Sefc *et al*., 2000; Baldoni *et al*., 2009; Sarri *et al*., 2006;

 ISSN 2663-1407; National Library of Libya, Legal number: 390/2018

Carriero *et al*., 2002; Cipriani *et al*., 2002; Belaj *et al*., 2003; De La Rosa *et al*., 2002). These were multiplexed using multiplex manager 1.2 software (Guichoux *et al*., 2011) to minimize overlap among the markers and to maximize similarity in the annealing temperature of each primer combination to reduce the variation and a total number of PCR reactions. Each cycle of multiplex PCR amplification was performed with combinations of three different primers labeled with specific fluorescent dyes that incorporated during multiplex PCR amplification giving a specific color tag to each PCR product (Table 1).

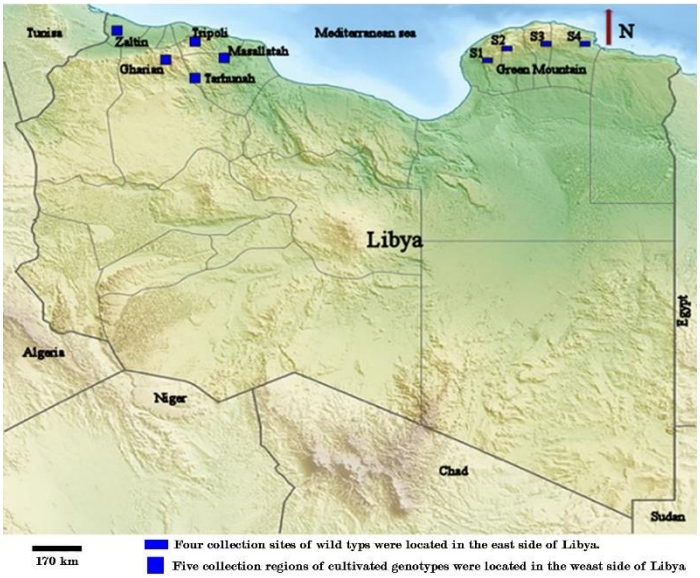

Fig. 1. Map of Libya that illustrates the collection sites of cultivated and wild olive.

Table 1

Locus names, Forward primers including nucleotide sequences and company references.

Locus Name	Forward dye label	Company	Primer sequence labeled with fluorescent probe (5' –3')
EMO-90-F	56-FAM	IDT	5'-/56-FAM/CAT CCG GAT TTC TTG CTT TT-3'
EMO-90-R	PIGtail	IDT	5'-GTT TCT T/AG CGA ATG TAG CTT TGC ATG T-3'
DCA3-F	56-FAM	IDT	5'-/56-FAM/CCC AAG CGG AGG TGT ATA TTG TTA C-3'
DCA3-R	PIGtail	IDT	5'-GTT TCT T/TG CTT TTG TCG TGT TTG AGA TGT TG-3'
DCA14-F	56-FAM	IDT	5'-/56-FAM/AAT TTT TTA ATG CAC TAT AAT TTA C-3'
DCA14-R	PIGtail	IDT	5'-GTT TCT T/TT GAG GTC TCT ATA TCT CCC AGG GG-3'
GAPU101-F	56-FAM	IDT	5'-/56-FAM/CAT GAA AGG AGG GGG ACA TA-3'
GAPU101-R	PIGtail	IDT	5'-GTT TCT T/GG CAC TTG TTG TGC AGA TTG-3'
DCA18-F	VIC	AB	5'-/VIC/AAG AAA GAA AAA GGC AGA ATT AAG C-3'
DCA18-R	PIGtail	IDT	5'-GTT TCT T/GT TTT CGT CTC TCT ACA TAA GTG AC-3'
DCA16-F	VIC	AB	5'-/VIC/TTA GGT GGG ATT CTG TAG ATG GTT G-3'
DCA16-R	PIGtail	IDT	5'-GTT TCT T/TT TTA GGT GAG TTC ATA GAA TTA GC-3'
DCA5-F	VIC	AB	5'-/VIC/AAC AAA TCC CAT ACG AAC TGC C-3'
DCA5-R	PIGtail	IDT	5'-GTT TCT T/CG TGT TGC TGT GAA GAA AAT CG-3'
DCA17-F	VIC	AB	5'-/VIC/GAT CAA ATT CTA CCA AAA ATA TA-3'
DCA17-R	PIGtail	IDT	5'-GTT TCT T/TA AAT TTT TGG CAC GTA GTA TTG G-3'
GAPU103A-F	PET	AB	5'-/PET/TGA ATT TAA CTT TAA ACC CAC ACA-3'
GAPU103A-R	PIGtail	IDT	5'-GTT TCT T/GC ATC GCT CGA TTT TTA TCC-3'
GAPU71B-F	PET	AB	5'-/PET/GAT CAA AGG AAG AAG GGG ATA AA-3'
GAPU71B-R	PIGtail	IDT	5'-GTT TCT T/AC AAC AAA TCC GTA CGC TTG-3'
UDO-043-F	PET	AB	5'-/PET/TCG GCT TTA CAA CCC ATT TC-3'
UDO-043-R	PIGtail	IDT	5'-GTT TCT T/TG CCA ATT ATG GGG CTA ACT-3'
DCA9-F	PET	AB	5'-/PET/AAT CAA AGT CTT CCT TCT CAT TTC G-3'
DCA9-R	PIGtail	IDT	5'-GTT TCT T/GA TCC TTC CAA AAG TAT AAC CTC TC-3'

Primers EMO90-F, DCA3-F, DCA14-F, and GAPU101-F were labeled with fluorescent dye (56-FAM) attached to the 5'-end of oligonucleotides from Integrated DNA Technologies (IDT) (IDT, Coralville, IA). The forward primers DCA18-F, DCA16-F, DCA5-F, and DCA17-F were attached with a green fluorescent dye (VIC) while GAPU103A-F, GAPU71B-F, UDO-043-F, and DCA9-F were attached with a fluorescent dye (PET) (both labeled groups were synthesized by Applied Biosystems (AB) (Foster City, CA). The reverse primers for all sets of 12 primer pairs were unlabeled and were obtained from Integrated DNA Technologies (IDT).

A small-tailed oligonucleotide or PIG-tail sequence (GTTTCTT) was added to all the unlabeled reverse primers to promote specific priming, full adenylation and reduce stutter bands (Brownstein *et al*., 1996). PCR amplifications were carried out in a final volume of 10µL in 2 mL 8-strip PCR tubes with 2 µM. The solution mix for PCR reactions consisted of the following: 2.0 µL of (20 ng/µL) genomic DNA; 3 µL of (Type-it microsatellite PCR –Maste mix; QIAGEN, USA); 2.0 µL of (2.0 µM) primer mix; and 3.0 µL of deionized water. All amplifications of multiplex PCR were performed in a 96-well thermocycler (Applied Biosystems, USA) under the following conditions of touchdown annealing temperature profile (Viljoen *et al.,* 2005): 2 min at 94°C; 10 cycles of 45 sec at 94°C, 1 min at 65°C (annealing temperature was reduced 1°C after every cycle), and 1 min and 30 sec at 72°C; 35 cycles of 45 s at 94°C, 1 min at 55°C, and 1 min and 30 s at 72°C; and a final extension step of 5 min at 72°C. The touchdown procedure was used to reduce non-specific priming during PCR amplification.

After successful amplification of the target region of isolated DNA, PCR samples were combined with LIZ 600 internal size standards. Fragment analyses were performed on an Applied Biosystems 3130 xL. The fragment data were scored using 'GeneMapper' software v.3.7 to size and genotype the alleles. Once allele sizes were determined (allele calling), the data set was formatted such that it could be converted to the various formats required by the software packages (Convert program Version) (Glaubitz, 2004).

2.3 Analytical methods

2.3.1 Quality control

Quality control was performed using a set of procedures to ensure the integrity, stability and consistency of SSR results. All amplifications of PCR for each sample three times. Negative and positive standard controls were applied. Quality was evaluated prior to exporting the results of the genotype samples as matrix data. Genotypes that have the same gene fragment to minimize the error estimation of genotyping. Filtering loci set to eliminate markers that have a missing data across all genotypes.

2.3.2 Population genetic analyses

Descriptive statistics were performed using FSTAT software version 2.9.3.2 (Goudet, 2002) and GDA software version 1.1. (Observed alleles, observed fragment size, private alleles, the probability of identity and power of discrimination) were estimated for each individual locus (Table 3) (probability of identity, power of discrimination, allele richness, expected heterozygosity, observed heterozygosity and population inbreeding coefficient).

2.4 Diversity and differentiation

2.4.1 Estimation of population structure and diversity

To estimate the dissimilarity or similarity of genetic data based on their populations or type of genotype. The pairwise distance matrix of SSR data was implemented as a (.txt) input file of allelic data in DARwin software v 5.0.158 (Raman *et al*., 2014). The constructed tree from *DARwin* software applied into the *Fig Tree* software v1.4.0 (Rambaut, 2012) to describe the relationship among olive samples using genetic distance as a tree based on (UPGMA) with the support of bootstrapped dissimilarities number of (1000) to assess the uncertainty of the tree structure.

2.4.2 Estimation of partition by assignment

Structure analysis was used to estimate genetic data to assign genotypes to specific groups without any prior information. The probability of membership into 1-4 K groups was determined by multiple runs (10 times) using STRUCTURE software Version 2.3.4 by (Pritchard *et al*., 2003). The STRUCTURE HARVESTER program (Earl, 2012) collects results generated by STRUCTURE program. This method allows assessment and visualizes the likelihood scores of multiple values of K, to evaluate the most likely level of genetic group subdivision. The probability of identity (IP) for each locus and all SSR loci set (accumulated IP) was calculated by means of the CLUster Matching and Permutation Program (CLUMPP) version 1.1.2 (Jakobsson and Rosenberg, 2007). This program assigns individuals on the basis of optimal membership coefficients within clusters. Molecular data were combined together with morphological data of stable phenotypic traits that were blocked by results of structure assignment of molecular data to evaluate the relationship between phenotypic and genotypic data.

3. Results

A matrix of 12 SSR primers by 99 individuals (Table 1) was used to evaluate the genetic relationships among genotypes of local cultivated, introduced cultivars and wild types. As a result of filtering loci and genotypes that have missing data, allelic data of DCA17 and DCA9 were removed from the dataset due to high failure rate. Eight duplicated accessions, based on their identical genotypes, were also excluded (Table 2). Consequently, a total of 10 SSR loci and 91 genotypes (39 local, 36 introduced and 16 wild) remained in the genetic data matrix.

3.1 Identification of duplicated genotypes

Ten SSRs loci (Table 3) were used to determine if duplicate olive cultivar samples were present in the dataset. Twelve genotypes (6 pairs) had the same names and were genetically identical as true duplicates (Table 2 and Fig. 2). Two sets of cultivars had different names but identical genotypes and were therefore considered to be (synonyms) (Table 2 and Fig. 2). One cultivar from each of these eight pairs was excluded from further analyses. A review of their morphological data and associated images indicated similarity in phenotypic traits (Fig. 3).

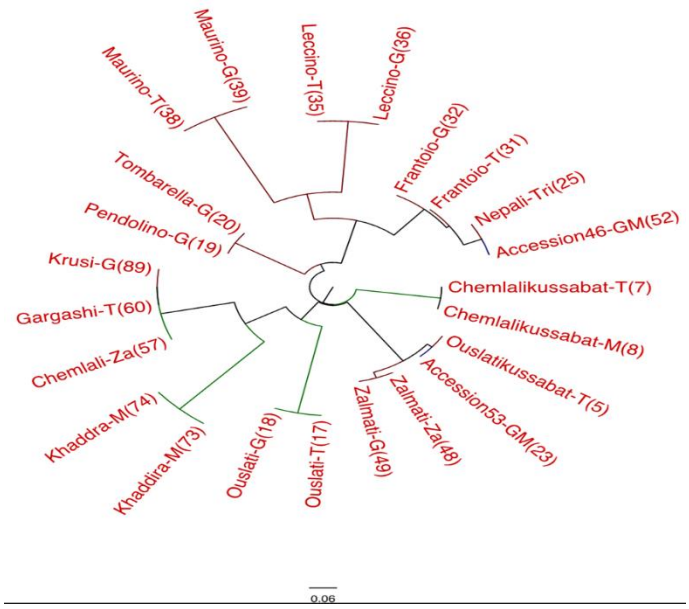

Fig. 2. A Neighbor-joining tree of 23 duplicated olive genotypes; each tip represents a single individual genotype with all pairs of duplicated genotypes similar.

Fig. 3. Phenotypic traits of the duplicated olive genotypes that illustrate similarity of genotypes.

Table 2

The same fragment sizes were considered to be duplicated or synonyms.

Variety name	Local location	Relationship	Bootstrap values (1000)
Chemlkussabat	Tharouna	Duplicated	99
Chemlkussabat	Mesalata	Duplicated	99
Khaddira	Mesalata	Synonyms	100
Khaddra	Mesalata	Synonyms	100
Ouslati	Tharouna	Duplicated	100
Ouslati	Gharian	Duplicated	100
Leccino	Tharouna	Duplicated	100
Leccino	Gharian	Duplicated	100

Variety name	Local location	Relationship	Bootstrap values (1000)
Maurino	Tharouna	Duplicated	100
Maurino	Gharian	Duplicated	100
Zalmati	Zaltin	Duplicated	59
Zalmati	Gharian	Duplicated	59
Frantoio	Tharouna	Duplicated	96
Frantoio	Gharian	Duplicated	96
Chemlali	Zaltin	Synonyms	98
Gargashi	Tharouna	Synonyms	98

3.2 Descriptive statistics of loci

A total of 109 alleles were identified, and the number of alleles per locus ranged from 4 alleles at the DCA5 locus to 20 alleles at the UDO043 locus, with an average of approximately 11 alleles per locus (Table 3). The combined discrimination power for all 10 loci was calculated with an average of (0.70) indicating that there is a moderate to high discrimination of the markers that were used, so there is a high probability that two individuals have different genotypes for each locus. The average probability of identity for all loci was low, indicating that there is a low (0.30) probability of accessions matching by chance.

Table 3

Descriptive statistics of 10 loci based on genetic data from 91 individual olive genotypes collected in Libya.

Locus	Sample size	Observed alleles (A)	Observed fragment size	Private alleles	Probability of identity (PI)	Power of discrimination (PD)
DCA14	90	10	168-188	3	0.22	0.78
DCA16	85	18	121-193	10	0.24	0.76
DCA18	92	10	154-180	3	0.20	0.80
DCA3	84	9	229-252	4	0.49	0.51
DCA5	83	4	194-206	1	0.85	0.15
EMO90	92	5	180-193	0	0.30	0.70
GAPU101	81	16	164-215	6	0.12	0.88
GAPU103A	88	11	134-189	4	0.21	0.79
GAPU71B	92	6	117-140	1	0.23	0.77
UDO043	69	20	154-227	9	0.10	0.90
All	85.6	10.9	161-198	4.1	0.30	0.70

3.3 Descriptive statistics of populations

Descriptive analysis of populations using GDA analysis (Table 4) revealed a higher inbreeding coefficient in the wild population (0.36) than the two sets of individuals, introduced (0.23) and local (0.24). The private allele frequency in the wild types was relatively higher than the other two populations. However, the discrimination power (PD) of private alleles in local and introduced genotypes was relatively high (0.99 and 0.98) respectively (Table 4). Results from the descriptive statistics of these populations provided insights into observed and expected heterozygosity. The value of expected heterozygosity (He) was higher than the value of observed heterozygosity for all three sets of individuals (Table 4) indicating there is more chance of heterozygosity at each population and they have some outbreeding resulting in disassortative mating and dissimilar traits.

Table 4

Descriptive statistics of three sets of individuals (Introduced, local and wild) collected from six locations in Libya

Sets of individuals	Sample size	Number of Private alleles	Probability of identity (PI)	Power of discrimination (PD)	Allele richness	He	Ho	Population inbreeding coefficient
Introduced	36	19	0.02	0.98	5.89	0.71	0.55	0.23
Local	39	4	0.002	0.99	4.88	0.68	0.52	0.24
Wild	16	18	0.13	0.87	5.88	0.64	0.41	0.36
Overall	30.33	13.67	0.05	0.95	5.55	0.68	0.49	0.28

z Six locations located as identified in Fig. 1.

In general, allelic richness was higher in wild and introduced genotypes (5.89 and 5.88) respectively than in local genotypes (4.88) (Table 4). There were more private alleles (observed once) in the introduced genotypes (19 private alleles), than in the wild (18 alleles) and local genotypes (4 alleles) (Table 4). Overall, all of the 41 private alleles were considered to be highly polymorphic across locations and could be used to assign individuals into a specific population based on their origins (Table 4). A total of 42 monomorphic alleles were estimated in all three different populations. These could not be used to assign any genotype to a specific population. Common alleles were most often observed in wild and introduced genotypes.

F-stats for the three sets of individuals (Introduced, local and wild) were estimated by performing a bootstrap analysis across loci to create 95% confidence intervals (Table 5). The pairwise Fst for the three sets of individuals were significantly different. Genetic differentiation of Fit, Fst and Fis was estimated by bootstrap test over all loci, and it was significant among all loci.

Table 5

Genetic differentiation as estimated by Fst with confidence intervals of 95% overall loci and three different locations.

Source	Fst	Fst confidence interval
Loci	0.025	–0.025-0.077
Sets of individuals	0.030	–0.030-0.080

3.4 Estimation of diversity and differentiation

3.4.1 Identification of mislabeled genotypes

Neighbor-joining relationships revealed that the 10 loci failed to distinguish a total of seven cultivars appeared to be similar when the molecular data were evaluated. These genotypes were Krusi, Pendolino, Tombarella, Ouslatikussabat, Accession53, Nepal and Aceession46. However, all seven cultivars had missing data for two loci (Table 6). A review of their morphological data and associated images (Fig. 4) indicated large differences in phenotypic traits across all of these cultivars.

Table 6

The seven cultivars had missing data that were considered to be mislabeled genotypes.

POP = Introduced	DCA18	DCA18	UDO043	UDO043	GAPU101	GAPU101	DCA3	DCA3	DCA5	DCA5
KrusiG	168	168	227	227	?	?	240	240	202	202
GargashiT	168	168	?	?	187	193	240	240	202	202
PendolinoG	174	174	204	204	189	203	240	240	202	202
TombarellaG	174	174	?	?	?	?	240	240	202	202
Ac#53	174	174	168	168	189	195	240	240	202	202
OuslatikussabatT	174	174	168	168	189	195	?	?	?	?
Ac#46	?	?	?	?	181	195	240	240	202	202
NepalTri	174	174	177	177	181	195	?	?	?	?
POP = Introduced	DCA14	DCA14	GAPU103A	GAPU103A	DCA16	DCA16	GAPU71B	GAPU71B	EMO90	EMO90
KrusiG	182	186	159	159	147	160	124	127	184	184
GargashiT	182	186	159	159	147	160	124	127	184	184
PendolinoG	186	186	150	150	147	147	121	127	183	189
TombarellaG	186	186	150	150	147	147	121	127	183	189
Ac#53	168	186	159	159	?	?	?	?	183	184
OuslatikussabatT	168	186	159	159	147	183	121	140	183	184
Ac#46	178	186	162	174	147	147	121	140	183	189
NepalTri	178	186	162	174	147	147	121	140	183	189

3.4.2 Identification of homonyms genotypes

There were 13 samples that had the same cultivar names but did not have matching genotypes (Table 7 & Fig. 5). This suggests that most of them (Chemlali-M, Chemlalisfax-T, Chemlalisfax-G, Coratina-T, Coratina-G, Jabbugi-T, Jabbugi-M, Mbuti-T, Mbuti-M, Mignolo-T, Mignolo-G, Moraiolo-T, Moraiolo-G, Rasli-T, Rasli-M, Zaafrani-T, Zaafrani-M, Zarrasi-M and Zarrasi-T) considered to be homonyms and were given the same names by human error, some of the labeled cultivars were misidentified because they matched other cultivars (Gargashi-T match Chemlali –Za, 53% bootstrap). Whereas other four cultivars (Hammudi-M, Hammudi-T and Marrari-M, Marrari-T) considered being close clones and were different from each other by 3 and 2 different alleles respectively. Comparisons of morphology images of each duplicate pair of genotypes showed distinct differences and supported the genetic results of polymorphism (Fig. 6). The problems associated with cultivar identification likely in landrace types than in introduced cultivars or wild type olives.

Table 7

Duplicated cultivars were considered to be mislabeled or homonyms genotypes

Variety name	Local location	Relationship
Chemlali	Masallatah	Homonyms
Chemlali	Zaltin	Homonyms
Chemlalisfax	Gharian	Homonyms
Chemlalisfax	Tharouna	Homonyms
Coratina	Gharian	Homonyms
Coratina	Tharouna	Homonyms
Gargashi	Masallatah	Homonyms
Gargashi	Tharouna	Homonyms
Hammudi	Masallatah	Homonyms
Hammudi	Tharouna	Homonyms
Jabbugi	Masallatah	Homonyms
Jabbugi	Tharouna	Homonyms
Marrari	Masallatah	Homonyms
Marrari	Tharouna	Homonyms

Variety name	Local location	Relationship
Mbuti	Masallatah	Homonyms
Mbuti	Tharouna	Homonyms
Mignolo	Gharian	Homonyms
Mignolo	Tharouna	Homonyms
Moraiolo	Gharian	Homonyms
Moraiolo	Tharouna	Homonyms
Rasli	Masallatah	Homonyms
Rasli	Tharouna	Homonyms
Zaafrani	Masallatah	Homonyms
Zaafrani	Tharouna	Homonyms
Zarrasi	Masallatah	Homonyms
Zarrasi	Tharouna	Homonyms

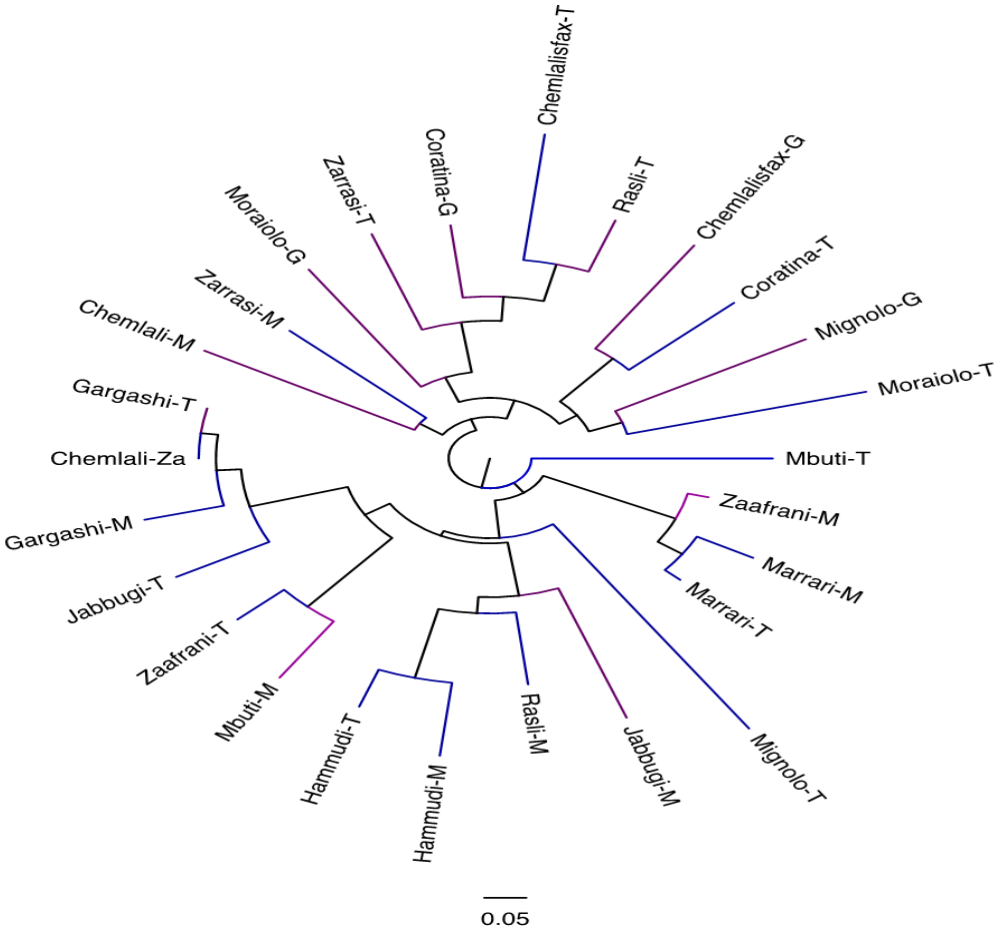

Fig. 5. Neighbor-joining tree of 13 duplicated pairs of olive genotypes; each tip represents a single individual accession with all pairs of duplicated genotypes different.

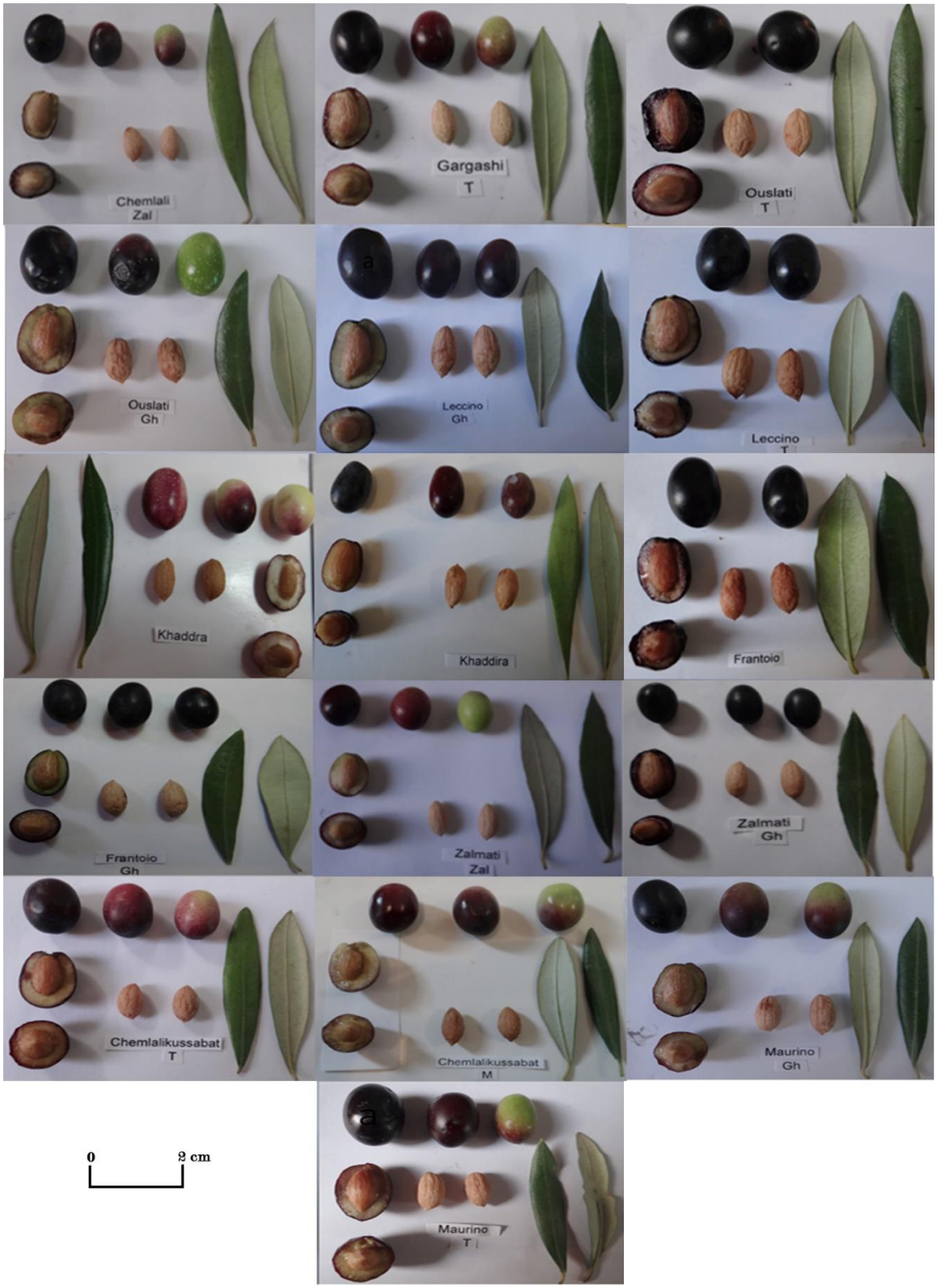

Fig. 6. Accessions identified by the same name (Homonyms accessions).

An UPGMA neighbor-joining tree (Fig. 7) was constructed to study the genetic relationships among the 91 different olive genotypes that were discriminated by the 10 SSR markers. Two primary clusters of individuals were identified (green color = landraces) and (intermixed color, red = introduced cultivars and blue = wild types). Most of the wild types were found within the intermixed wild and introduced genotypes (Fig. 7).

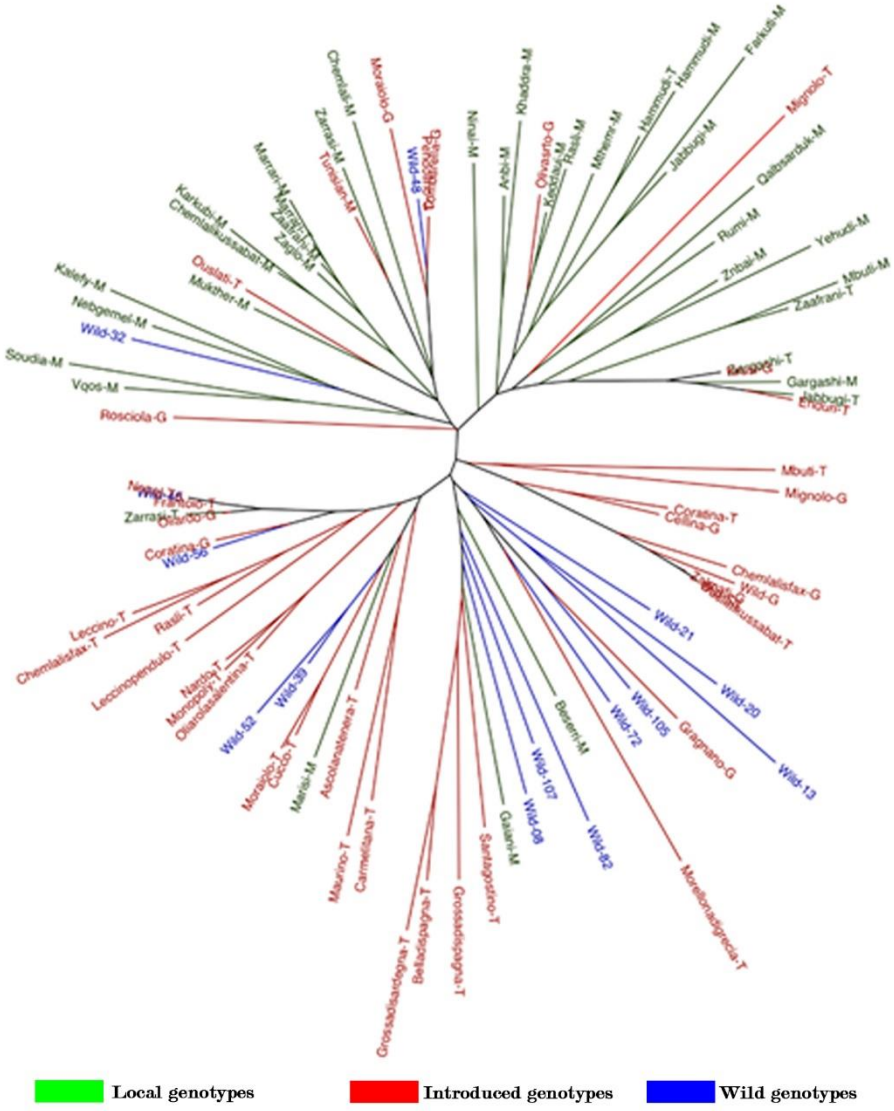

Fig. 7. Neighbor-joining tree of 91 individuals, each tip represents a single olive genotype and the colors of clades indicate the populations of origin (Local, introduced and wild).

3.5 Estimation of partition by assignment

Structure analysis using the admixture model without prior information was used to identify the genetic relationships of Libyan landraces, wild, and introduced cultivars. It was also used to differentiate individuals within each population. The most likely number of clusters inferred by structure software were at K=3. The local genotypes clustered together and two distinct sub-groups were identified. The first group consisted of the 20 most popular local genotypes (blue color) that are used mainly to produce olive oil. The second group consisted of 11 hybrid genotypes (blue and red color) between local and introduced cultivars (Fig. 8). These accessions are not widely grown and are not preferred for oil production. Those cultivars that were primarily local cultivars genetically were ancient ones grown in the Masallatah region where they are widely grown for their valuable oil characteristics. This group includes the main two cultivars Rasli and Gargashi that are used mainly for their oil production under extremely dry climates. There were six genotypes (ZarrasiM, ChemlaliM, MoraioloG, Ac#48, PendolinoG and TombarellaG) that were considered to be local genotypes in neighbor-joining tree cluster (Fig. 7) but based on the structure analysis were included in the introduced genotype grouping. This is perhaps best explained by saying that they are really introduced genotypes especially given the derivation of the names of 4 of them is not Arabic but Italian. In the case of ZarrasiM relative fruit size is similar to the introduced genotypes that have larger fruit size as compared to the smaller fruit of the local types. The wild and introduced accessions remained unchanged and were clustered the same as the UPGMA of the neighbor-joining tree (Fig. 7). They had an intermixed genetic background (red color) as shown in (Fig. 8). There were 13 genotypes that had a lot of admixture and mixed genetic background of all populations (Fig. 8). Most of these genotypes (Beserri-M, Oliarolasalentina-T, Santagostin-T, Mignolo-T, Gragnano-G, Ouslati-T, Nebgemel-M and Kalefy-M) were previously reported to be clustered as individual genotypes with Fig Tree cluster too (Fig. 7), also they have proportions of their membership in three different gene pools. Finally, the results from population structure analyses clearly distinguished the known ancient local cultivars, introduced cultivars and wild types into specific clusters associated with their origin (local, introduced and wild), but not always due to their use (oil, table and dual purpose) as reported in previous studies (Besnard *et al*., 2001; Belaj *et al*., 2010).

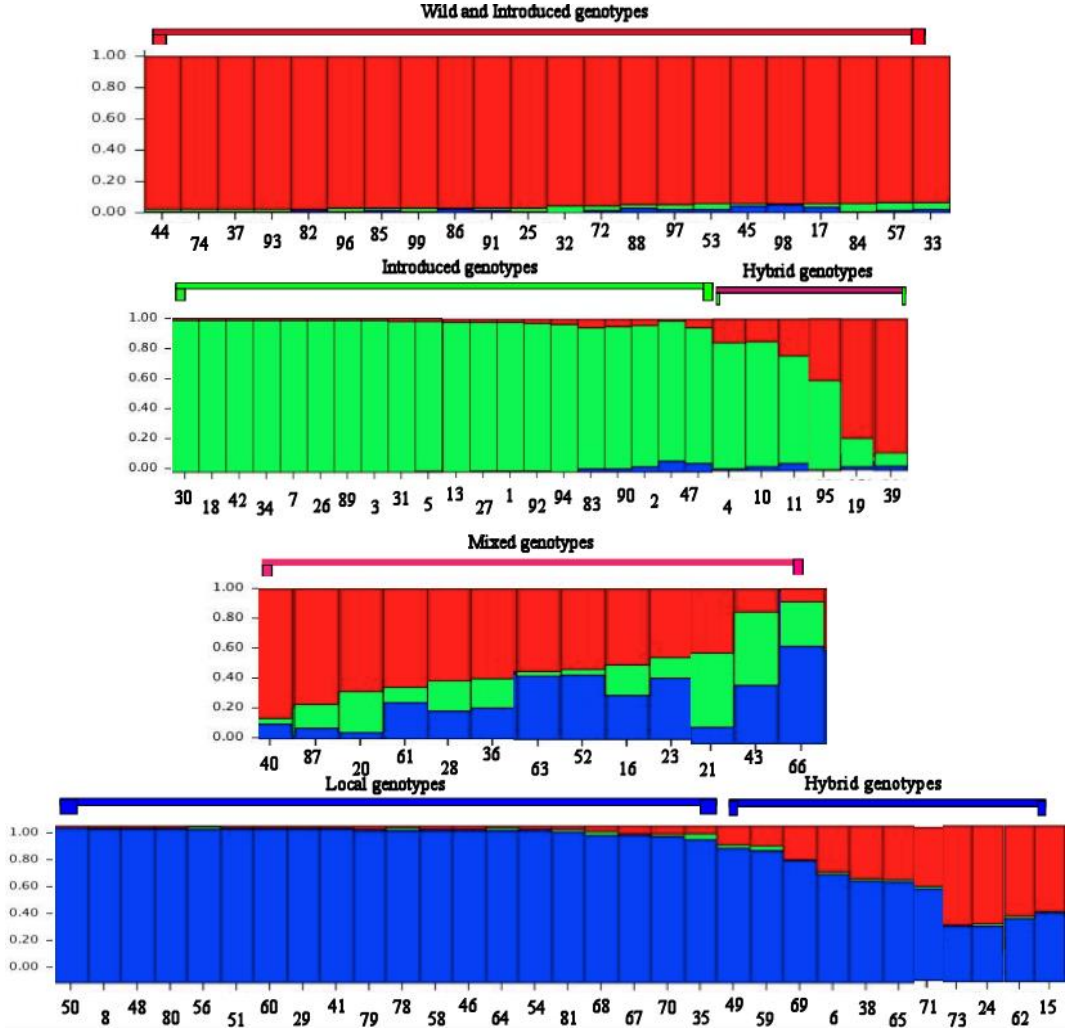

Fig. 8. Separation of the structure analysis into specific groups; intermixed group between introduce and wild genotypes (red color), Introduced genotypes (green color) and hybrid genotypes (mixed color) and local genotypes (blue color). Every single vertical strain is represented by an individual genotype.

3.6 Genotype-phenotype comparison

We sought to determine if independent stable phenotypic traits could be used to predicate the genetic classification of olive genotypes to verify if there is a strong correlation between the phenotypic and genotypic traits. Highly significant differentiation (P<0.0001***) (Fig. 9 A and Fig. 9 B) of stable phenotypic traits were observed when using the average q values of structure membership coefficient (1=local, 2=mixed and 3=introduced) or structurama partition assignment (1=mixed, 2=Introduced and 3=Landraces) respectively as a categorical data for all 90 genotypes based on the cultivar origin (introduced or local).

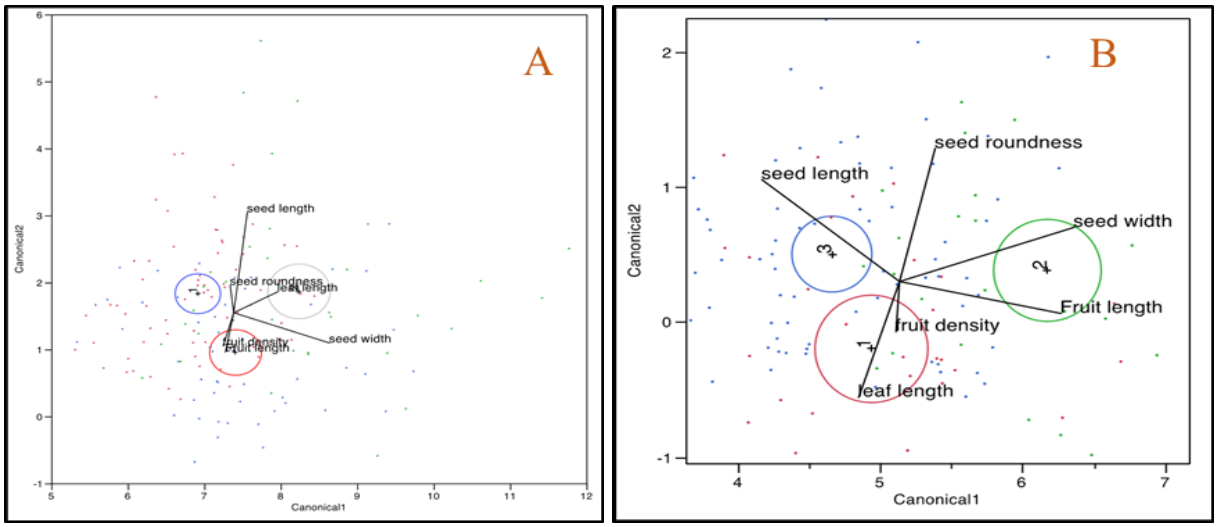

Fig. 9 Discriminant analysis was used to differentiate among all 90 genotypes based on membership q values of structure (p<0.0001***) A, and structurama assignment (p<0.0001***) B.

4. Discussion

The SSR markers (Table 1) used in this study were selected based on previously published reports (Baldoni *et al*., 2009; Erre *et al*., 2010; Dı´ez *et al*., 2011 and Ipek *et al*., 2012). The identification of duplicated, mislabeled or homonymes genotypes (Table 2, 6 and 7) respectively, found within the Libyan olive collection illustrates one of the most important problems associated with olive production in Libya. This misidentification may growers planting genotypes that are not those of yield potential in their specific area. A source of this misidentification may be due to phenotypic variation (Fig. 3) associated with environmental conditions when grown in diverse locations, to the description of the same genotype with different names. Rao *et al*. (2009) showed that synonyms and homonyms occur more frequently among landraces than in common cultivars. However, phenotypic data (fruit, seed and leaf) may be important in distinguishing different genotypes when molecular data indicates no differences due to missing or limited data. This is especially true when stable phenotype characteristics indicate differences between genotypes. Seven cultivars (Table 6) were determined to be identical based on the data from eight loci. However, this data was insufficient to discriminate all seven cultivars due to missing data of two additional loci. The combination of phenotypic traits (Fig. 4) clearly indicated that these cultivars were different.

The genetic descriptive analysis identified the most informative with a total of 20 alleles as similarly reported by D´ıez *et al.* (2011). In general, loci that have many different alleles were preferred to distinguish between two different individuals. (*http://www.mathcs.citadel.edu*). The lowest probability of identity (PI) (0.1) was observed for locus UDO43 that was the most informative locus the highest discrimination power (0.90). The highest probability of identity (0.85) observed was for locus DCA5 that had the lowest power of discrimination (PD) (0.15) with (Table 3).

Overall, loci probability were generally low (0.30), particularly at loci that have a high allelic number as noted also in previous results (Roubos *et al*., 2010). Overall, the values observed for the expected and observed heterozygosity, for all three sets of individuals (0.68 and 0.49), respectively, were somewhat higher than reported by the authors using similar sets of SSR markers (Erre *et al*., 2010; Belaj *et al*., 2010; Muzzalupo *et al*., 2010; Baldoni *et al*., 2009; Zaher *et al*., 2011 and Erre *et al*., 2010). Reason for the number of alleles observed in the study could be due to the use of a large number of exotic genotypes.

Wild types have a higher inbreeding coefficient (0.36) than the two cultivated populations, introduced (0.23) and local (0.24). This may be the result of continued breeding of closely related individuals since the area in which the wild genotypes grow is far away from cultivated genotypes. In addition, it has the highest number of private alleles and the highest level of genetic diversity found in this area in spite of the low number of wild types. This may be useful information for the preservation traits of the wild type in the same genetic pool. The result is that the wild type may then be a source of some genes for potential improvement of local cultivars. Genetic diversity studies of the local ancient olive cultivars (Banilas *et al*., 2003 and Baldoni *et al*., 2006) have revealed that only a few of these landraces matched current olive cultivars grown today. These studies comparable to our results, which clearly indicate large differences observed in the Libyan collection.

Distinct groups of local landraces differed from introduced and wild genotypes as indicated in both the neighbor-joining tree (Fig. 7) and the admixture analysis (Fig. 8). This was also noted by (Zaher *et al*., 2011) distinct clustering of the landraces from the same region a unique genetic background and did not have matching genotypes form the other two sets of individuals. In contrast, early (Hannachi *et al*., 2010) that 'Roumi' could be a progeny of 'Chemlali', but our results from the dendrogram the major proportion of ancient Libyan local landraces did not match any other introduced or wild olive genotypes. The local Libyan cultivars may represent early stages of olive cultivation (D´ıez *et al*., 2011 and Belaj *et al*., 2010) that remain as unexploited genetic diversity and therefore important germplasm resources Among the three sets of individuals (local, introduced and wild) that were assumed to be different not as different as expected. Neighbor-joining tree (Fig. 7) and STRUCTURE analysis (Fig. 8) demonstrated a strong between wild and introduced genotypes. The wild types were genetically more closely related to the introduced. This was unexpected since one would most commonly assume that the local cultivars were descended from the native wild types. However, samples of wild-32 and wild -48 were an exception they were phenotypically and genetically related to the landraces than the wild type. This may be due to errors of the propagation process. Therefore, the idea of Libyan ancient local cultivars maybe descendants from the wild types not supported by either neighbor-joining tree or the structural analyses. This is likely due to the result of gene flow based on geographical proximity over the years. Our results are comparable with previous studies (Hannachi *et al*., 2008 and Hannachi *et al*., 2010) that showed there are close genetic relationships between oleaster types and cultivated genotypes using SSR data with NJ method. Although some oleaster types were intermixed within cultivated genotypes, others only clustered from wild types alone.

Most of the wild type accessions were collected from the Eastern side of Libya (Fig. 1), which is closer to Europe from which introduced genotypes came to Libya in 1954 during the years of colonization by Italy. D´ıez (2011) noted the exchange genetic material between North Africa and Europe took place during the Arab expansion through Andalusia between the eighth and fourteenth centuries. This offers the archaeological evidence to support the gene flow of olives with human migration. Wild olive genotypes are currently thought to have a common gene pool in the entire Mediterranean Basin (Kole, 2011). This may be why the wild Libyan accessions are closely related to the introduced lines from Europe. Several morphological traits can differentiate between wild and cultivated olive (Hannachi *et al*., 2008). Phenotypic traits not as informative as molecular data and limited in discriminatory power to evaluate the relatedness and the level of genetic similarity (Corrado *et al*., 2009 and Hannachi *et al*., 2008). In addition, Rao *et al.* (2009) reported that biometry values alone were unable to differentiate between similar genotypes that were evaluated by morphological traits.

It seems, there is a strong correlation of comparison between the genotype and phenotype data (Fig. 9 A and Fig. 9 B) that were based on independent phenotypic stable traits and blocked by structure membership coefficient (1=local, 2=mixed and 3=introduced) or structurama partition assignment (1=mixed, 2=introduced and 3=local) (Fig. 9 A and Fig. 9 B) respectively. The results showed that stable phenotypic data could be used the same as genetic data to assign each individual to a specific group of cultivars based on their origin (local, introduced or wild). The resemblance between molecular and morphological relationships within olive varieties expected when there is a little effect of genetic and environment interaction observed. Our results are relevant to the most recent olive. Recently, both morphological and molecular aspects have been combined to clarify the identity of genotypes within other crops (Corrado *et al*., 2009; Hannachi *et al*., 2010; D´ıez *et al*., 2011 and Belaj *et al*., 2012).

5. Conclusion

The study of local ancient cultivars and wild types of the Libyan collection is increasingly important in order to conserve those genotypes as a potential genetic resource; they may have valuable genes that could provide a novel and useful phenotypic traits for advanced plant breeding. This study provides useful information a general molecular database of Libyan olive cultivars. There is a high heterozygosity within the Libyan collection studied, which identified all genotypes with limited similarity. The current set of 10 SSR loci amplified the corresponding microsatellite fragments in all 91 genotypes; also, it can be used to genotype the Libyan olive collection and to assign each individual into a genetic relatedness group. In this study, molecular data led to the clear identification

of 91 distinct genotypes (39 local, 36 introduced and 16 wild) out of the 99 accessions included in this study, also it revealed the existence of a high level of genetic variability among Libyan collection. It is interesting that changes of the denominations are more frequently within landraces than other cultivated and wild types. Identification of additional new candidate loci with the use of a reference sample could lead to a more robust molecular database, which could be used to characterize the Libya olive collection. This may then be used to optimize the management strategy of the Libyan olive germplasm. The combination based on morphological traits and molecular data were highly useful to separate closely related genotypes and facilitate genetic differentiation among olive genotypes.

Reference

Baldoni, L., Cultrera, N.G., Mariotti, R., Ricciolini, C., Arcioni, S., Vendramin, G.G., Buonamici, A., Porceddu, A., Sarri, V., Ojeda, M.A., Trujillo, I., Rallo, I., Belaj, A., Perri, E., Salimonti, A., Muzzalupo,I., Casagrande,A., Lain,O., Messina,R., and Testolin, R. (2009) 'A consensus list of microsatellite markers for olive genotyping ', *Mol Breeding*, 24, pp.213–231.

Baldoni, L., Tosti, N., Ricciolini, C., Belaj, A., Arcioni, S., Pannell, G., Germana, M. A., Mulas, M., and Porceddu, A. (2006) 'Genetic structure of wild and cultivated olives in the central Mediterranean Basin ', *Annals of Botany*, 98, pp.935–942.

Banilas, G., Minas, J., Gregoriou, C., Demoliou, C., Kourti, A., and Hatzopoulos, P. (2003) 'Genetic diversity among accessions of an ancient olive variety of Cyprus ', *Genome* 46, pp.370–376.

Belaj, A., del Carmen Dominguez-García, M., Atienza, S. G., Urdíroz, N. M., De la Rosa, R., Satovic, Z., and Del Río, C. (2012) 'Developing a core collection of olive (*Olea europaea* L.) based on molecular markers (DArTs, SSRs, and SNPs) and agronomic traits ', *Tree Genetics & Genomes*, 8(2), pp.365-378.

Belaj, A., Munoz-Diez, C., Baldoni, L., Satovic, Z., and Barranco, D. (2010). 'Genetic diversity and relationships of wild and cultivated olives at regional level in Spain ', *Scientia Horti culturae*, 124, pp.323–330.

Belaj, A., Satovic, Z., Cipriani, G., Baldoni, L., Testolin, R., Rallo, L., and Trujillo, I. (2003) 'Comparative study of the discriminating capacity of RAPD, AFLP and SSR markers and of their effectiveness in establishing genetic relationships in olive ', *TheorAppl Genet*. 107, pp.736–744.

Besnard, G., Baradat, P., and Berville. A. (2001) 'Genetic relationships in the olive (*Olea europaea* L.) reflect multifocal selection of cultivars ', *Theor. Appl. Genet.* , 102, pp.251–258.

Brownstein, M. J., Carpten, J. D., and Smith, J. R. (1996) 'Modulation of non-templated nucleotide addition by Taq DNA polymerase: primer modifications that facilitate genotyping ', *Biotechniques*, 20(6), pp.1004 -6, 1008-10.

Carriero, F., Fontanazza, G., Cellini, F., and Giori, G. (2002) 'Identification of simple sequence repeats (SSRs) in olive (*Olea europaea* L) ', *Theor Appl Genet*, 104, pp.301–307.

Cipriani, G., Marrazzo, M.T., Marconi, R., Cimato, A., and Testolin, R. (2002) 'Microsatellite markers isolated in olive (*Olea europaea* L.) are suitable for individual fingerprinting and reveal polymorphism within ancient cultivars ', *Theor. Appl. Genet*. 104, pp.223–228.

Corrado, G., La Mura, M., Ambrosino, O., Pugliano, G., Varricchio, P., and Rao, R. (2009) 'Relationships of companion olive cultivars: comparative analysis of molecular and phenotypic data ', *Genome*, 52, pp.692–700.

De La Rosa, R., James, C. M., and Tobutt, K. R. (2002) 'Isolation and characterization of polymorphic microsatellites in olive (*Olea europaea* L.) and their transferability to other genera in the Oleaceae ', *Molecular Ecology Notes*, 2, pp .265–267.

D íez, C. M., Trujillo, I., Barrio, E., Belaj, A., Barranco, D., and Rallo, L. (2011) 'Centennial olive trees as a reservoir of genetic diversity. *Annals of Botany*, 108(5), pp.797-807.

Earl, D. A. (2012) 'STRUCTURE HARVESTER: a website and program for visualizing STRUCTURE output and implementing the Evanno method ', *Conservation Genetics Resources*, 4(2), pp.359-361.

Ercisli, S., Bencic, D., Ipek, A., Barut, E., and Liber, Z. (2012) 'Genetic relationships among olive (*Olea europaea* L.) cultivars native to Croatia and Turkey ', *Journal of Applied Botany and Food Quality*, 85(2), pp.144-149.

Ercisli, S., Ipek, A., and Barut, E. (2011) 'SSR marker-based DNA fingerprinting and cultivar identification of olives (*Olea europaea* L.) ', *Biochem Genet*. 49(9-10):555-61.

Erre, P., Chessa, I., Muñoz-Diez, C., Belaj, A., Rallo, L., and Trujillo, I. (2010) 'Genetic diversity and relationships between wild and cultivated olives (*Olea europaea* L.) in Sardinia as assessed by SSR markers ', *Genetic Resources and Crop Evolution*, 57(1), pp.41-54.

Glaubitz, J. C. (2004) 'Convert: A user-friendly program to reformat diploid genotypic data for commonly used population genetic software packages ', *Molecular Ecology Notes*, 4(2), pp.309-310.

Goudet, J. (2002) 'Fstat Vision (1.2): A Computer Program to Calculate F-Statistics ', *Journal of Heredity*, 86, 485-486.

Guichoux, E., Lagache, L., Wagner, S., Chaumeil, P., Léger, P., Lepais, O., and Petit, R. J. (2011) 'Current trends in microsatellite genotyping ', *Molecular ecology resources*, 11(4), pp.591-611.

Hannachi, H., Breton, C., Msallem, M., Ben El Hadj, S., El Gazzah,M., and Berville, A. (2010) 'Genetic relationships between cultivated and wild olive trees (*Olea europaea* L. var. *europaea* and var. *sylvestris*) based on nuclear and chloroplast SSR markers', *Natural Resources*, 1, pp. 95-103.

Hannachi, H., Breton, C., Msallem, M., Ben El Hadj, S., El Gazzah, M., and Berville, A. (2008) 'Differences between native and introduced olive cultivars as revealed by morphology of drupes, oil composition and SSR polymorphisms: A case study in Tunisia', *Scientia Horti culturae*, 116(3), pp.280–290.

http://*www.mathcs.citadel.edu/trautmand/stuff/dnapapers/little.htm*

Ipek, A., Barut, E., Gulen, H., and Ipek, M. (2012) 'Assessment of inter-and intra-cultivar variations in olive using SSR markers', *Scientia Agricola*, 69(5), pp.327-335.

Jakobsson, M., and Rosenberg, N. A. (2007) 'CLUMPP: a cluster matching and permutation program for dealing with label switching and multimodality in analysis of population structure', *Bioinformatics*, 23, pp.1801–1806.

Kole, C. (2011) 'Wild crop relatives: Genomic and breeding resources: Temperate fruits. Springer Heidelberg Dordrecht London, New York', *Vegetables*, pp.217-246.

Leon, L., Garrido, V. A., and Downey, G. (2005) 'Near infrared spectroscopy (NIRS) as a promising selection tool in olive breeding programs. *FRUTIC*, 05, pp.12-16.

Mace, E. S., Hutokshi K. Buhariwalla, H., and Crouch, J. H. (2003) 'A high-throughput DNA extraction protocol for tropical molecular breeding programs', *Plant Molecular Biology Reporter*, 21, pp.459a–459h.

Mariotti, R.; Cultrera, N. G. M.; Munoz-Diez, C.; Baldoni, L. and Rubini, A. (2010). 'Identification of new polymorphic regions and differentiation of cultivated olives (*Olea europaea* L.) through platome sequence comparison', *BMC Plant Biol*, 10, pp. 211.

Muzzalupo, I., Chiappetta, A., Benincasa, C., and Perri, E. (2010) 'Intra-cultivar variability of three major olive cultivars grown in different areas of central-southern Italy and studied using microsatellite markers', *Scientia Horticulturae*, 126(3), pp.324-329.

Pritchard, J. K., Wen, W., and Falush, D. (2003) 'Documentation for STRUCTURE software: version 2', http://*pritch.bsd.uchicago.edu*

Raman, R., Cowley, R. B., Raman, H., and Luckett, D. J. (2014) 'Analyses Using SSR and DArT Molecular Markers Reveal that Ethiopian Accessions of White Lupin (*Lupinus albus* L.) Represent a Unique Genepool', *Open Journal of Genetics*, 4, pp.87-98.

Rambaut, A. (2012) 'FigTree version 1.4. 0. Computer program distributed by the author', http://*tree. bio. ed. ac. uk/software/figtree*.

Rao, R., La Mura, M., Corrado, G., Ambrosino, O., Foroni, I., Perri, E., and Pugliano, G. (2009) 'Molecular diversity and genetic relationships of southern Italian olive cultivars as depicted by AFLP and morphological traits', *J. Hortic. Sci. Biotechnol*, 84(3), pp.261-266.

Roubos, K., Moustakas, M., and Aravanopoulos, F. A. (2010) 'Molecular identification of Greek olive (*Olea europaea*) cultivars based on microsatellite loci', *Genet. Mol. Res*, 9, pp.1865-1876.

Sarri, V., Baldoni, L., Porceddu, A., Cultrera, N.G.M., Contento, A., Frediani, M., Belaj, A., Trujillo, I., and Cionini, P.G. (2006) 'Microsatellite markers are powerful tools for discriminating among olive cultivars and assigning them to geographically defined populations', *Genome*, 49, pp.1606-1615.

Sefc, K. M., Lopes, S., Mendonca, D., Dos Santos, M. R., Machado, M. L. D., and Machado, A. D. (2000) Identification of microsatellite loci in olive (*Olea europaea*) and their characterizationin Italian and Iberian olive trees', *Mol. Ecol*. 9, pp.1171–1173.

Viljoen, G. J., Nel, L. H., and Crowther, J. R. (2005) 'Molecular diagnostic PCR handbook Dordrecht', *Springer*, pp. 13-14.

Zaher, H., Boulouha, B., Baaziz, M., Sikaoui, L., Gaboun, F., and Udupa, S. M. (2011) 'Morphological and genetic diversity in olive (*Olea europaea* subsp. *europaea* L.) clones and varieties', *Plant Omics Journal*, 4(7), pp.370-376.

Libyan Journal of Science & Technology 9:2 (2019) 142–145

Faculty of Science - University of Benghazi

Libyan Journal of Science & Technology

journal home page: www.sc.uob.edu.ly/pages/page/77

Study Influence of adding Surfactant to polymers in Reduce Friction in Pipelines

Emsalem F. Hawege*, Almaki A. Abushina

Department of Chemical Engineering, University of Elmergib, Al-Khoms Libya

Highlights

- **Polymers used as drag reduction agent but are not economical.**
- **The efficiency of surfactant is very low.**
- **The use complexes of polymer and surfactant decrease friction in pipeline.**
- **Rotating Disk Apparatus to check degradation of additives.**

ARTICLE INFO

Article history:
Received 16 January 2019
Revised 11 May 2019
Accepted 18 May 2019
Available online 17 June 2019

Keywords:
Poly (acrylamide-co-diallyl-dimethylammonium chloride); Tween 20; Drag reduction; Reynolds number; RDA.

* Corresponding author:
E-mail address: emsalemfrg@yahoo.com
E. F. Hawege

ABSTRACT

When polymers (DRA) passes through high shear force areas like pumps and elbows that causes from turbulent flow will lose their drag reduction abilities. In this research, the effect of adding a nonionic surfactant (tween 20) to the cationic polymer (Poly (acrylamide-co-diallyl-dimethylammonium chloride)) in reducing friction in the pipeline has been examined by using rotating disk apparatus to verify its ability in decrease the friction in pipelines. The influence of adding polymer, surfactant and Reynold number in enhancing flow in pipelines were examined. The results appeared that 40% drag reduction could be obtained by using this complex.

1. Introduction.

In the oil and gas industry, transporting liquids (particularly crude oils) through pipelines is one of the applications that consume the most power because of the turbulent flow modes by which liquids are transported. Turbulent flow modes can cause a massive dissipation of pumping power as a result of the reverse and chaotic movements of the structures inside the pipes (eddies), which grow and massively multiply through the pipe length. Drag forces can occur between moving fluids and stagnant pipe walls or even between two fluid layers. They are proportional to the velocity of laminar flows and to the squared velocity of turbulent flows (Benzi, 2010).

Over the last few decades, many scientists have suggested various techniques to reduce drag (i.e., drag reduction methods) and therefore improve liquid flow through pipelines. These methods can be classified into either passive or active, depending on their implementation. Passive methods take their inspiration from nature and simulate sharkskin microstructures, creating what are called "Riblets" (El-Samni *et al*., 2007). Different passive techniques have been invented and implemented, including dimples, oscillating walls, compliant surfaces, and even microbubble injection in pipelines. However, these techniques have failed to efficiently reduce the drag and have high implementation cost (Du *et al*., 2002).

Polymeric additives are proven to have a massive impact on the behavior of turbulent flow in pipelines because of their unique viscoelastic properties that suppress turbulent eddies. In many cases, polymeric DRA loses its drag reduction abilities when exposed to high shear forces exerted by the turbulent flow caused by pumps. This action is irreversible, thereby requiring the re-injection of fresh polymers (Abdulbari *et al*., 2012).

Surface active agents have since been tested as DRAs by many scientists. Used as DRA, these additives have no real commercial or industrial application because of their low drag reduction efficiency and high concentrations. On the other hand, the advantage of using surfactant molecules as DRA is their ability to reform their shape, pass through high shearing areas, and capacity to regain their drag reduction ability, which is nevertheless relatively lower than that of polymeric DRA (Alramadhni *et al*., 2013).

The adding surfactants to the polymers can improve the performance of the polymers because this complex will form micelles and these micelles will rearrange their form after they passing pumps (Xiaodong Dai *et al*., 2017).The objective of this study is to investigate the interaction between polymer and surfactant. The polymer selected was Poly (acrylamide-co-diallyl-dimethylammonium chloride) (PAMC), and non-aionic (Tween 20) were selected as surfactant. The drag reduction of mixture was calculated and compared to the drag reduction achieved by pure polymer and surfactant. The effect of additive concentration and reynolds number on the friction in pipeline also have been examined in this research.

2. Materials and methods.

2.1 Materials.

In general, two types of materials were investigated in the present work, polymer, and surfactant with different polarities cationic and non-ionic. The cationic Polymer **(PAMC)** 10 wt. % in H_2O and non-ionic surfactant Tween 20 used without further purification.

 ISSN 2663-1407; National Library of Libya, Legal number: 390/2018

2.2. Method.

2.2.1 Preparation of Solutions,

All the purchased additives are water soluble and the tested solutions from these additives are created by adopting the following steps:

1. The concentration of the additives was determined in weight parts per million (ppm) by adopting the weight/weight basis.
2. The stock solution was prepared by dissolving the desired weight of the additives into distilled water and by stirring using a magnetic stirrer for 4 h.
3. The final solution for RDA testing was left for 24 h. to allow for maximum additive penetration.

2.2.2 Rotating disk apparatus.

The RDA in the present work was designed and fabricated for the purpose of testing drag reduction and mechanical stability of the investigated liquids by applying shearing force and measuring the torque. Fig. 1 shows a photo of the fabricated RDA. The Reynolds number in the RDA was calculated using the formula presented in Eq. (1).

$$Re = \frac{\rho \times R^2 \times \omega}{\mu} \quad (1)$$

Where

Re= Reynolds number (dimensionless)

ρ= density of the fluid, 1000 (kg/m^3)

R = radius of the disk, (14 cm)

ω = rotational speed of the disk, (rpm)

μ= viscosity of the fluid = 0.001 n. s /m^2(c.p)

Because the amount of additives (polymer, surfactant or mixture) are very little, the properties of fluid (density and viscosity) were taken for pure water.

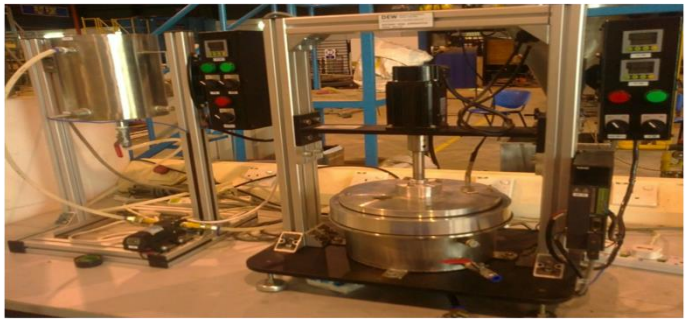

Fig. 1. Rotating Disk Apparatus rig.

3. Result and discussion.

Fig. 2. displays influence concentration of PAMC on the drag reduction at different Reynolds number. The drag reduction of 50 ppm PAMC has achieved 10% at Re = 980000. By increasing concentration of PAMC to 700 and 1000 ppm the drag reduction enhanced to 27% and 34% respectively at the same value of Re. As a result, the torque of polymer additive reduces clearly, when the concentration of additive increase and this is more obviously at higher Reynolds number values. Fig. 3. displays influence concentration of surfactant on the drag reduction at different Reynolds number values. The drag reduction efficiency of surfactant solution not enhanced by rising surfactant concentration from 50 to 1000 ppm at different Reynolds number values.

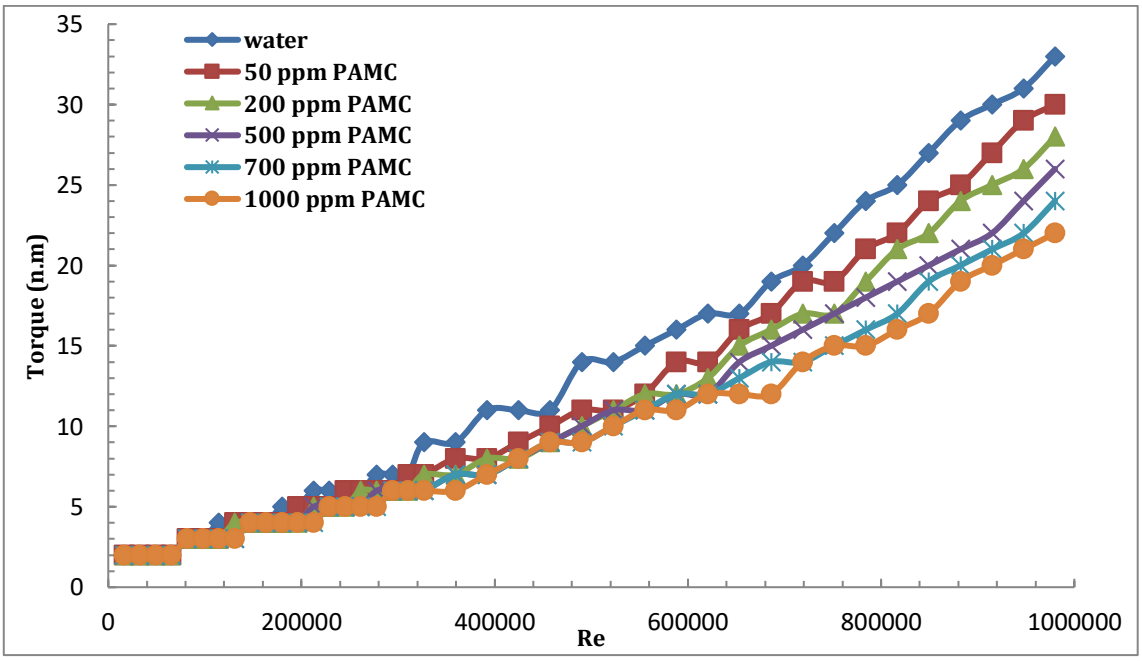

Fig. 2. Influence increment concentration of polymer on the torque as a function of Reynold number.

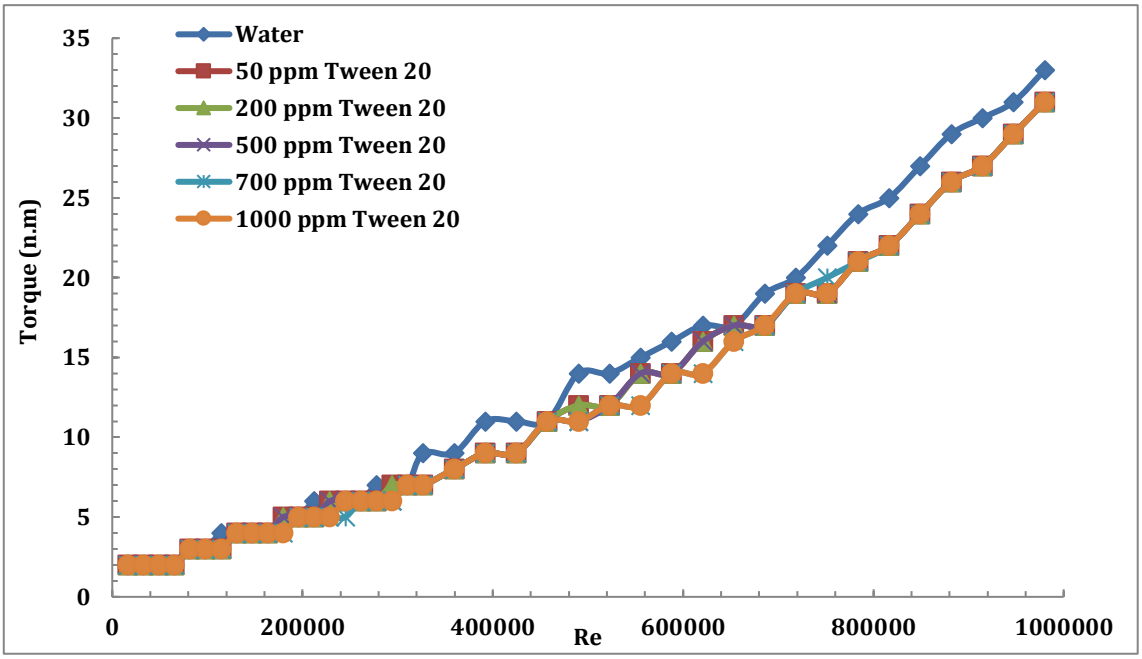

Fig. 3. Influence surfactant concentration on the drag reduction at different Reynolds number values

The influence of adding the surfactant to the polymer on drag reduction at different Reynolds number values shown in Fig. 4. It is clear that the drag reduction efficiency enhanced by using polymer surfactant mixture. The drag reduction efficiency of PAMC-Tween 20 mixture at Re = 980000 and 500 ppm was 24% while the percentage drag reduction of PAMC was 20% at the same conditions. This enhancing in drag reduction was a result of interaction between the polymer and surfactant. By using a TEM test we can see the picture of the interaction between these materials clearly.

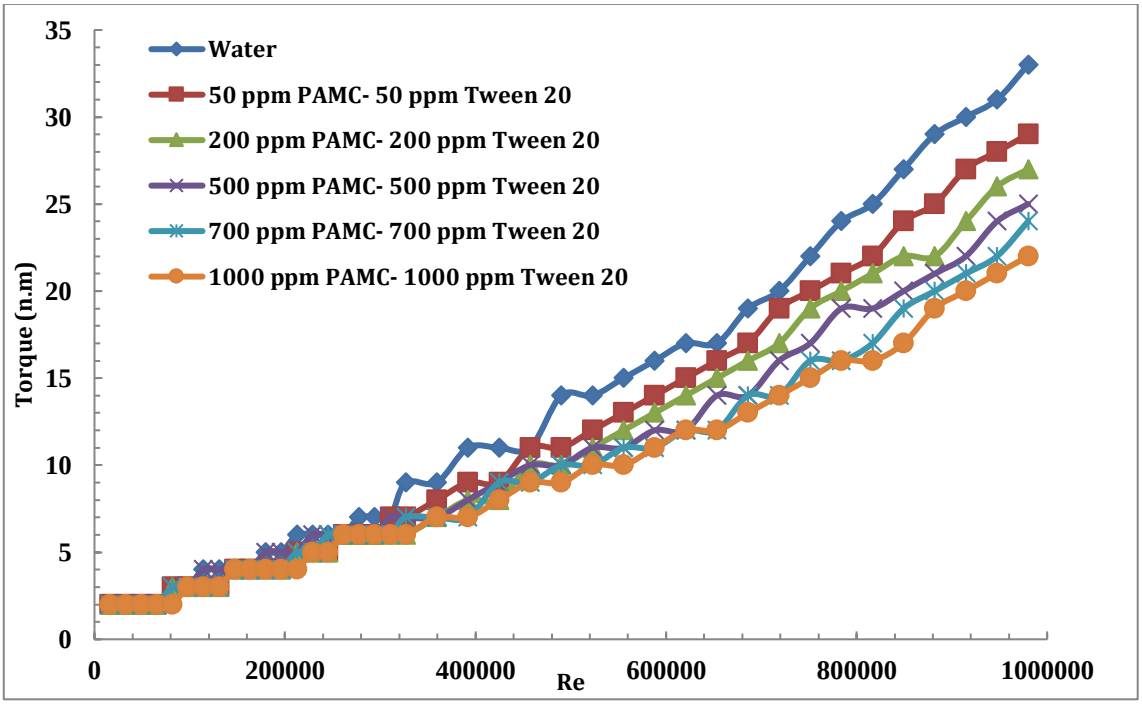

Fig. 4. Displays effect adding a surfactant to the polymer on the drag reduction.

4. Conclusion.

In conclusion, the influence of polymer concentration, surfactant concentration, Reynold number and mixture of polymer-surfactant on the drag reduction efficiency have been studied. The drag reduction efficiency resulting by mixture 1000 ppm PAMC–Tween 20 was 40%. In other words, the interaction between polymer-surfactant solution plays a vital role in enhancing the flow in pipes and declining the friction between the fluid and surface of the pipe.

References

Abdulbari, H., Kamarulizam, N. and Nour, A. (2012) 'Grafted natural polymer as new drag reducing agent: An experimental approach', *Chemical Industry and Chemical Engineering Quarterly,* 18, 3, pp. 361-371.

Alramadhni, S., Saleh, N. and Rassol, G. (2013) 'Experimental Study of Drag Reduction Phenomena within Pipe-Flow in a Closed Circuit System Using Surfactant Additives', *Eng. &Tech.Journal,* 3, pp. 11-13.

Al-Sarkhi, A. (2012) 'Effect of mixing on frictional loss reduction by drag reducing polymer in annular horizontal two-phase flows', *International Journal of Multiphase Flow,* 39, pp. 186-192.

Benzi, R. (2010) 'A short review on drag reduction by polymers in wall bounded turbulence', *Physica D,* 239, 14, pp. 1338-1345.

Du, Y., Symeonidis, V. and Karniadakis, G. (2002) 'Drag reduction in wall-bounded turbulence via a transverse travelling wave', *Journal of Fluid Mechanics,* 45, 7 ,pp. 1-34.

El-Samni, O., Chun, H. and Yoon, H. (2007) 'Drag reduction of turbulent flow over thin rectangular riblets', *International Journal of Engineering Science,* 45, 2, pp. 436-454.

Kim, J., Kim, C., Zhang, K., Jang, C. and Choi, H. (2011) 'Effect of polymer–surfactant interaction on its turbulent drag reduction', *Colloids and Surfaces A: Physicochemical and Engineering Aspects,* 391, 1–3, pp. 125-129.

Malcher, T. and Gzyl-Malcher, B. (2012) 'Influence of polymer–surfactant aggregates on fluid flow', *Bioelectrochemistry,* 87, pp. 42-49.

Moaven, K., Rad, M. and Taeibi-Rahni, M. (2013) 'Experimental investigation of viscous drag reduction of superhydrophobic nano-coating in laminar and turbulent flows', *Experimental Thermal and Fluid Science,* 51, pp. 239-243.

Pérez-Gramatges, A., Matheus, C., Lopes, G., da Silva, J. and Nascimento, R. (2013) 'Surface and interfacial tension study of interactions between water-soluble cationic and hydrophobically modified chitosans and nonylphenol ethoxylate', *Colloids and Surfaces A: Physicochemical and Engineering Aspects,* 418, pp. 124-130.

Xia, G., Liu, Q., Qi, J. and Xu, J. (2008) 'Influence of surfactant on friction pressure drop in a manifold microchannel', *International Journal of Thermal Sciences,* 47, 12, pp. 1658-1664.

Xiaondong, D., Guicai, Z., Bing, L., Jijiang, G., Xuewu, W. and Shuming, Y. (2017) 'Enhanced Drag Reduction Performance of Nanocomposites', *Advanced Composites Letters*, 26, 4, pp. 118-126.

Zadrazil, I., Bismarck, A., Hewitt, G. and Markides, C. (2012) 'Shear layers in the turbulent pipe flow of drag reducing polymer solutions', *Chemical Engineering Science*, 72, pp. 142-154.

Libyan Journal of Science & Technology 9:2 (2019) 146–148

Faculty of Science - University of Benghazi

Libyan Journal of Science & Technology

journal home page: www.sc.uob.edu.ly/pages/page/77

Preliminary results on feeding habits of the invasive fish *Fistularia commersonii* (Ruppell, 1862) in the coast of Benghazi, Libya

Asma Elhadi Bashir and Houssein Elbaraasi*

Department of Zoology, Faculty of Science, University of Benghazi, Benghazi, Libya

Highlights

- **The feeding habits of the invasive fish Fistularia commersonii in the coast of Benghazi were studied by investigating the natural diet of monthly collected specimens.**
- **Generally, the food items found in the examined stomachs were grouped into six categories namely fish, crustacean, mollusca, empty stomach, digested matter, and other.**
- **The first group found in large quantities was Fish (87%) of total food composition. Sand grains, and the unidentified matter was 5% of total food composition followed by digested matter (4%), crustacean (2%), mollusca (1%) and an empty stomach (2%).**

ARTICLE INFO

Article history:
Received 24 February 2019
Revised 19 May 2019
Accepted 26 May 2019
Available online 18 June 2019

Keywords:
Lessepsian, feeding, *Fistularia commersonii*, Benghazi, Libya.

* Corresponding author:
E-mail address: albrasi2000@gmail.com
H. M. Elbaraasi

ABSTRACT

The feeding habits of the exotic fish *Fistularia commersonii* off the coast of Benghazi, Libya were investigated. A total of 189 specimens were collected throughout the year of 2012-2013. The mean total length (TL) and mean weight was 99.08±6.45cm and 545.33±116 g, respectively. The condition factor (K) ranged between 0.7 and 0.8. Fish were found in large quantities (87%) in the stomach of the bluespotted cornetfish. While crustaceans (2%) and mollusks (1%). The results showed also that *F. commersonii* feeds on prey from diverse habitats as well as depths.

1. Introduction

Although the Suez Canal was constructed to provide a better trade route between Europe and the Far East countries, it truly initiated an ecological disturbance between two totally different bodies of water which are the Red Sea and the Mediterranean Sea. From that point on numerous marine species were introduced into the Mediterranean Sea, this introduction was termed lessepsian migration after the engineer Ferdinand de Lesseps (Por 1978, 1990) who designed the canal. The bluespotted cornetfish, *Fistularia commersonii* (Ruppell, 1862), is a great example of the fish species taking part in the migration process from the Red Sea to the Mediterranean Sea. The first report of *F. commersonii* was in the year of 2000, off the coast of Israel (Golani 2000, Elbaraasi *et al.* 2014). Since this initial report, it has become a comparatively common fish in the Mediterranean Sea. It recorded for the first time in Libya by the year of 2007 (Elbaraasi & Elsilini, 2009; Shakman and Kinzelbach, 2007).

It is flattened from the ventral side; the dorsal and anal fins are opposite to each other. The caudal fin is forked, with very elongated and filament middle rays (Deidun and Germana 2011). It is green dorsally and silvery white ventrally, with two blue stripes of blue spots on the back. The head (consisting of a protracted, tubular snout) constitutes more than one-third of the entire body length, ending in a small mouth.

F. commersonii is a benthopelag species with tropical and subtropical distribution (Froese and Pauly 2010). It lives either solitary or in schools (Fischer and Bianchi 1984, Nakamura *et al.* 2003, Karachle *et al.* 2004). It founds in many different habitats, such as rocky, reef, muddy and sandy bottoms also in seaweed meadows to mixed environments (Bilecenoglu *et al.* 2002, Garibaldi and Orsi-Relini 2008, Kara and Oudjane 2009, somadakis *et al.* 2009).

The diet composition of *F. commersonii* in the Mediterranean has rarely been studied. However, it is carnivorous, seeking food over reefs and seagrass beds, as well as benthic fish and sometimes shrimps (Golani 2000). It feeds on bottom-living, water column dwelling local fishes like *Atherina sp.* and native populations of economic importance mainly *Spicara smaris* and *Mullus surmulentus* (Corsini *et al.* 2002). The prey families known are grouped as either pelagic fish or bottom-dwelling reef fish (Takeuchi *et al.* 2001). The objective of this study is to provide essential information on the feeding habits of *F. commersonii* on the Libyan coast off Benghazi during some months of the year of research.

2. Materials and methods:

The bluespotted cornetfish, *Fistularia commersonii* Samples (Fig. 1) were collected by fishermen using commercial fishing vessels along the coast of Benghazi, Libya (Fig. 2). A total of 189 individuals were sampled monthly from November 2012 to October 2013, taking into account the absence of samples in some months. Fish Samples, after that, were transferred in ice to the Aquaculture and Fisheries lab, Zoology Department, Benghazi University.

For each specimen, the total length (TL) were calculated to the closest cm and total weight (BW) to 0.1 gr. For feeding habit investigation, the stomachs were dissected out, and the food was preserved in 5% formaldehyde for further study. The analysis of food

 ISSN 2663-1407; National Library of Libya, Legal number: 390/2018

contents within the digestive tract was done by recording the degree of stomach fullness. The stomachs were classified as gorged, full, three-quarter full, half full, quarter full, trace and empty depends upon the degree of fullness and consequently, the amount of food contained in them converted to a percentage (Bapal and Bal, 1958).

Fig. 1. Samples of the blue spotted cornetfish, *Fistularia commersonii.*

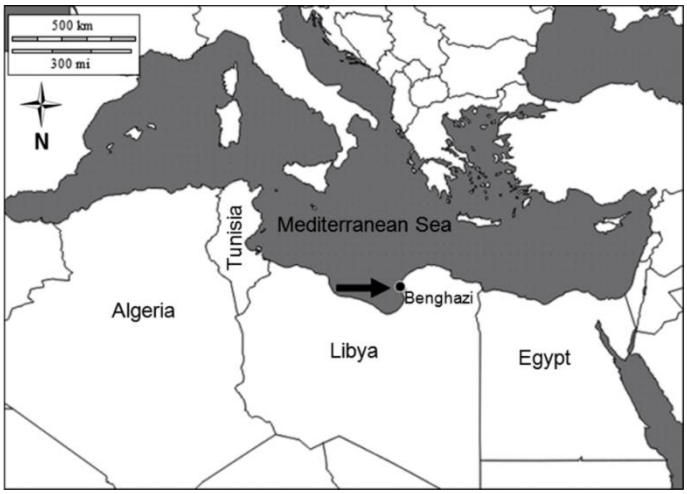

Fig. 2. Map showing the location of sampling *F. commersonii* in the coast of Benghazi, Libya.

The condition factor (K) was calculated according to Pauly, 1983 by the formula:

$$K = 100w / L^3$$

Where W= weight (g), L= Total length (cm).

3. Results and Discussions

Total length (TL) of bluespotted cornetfish collected during this study ranged from 55.0 to 198.5 cm with mean TL of 99.08±6.45cm (mean±SD), weight of bluespotted cornetfish collected during this study ranged from 179 to 1032 g with mean weight 545.33±116 g (mean±SD). However, the biggest individual inspected (198.5 cm, TL) is in accordance with greatest sizes recorded from the Mediterranean in past investigations (Kalogirou *et al.*, 2007; Bariche *et al.*, 2009, Bariche and Kajajian 2012). The calculated values of Condition factor (K) of bluespotted cornetfish off the coast of Benghazi ranged between 0.7 and 0.8. However, the mean value of K in April was 0.7±0.01, in May was 0.7±0.01, in June was 0.7±0.02, in August was 0.7±0.01, in September was 0.8±0.01, and finally in November was 0.7±0.01. Furthermore, the condition of fishes is influenced by gonadal development, feeding activity and several other factors (Doddamani *et al.*, 2001). In the present investigation, comparing K bluespotted cornetfish collected from Benghazi showed that there were no differences in condition factor during the year, which may explain that the population off Benghazi coast living in same conditions of food availability.

The various food items recorded from the stomach of the bluespotted cornetfish during the study period are presented in (Fig. 3). Generally, the food items found in the examined stomachs were grouped into six categories namely fish, crustacean, mollusca, empty stomach, digested matter, and other. The first group found in large quantities was Fish (87%) of total food composition. Thus, it forms the major food items in the stomach. However, other matter (which include sand grains, and the unidentified matter was 5% of total food composition followed by digested matter (4%), crustacean (2%), mollusc (1%) and an empty stomach (2%).

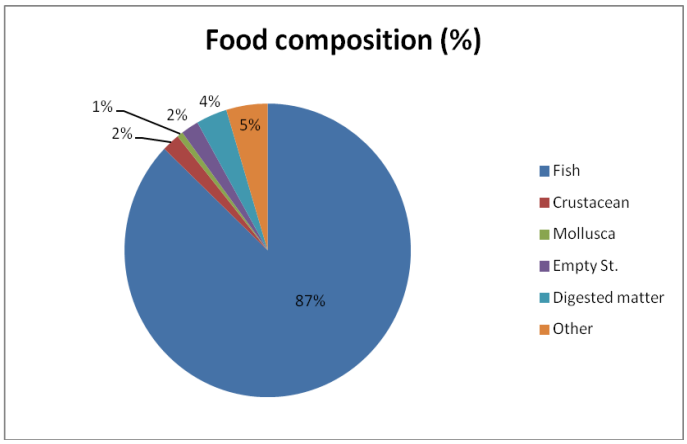

Fig. 3. The average percentage of main food items in the stomach of *Fistularia commersonii* in the coast off Benghazi, Libya.

The variation in percentage composition of food items in *Fistularia commersonii* during different months are shown in (Fig. 4). It revealed that the percentage composition of different food items varied in different months according to their availability and preference of fish. However, fish was the main food composition for all months. Furthermore, In April, fish was 81% of total food composition, crustacean was 2%, mollusca was 1%, empty stomach was 4%, digested matter 8%, and other was 4%.

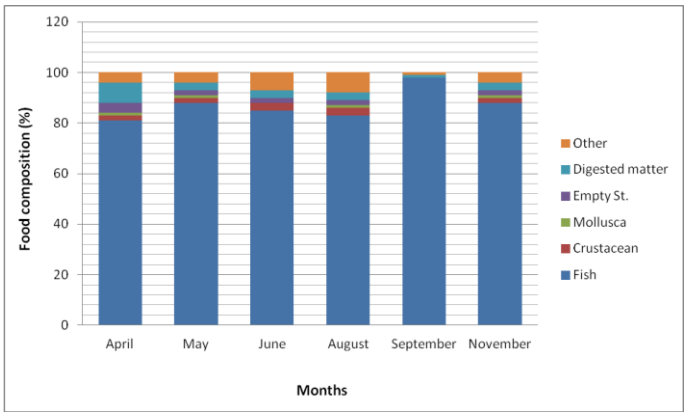

Fig. 4. Monthly variation of food composition of *Fistularia commersonii* in the coast of Benghazi, Libya.

In May, fish was 88% of total food composition, the crustacean was 2%, mollusca was 1%, empty stomach was 2%, digested matter 3%, and the other was 4%. In June, fish was 85% of total food composition, the crustacean was 3%, mollusca was 0%, empty stomach was 2%, digested matter 3%, and the other was 7%. In August, fish was 83% of total food composition, crustacean was 3%, mollusca was 1%, the empty stomach was 2%, digested matter 3%, and other was 8%. In September, fish was 98% of total food composition, crustacean was 0%, mollusca was 0%, the empty stomach was 0%, digested matter 1%, and the other was 1%. In

November, fish was 88% of total food composition, crustacean was 2%, mollusca was 1%, an empty stomach was 2%, digested matter 3%, and the other was 4%.

Feeding habits influence on the length of the gut of fishes. Moreover, carnivore fishes commonly have a stomach with a short and less straight gut. This can be as a result of the meat gets digested more simply, whereby herbivores fishes the gut is long and extremely whorled as a result of the vegetable food take longer for digestion (Bond 1996, Moyle and Cech 2000). In the present species, the alimentary canal is short; hence, the stomach was only considered in this study. The analysis of stomach content of bluespotted cornetfish from Benghazi coast revealed that these species consume a variety of bony fish as food items in this region of Libya. Differences within the dominance of various food classes are often attributed to their accessibility and also the environment wherever the fish lived at a selected time. Prevalence of crustacean and mollusks even in little proportion is maybe because of the abounding of them throughout this time. They additionally indicate a bottom-feeding tendency. Incidence of sand grains throughout the study period with comparatively low quantities indicates that sand could also be taken by accident (Kalogirou *et al*. 2007).

4. Conclusion

The bluespotted cornetfish in Benghazi coast became abundant lately which might be dangerous to many indigenes fish species that have commercial importance in the fishery sector, therefore, more studies need to be done in the future to understand the life history of this species along the coast of Libya.

References

Bapal S., Bal D. (1958) Food of some Young Fishes from Bombay Waters; *Proc. Ind. Acad*. Sci.; 35: 78-92.

Bariche M., Alwan N., El-Assi H., Zurayk R. (2009) 'Diet composition of the Lessepsian bluespotted cornetfish *fistularia commersonii* in the eastern Mediterranean', *Journal of Applied Ichthyology*, 25, pp. 460-65.

Bariche M., Kajajian A. (2012) 'Population structure of the bluespotted cornetfish *fistularia commersonii* (Osteichthyes: Fistulariidae) in the eastern Mediterranean', *Journal of Biological Research- Thessaloniki*, 17, pp. 74-08.

Bilecenoglu M., Taskavak E., Kunt B. (2002) 'Range extension of three Lessepsian migrant fish (*fistularia commersonii, sphyraena flavicauda*, *Lagocephalus suezensis*) in the Mediterranean Sea', *Journal of the Marine Biological Association of the United Kingdom*, 82, pp. 525-526. DOI: 10.1017/S0025315402005829.

Bond C. (1996) Biology of Fishes, 2nd ed., Saunders College pub., Florida. 750p.

Corsini M., Kondilatos G., Economidis S. (2002) Lessepsian migrant *fistularia commersonii* from the Rhodes marine area', *Journal of fish Biology*, 60, pp. 1061-1062. DOI:10.1111/j.1095-8649.2002.tb01865.x.

Deidum A., Germana A. (2011). 'On the increasing occurrence of the Bluespotted cornetfish *fistularia commersonii* (Rüppell, 1838) in the central Mediterranean (Osteichthyes, fistulariae)', *Biodiversity Journal*, 2(1), pp. 19-26.

Doddamani M., Rameshaand T., Shanbhogne S. (2001) 'Length-weight relationship and condition factor of stolephorus bataviensis from mangalore area', *Indian Journal of fisheries*, 48, pp. 329-332.

Elbaraasi H., Elsalini O. (2009) A record of the bluespotted cornetfish, Fistularia commersonii, off the coast of Benghazi, Libya (southern Mediterranean), *Acta Ichthyologica et Piscatoria*, 39, pp. 63-66.

Elbarassi, H., Bashir, A. E., Azzurro, E., (2014) '*Fistularia commersonii* Rüppell, 1838 in the Mediterranean Sea: filling the Libyan gap', *Journal of Applied Ichthyology*, 30(5), pp. 1047-1049.

Fischer W., Bianchi G. (1984) FAO species identification sheets for fishery purposes. Vol.2. Western Indian Ocean (Fishing Area 51). FAO, Rome.

Froese R., Pauly D. (2010) FishBase. World Wide Web electronic publication, http://www. Fishbase. org, version 03/2011.

Garibald F., Orsi-Relini L. (2008) 'Record of the bluespotted cornetfish *Fistularia commersonii* Rüppell, 1838 in the Ligurian Sea (NW Mediterranean)', *Aquatic Invasions*, 3, pp. 471-474.

Golani D. (2000) 'First record of bluespotted cornetfish from the Mediterranean Sea', *Journal of Fish Biology*, 56, pp. 1545-1547.

Kalogirou S., Corsini M., Kondilatos G., Wennhage H. (2007) 'Diet of the invasive piscivorous fish *Fistularia commersonii* in a recently colonized area of the Mediterranean', *Biological Invasions*, 9, pp. 887-896.

Kara M., Oudjane F. (2009) First observation of the Indo-Pacific bluespotted cornetfish *fistularia commersonii* (Fistulariidae) from Algerian coasts. Marine Biodiversity Records 2:e83. 4 pages.

Karachle K., Triantaphyllidis C., Stergiou I. (2004) 'Bluespotted cornetfish, Fistularia commersonii Rüppell, 1838: 'A lessepsian sprinter', *Acta Ichthyologica et piscatorial*, 34, pp. 103-108.

Moyle P., Cech J. (2000) Fishes, An Introduction to Ichthyology, 4th edition, prentice Hall, Upper Saddle River, UJ. 612P.

Nakamura Y., Horinouchi M., Nakai T., Sano M. (2003) 'Food habits of fishes in a seagrass bed on a fringing coral reef at Iriomote Island, southern Japan', *Ichthyological Research*, 50, pp. 15-22. DOI: 10.1007/s 102280300002.

Pauly D. (1983) Some simple methods for the assessment of tropicalfish stocks. FAO Fisheries Tech. pap. 234, FAO. Rome 52p.

Por F. d. (1978) Lessepsian migration: the influx of Red Sea biota into the Mediterranean by way of the Suez Canal. Ecological studies. Berlin: Springer- Verlag: 23:228.

Por F., D. (1990) Lessepsian migration. An appraisal and new data. Bulletin de l'lstitut océanographique (Monaco). N. S.7: 1-10.

Psomadakis P. N., Scacco U., Consalvo L., Bottaro M., Leone F., Vacchi M. (2009) New records of the Lessepsian fish *Fistularia commersonii* (Osteichthyes: Fistulariidae) from the central Tyrrhenian Sea: signs of an incoming colonization? JMBA 2 – Biodiversity records 2008 (6123): 1-7. http://www.mba.ac.uk/jmba/pdf/6123.pdf.

Shakman E., Kinzelbach R. (2007) 'Distribution and characterization of Lessepsian migrant fishes along the coast of Libya', *Acta Ichtyological Et Piscatoria*, 37, pp. 7-15.

Takeuchi N., Hashimoto H., Gushima K. (2001) 'Short- term foraging patterns of individual cornetfish, *fistularia commersonii*, based on stomach content analysis', *Ichthyological Research*, 49, pp. 76-80.

Libyan Journal of Science & Technology 9:2 (2019) 149–154

Faculty of Science - University of Benghazi

Libyan Journal of Science & Technology

journal home page: www.sc.uob.edu.ly/pages/page/77

Anatomical Studies of the Gastrointestinal Tract of snake *Malpolon monspessulanus insignitus* (Geoffroy, 1809)

Ezaldin A. M. Mohammed [a,*], Youssef K. A. Abd-Alhafid [a], Hamed A. N. Jala [b]

[a]*Zoology Department, Faculty of Science, Omar Al-Mukhtar University, Al Bayda, Libya.*

[b]*Zoology Department, Faculty of Science, Azzaytuna University, Tarhona, Libya*

Highlights

- **The gastrointestinal tract is a straight tubular organ from oral cavity to cloaca.**
- **The wall of the esophagus, stomach, small intestine and large intestine was built up of the following layers from outside inwards; serosa, muscularis, submucosa and mucosa**
- **The entire length of the gastrointestinal tract was lined by simple columnar epithelium (ciliated in the esophagus) and contains goblet cells except in the stomach and rectum where these cells are absent.**
- **In the small intestine, lining the mucosa consists of three types of cells. Simple vertical cells, cup cells and lymph nodes.**

ARTICLE INFO

Article history:

Received 04 October 2018
Revised 15 June 2019
Accepted 27 June 2019
Available online 29 June 2019

Keywords:

Anatomical, Gastrointestinal Tract, *Malpolon monspessulanus insignitus*.

* Corresponding author:

E-mail address: ezaldine5@gmail.com
E. A. Mohammed

ABSTRACT

Studies aim to study the morphometrical and anatomical features of a gastrointestinal tract *of Malpolon insignitus*, and compared with that of other examined reptiles So, It is clear that the tissues in the gastrointestinal tract adapt to feed the meat. The wall of the esophagus, stomach, small intestine, and large intestine is a buildup of four layers from outside inwards are serosa, muscularies, submucosa and mucosa. The esophagus was longer than the stomach and It may measure one-quarter the body length of the snake it is highly stretch to facilitate movement the food to the stomach. The mucosal epithelium was consist of simple and compound stomach glands and consist of three types of glands; they are the cardiac glands, pyloric glands, and fundus glands. The majority of the mucosal folds were primary folds as for secondary folds were rare. The small intestine is long on and that of the animal is purely carnivorous. The small intestine is composed of short transverse loops in snakes. The intestine consists of many longitudinal folds that allow the surface area to increase digestion. The mucosa of the small intestine members in the form of leaf-like villi provided with shallow branched Lieberkühn crypts at their bases. It consists of three types of cells; the endocrine cells, the goblet and the absorptive. The large intestine is short and has a larger diameter and consists of colon and rectum. The mucous membrane of the colon consists of cavernous and vertical cells, while that of the rectum is, straight and is rich in lymph spaces and goblet cells.

1. Introduction

Snakes have an important role in preserving the environment, as they play a role in the ecological balance and feed them on rodents and insects (Shine., 1995; Farooq *et al*., 2007). The diversity of snakes is not fully explored in Libya. The increased use the reclaimed land area at the expense of the natural environment of wild animals of the increased use pesticides and chemical fertilizers has significantly threatened the lives of these animals (Akram and Qureshi, 1995; Farooq *et al*., 2007). Despite the destruction of their environment, snakes remain abundant in most parts of Africa (Farooq *et al*., 2007; Amr and Disi, 2011). Snake *Malpolon insignitus* it brown color soft texture long and medium movement. Eyes are relatively large and surrounded by armor (Schleich, H. H., 1987). Frontal twice to two and a half as long as broad, about half as broad, in the middle, as the subocular, as long as or a little longer than its remoteness from the end of the snout, as long as the parietals. Loreal three to four times as long as deep (Cottone and Bauer, 2009). The maximum length may reach 200 cm. (Carranza *et al.*, 2006). In Libya, *Malpolon insignitus* is found in mountainous and coastal areas and is very common in forest areas where as well as agricultural areas it can easily get its prey (Schnurrenberger and Hans, 1963), see Fig. 1.

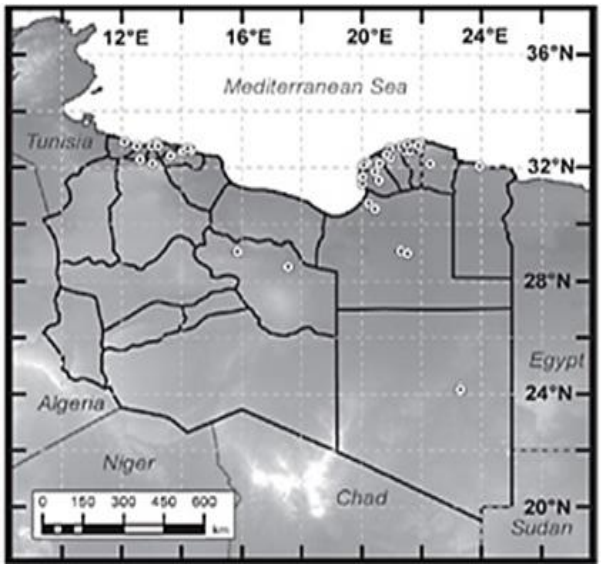

Fig. 1. Distribution of *Malpolon insignitus* in Libya, Schnurrenberger and Hans, (1963)

 ISSN 2663-1407; National Library of Libya, Legal number: 390/2018

An agile and active daytime predator he strong and courageous, a force of up to 16 kilometers per hour when chasing prey (Sindaco *et al*., 2013). Prey Species includes Insects, lizards, small birds, rodents and other Small snakes (Nagy *et al*., 2004). They are a venomous species, but venomous is not dangerous to humans, and the best defense in response to threats is its speed to escape (Bauer *et al*., 2017).

The digestive system is responsible to break up and absorb the nutrients into the bloodstream in the diet of the snake for use by the metabolism and energy production of the body (Kardong, 2002). The mouth is the beginning of the digestive system and in it begins digestion where the secretion of digestive enzymes working on the decomposition of prey after being fixed my teeth. (Zug *et al*., 2001). The venom gland produces Poisoning enzymes that are injected into the prey working to paralysis, kill prey, and then begin the process of digestion (Goin, 1962; Spellerberg, 1982; Mehrtens, 1987). The esophagus receives food from a mouth, Waves of contraction of the relatively long esophagus coupled delivers food to stomach (Romer, A. S. and Parsons T., 1986). Then to the large intestine. From there the waste enters the colon, which comes out of the cloaca. (Kardong, 2002).

2. Materials and methods

The animal used in this studying is the *Malpolon monspessulanus insignitus* (Geoffroy, 1809). It was caught localities in Wasita region, 20 km from Bayda City, Libya. Only adult-stage specimens were used [total body length (TL), 164±20 cm and total weight, 1150±100 g]. *Malpolon insignitus* were anesthetized by an overdose of 0.05% tricaine methane sulfonate by injection under the skin. Animals were dissected and the different regions of the alimentary canal; esophagus, stomach, Parts of the gastrointestinal tract of the esophagus, Stomach, the small intestine and the large in Bouin's fluid and were subjected to processing for sectioning. Section 7 µm thick were stained with haematoxylin and eosin.

3. Results

Anatomical observations

- *Malpolon monspessulanus* is a type of snake that changes its skin, a family of Colubridae. It is a poisonous opistoglifa snake. It is rarely involved in human poisoning. Since the quality of the toxins is ineffective for large mammals. The male and female adult samples were about 1.60 m long. Her weight was about 1.40 kg. The tail represents about 1/4 of the total length with a a uniform dark brown or light brown color, males are larger than females (Fig. 2a).
- The head of *Malpolon monspessulanus* is Looks like hanging, and bears eight large dorsal shields, the head shields are of great importance in Knowing the type of snake and taxonomy, It is called shields (Rostral, Internasal, Nasal, Parietal reocular, Prefrontal, Supraocular and Frontal, parietal) (Fig. 2b).
- The digestive system directly inside the snake's mouth is the buccal cavity. This is known as the esophagus of the snake. In snakes, the esophagus is long and can be half-length of the body. The esophagus connects to the anterior region of the stomach, which in turn connects to the intestines, the rectum and finally the cloaca.
- The esophagus has a relatively thin wall and as the axial musculature plays a role in the transportation of food to the stomach, it becomes muscular. The esophagus is extremely distensible to allow large prey. The mean length of the esophagus was 40±5 cm. The only distinguishing feature between the stomach and esophagus is that the stomach has a glandular mucosa. The esophagus is fusiform, having longitudinal folds (proximal esophagus) and broad and flat folds (distal esophagus).
- The stomach is responsible for the secretion of digestion enzymes, and the stomach is clear as it has a diameter larger than the intestines and also have large folds allow to increase their size when entering food, and the length of the stomach about 20 cm. The stomach is divided into four regions: the cardiac region continued with the esophagus, the long saccular body with a terminal region, and the pyloric region continuous with the intestine.
- The intestine was continues the digesting process started in the stomach. It has extensive longitudinal folds to increase surface area for absorption and allows distension to accommodate large prey; the mean length was 55±5 cm. The transition from small intestines to the large intestines was clear. The spleen is adherent to the pancreas, forming the splenopancreas. The pancreas is found caudal to the pylorus, near the gallbladder and spleen those three organs being referred to as the triad. Cloaca is the terminus of the gastrointestinal tract. In snakes, the cloaca is linear rather than round and is divided into three sections by mucosal folds: urodeum, coprodeum and proctodeum (Fig. 2c).

Fig. 2 (a) Snake *Malpolon monspessufanus insignitus* (Geoffroy, 1809).

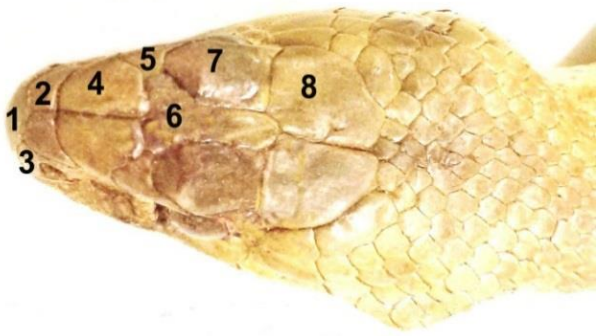

Fig. 2. (b) *Malpolon monspessulanus*. Top of head called shields: 1- Rostral. 2- Internasal. 3- Nasal. 4- Parietal reocular. 5- Prefrontal. 6- Supraocular. 7- Frontal. 8- Parietal.

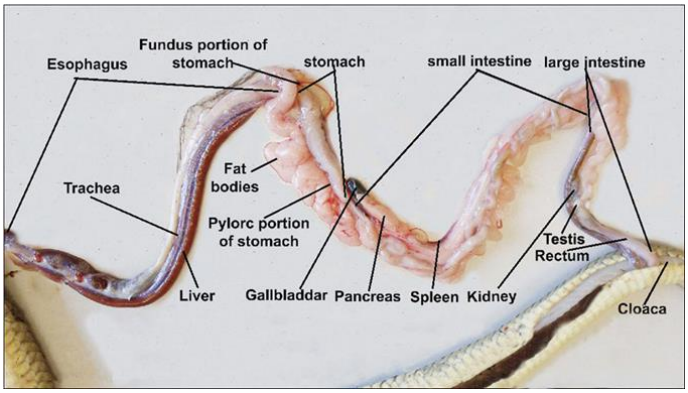

Fig. 2. (c) Gastrointestinal Tract of snake *Malpolon monspessulanus* insugnitus (Geoffroy, 1809)

Histological observations

- Esophagus: The esophagus was composed of four layers; mucosa, submucosa, muscularis, and serosa. The majority of the mucosal folds were primary folds, and secondary folds were

rare. The mucosal epithelium was composed of stratified cells; there were no glands in the wall of the esophagus. Brush cells were present among the columnar epithelial cells in the distal portion of the esophagus. The muscularis was composed of an inner longitudinal layer and an outer circular) layer, both of which were striated muscles (Fig. 3).

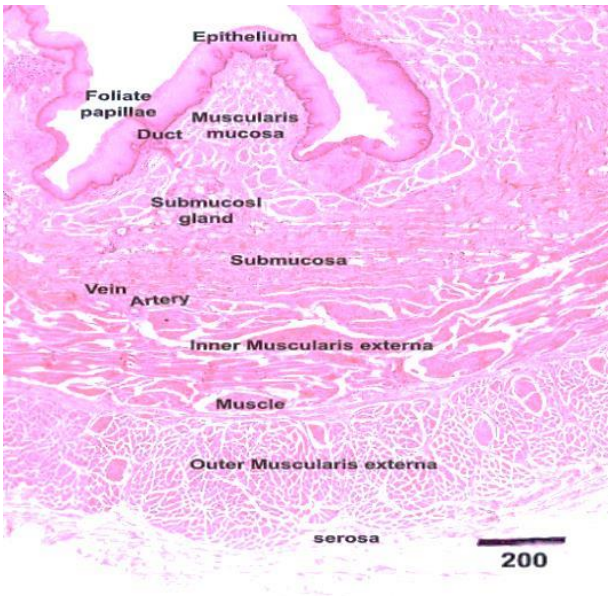

Fig. 3. Photomicrograph in the oesophagus of psammophis schokari. H&E stain.

- Stomach: All regions of the stomach had four layers; mucosa, submucosa, muscularis, and serosa. From the esophagus to the cardiac region of the stomach, cells comprising the mucosal epithelium transitioned from stratified cells mixed with saccular mucous cells to simple columnar cells (Fig. 4a).

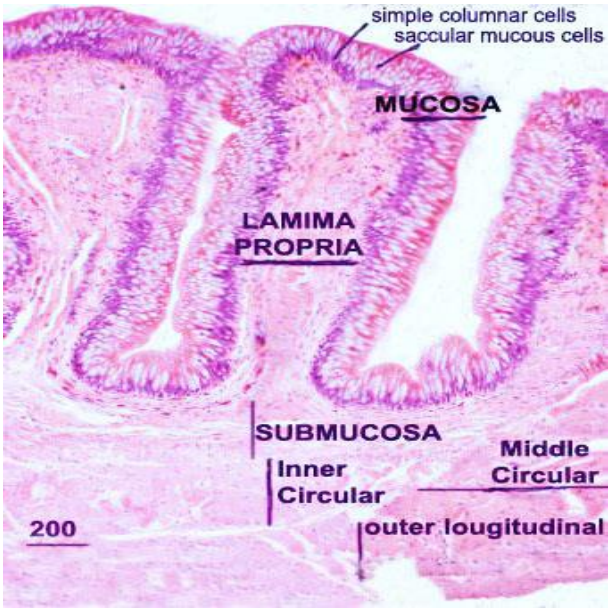

Fig. 4. (a) LM in the esophagus the terminal region of the stomach. H&E stain

- The inner longitudinal striated muscle layer in the esophagus was present within the submucosa in the cardiac region of the stomach. The circular striated muscle layer is finished at the beginning of the stomach in a cardiac region of the stomach.
- The cardiac region of stomach: Is the first part is the cardia which surrounds the cardial orifice, the mucosal epithelium composed of simple columnar epithelial cells, and no goblet cells were observed within the lamina propria which is atypical loose connective tissue. The muscularis was composed of inner longitudinal, middle circular and outer longitudinal layers (Fig. 4b).

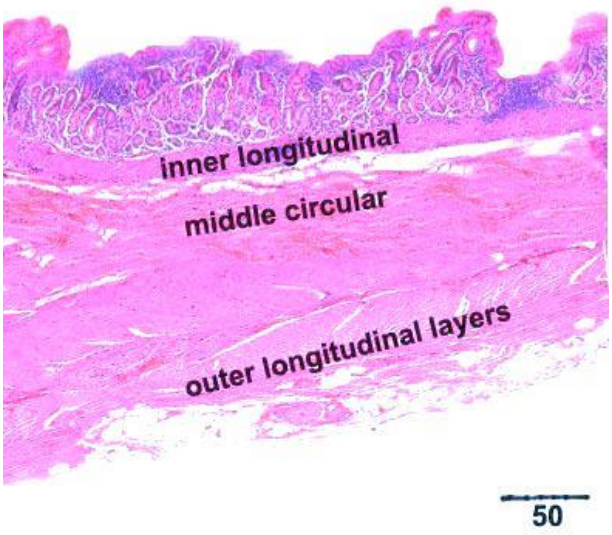

Fig. 4. (b) muscularis in the cardiac region of stomach. E&E stain.

- The Stomach layers consisted of both longitudinal and circular smooth muscle layers, the circular smooth muscle layers were thin when they are compared with smooth muscle layer in the body region of the stomach, the longitudinal smooth muscle was considerably thicker when compared with smooth muscle layer in the body region of the stomach, and a muscularis mucosa was not observed. The pyloric region of the stomach: The mucosal epithelium was composed of simple columnar cells, and no gastric glands were observed within the lamina propria (Figs. 4c & 4d).

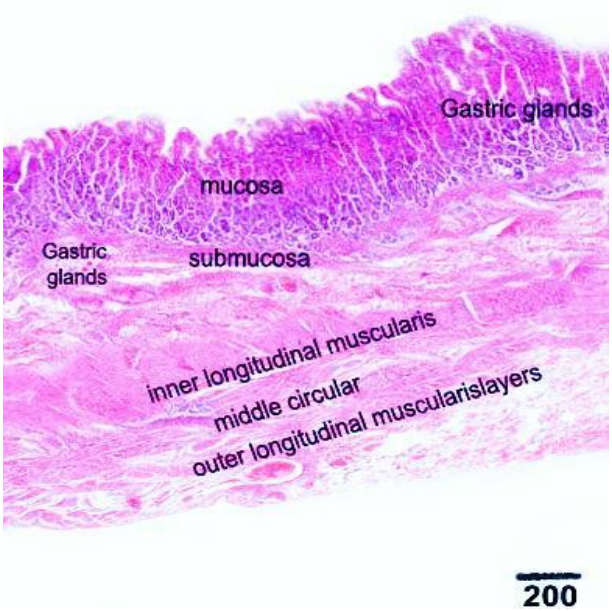

Fig. 4. (c) The body region of the stomach. H&E stain.

- The small intestine is a long and narrow 'tube' with a structure and epithelium that maximises surface area due to the presence of many largely longitudinal folds. Ileocecal valve is absent in *Malpolon insignitus*. The small intestine is composed of four layers typically present in the alimentary system. Its four layers are the mucosa, submucosa, the smooth muscles and serous membrane.
- The muscularis was composed of inner circular and outer longitudinal layers. The circular and longitudinal layer was as thick. The intestinal epithelium presenting a large number of

goblet cells with mucopolysaccharides. The intestine had many branched and intensive villi, which was a very thick wall when compared to the stomach (Figs. 5a & 5b).

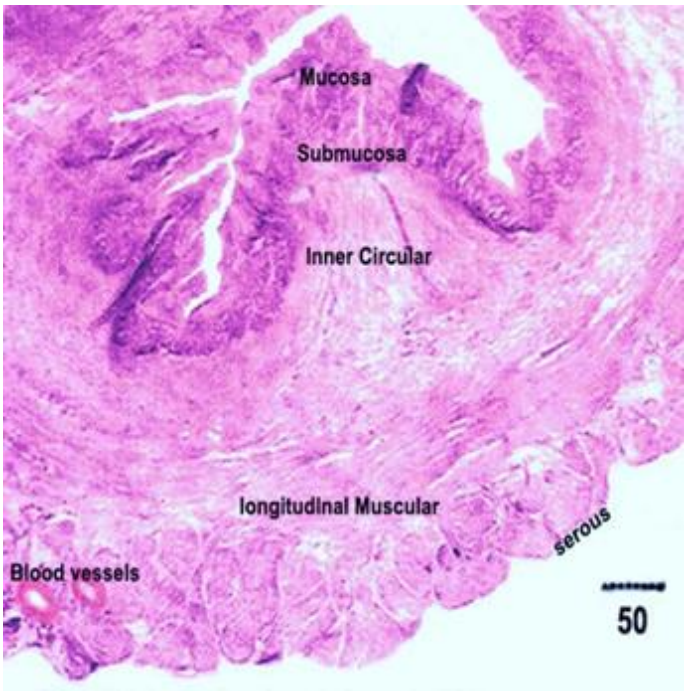

Fig. 4. (d) Terminal region of stomach. H&E

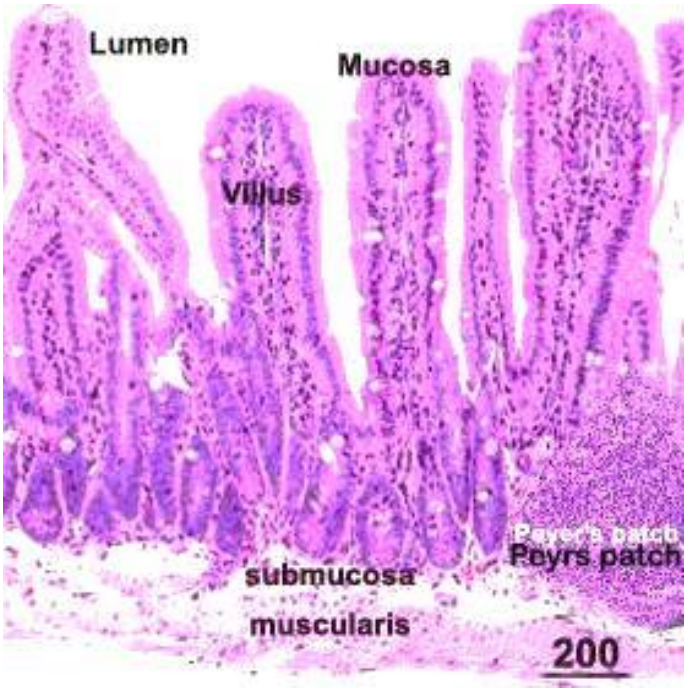

Fig. 5. (a). Anterior intestine. H&E stain

- Large Intestine: The mucous showed villi and an intestinal wall thin when compared to the Small intestine and Short and unclear primary folds were observed. The intestinal epithelium presenting a little of simple columnar cells and numerous goblet cells. The muscularis was composed of inner circular and outer longitudinal layers. Both layers were thinner than those of the anterior intestine. The inner longitudinal striated muscle layer in the cardiac region of the stomach is an extension of the inner longitudinal striated muscle layer in the esophagus (Figs. 5c & 5d).

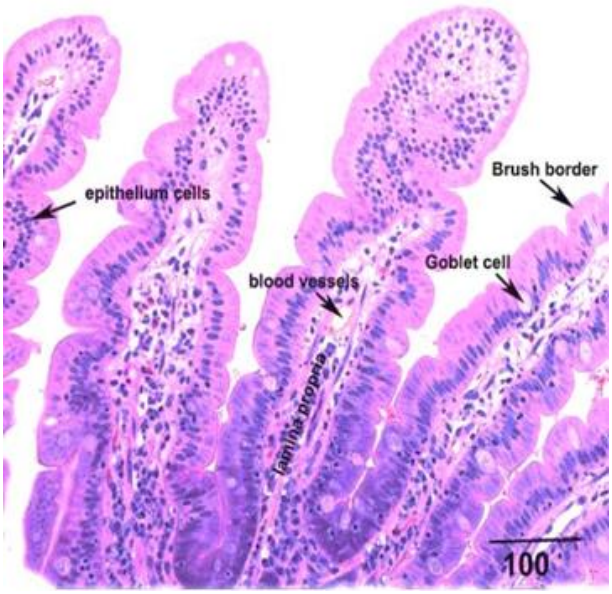

Fig. 5. (b) Simple columnar epithelim cell and few goblet cells

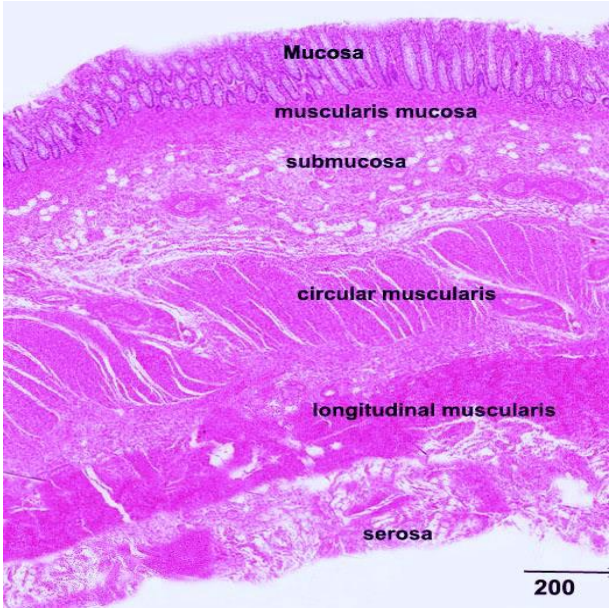

Fig. 5. (c). Posterior intestine. H&E stain.

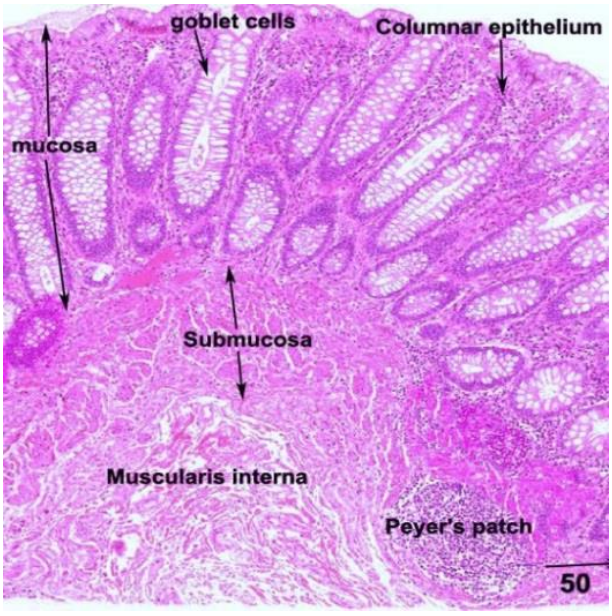

Fig. 5. (d). Posterior intestine. H&E stain.

4. Discussion

Histological examination of the oesophageal mucsa of species of reptiles showed a considerable difference in their histological structure. The present study and examination revealed that the oesophageal mucosa of the colubrid snake *Malpolon insignitus* is represented by goblet cells and simple columnar ciliated (Khamas, 2011; Reeves, 2011). Such a structure is similar to the observations obtained in Mauremys (Taib, N. T. Jarrar, B. and EL- Ghandour, M. H., 1985). Caspica (Taib and Jarrar., 1983), Acanthodactylus and Cnalcides (Dehlawi and Zaher, 1989). However, in Uromastyx aegyptia (EL-Toubi and Bishai, 1958), Chameleon vulgaris (Bishai, 1960) and in Uromastyx philbyi (Farag, 1982). Only the anterior region of the esophageal mucosa assumes structure is similar to the observations obtained, while the posterior region was found to consist of a layer of goblet cells and ciliated columnar. This latter layer is followed by two or three layers of replacing cells (Al-Nassar, 1976). Thus, comparing the data obtained by this experiment with the available literature, it is possible to conclude that the findings described here confirm that the predominant esophagus-lining epithelium of the studied samples was prismatic simple epithelium, which is compatible with previous works (Frye., 1991; Abdeen, *et al*., 2013), although no pseudostratified epithelium has been found, as described by Khamas and Reeves (2011). In *Malpolon monspessulanus insignitus*, the oesophageal mucosa is only primarily of mucous secreting cells (goblet cells). Moreover, in the snake Natrix natrix, and Vipera berus (Dehlawi and Zaher, 1989), the ciliated cylindrical cellsoccurring in the anterior portion of the oesophagus are replaced posteriorly by large mucous cells and simple squamous cells on the surface and more cubical cells devoid of cilia. In many snakes' species, the posterior portion of the oesophagus is devoid of ciliated cells (Dehlawi and Zaher, 1989; Dilmuhamedov, 1975).

The presence of oesophageal glands in reptiles, in general, was a matter of great dispute between several authors. The present Observational Study revealed the absence of such glands as in many previous examined reptiles as in Alligators (Beguin, F. 1904), Ablephorius pannonicus (Greschik, E., 1917), Scincus officinalis (El-Toubi, M. R., 1936), Typhlops vermicularis, Agama stellio (Heyder, G., 1974), the colubrid snak N. natrix and V. berus (Dehlawi and Zaher, 1989).

The esophageal wall exhibited a thickening in the cranial-caudal sense, especially regarding the muscle layer and, secondarily, the muscularis mucosae and even the adventitia, according to the terms used by Jacobson (2007), as similarly found in this work Abdeen *et al*., (2013) describes that the esophageal-gastric transition is abrupt and that the mucosa of the gastric fundus, the main glandular portion of the organ, is composed of stratified columnar epithelium with cylindrical cells and glands, which, in turn, are outlined by neck cells (Frye, 1991; Jacobson, 2007). These gastric glands exhibit two clearly distinguishable cell types: one characterized by dark cells (pale blue stain or light basophilia) and the other by light cells (eosinophilic) (Frye, 1991; Jacobson, 2007). The points of the discrepancy between the cited works involve the types and functions of the cells present in the gastric glands, the characterization of the cardiac and pyloric portions and finally the number of layers of the muscularis mucosae.

The esophagus and cardia could not be distinguished, as pylorus and fundus could not either. Frye (1991) and Helmstetter *et al*., (2009) describe the cardia as an epithelium identical to the esophagus, with an abrupt transition to the glandular epithelium of the fundic portion, which, in turn, is the major glandular portion of the stomach. The pyloric portion is characterized by a discrete reduction in the number of gastric glands, epithelial projections resembling intestinal folds, and a lining with a single, strongly eosinophilic cell type (Frye, 1991). Thus with respect to the fundus and the pylorus, the descriptions are very similar, in the sense of the present study. However, Jacobson (2007) divided the stomach only in fundus and pylorus, with the latter portion characterized by shorter and less branched glands, still poorly distinguishable from the anterior portion.

This apparent discrepancy seems merely nominal to us and not analytical, given that Jacobson (2007) simply did not name the transition between the esophagus and cardia, as it is histologically indistinguishable and only macroscopically visible. The abrupt microscopic transition, which is a consensus between both works cited, occurs only between the cardia and the fundus, corroborating the findings of the present study. Concerning the cell types constituting the gastric glands, the samples examined in the present study exhibited one type composed of a pale and heterogeneous cytoplasm.

In lower part of the epithelial tissue of the small intestine, muscularis mucosa was narrow and composed of a layer of smooth muscle cells. Similar to other reptiles, muscularis layer of small intestine was smooth and consisted of two layers (Putterill and Soley, 2003). There were no glands in the small intestine of H. cyanocincyus as indicated by Holmberg *et al*., 2002. The mucosal epithelium of large intestine was Existence up simple columnar cells with several sporadic goblet (Firmiano *et al*., 2011).

Abdeen *et al*., (2013) while studying the large intestine of the Ramphotyphlops braminus snake reported that in mucosa, a thin layer of muscle was present, which is the same layer as muscularis mucosa in this study. Then, was the submucosa layer, which is equivalent to the connective tissue, rich in blood vessels. Muscularis was made of a thick layer of longitudinal cells on the inside and a thin layer of circular cells on the outside. Serosa was located in the outermost part of the wall. Similar to most reptiles, the intestinal gland in the large intestine was not found in H. cyanocinctus (Gasperetti, 1988; Hamdi *et al*., 2014).

References

Abdeen, A. M., Mostafa, N. A., Abo-Eleneen, R. E., Elsadany, D. A. (2013) 'Anatomical studies on the alimentary tract of the Egyptian Typhlopid Snake', *Journal of American Science*, 9, 5, pp. 504-517, doi: 10.7537/marsjas090513.65.

Akram, S. and Qureshi, J. (1995) Snake-Nittagun, 27, pp. 25-30.

Al-Nassar, N. A. (1976) Anatomical studies osteology and gut histology of the amphisbaenian Diplometopon zarudnyi inhibiting Kuwait. M.Sc. Thesis, Kuwait University.

Amr, Z. and Disi, A. M. (2011) 'Systematics, distribution and ecology of the snakes of Jordan', *Vertebrate Zoology*, 61, pp. 179-266

Bauer, Aaron M., Jonathan C. Deboer, Dylan J. Taylor (2017) 'Atlas of the Reptiles of Libya. Proc', *Cal. Acad. Sci*., 64(8), pp. 255-256.

Beguin, F. (1904) 'L intestine pendant le jeune et l intestine pendant la digestion. Etudes faites sur le Crapaud de joucs et le lezard des murailles', *Arch. Anat. Micr*., 6, pp. 385-454.

Bishai, H. (1960) 'The anatomy and histology of the alimentary tract of Chameleon vulgaris', *Fac., Sci., Cairo Univ*., 15(29), pp. 44-61.

Carranza, S., Arnold, E. N. and Pleguezuelos, J. M. (2006) 'Phylogeny, biogeography, and evolution of two Mediterranean snakes, *Malpolon monspessulanus* and Hemorrhois hippocrepis (Squamata, Colubridae), using mtDNA sequences', *Molecular Phylogenetics and Evolution*., 40(2), pp. 532–546. doi:10.1016/j.ympev.2006.03.028. PMID 16679033.

Cottone, A. M. and Bauer, A. M. (2009) 'Sexual size dimorphism, diet, and reproductive biology of the Afro-Asian Sand Snake, Psammophis schokari (Psammophiidae)', Amphibia-Reptilia, *Leiden*, 30, pp. 331-340.

Dehlawi, G. Y. and Zaher, M. M. (1989) 'Histological studies on the alimentary tract of the colubrid snake, Coluber florudentus (Family: Colubridae)', *Proceedings of the Zoological Society. A. R. Egypt*, (1), pp. 95-112

Dilmuhamedov, M. E. (1975) The comparative morphology of the digestive tract of some reptiles. Dissertation, Alma-Ata.

El-Toubi, M. and Bishai, H. (1958) The anatomy and histology of the alimentary tract of the lizard Uromastyx aegyptia Forskal, *Bull. Fac. Sci*. 34, pp. 5-13.

EL-Toubi, M. R. (1936) Macroscopic and microscopic anatomy of Scincus officinalis. M.Sc. Thesis, Fac. Sci, Cairo University.

Farag, A. A. (1982) Histological studies on the mucosal epithelium of the anmentary tract of the agamid lizard, Uromastyx philbyi parker. The Annals of Zoology. Published by Academy of Zoology. XLX, (1), pp. 1-23.

Farooq, Z., Akram, S. M. and Tahir, T. (2007) Ecological Assortment of Snakes in Southern Punjab, Pakistan. Life Sci. Int. J., 1, pp. 330-334.

Firmiano, E. M., Cardoso, N. N., Vieira, D. A., Sales, A., Santos, M. A. (2011) 'Histological study of the liver of the lizard, Tropidurus torquatus Wied 1820, (Squamata: Tropiduridae)', *Journal of Morphological Science*, 28, pp. 165-170.

Frye, F. L. (1991) Reptile care: an atlas of diseases and treatments. Neptune: TFH Publications,

Goin, C. (1962). Introduction to Herpetology. San Francisco: W.H. Freeman and Company

Greschik, E. (1917) Uber den Darmkanal von Albepharus pannonicus Fritz, und Anguis fragilis L. *Anat. Anz*., 50, pp. 70-80.

Hamdi, H., El-Ghareeb, A. W., Zaher, M., Essa, A., Lahsik, S. (2014) 'Anatomical, histological and histochemical adaptations of the reptilian alimentary canal to their food habits: II-Chamaeleona fricanus', *World Applied Sciences Journal*, 30, pp. 1306-1316.

Helmstetter, C., Reix, N., Tflachebba, M. Pope, R. K.; Secor, S. M.; Le maho, Y.; Lignot, J. H. (2009) 'Functional changes with feeding in the gastro-intestinal epithelia of the Burmese python (Python molurus)', *Zoological Science*, 26, 9, pp. 632-638. doi: 10.1242/jeb.015313.

Heyder G. (1974) 'Das verdaungs system Von Typhlops vermiucularis Marrem. 1920', *Morph Journal of biology*, 120, pp. 185-197.

Holmberg, A., Kaim, J., Persson, A., Jensen, J. (2002) 'Effects of digestive status on the reptilian gut. Comparative Biochemistry and Physiology Part A', *Molecular & Integrative Physiology*, 133, pp. 499-518.

Jacobson, E. R. (2007) Infectious diseases and pathology of reptiles: color atlas and text. Boca Raton: CRC Press. https://doi.org/10.1201/9781420004038

Kardong, Kenneth V. Ph.D. (2002) Vertebrates-Comparative Anatomy, Function, Evolution. 3rd Ed. McGraw Hill: New York.

Khamas, W., Reeves R. (2011) 'Morphological study of the esophagus and stomach of the gopher snake pituophis catenifer', *Journal of Veterinary Medicine Series C: Anatomia Histologia Embryologia*, 40, 4, pp. 307-313. doi: 10.1111/j.

Mehrtns, J. M. (1987) Living Snakes of the World in Color. New York City, NY, USA: Sterling Publishers: 480.

Nagy, Z. T., Lawson, R., Joger, U. & Wink, M. (2004) 'Molecular systematics of racers, whipsnakes and relatives (Rep tilia: Colubridae) using mitochondrial and nuclear markers', *Journal of Zoological Systematics and Evolutionary Research*, 42, pp. 223 – 233.

Putterill, J. F., Soley, J. T. (2003) 'General morphology of the oral cavity of the Nile crocodile, Crocodylus niloticus (Laurenti, 1768). I. Palate and gingivae Onderstepoort', *Journal of veterinary research*, 70, pp. 281-297.

Romer, A. S. and Parsons, T. (1986) The Vertebrate Body. W.S. Saunders Co. Philadelphia. 679.

Schnurrenberger, Hans. (1963) 'Fishes, amphibians, and reptiles of two Libyan oases', *Herpetologica*, 18(4), pp. 270-273.

Shine, R. (1995) Australian snakes: A natural history. Cornell University Press.

Sindaco, R. & Venchi, A. & Grieco, C. (2013) The reptiles of the Western Palearctic. 2. Annotated checklist and distributional atlas of the snakes of Europe, North Africa, Middle East and Central Asia, with an update of the vol. 1.

Spellerberg, I. (1982) Biology of Reptiles. NY: Chapman and Hall, spring 2010.

Taib, N. T. and Jarrar, B. (1983) 'Morphology and histology of the alimentary canal of Mauremys caspica (Reptilia, Emydidae)', *Ind. J. Zool*., 11, pp. 1-12.

Taib, N. T. Jarrar, B., and EL-Ghandour, M. H. (1985) 'Morphology and histology of the alimentary canal of Chalcides levitoni (Reptilia, Emydidae)', *Bangladesh J. Zool*., 10, pp. 1-14

Zug, George R., Laurie J. Vitt, Janalee P. Caldwell (2001) Herpetology–An Introductory Biology of Amphibians and Reptiles.2nd Ed. Academic Press: California.

Libyan Journal of Science & Technology 9:2 (2019) 155–164

Faculty of Science - University of Benghazi

Libyan Journal of Science & Technology

journal home page: www.sc.uob.edu.ly/pages/page/77

Taxonomy of Miocene Bryozoans from As Sahabi area, Ajdabiyah Trough, NE Sirt Basin, Libya

Ahmed M. Muftah[a,*] and Yasser A. El-Safori[b]

[a]*Department of Earth Sciences, Faculty of Science, University of Benghazi, P. O. Box 9480, Benghazi, Libya.*

[b]*Department of Geology, Faculty of Science, University of Ain Shams, P.O. Box 11566 Cairo, Egypt.*

Highlights

- **Bryozoan taxa have retrieved from the formation "M" in As Sahabi area of Sirt Basin, Libya.**
- **Fourteen species are classified and described in this study.**
- **The assemblage is closely similar to the equivalent sediments from Egypt and Libya.**
- **According to the assemblage, a shallow marine environment with low energy condition has been interpreted.**

ARTICLE INFO

Article history:
Received 04 December 2018
Revised 26 June 2019
Accepted 29 June 2019
Available online 01 July 2019

Keywords:
As Sahabi, Bryozoa, Tortonian, Sirt Basin, Libya, Taxonomy, Paleogeography.

* Corresponding author:
E-mail address: ahmed59muftah@gmail.com
A. M. Muftah

ABSTRACT

The exposed Pre-Sahabi rock unit formation "M" at As Sahabi area in Sirt Basin is analyzed micro paleontologically for bryozoans. Fourteen species belonging to eleven genera of bryozoan have been identified, described for the first time. In addition, the importance of the present study is to determine the paleo environmental occurrences as is performed herein with particular attention to their paleo geographical distribution. A comparison with the coeval sites from Siwa Oasis, the Cairo-Suez Road section in Egypt, as well as the Maradah Formation from Sirt Basin in Libya, has been revealed some similarities between these sites.

1. Introduction

The As Sahabi study area is located in the northeastern part of Sirt Basin, covering an area of ≈375km². It is bounded by longitudes 20° 48' 08" to 20° 54' 45" E and latitudes 30° 10' 58" to 30° 17' 36" N within a tectonic province called the Ajdabiya Trough (Fig. 1).

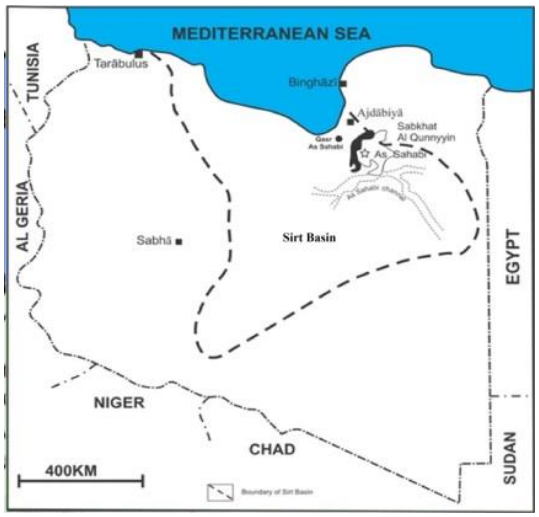

Fig. 1. Location of the As Sahabi area in Sirt Basin of Libya (Muftah, 2013).

The studied samples came from a small exposure profile at locality P53 called Inselberg Hill (Fig. 2). It is located at latitudes (30° 14' 5.78" N) and longitudes (20° 53' 54.18" E) along the western margin of the Sabkhat Al Qunnyyin. It is the oldest exposed rock unit in As Sahabi area and belongs informally to formation "M", which consists of clay and fossiliferous semi consolidated carbonates (Fig. 2).

Thirteen samples were collected from the locality P53 exposure (Fig. 2) which are prepared according to standard micropaleontological techniques and examined for their bryozoan content.

Fig. 2. Inselberg Hill (P53) located at the western edge of Sabkhat Al Qunnyyin (facing NW) (see Fig. 4 for lithology).

Selected bryozoan species are examined using a Jeol JSM 6360 Scanning Electron Microscope, at the University of Athens, Department of Historical Geology and Paleontology, for taxonomic and illustrative purposes. All materials (rock samples and micro paleontological slides) are stored in the micro paleontological section of the Earth Sciences Department of Benghazi University, Benghazi, Libya.

 ISSN 2663-1407; National Library of Libya, Legal number: 390/2018

2. Geological setting and Stratigraphy of As Sahabi

2.1 Tectonics

The Sirt Basin is the largest and youngest sedimentary basin in Libya, with an NW-SE trending pattern, covering an area of about 300.000 km2 (Fig. 3). It is bounded by the Hun graben to the west, a major fault of dip-slip nature including the Antelat uplift, which separates the basin from the Cyrenaica platform to the east, by the Mediterranean Sea to the north and by the major Tibisti Sirt uplift to the south (Fig. 3). Sirt Basin was formed in the Cenomanian, during which a series of NW-SE trending horsts and grabens were developed. The deeper part of the basin (troughs), including the Ajdabya (≈Agedabia) trough where As Sahabi area is located, is considered as the eastern graben of the horst - graben system of Sirt Basin complex (El-Arnauti and El Sogher, 2004). This trough has received more than 15.000 ft. thick sequences of Mesozoic and Tertiary marine sediments, as they are recorded in the subsurface drilled oil wells in this Basin.

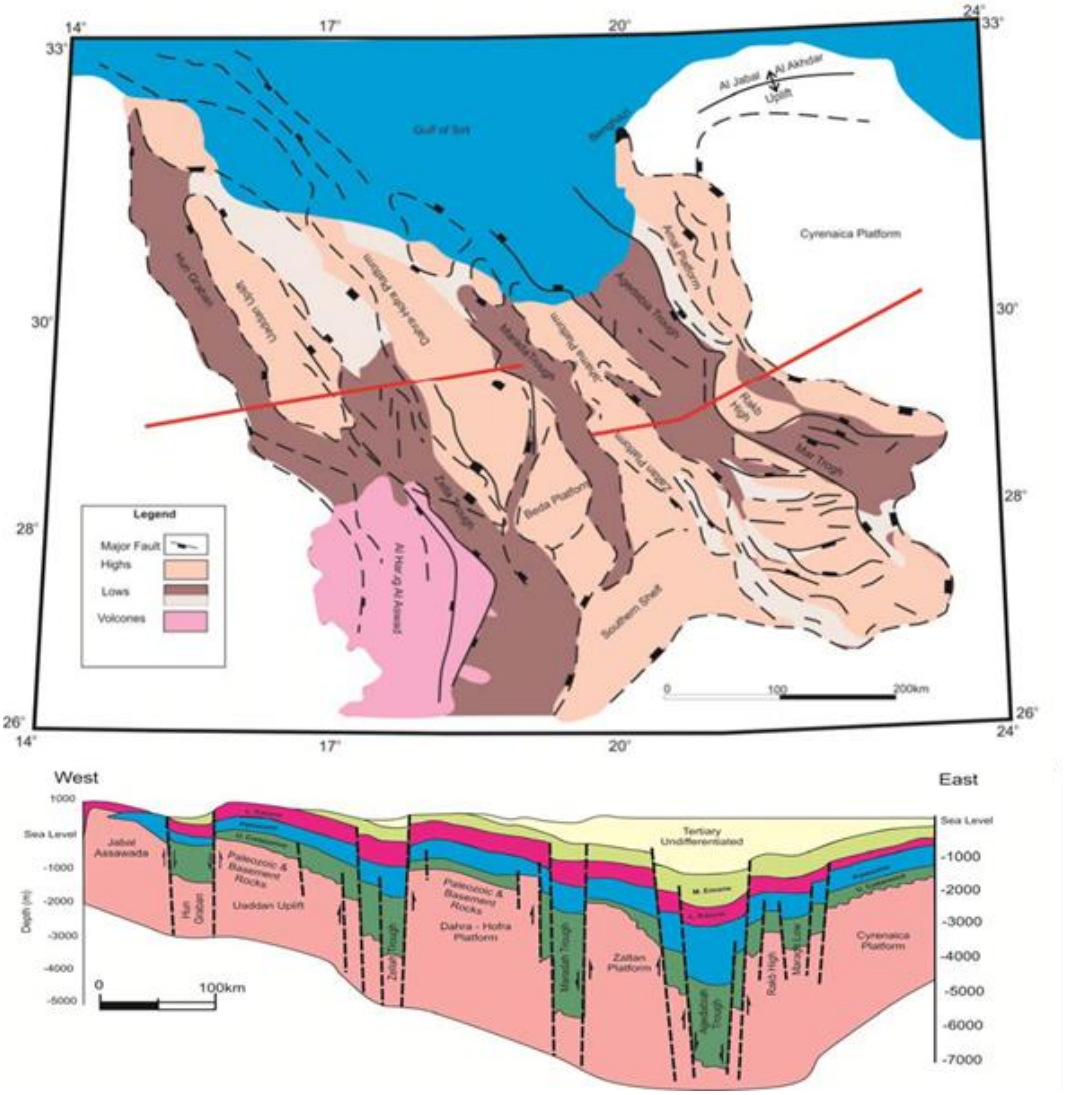

Fig. 3. Tectonic map of Sirt Basin shows the Ajdabya Trough and geological cross section through the Basin (after Roohi, 1993).

2. 2. Stratigraphy of As Sahabi area

The Neogene strata in the As Sahabi area are exposed along the western edge of the Sabkhat Al Qunnyyin. The stratigraphy of these rocks has been introduced by De Heinzelin and El Arnauti (1982, 1983, and 1987); Giglia (1984) and Muftah *et al*. (2008b) from several surface exposures in As Sahabi area (Fig. 3). The exposed rock units are named informally, from bottom to top: formation "M", formation "P", and the Sahabi Formation. The latter is subdivided into five informal members (T, U1, UD, U2 and V) and formation "Z" as the topmost rock units at some localities (De Heinzelin and El-Arnauti, 1987; Muftah, 2013, Muftah *et al*., 2013). However, El-Shawaihdi *et al*. (2014), El-Shawaihdi, *et al*. (2016) and El-Shawaihdi, *et al*. (2019) amended the lithostratigraphic nomenclatures of the As Sahabi area based on stable isotopes dating of few samples to modify formation "M" and regional correlation to introduced new “lower member” and “upper member” of Sahabi Formation, Qarrat Waddah Formation and formation "Z" (Fig. 3). The present study focuses only on the formation "M".

Formation "M" composes of semi-consolidated lithofacies with maximum exposed thickness reaching up to 13 meters, among which the main bryozoan-productive horizon is accommodated (*i.e.* the lower two units) (Fig. 4). It is highly fossiliferous with most common invertebrate fossil groups, including echinoids, pelecypods, gastropods, corals and bryozoans in addition to several microfossils groups such as foraminifera, calcareous nannofossils and ostracods (De Heinzelin and El-Arnauti, 1983; Willems and Meyrick, 1982; and Muftah *et al*., 2008a, b). Petrographically formation “M” is differentiated into the following five units, (Fig. 4), on the basis of the lithology, texture and fossil content; from bottom to top they are: i) Foraminifera-echinodermal packstone unit; ii) Sandy-pelletal packstone unit; iii) Gypsiferous dolostone unit; iv) Clay unit; and v) Fossiliferous limestone unit.

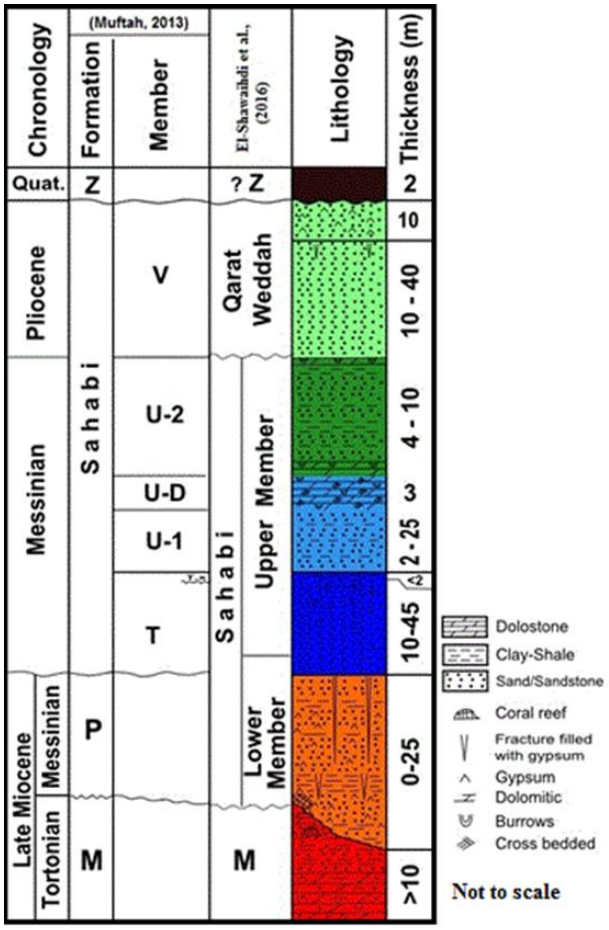

Fig. 3. Stratigraphic column of exposed rock units in As Sahabi area (Muftah *et al*., 2019, *in press*).

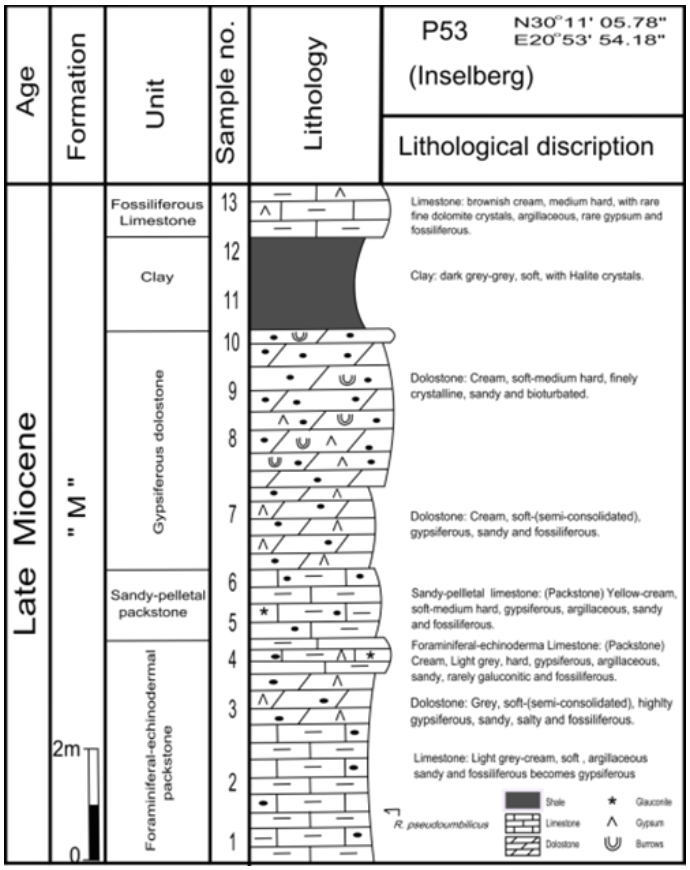

Fig. 4. Columnar section of Pre-Sahabi rock unit at P53 As Sahabi area (Muftah, 2013).

3. Taxonomy

Taxonomic study of all recorded species is based primarily on the classification of Bassler (1953) with modifications. In addition, description, micrometric measurements, distribution, and habitat for each species are given. The parameters, statistics and abbreviations, as well as the form in which are presented, are as follows:

Parameter	No. of measured (Zoaria, Zooecia)	Range (mm)	Standard deviation	Mean (mm)
X*	(4, 8)	0.125–0.301	0.021	0.332

*Dz= Zoarial diameter; Dp= Peristomes diameter; Do= Orifice diameter; Lz= Aurozooidal length; lz= Aurozooidal width; Lo= Apertural or Opesial length; lo= Apertural or Opesial width; Lov= Ovicell length; Iov= Ovicell width; Lav= Avicularian length; Iav= Avicularian width. The bryozoan suite in the formation "M" is in general of very low diversity and is represented by fourteen species (Fig. 5).

Age	Formation	Samole No.	*Crisia eburnea*	*Crisia elongata*	*Crisia hornesi*	*Tretocycloecia dichotoma*	*Steginoporella iberica reussi*	*Calpensia nobilis*	*Thalamoporella zaltaniensis*	*Cellaria salicornioides*	*Nellia tenella*	*Scrupocellaria elleptica*	*Margretta cereoides*	*Celleporaria desioi*	*Celleporaria polythele*	*Schedocleidochasma incisa*
Late Miocene (Tortonian)	"M"	8-13	BARREN													
		7	R	R					R	R	R		R			C
		6									R					
		5		R		R	R				R	R	R	F	R	R
		4		C						R	F					
		3		C	R			R		A	C	R				
		2		C				C			F					
		1		F				C		C	F	F				R

Fig. 5. Bryozoans distribution chart of the P53 section at As Sahabi area.

(R: Rare 1-2; C: Common 3-5; F: Frequent: 6-10; A: Abundant >10)

Phylum: Bryozoa Ehrenberg, 1831
Order: Cyclostomata Busk, 1852
Family: Crisidae Johnston, 1847
Crisia eburnea (Linnaeus, 1758)

Sertularia eburnea Linnaeus, 1758: 810.

Crisia eburnea Winston, 1982: 155, fig. 91; Hayward and Ryland, 1985: 49, fig. 13a-c; Dulai *et al*., 2010: 37, pl. 3, Fig. 2.

Measurements:

Dz (3) 0.253-0.260 (0.022) 0.267 mm,
Lz (1, 3) 0.342-0.371 (0.043) 0.364 mm
Do (1, 10) 0.062-0.064 (0.021) 0.063 mm
Dp (1, 10) 0.078-0.085 (0.042) 0.083 mm

Description. Zoarium erect, flat, internodes short and composed of 5–7 Autozooids, ornamented by dark common slit-like and few circular pseudopores and annual lines. Autozooids with a definite little salient, gently and frontally curved peristome and circular orifice. Gonozooid not observed. Non-cellular surface, gently curved, ornamented by the same pseudopores as the cellular one.

Occurrences: Sirt Basin, Sahabi area, locality P53 formation "M", Sample no. 7 (Fig. 4).

Distribution: Common in the cold waters of Europe and America, western Atlantic, Mediterranean Sea and West Africa.

Habitat: It is always dominant at 50 m, with a maximum depth of 300 m (Hayward and Ryland, 1985).

Crisia elongata Milne-Edwards, 1838

(Pl. I, Fig. 1)

Crisia elongata Milne-Edwards, 1838: 203, pl. 7, Fig. 2; Braga and Barbin, 1988: 505, pl. 1, Fig. 2; Ziko and Hamza, 1987: 320, Fig. 2-4; Ziko and El-Sorogy, 1995: 82, Fig. 3: 1-2.

Description: Zoarium free, erect, articulated cylindrical stems with a tapering initial part, circular cross section and slightly depressed lateral parts, cellariiform (Crisiid). Autozooidal tubes cylindrical, only obvious near apertures, biserially arranged in alternating manner. Frontal convex. Orifice circular; peristome thin, little salient. Distance between peristomes exceeds the internode distance. Dorsal convex, smooth. Ovicell subglobular located between nodes.

Measurements:

Dz (4) 0.223-0.257 (0.021) 0.243 mm
Lz (1, 10) 0.402-0.432 (0.025) 0.418 mm
Do (2, 10) 0.060-0.073 (0.020) 0.062 mm
Dp (2, 10) 0.065-0.082 (0.019) 0.079 mm
Lov (2, 2) 0.490-0.510 (0.018) 0.498 mm
Iov (2, 2) 0.275-0.302 (0.012) 0.286 mm

Occurrence: Sirt Basin, As Sahabi area, locality P53 formation "M", Sample nos. 1- 5, 7 (Fig. 4).

Distribution: Eocene (France, and North America); Oligocene (France, Germany, and Italy); Miocene (Egypt, CSSR, France, Hungary, Italy, and Austria); Pliocene (Italy), Pleistocene (Egypt).

Habitat: Atlantic, Mediterranean, Red Sea, Japan, with a depth range of 0-59 m (Vavra, 1977).

Crisia hornesi Reuss, 1847

(Pl. 1, Fig. 2)

Crisia hornesi Reuss,1847: 54, Pl. 7, Fig. 21; Canu and Bassler, 1923: 704, pl. 141, Figs. 1-4; Vavra, 1977: 14; Ziko, 1994: 224; Ziko *et al*., 2000: 1465, Pl. 1, Fig. 1; El Safori. 2002: 426, Pl. 2, Fig. 3; Dulai et al., 2010: 40, pl. 3, Fig. 4.

Description: Zoarium free, erect, subcylindrical stem, cellariiform (crisiid). Frontal little convex, finely perforated. Autozooidal tubes little distinct, biserially arranged in an alternating manner. Orifice circular; peristome thin, little salient, rounded. Dorsal little convex, Ovicell not observed.

Measurements:

Dz (3) 0.503-0.522 (0.015) 0.513 mm
Lz ((1, 3) 0.362-0.394 (0.020) 0.374 mm
Do (2, 10) 0.065-0.078 (0.012) 0.071 mm
Dp (2, 10) 0.083-0.089 (0.006) 0.085 mm

Occurrence: Sirt Basin, As Sahabi area, locality P53 formation "M", Sample no. 3 (Fig. 4).

Distribution: Middle Miocene north of Western Desert and the western side of the Gulf of Suez; Eocene of France, Italy and North America; Oligocene of Germany, France, Italy and USA; Miocene of CSSR, Greece, Italy, Poland, Romania, Hungary, Portugal, Egypt; Pliocene – Pleistocene of Italy (Ziko, 1973; Vavra, 1977; El-Dera, 1996; El-Sorogy *et al*., 2001).

Habitat: Red Sea, Philippines at depth from 100 to 300m, temperature: 11.2ºC (Canu and Bassler, 1929; Ziko *et al*., 2000; El-Sorogy *et al*., 2001).

Family: Heterocycloeciidae, Canu, 1919
Tretocycloecia dichotoma (Reuss, 1848)

(Pl. I, Fig. 3)

Heteropora dichotoma Reuss, 1848: 35, pl. 5, Fig. 20.

Tretocycloecia dichotoma Vavra, 1977: 65; Vavra, 1979: 388, pl. 2, Fig. 2, Ziko, 1996: 69, pl. 7, Figs. 3, 4, 6, 7, 8, El Safori, 2002: 431, pl. 3, Fig. 3; Ziko *et al*., 2010: 92, pl. 4, Fig. 12, pl. 5, Fig. 1.

Description: Zoaria free, globular, vesicular, multilamellar, adeoniform. Autozooidal orifices subcircular, branching. Kenozooids very abundant arranged around autozooidal apertures in an irregular quincuncial pattern. Gonozooecium not observed. numerous separated by smaller polygonal mesopores, no peristome.

Measurements:

Dz (2) 1.356-1.510 (0.083) 1.433 mm
Do (1, 10) 0.084-0.095 (0.003) 0.087 mm
Dp (1, 10) 0.096-0.145 (0.088) 0.122 mm

Occurrence: Sirt Basin, As Sahabi area, locality P53 formation "M", Sample no. 5 (Fig. 4).

Order Cheilostomata Busk, 1852
Suborder: Anasca Levinsen, 1909
Family: Steginoporellidae Bassler, 1953
Steginoporella iberica reussi Pouyet and David, 1979.

Steginaporella iberica reussi, Poyet and David, 1979: 780, pl. 4, Fig. 3, text Fig. 3; Vavra, 1980, 55.

Description: Zoarium encrusts a fragment of *Pecten* sp., often represented by fragmented parts. Unilamellar, membraniporiform. Autozooids elongated hexagonal, arranged in alternating longitudinal rows, separated by thin furrows. Mural rim convex, thick, salient, finely granulated. Cryptocyst almost flat, perforated; the distal part, elevated, imperforated, grooved by two subsymmetrical, subcircular opesiules, placed just below the proximal border. Opesia large, subterminal, semicircular, transverse, with rounded distal and slightly concave proximal border; peristome thick, raised. B-zooids rarely observed.

Measurements:

Lz (1, 8) 0.856-1.047 (0.065) 0.875 mm
Iz (1, 8) 0.643-0.716 (0.048) 0.664mm
Lo (1, 8) 0.124-0.2336 (0.093) 0.225 mm
Io (1, 8) 0.335-0.390(0.013) 0.382 mm

Distribution: Miocene (Vienna Basin-Austria, Rhone Basin).

Occurrence: Sirt Basin, As Sahabi area, locality P53 formation "M", Sample nos 1, 5 (Fig. 4).

Family: Calpenciidae Canu and Bassler, 1923
Calpensia nobilis (Esper, 1796)

Cellepora nobilis Esper, 1796: 145.

Calpensia nobilis Zabala and Maluquer, 1988 : 90; Moissette, 1988: 96, pl. 4, Fig. 8; pl. 16, Figs. 11, 12; Hayward and McKinney, 2002: 31, Figs. 13 A-C.

Description: Colony encrusting unilamellar, multiserial. Autozooids distinct, elongated rectangular, arranged in alternating longitudinal rows, separated by thin furrows. Mural rim convex, thin, salient, granulated. Cryptocyst deep, little convex to flat, perforated and granulated, pierced by two small, rounded opesiules, placed at a little distance of opesium and close to mural rim. Opesia elliptical, transverse with rounded distal and concave to the little convex proximal border; peristome thick, salient. Ovicell not recognized.

Measurements:

Lz (1, 10) 0.598-0.702 (0.024) 0.657 mm
Iz (1, 10) 0.390-0.464 (0.015) 0.438 mm
Lo (1, 10) 0.090- 0.110 (0.010) 0.104 mm
Io (1, 10) 0.130- 0.200 (0.010) 0.148 mm

Occurrence: Sirt Basin, Sahabi area, locality P53 formation "M", Sample nos. 1, 2, 3 (Fig. 4).

Distribution: Miocene (Egypt, France, Italy, and Algeria); Pliocene (Italy and Tunisia); Pleistocene (Italy); Recent (the Mediterranean Sea and the Atlantic Ocean).

Family Thalamoporellidae Levinsen, 1902
Thalamoporella zaltaniensis El Safori and Muftah, 2019, (*in Press*)

Description: Zoarium encrusts and membraniporiform. Zooecia distinct, arranged in alternating longitudinal rows and separated by thin furrows. Mural rim thin, convex, slightly salient, granulated, basal part pierced by two and rarely one small spine with a thick base and abraded shaft. Cryptocyst shallow, little convex to flat, finely granulated and perforated, grooved by two small symmetrical rounded opesiuels, placed just below the proximal border of the opesia. Opesia elliptical with rounded distal and concave to the little concave proximal border; peristome thin, salient. Ovicells are not observed.

Measurements:

Lz (2, 7) 0.391-0.492 (0.036) 0.449 mm
Iz (2, 7) 0.187-0.282 (0.042) 0.253 mm
Lo (2, 7) 0.043- 0.057 (0.013) 0.050 mm
Io (2, 7) 0.101- 0.108 (0.006) 0.104 mm
Lav (1, 2) 0.558- 0.565 (0.013) 0.561 mm
Iav (1, 2) 0.276- 0.284 (0.006) 0.280 mm

Occurrences: Sirt Basin, As Sahabi area, locality P53 formation "M", Sample no. 7 (Fig. 4).

Family Cellaridae Fleming, 1828
Cellaria salicornioides Lamoroux, 1816

(Pl. 1, Fig. 4)

Cellaria salicornioides Lamouroux,1816: 127; Moissette, 1988: 104, pl. 17, figs. 1, 2; Hayward and McKinney, 2002: 36, Fig. 15F-K; Dulai *et al*., 2010: 36, pl. 2, Fig. 7.

Description: Colonies erect and branching, with cylindrical internodes consisting of alternating 8-10 autozooidal rows. Autozooids oval to hexagonal, with a regular quincuncial arrangement. Opesia subterminal, semicircular, mural rim short, bluntly tapered. Cryptocyst concave, finely granulated. Avicularia not common, distinct as large autozooid, with large subcircular rostrum. Ovicell is a simple round opening distal to the opesia.

Measurements:

Zd (1, 3) 0.730-0.832 (0.024) 0.760 mm
Lz (1, 10) 0.288-0.400 (0.024) 0.311 mm
Iz (1, 10) 0.266-0.311 (0.015) 0.297 mm
Lo (1, 10) 0.044- 0.067 (0.010) 0.057 mm
Io (1, 10) 0.097- 0.124 (0.010) 0.120 mm

Occurrences: Sirt Basin, As Sahabi area, locality P53 formation “M”, Sample no. 3 (Fig. 4).

Distribution: Miocene (Portugal, Italy); Pliocene (Italy); Pleistocene (Italy); Recent (Mediterranean Sea, Atlantic Ocean, Red Sea) (Moissette, 1988).

Habitat: Shallow coastal sublittoral waters (50 m-80 m).

Family Quadricellariiidae Gordon, 1984

Nellia tenella (Lamarck, 1816)

(Pl. 1, Fig. 5)

Cellaria tenella Lamarck, 1816: 135.

Nellia tenella Cheetham,1963: 59, pl. 1, Fig. 14; Braga, 1963: 27; El Safori, 2002: 426, pl. 5, Fig. 7; Di Martino *et al*., 2017: 109.

Description: Zoarium free, erect, straight, sometimes slightly curved, composed of four identical alternating autozooidal rows, open on four sides with square cross-section, cellariiform. Autozooids distinct, elongated, rectangular, separated by thin furrows. Mural rim convex, thin, salient. Gymnocyst smooth, slightly convex. Cryptocyst proximally placed, smooth, flat or slightly concave. Opeisa narrow elliptical to oval. Avicularia small paired, placed on gymnocyst at the proximelateral corners of autozooids, oval, pointing to the outside, with small central oval opesia. Ovicell endotoichal.

Measurements:

Lz (2, 10) 0.431-0.463 (0.007) 0.442 mm
Iz (2, 10) 0.243-0.274 (0.012) 0.261 mm
Lo (2, 10) 0.251- 0.267 (0.022) 0.264 mm
Io (2, 10) 0.112- 0.129 (0.013) 0.118 mm

Occurrence: Sirt Basin, As Sahabi area, locality P53 formation “M”, Sample nos. 1-7 (Fig. 4). Also reported from the overlying members "U1 and UD" of Sahabi Formation in the locality P96c section.

Distribution: Eocene (France); Eocene-Oligocene (USA); Miocene (Egypt, Jamaica, Austria); Pliocene-Pleistocene (USA).

Family Scrupocellariidae Levinsen, 1909
Scrupocellaria elleptica (Reuss, 1848)

(Pl. 1, Fig. 6)

Bactridium elleptica Reuss,1848: 148, pl. 11, Fig. 1-9.

Scrupocellaria elleptica Neviani,1900: 149, pl. 16, Figs. 2, 3; Vavra, 1979: 598, pl. 1, Fig. 1; Pouyet and Moissette, 1992: 47, pl. 6, Fig. 1, 2; Haddadi-Hamdane, 1996: 73, pl. 5, Fig. 5.

Description: Zoarium free, erect, subcylindrical stems, oval cross-section, tapering basal part, cellariform. Autozooids distinct rhomboidal cylindrical, more narrow at the proximal part, arranged biserrially in alternating rows on the zoarial front, separated by thin furrows. Mural rim convex, thick, provided by a triangular tubercles distally and laterally directed, granulated. Opesia distal, elongate elliptical. Avicularia lateral, salient, triangular. vibracula dorsal, sub-triangular, inconstant. Dorsal convex, finely granulated. Ovicell not observed.

Measurements:

Lz (2, 5) 0.368-0.437 (0.035), 0.410 mm
Iz (2, 5) 0.138-0.184 (0.016) 0.176 mm
Lo (2, 5) 0.189-0.253 (0.028), 0.228 mm
Io (2, 5) 0.069-0.119 (0.030) 0.103 mm

Occurrence: Sirt Basin, As Sahabi, locality P53 formation “M”, Sample nos. 1, 3, 5, 7 (Fig. 4). Also reported from the overlying member "U1" of Sahabi Formation in the locality P96c section.

Distribution: Eocene (France, Italy, Hungary, and France); Oligocene (Italy and France); Miocene (Egypt, Libya, France, Iran, Portugal, Austria, and Belgium); Pliocene (Portugal, Spain, Italy, and Tunisia); Pleistocene (Egypt, Algeria, and Italy).

Suborder Ascophora Levinsen, 1909
Family: Margarettidae Harmer, 1956
Margaretta cereoides (Ellis and Solander, 1786)

(Pl. 1, Fig. 7)

Cellaria cereoides Ellis and Solander, 1786: 26, pl. 5, Figs. B-E.

Margaretta cereoides Buge and Debourle, 1977: 344, pl. 8, Fig. 3; Vavra, 1979: p. 603, pl. 1, Fig. f ; Ziko and Hamza, 1987: p. 305, Fig. 77; Schmid, 1989: p. 52, pl. 15, Figs. 4, 5, 7, 8; Ziko, 1996: p. 136, Figs. 4-5; El Safori, 2002: 450, pl. 7, Fig. 6; Dulai *et al*., 2010: 37, pl.4, Fig. 3

Description: Zoarium free, erect, dishotomous, cylindrical stems, elliptical, arranged in alternating longitudinal rows separated by shallow furrows. Frontal convex, thick, tremocyst with numerous, large pores. Aperture subterminal, subcircular; proximal border concave; peristome thick, short. Avicularia peristomial, median, small, elongate, oval, sometimes not observed.

Measurements:

Lz (2, 10) 1.230-1.432 (0.095) 1.389 mm
Iz (2, 10) 0.464-0.497 (0.012) 0.477 mm
Lo (2, 10) 0.122- 0.142 (0.024) 0.132 mm
Io (2, 10) 0.164- 0.178 (0.017) 0.171 mm

Occurrence: Sirt Basin, As Sahabi area, locality P53 formation “M”, Sample nos. 5, 7 (Fig. 4).

Distribution: Eocene (Spain, Italy, France, and Egypt); Oligocene (Italy, Germany, Austria, Poland, and USA); Miocene (Italy, France, Egypt, Austria, Poland, Romania, Libya, Algeria, and Morocco); Pliocene (Italy, North Africa, and Central America).

Habitat: Adriatic, Mediterranean, Pacific, and Red Sea; Atlantic in tropical and subtropical regions (Schmid, 1989).

Family: Celleporidae Busk, 1852
Celleporaria desioi (Cipolla, 1929)

(Fig. 6)

Holoporella desioi Cipolla, 1929: 379, pl. 43, Figs. 4-8, pl. 44, Figs. 2, 6; Annoscia, 1969: 88, pl. 1, Figs. 16-18.

Celleporaria desioi El Safori, 2002: 453, pl. 7, fig. 8.

Description: Zoarium cap-shaped, large-sized, multiserial, multilayered with a pimply surface, sometimes ovoid (Fig. 6). Autozooids ovoid, distinct, irregularly arranged in rows, separated by thin furrows. Frontal thin, convex, finely granulated. Aperture subcircular, umbonate with a slightly concave narrow poster. Adventitious

avicularia suboral on the top of the apertures mucrons. Vicarious avicularia absent. Ovicells not observed.

Measurements:

Lz (1, 10) 0.238-0.362 (0.074) 0.310 mm
Iz (1, 10) 0.187-0.243 (0.120) 0.238 mm
Lo (1, 10) 0.066- 0.075 (0.093) 0.064 mm
Io (1, 10) 0.065- 0.093 (0.040) 0.082 mm

Occurrence: Sirt Basin, As Sahabi area, locality P53 formation “M”, Sample nos. 5 (Fig. 4).

Distribution: Miocene (Egypt, and Libya).

Fig. 6. *Celleporaria desioi,* formation "M", P53 As Sahabi area (scale bar=2 cm).

Celleporaria polythele (Reuss, 1848)

Cellepora polythele Reuss, 1848: 77, pl. 9, Fig. 18.

Holoporella polythele Canu, 1912: 217, pl. 12, Figs. 1-5, pl. 13, Figs. 6, 7; Souaya, 1965: 1141, pl. 139, Figs. 1, 2.

Celleporaria polythele David *et al*., 1970: 45; El Safori, 2000: 405, fig. 5: 7; El Safori, 2002: 451.

Description: Zoarium free, massive, thick, globular, multilamellar, celleporiform. Autozooids crowded, distinct, salient, disoriented represented by variable sizes. Frontal oloyest, very convex, bordered by areolar pores, which are more definite in large Autozooids. Orifice subcircular; proximal border convex, obliques. Avicularia rest on mucron, small, triangular, median, inconstant. Vicarious avicularia, rare or absent. Ovicell hyperstomial, commonly broken.

Measurements:

Lz (2, 10) 0.334-0.350 (0.032) 0.345 mm
Iz (2, 10) 0.376-0.395 (0.028) 0.387 mm
Lo (2, 10) 0.105- 0.123 (0.026) 0.110 mm
Io (2, 10) 0.110- 0.132 (0.017) 0.119 mm

Occurrence: Sirt Basin, As Sahabi area, locality P53 formation “M”, Sample no. 5 (Fig. 4).

Family Phidoloporidae Gabb and Horn, 1862
Schedocleidochasma incisa (Reuss, 1874)

(Pl. 1, Fig. 8)

Lepralia incisa Reuss, 1847: 168, pl. 3, Fig. 4.

Buffonellodes incisa David and Pouyet, 1974: p. 170, pl. 9, Fig. 7; Pouyet and Moissette, 1992: 61, pl. 9, Fig. 3; Pouyet, 1997, p. 62, pl. 6, Fig. 5.

Schedocleidochasma incisa Berning, 2005: 120, pl. 12, Figs. 8, 9, 12.

Description: Colony encrusting unilaminar, multiserial. Autozooids elliptical to hexagonal, separated by either distinct grooves or indistinct sutures on marked ridges; frontal wall convex, smooth, with two large elongated pores in marginal corners at mid-distance. Orifice large, comprising more than one-third of zooid length, cleithridiate, anter large, round, set off from the smaller, round or semielliptical poster by a pair of pointed condyles directing downwards and proximally; three distal oral spines (up to five in astogenetically young zooids). Ovicell globular, recumbent on distal zooid, slightly longer than wide, surface imperforate, smooth and flattened frontally, with a pair of narrow proximolateral fissures delimiting a simple labellum with a straight or slightly concave proximal edge. Interzooidal avicularium common, single, originating from a marginal corner at mid-distance from an areolar pore, situated lateral or proximolateral to poster; cystid slightly was swollen; rostrum elongated triangular, directing laterally or distolaterally; crossbar complete without columella.

Measurements:

Lz (1, 10) 0.268-0.320 (0.074) 0.289 mm
Iz (1, 10) 0.219-0.289 (0.030) 0.244 mm
Lo (1, 10) 0.097- 0.121 (0.023) 0.109 mm
Io (1, 10) 0.060- 0.116 (0.018) 0.075 mm
Lov (1, 10) 0.152-0.180 (0.013) 0.164 mm
Iov (1, 10) 0.182-0.195 (0.010) 0.189 mm
Lav (1, 10) 0.112-0.125 (0.023) 0.120 mm
Iav (1, 10) 0.050-0.065 (0.020) 0.061 mm

Occurrence: Sirt Basin, As Sahabi area, locality P53 formation “M”, Sample nos. 1, 7 (Fig. 4).

Distribution: Miocene (Egypt, Portugal, France, Italy, Austria, Poland, Guadalquivir, Spain, Algeria, Morocco); Pliocene (Spain, Italy).

4. Results and discussions

The Miocene bryozoans of North Africa and South Europe are represented in stratigraphic levels without specific new occurrences (Moissette, 1988; El Hajjaji, 1992). However, evidences for a bryozoan event during Badenian (a central Paratethys stage) of Middle Miocene time were recognized in several sections in North-South transect through the Paratethys (Zagoršek, 2015). As indicated by Holcová and Zágoršek (2008), the main factor for bryozoan accumulation is probably changes in trophic condition, together with high variability of temperature. Evidences from Paratethys Middle Miocene bryozoans without major occurrences in the bryozoan species but rather they show changes in growth from North (erect) to South (encrusting) along the Paratethys. The slight changes in bryozoan event can be recognized from their stratigraphic distributions and the domain of some species on certain horizons. El Safori (2002) recognized two bryozoan assemblage zones from Siwa Oasis accompanied by the water transgression of middle Serravallian (Siwa sequence). These assemblages are close to equivalent assemblages from the Ar Rahla Member of the Maradah Formation (El Safori and Muftah, in press). The Pre-Sahabi succession of formation "M" is dated Tortonian based on the presence of foraminifers and calcareous nannofossils (Muftah *et al*., 2013) as well as Strontium isotopic dating (El-Shawaihdi *et al*., 2014) which representing the Late Serravallian 2nd bryozoan assemblage defined from Siwa. In addition, it is the equivalent to Serravallian-Tortonian bryozoan Member that defined from the Cairo-Suez Road section (Cherif and Yahia, 1977) on a stratigraphical basis.

A shallow neritic depositional environment for formation "M" has been interpreted by De Heinzelin and El-Arnauti (1982, 1983 and 1987) according to the lithological nature and faunal contents. The macro/microfossil contents suggest a depositional setting under transgressive inner neritic marine environment. The presence of low diversity bryozoans (*Nellia tenella, Crisia* spp., *Celleporaria desioi, Calapensia* sp., *Cellaria* sp., *Scrupocellaria elleptica* and *Steginoporella iberica reussi*) at some levels is clearly indicative of shallow water with low rate of sedimentation (Lagaaij and Gautier, 1965; El Safori, 2000). The presence of the membranous type *Cel-*

leporaria desioi is very characteristic in this formation (Fig. 6), altogether with the associated species that listed in Fig. 5 are indicating the shallow marine environment of low energy conditions (Lagaaij and Gautier, 1965; El Safori, 2000). On the other hand, only three species of the above-mentioned list (*Nellia tenella, Scrupocellaria elleptica* and *Crisia* sp) are reported from the locality P96c Profile of Sahabi Formation in members "U1" and "UD" (Muftah, 2013). The presence of these three species alone indicates low energy shallow marine environment of less than 50 m.

5. Conclusions

The shallow marine carbonates of formation "M", the Late Miocene (Tortonian) pre-Sahabi Formation at P53 in the As Sahabi area, Sirt Basin contained low diverse and bryozoan remains. A descriptive taxonomy has been performed for fourteen species from this measured Tortonian formation "M". The reported assemblage is closely similar to that described by Cherif and Yahia, (1977) in Cairo-Suez roadcut section and partly to which represents the 2nd bryozoan assemblage defined from Siwa (El-Safori, 2002) and from the Ar Rahlah Member of Maradah Formation El-Safori and Muftah, 2019 (*in press*). Most of the bryozoan taxa described herein are indicative to shallow marine warm water with low sedimentation energy. The concerned taxa more or less inhabit wide geographical distribution with shallow marine environment.

Acknowledgments

We would like to thank East Libya Neogene Research Project (ELNRP) for the logistic support of the field trip. Our gratitude is also to Ain Shams University, Athens University and Benghazi University for giving us all means of support to produce this paper.

References

Annoscia E., (1969) The bryofauna of mesomiocenic al Jaghbub formation in eastern Cyrenaica (Lybia), Proc. Third Afr. Micropaleontology, Colloquium (1968), Le Caire: 37-94.

Bassler, R. S. (1953) Bryozoa. In: Moore, R.C. (Ed.) Treatise on Invertabrate Paleontology, Part G; Geol. Soc. America, University of Kansas Press, 175 p.

Berning B. (2005) The late Tortonian cheilostome Bryozoa from Niebla (Guadalquivir Basin, SW Spain): implications for Atlantic-Mediterranean environment and biogeography during the late Neogene Dissertation, zur Erlangung des Doktorgrades der Naturwissenschaften im Fachbereich Geowissenschaften der Universität Hamburg vorgelegt von: 170p.

Braga, G. (1963) 'I Briozoi del' Terziario veneto. l° Contributo', *Boll. Soc. Paleont. Ital., Modena*, 2, 1, pp. 16-55.

Braga, G. and Barbin, V. (1988) 'Les bryozoaires du Priabonien Stratotypique (Province Vicenza, Italy)', *Rev. Paleobiol.*, 7, pp. 495-565.

Buge, E. and Debourle, A. (1977) 'Ecologie de la faune de Bryozoaires d'un plage des environs de Tripoli (Libye)', *Bull. Cent. Rech. Pau*, 1, 2, pp. 321-377.

Canu, F. (1912) "Etude comparée du Bryozoaires helvétiens de l' Égypt avec les Bryozoaires vivants de la Méditerranée et de La Mer Rouge', *Mém. Inst. Egypt., Paris*, 6, 3, pp. 185-236.

Canu, F. and Bassler, R. S. (1923) 'North American later Tertiary and Quaternary Bryozoa', *United States National Museum Bulletin*, 125, pp. 1-302.

Canu, F. and Bassler, R. S. (1929) 'Bryozoa of the Philippine Region', *Proc US Nat Mus*., 100, 9, pp. 1–685.

Cheetham, A. H. (1963) 'Late Eocene zoography of the Eastern Gulf Coast region', *Mem. Geol. Soc. Amer*., 93, pp. 1-113.

Cherif, O. H., Yehia, M. A. (1977) 'Stratigraphy of the area between Wadi Gimal and Wadi Hommath, Gulf of Suez, Egypt', *Egyptian Journal Geology*, 21, 2, pp. 185-203.

Cipolla, F. (1929) Briozoi, Resultati Scientifici della Missione alla Oasi di Giarabub (1926-1927). Fasc. III: La Paleontologia; R. Soc. Geogr. Roma 351-396 p.

David, L., Mongereau, N., and Pouyet, S. (1970) 'Bryozoaires du Néogéne du Bassin du Rhône Gisements burdigaliens de Taulignan (Drôme). Docum. Lab. Góol', *Fac. Sci. Lyon*, 40, pp. 97-175.

David, L., and Pouyet, S. (1974) 'Révision des Bryozoaires Cheilostomes Miocénes du Bassin de Vienne- Autriche. Doc. Un. Lab. Géol', *Fac. Sci. Lyon.*, 60, pp. 83-257.

De Heinzelin, J., El-Arnauti, A. (1982) 'Stratigraphy and geological history of the Sahabi and related formations', *Garyounis Scientific Bulletin, Special Issue*, 4, pp. 5-12.

De Heinzelin, J., El-Arnauti, A. (1983) Geology of the Sahabi area with a geological map at scale 1:25000. Research Centre of Garyounis University, Benghazi, Libya. (Edited by the section of Cartography and Photo-Interpretation of the Royal Museum for Central Africa, Tervren, Belgium) in commission of the Research Centre, Caryounis University, Benghazi, Libya.

De Heinzelin, J., El-Arnauti, A. (1987) The Sahabi Formation and related deposits. In: (eds. Boaz, N., El-Arnauti, A., Gaziry, A., De Heinzelin J., Boaz, D.D.). Neogene Paleontology and Geology of Sahabi. Alan R. Liss, New York: 1-21.

Di Martino, Emanuela, Taylor, Paul D. & Portell, Roger W. (2017) 'Bryozoans from the Lower Miocene Chipola Formation, Calhoun County, Florida, USA', *Bulletin of the Florida Museum of Natural History*, 53, 4, pp. 97-200.

Dulai, A., Moissette P. and Muller, P. (2010) Badenian (Middle Miocene) bryozoan fauna of Hungary; basic data of localities and samples, Fragmenta Palaeontologica Hungarica 28, pp. 33-69.

El-Arnauti, A. and El Sogher, A. (2004) Short Notes and Guidebook on the Geology of Qasr As Sahabi Area. Tripoli, Earth Science Society of Libya, pp. 1-95.

El-Dera, N. (1996) Miocene Bryozoa of Mersa Matruh area. (Unpublished Ph.D. thesis) Zagazig University, 1-220. Geol. Dept., Zagazig Univ. Zagazig, pp. 1-156

El Hajjaji, K. (1992) 'Les bryozoaires du Miocene superieur du Maroc Nord-oriental, Docum. Lab. Geol', *Fac. Sci. Lyon*, 123, 355p.

Ellis, J. and Solander, D. C. (1786) The natural history of many curious and uncommon zoophytes, collected from various parts of the globe Vol, White & Elmsly, London, pp. 1-206.

El Safori, Y. A. (2000) Early Eocene bryozoans of the Farafra Oasis, Egypt. Proceeding of the 11th International Bryozoology Association Conference, Panama: 232-237.

El Safori, Y. A. (2002) 'Taxonomy, stratigraphy, and paleoecology of the Miocene bryozoans of Siwa Oasis, Egypt. Egypt', *Jour. Paleontol*., 2, pp. 417-464.

El Safori, Y. A., and Muftah, A. M. (2019) Miocene Bryozoans from Jabal Zaltan, NE Sirt Basin, Libya, *Egyptian Journal of Paleontology*, (in press).

El-Shawaihdi, M. H., Muftah, A, M., Mosely, P. S., Boaz, T. N. (2014) 'New age constraints for Neogene sediments of the Sahabi area, Libya (Sirt Basin) using strontium isotope (87Sr/86Sr) geochronology and calcareous nannofossils', *Journal of African Earth Sciences*, 89, pp. 42-49.

El-Shawaihdi, M.H., Mozley, P.S., Boaz, N.T., Salloum F., Pavlakis P., Muftah, A., Triantaphyllou, M. (2016) 'Stratigraphy of the Neogene Sahabi Units in the Sirt Basin, northeast, Libya', *Journal of African Earth Sciences*, 118, pp. 87-106

El-Sorogy, A. S., Abdelwahab, M., Ziko, A. and El-Dera, N. (2001) 'New Bryozoan Records from the Recent coral reefs, Dahab Bay, Gulf of Aqaba, Egypt. Egypt', *Jour. Paleontol*., 1, pp. 53-80.

Esper, E. J. C. (1796) Forsetzungen der Pflanzenthiere in Abbildungen nach der Natur mit Farben erleuchtet hebst Beschreibungen Vol. Theil 1, pp. 1-230. Nürnberg.

Giglia, G. (1984) Geological Map of Libya 1:250.000 Sheet: Ajdabia (NH34-6). Industrial Research Center. Tripoli Libya, pp. 1- 93.

Haddadi-Hamdane A. (1996) Bryozoaires du Pliocène du Sahel d'Alger. Documents des Laboratoire de Géologie de Lyon 140, pp. 1–189.

Hayward, P. J., and Ryland, J. S. (1985) Cyclostome bryozoans. In Kermack, D.M. and Barnes, R.S.K. (eds.), Synopses of the British Fauna (new series); Linn. Soc. London, pp. 1-147.

Hayward, P. J. and McKinney, F. K. (2002) Northern Adriatic bryozoa from the vicinity of Rovinj, Croatia. Bull. Amer. Mus. Nat. Hist. New York, 270, pp. 1-139 .

Holcová, K. and Zágoršek, K. (2008) 'Bryozoa, foraminifera and calcareous nannoplankton as environmental proxies of the âœbryozoan eventâ in the Middle Miocene of the Central Paratethys (Czech Republic)', *Palaeogeography Palaeoclimatology Palaeoecology*, 267, pp. 216-234.

Lagaaij, R. and Gautier, Y. V. (1965) 'Bryozoan assemblages from marine sediments of the Rhone delta, France', *Micropaleontology*, 11, 1, pp. 39-58.

Lamarck, J. B. (1816) Histoire naturelle des Animaux sans Vertébres. Paris, Lére édit., 568 p.

Lamouroux, J. V. F. (1816) Histoire des polypiers Coralligènes Flexibles, vulgairement nommés Zoophytes Vol. pp. 1-559.

Linnaeus, C. (1758) Systema Naturae per regna tria naturae, secundum classes, ordines, genera, species, cum characteribus, differentiis, synonymis, locis. Editio decima, reformata. Laurentius Salvius: Holmiae. ii, 824p.

Milne-Edwards, H. (1838) 'Mémoire sur les Crisies, les Horneres et plusieure autress Polypes vivants ou fossiles dont l'organisation est analogue a celle des Tubulipores', *Ann. Sci. Nat.*, Paris, 2, 9, pp. 193-238;

Moissette, P. (1988) 'Faunes de bryozoaires du Messinien d' Algérie occidentale', *Doc. Lab. Géol. Lyon*, 102, 351p.

Muftah, A. M. (2013) Biostratigraphic and temporal relations between the Neogene Sahabi and Maradah formations, Libya. Contribution to the age determination of their contained mammalian paleofaunas. (Ph.D. Thesis), University of Athens, Greece. 227p.

Muftah, A. M., El Mehaghag, A. A., Starkie, S. (2008a) Biostratigraphical notes on the As Sahabi stratigraphic boreholes 1 and 2, Sirt Basin, Libya. in: Boaz, N. T., El-Arnauti, A., Pavlakis, P., Salem, M. J. (Eds.), *Garyounis Scientific Bulletin*, *Special Issue*, No. 5, pp. 47-57.

Muftah, A. M., Salloum, F., El-Shawaihdi, M. H., Al-Faitouri, M. S. (2008b) A contribution to the stratigraphy of Formations of the As Sahabi Area, Sirt Basin, Libya. In: Boaz, N. T., El-Arnauti, A., Pavlakis, P., Salem, M. J. (Eds.), *Garyounis Scientific Bulletin, Special Issue*, No. 5, pp. 33-45.

Muftah, A.M., Pavlakis, P., Godelitsas, A., Gamaletsos, P. and Boaz, N. (2013)' Paleogeography of the Eosahabi River in Libya: New insights into the mineralogy, geochemistry and paleontology of Member U-1 of the Sahabi Formation, northeastern Libya, *Journal of African Earth Sciences*, 78, pp. 86-96.

Muftah, A. M., El-Shawaihdi, N. H. and Al Riaydh, M. H. (2019) Coprolites from the Neogene Sahabi Formation, northeastern Sirt Basin of Libya. Arabic Journal of Geoscience, (*in press*)

Neviani, A. (1900) 'Briozoi neogenici delle Calabrie', *Palaeontographia, Ital., Pisa*, 6, pp. 115-265.

Pouyet, S. (1997) 'Les Bryozoaires du Badenien (Miocene Moyen) d'Olimpow (Pologne)', *Doc. Lab. Geol. Lyon*, 145, 1-124.

Pouyet, S. and David, L. (1979) Revision systematique du genre steginoporella Smitt, 1873. (Bryozoa Cheilostomata). Geobios, Lyon, 12, 6, pp. 763-817.

Pouyet, S., and Moissette, P. (1992) 'Bryozaires du Pliocene D'altavilla (Sicile-Italie): Revision de la collection Cipolla, Nouvelles donnees, paleoecologi', *Palaeontographica, Stuttgart, No. 223*: 19-101.

Reuss, A. E. (1847) Die fossilen Bryozoen des Oesterreichisch ungarischen Miocäns. Denks. K. Akad/Wiss., (Math. Natur. Cl.), 33, 1, pp. 141-190.

Reuss, A. E. (1848) Die fossilen polyparien des Wiener Tertiarbeckens. Haiding. Naturwiss. Abh., Wien, 2, 1, pp. 1-109.

Roohi, H. (1993) A geological view of source reservoir relationships in the western Sirt Basin. M. J. Salem, A. S. El Hawat and A. M.Sbeta (Eds.) In: The Geology of Sirt Basin, Volume II: 323-336. Tripoli-Libya.

Schmid, B. (1989) 'Cheilostome Bryozoen aus dem Badenien (Miozän) von Nussdorf (Wien)', *Beitr. Paläont. Oesterr*., 15, 101p.

Souaya, F. J. (1965) 'On the foraminifera of Gebel Gharra (Cairo-Suez Road) and some other Miocene samples', *Journal of Paleontology*, 37, 2, pp. 433-457.

Vavra, N. (1977) Bryozoa tertiaria In. zapfe, H: Catalogus Fossilium Austriae. Oesterreich. Akad. Wiss., Vol. 3, 210p.

Vavra, N. (1979) Die Bryozoenfaunen des Öesterreichischen Teritäirs (Bryozoa from the Austrian Tertiary). Neues Jahr. Geol. Paläont. Abh., Vol. 157, No. 3, pp. 366-392.

Vávra, N. (1980) Tropische Faunenelemente in den Bryozoenfaunen des Badenien (Mittelmiozän) des Zentralen Paratethys. Sitzungberichte öst. Akad. Wiss., 189, pp. 49-63.

Willems, W. and Meyrick, R. (1982) 'Preliminary report on the marine microfauna (Foraminifera, Ostracoda) of the Sahabi and related formations in Northern Libya', *Garyounis Scientific Bulletin, Special Issue,* 4, pp. 19-25.

Winston, J. E. (1982) Marine bryozoans (Ectoprocta) of the Indian River area (Florida). Bulletin of the American Museum of Natural History, 173, pp. 99–176.

Zabala, M., and Maluquer, P. (1988) Illustrated keys for the classification of Mediterranean Bryozoa. Treballs del Museu de Zoologia, Barcelona, 4, pp. 1-294.

Zagoršek K. (2015) Palaeobiography of selected taxa of Miocene Bryozoa, Hantkeniana 10, Budapest Barnabás GÉCZY Jubilee Volume, pp. 125–134.

Ziko, A. (1973) A study on some Tertiary Bryozoa from Egypt.- Unpubl. M.Sc. thesis, Geol. Dept., Ain Shams Univ., Cairo: 141p., 24 pls.

Ziko, A. (1994) Paleoenvironmental implications of thee Miocene bryozoans of Egypt: a preliminary note. In: Hayward,P.J., Ryland,J.S. & Taylor, P. D., (Eds.): Biology and Palaeobiology of Bryozoans, Olsen & Olsen: 223-226.

Ziko, A. (1996) 'Middle Miocene byrozoa of West-Centeral Sinai, Egypt.- M.E.R.C.', *Ain Shams Univ., Earth Sci. Res*., 10, pp. 124-146.

Ziko, A. and El-Sorogy, A. S. (1995) 'New Bryozoan records from the Pleistocene coral reefs, Red Sea coast, Egypt. M. E. R. C.', *Ain Shams Univ., Earth Sci*., 9, pp. 80-92.

Ziko, A., and Hamza, F. (1987) Bryozoa fauna from a post-Pliocene outcrop North of the Giza Pyramids plateau, Egypt. In: Ross. J.R.P. (Ed.) Bryozoa Present and Past. Water in Washington. Univ. Bellinghom, pp. 301-308.

Ziko, A., Eweda, SH. and El-Khawaga, S. (2010) 'Middle Miocene cyclostomatous bryozoans from Cyrenaica, North Western Desert, Egypt', *Jour. Paleont*., 10, pp. 61-106.

Ziko, A., El-Sorogy, A., Zalat, A., Eweda, SH. and Saber, N. (2000) Middle Miocene Bryozoa from Siwa Oasis, Western Desert, Egypt. 5th intern. Conf. on the Geol. of the Arab.

Plate 1

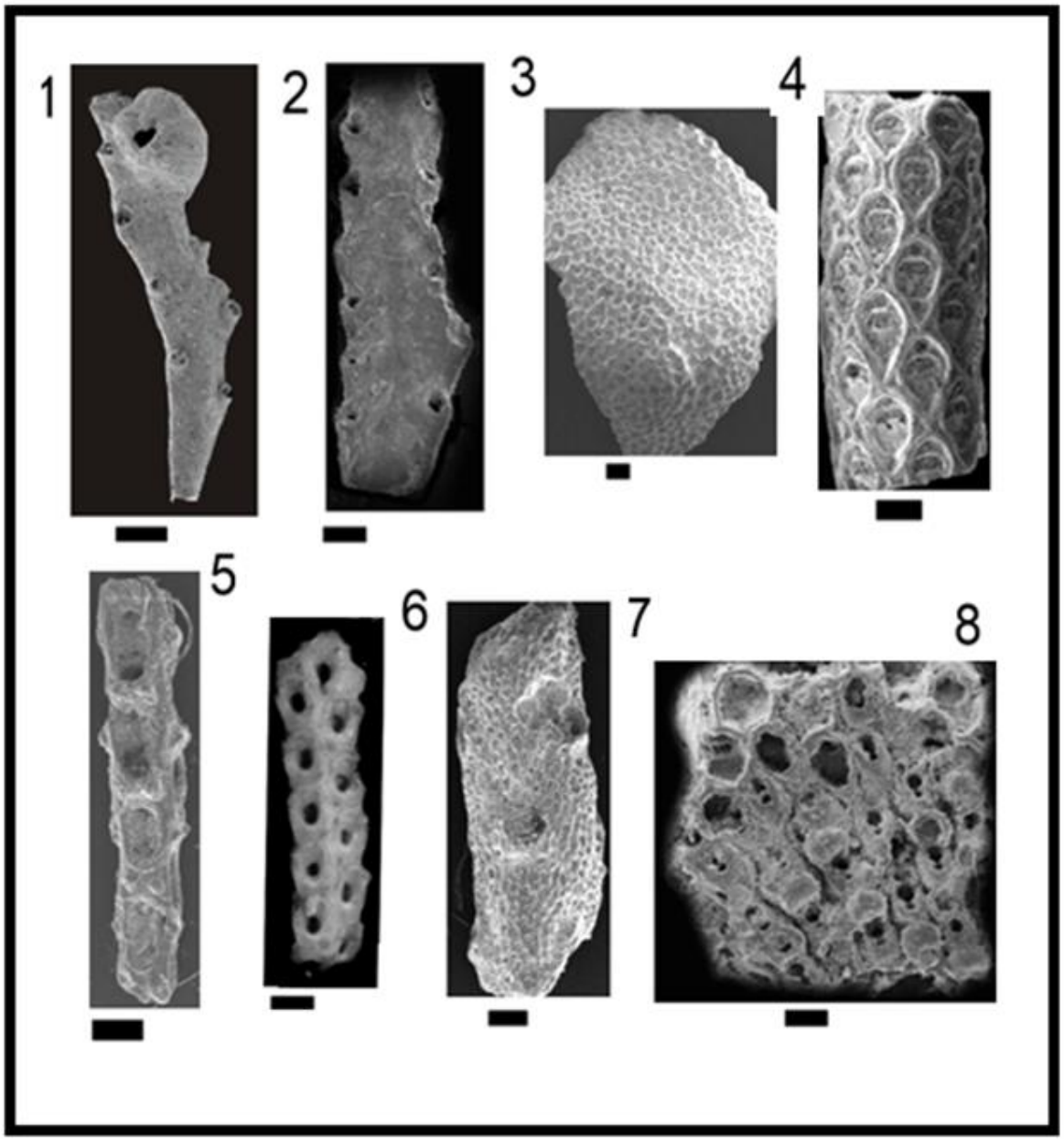

Explanation of Plate I (Scale bar =100 µm)

1. *Crisia elongata* (Linnaeus, 1758)
2. *Crisia hornesi* Reuss, 1847
3. *Tretocycloecia dichotoma* (Reuss, 1848)
4. *Cellaria salicornioides* Lamoroux, 1816
5. *Nellia tenella* (Lamarck, 1816)
6. *Scrupocellaria elleptica* (Reuss, 1848)
7. *Margaretta cereoides* (Ellis and Solander, 1786)
8. *Schedocleidochasma incisa* (Reuss, 1874)

Libyan Journal of Science & Technology 9:2 (2019) 165–167

Faculty of Science - University of Benghazi

Libyan Journal of Science & Technology

journal home page: www.sc.uob.edu.ly/pages/page/77

Measurement of Radium Equivalent Activity from Natural Occurring Radionuclides in Soil in the East Coast of Libya

Saeid Y. Elorfi*, Marai M. Imsallim, Yasin K. Abdalla

Department of Physics, Faculty of Science, University of Benghazi, Benghazi, Libya

Highlights

- **The measurement of the concentration of background radionuclides in soil in the East Coast of Libya indicated that the levels of the average activity to be within world average.**
- **It is observed that the concentrations of naturally occurring radionuclides increase with increasing altitude of the sample site locations.**
- **There is good correlation between soil structure and radioactivity content especially grain size.**
- **Radioactivity from natural occurring radionuclides is present everywhere at different levels, which could be attributed to geological and geographical conditions.**

ARTICLE INFO

Article history:
Received 27 September 2018
Revised 26 June 2019
Accepted 30 June 2019
Available online 01 July 2019

Keywords:
Radium equivalent, soil, absorbed dose, concentration.

* Corresponding author:
E-mail address: saeidelorfi@gmail.com
S. Y. Elorfi

ABSTRACT

The technological development, using atomic, and nuclear energy in industry, agriculture, nuclear medicine, nuclear wars and tests may increase environmental pollution with noticeable concentrations of man-made radionuclides in the environment. This experimental work aims at the determination of radium equivalent activity from the soil samples collected from sites extending from Benghazi city to the Libyan-Egyptian borders, along 600 km. Samples collected from fifty chosen sites, kept for four weeks to get a secular equilibrium between ^{226}Ra and ^{232}Th and their corresponding daughters. The result indicated that the value of radium equivalent (Ra_{eq}) ranged from 208.919 to73.881 Bq/kg, with an average of 117.587 Bq/kg

1. Introduction

Industry and all form of life on earth have been unavoidably exposed to radiation from all kind of sources. Exposer to natural sources vary little from year to year and involves the whole world population to almost the same extent. The exposure dose from natural sources depends mainly on the place of residence, and altitude. For most world population, the range of individual effective dose from natural sources is between one-half and two times the average global value at sea level which is 2.4 *mSv per year* (UNSCEAR, 1988).

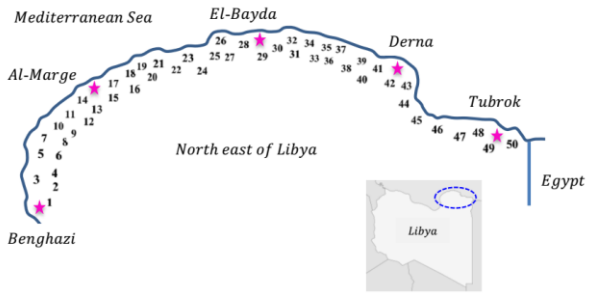

Fig. 1. Shows the sites of collected samples in the area extended from Benghazi city to the Libyan-Egyptian borders

Study of natural radiation background and exposure of human beings are of great importance, not only for practical reasons but also for the radiological impact of nuclear activities. Radioactivity is present everywhere due to geological and climate conditions. The activities of mankind may also enhance the level of radioactivity in our world. Radiation comes from different sources; mainly, electromagnetic rays such as gamma-ray emitters in soils, water, food, building materials, and air. Levels of radionuclide distribution in the environment have been studied providing essential radiological information. Soils may contain a significant amount of radioactivity. Several studies worldwide have measured the activity concentration of natural radionuclides in soil and gave valuable information about the levels of contamination (Quinds *et al.*, 1994; Taiwo *et al.*, 2014). A number of human activities contribute to our natural radiation environment and may result in the production of radioactive nuclides (Scholten *et al.*, 2005; Malik, 1994). Ingesting and inhaling such levels of radionuclides contribute significantly to the radiation dose that people receive (Saleh, *et al.*, 2007).

2. Sampling Procedures

Soil samples were collected from the fifty chosen sites shown in Fig. 1, using template a 25 cm×25 cm area sample was cut out using the template for guidance to a depth of 5 cm. Each sample was air-dried to avoid loss of radionuclides (IAEA, 1989). The dried samples each were thoroughly ground to ensure equal representation of samples. The samples were transferred to plastic Marinelli beakers (100 or 1000 ml capacity) made to fit on the high purity germanium detector. Each sample was sealed with adhesive tape and left for 21 days for the short-lived radionuclide to allow radon and its short-lived progenies attain secular equilibrium. Samples were analyzed by high-resolution gamma-ray spectroscopy using high purity germanium detector type Tennelec model CPCVS 30-30195 (active volume 155cc) with 30% photo peak efficiency and 1.95 keV FWHM for 1.33 MeV of Co-60 gamma transition connected

 ISSN 2663-1407; National Library of Libya, Legal number: 390/2018

to an Ortec series multichannel analyzer (MCA). The gamma-ray spectrometer is coaxial of vertical configuration and consists of a preamplifier, a linear amplifier, an analog-to-digital converter (ADC).

3. Radium Equivalent Activity Calculations

To assess the radiological hazard of possible changes of soil due to various geological processes or any artificial influences, it is useful to calculate an index called radium equivalent Ra_{eq} expressed in Bq/kg. The radium equivalent Ra_{eq} is defined according to the estimation that 10 Bq/kg of ^{226}Ra, 7 Bq/kg of ^{232}Th and 130 Bq/kg of ^{40}K produce the same ϒ-ray dose. (Beretka *et al.*, 1985; El-Tahawy *et al.*, 1992). The radium equivalent (Ra_{eq}) expressed in Bq/kg was calculated using the following equation:

$$Ra_{eq}(Bq.kg^{-1}) = A_{Ra} + 1.43\,A_{Th} + 0.077\,A_K$$

Where A_{Ra}, A_{Th} and A_K are the activity concentrations of ^{226}Ra, ^{232}Th and ^{40}K, respectively, in this calculations we used ^{238}U for (^{226}Ra), ^{232}Th and ^{40}K radionuclides. (Girigisu *et al.* 2013; Darwish *et al.*, 2015). The results are shown in Table 1 where maximum and minimum values are shown in bold.

Table 1.

Concentration of radionuclide in soil Bq/kg and Radium equivalent

Site No.	^{40}K	^{238}U	^{232}Th	Radium equivalent (Ra_{eq}Bq/kg)
1	660.9±21.9	29.4±1.4	31.9±2.3	125.906
2	638.6±32.5	32.5±1.1	43.9±1.5	144.449
3	780.3±25.6	41.7±2.2	48.2±2.6	170.709
4	754.1±11.9	44.1±0.8	50.1±0.8	173.809
5	744.0±47.5	47.5±2.2	49.2±2.8	175.144
6	725.8±14.4	43.9±1.2	48.5±1.5	169.142
7	644.1±25.9	42.7±2.8	51.7±2.9	166.227
8	688.0±14.4	41.9±1.2	50.1±1.6	166.519
9	845.0±33.6	46.9±3.3	67.8±4.3	**208.919**
10	830.0±37.0	48.7±3.3	61.2±1.8	200.126
11	858.7±32.7	44.0±3.4	60.2±3.6	196.206
12	807.1±12.7	38.0±0.8	58.8±1.1	184.231
13	669.6±28.9	43.8±2.6	43.4±3.5	157.421
14	714.0±15.2	46.4±1.3	52.8±1.7	176.882
15	714.6±13.6	48.3±1.2	51.8±1.5	177.398
16	711.0±14.3	47.0±2.1	50.1±1.3	173.390
17	223.4±8.1	42.0±1.3	28.2±1.2	99.528
18	234.3±7.5	39.8±1.4	30.3±1.5	101.170
19	213.5±7.1	38.9±1.0	24.5±1.1	90.375
20	198.2±6.6	36.4±1.0	25.5±1.0	88.126
21	475.4±19.3	29.2±1.9	29.3±2.5	107.705
22	483.8±26.6	23.6±2.5	29.1±2.9	102.466
23	485.0±25.6	26.7±2.1	29.4±2.8	106.087
24	488.8±11.2	26.6±0.9	27.8±1.2	103.992
25	452.4±20.9	27.5±2.1	24.6±2.2	97.513
26	475.2±23.9	23.6±1.9	26.0±2.5	97.370
27	462.3±22.2	24.3±2.3	26.9±2.9	98.364
28	392.5±10.6	25.2±0.9	21.3±1.0	85.882
29	475.4±19.3	27.5±2.1	24.5±1.1	99.141
30	483.8±26.6	23.6±1.9	25.5±1.0	97.318
31	475.0±25.6	26.6±0.9	29.3±2.5	105.074
32	234.3±7.5	23.6±2.5	29.1±2.9	83.254
33	457.4±20.9	26.7±2.1	29.4±2.8	103.962
34	475.4±19.3	26.6±0.9	23.8±1.2	97.240
35	383.8±26.6	27.5±2.1	23.6±2.3	90.801
36	385.0±25.6	23.6±1.9	26.0±2.5	90.425
37	388.8±11.2	24.3±2.3	24.9±2.8	89.845
38	352.4±20.9	24.2±0.9	21.3±1.0	81.794
39	383.8±26.6	27.5±2.1	24.5±1.1	92.088
40	385.0±25.6	23.6±0.9	22.5±1.0	85.420
41	388.8±11.2	23.5±2.1	28.3±2.5	93.907
42	252.4±20.9	23.6±1.9	29.1±2.2	84.648
43	235.4±19.3	22.3±2.3	29.4±2.8	82.468
44	383.8±26.6	22.2±0.9	25.8±1.2	88.647
45	385.0±25.6	22.5±2.1	24.4±2.2	87.037
46	298.8±11.2	21.6±1.9	26.5±2.5	82.503
47	252.4±20.9	21.3±2.3	24.2±2.9	75.341
48	283.8±26.6	22±0.9	21.3±1.0	74.312
49	285.0±25.6	20.5±2.1	22.9±2.9	75.192
50	288.6±11.2	21.2±0.9	21.3±1.0	**73.881**

4. Results and Discussion

The efficiency calibration of HpGe-detector was achieved using ^{226}Ra source and KCl solutions of different concentrations (El-Tahawy *et al.* 1992) and reference materials (RM) obtained from the Analytical Quality Control Service (AQCS) of the International Atomic Energy Agency (IAEA).

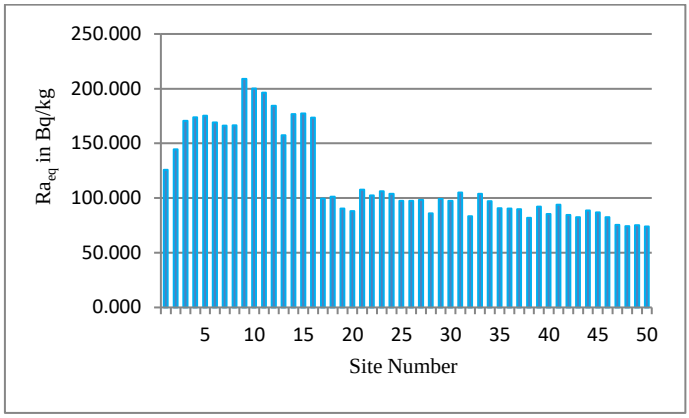

Fig. 2. The Radium Equivalent Activity and their Respective Site Locations

Fig. 2. Radium equivalent activity plotted against the site number. It is observed that the calculated radium equivalent in soils is lower than the allowed maximum value of 370 Bq/kg.

5. Conclusion

The calculated radium equivalent activity in fifty (50) soil samples collected from the East Coast of Libya have been investigated as part of the radiological impact of natural radionuclides. These in addition to man-made radionuclides behave differently in environmental samples according to sample type, and nature; for example in soil their behavior depends mainly on the rocks from which soil is formed (IAEA, 2003). Furthermore, the increase in the value of radium equivalent in samples from 1 to 9 can be attributed to the type of soil in that area. Samples from 9 to 16 have higher values than all other samples which may be due to the relative abundance of rocks from which soil is formed since this area is the Green mountain area the reason is that potassium-40 and radionuclides of uranium and thorium series contribute most of the naturally occurring radioactivity in rocks (Zebracki *et al.*, 2015).

Distribution of uranium and thorium depends upon the geological history of the rock, and the abundance of radioactive elements. From our measurements, it was found that the maximum value for the radium equivalent activity is 208.919 Bq/kg which was obtained from sample 9 as shown in Fig. 2 and tabulated in Table 1, and it is within the maximum allowed world average value of 370 Bq/kg. This study could be used as baseline data for a radiological map for the East Coast of Libya.

Reference

Ahmad, N. M. and Khatibeh, A. J. A. H. (1997) 'Indoor Radon Levels and Natural Radioactivity in Jordanian Soils' *Radiat. Prot. Dosim.*, 71(3), pp. 231–233

Beretka, J. and Mathew, P. J. (1985) 'Natural Radioactivity of Australian Building Materials, Industrial Wastes and By-Products' *Health. Phys.*, 48, pp. 87-95

Bhatti, T. M. and Malik, K. A. (1994) 'Phosphate Fertilizers a Potential Source for Uranium Recovery as by Product', *National Institute for Biotechnology &Genetic Engineering (NIBGE) Faisalabad, Technical Report*, No PAEC/NIBGE-2

Darwish, D. A. E., Abul-Nasr, K. T. M. and El-Khayatt, A. M. (2015) 'The assessment of natural radioactivity and its associated radiological hazards and dose parameters in granite samples

from South Sinai , Egypt' Journal of Radiation Research AND Applied Science, 8 (2015), pp. 17-25

El-Tahawy M. S., Farouk M. A., Hammad, F. H. and Ibrahiem, N. M. (1992) 'Natural potassium as standard source for absolute efficiency calibration of germanium detectors', *Nuclear science J.*, 29, 5, pp. 361-363

Girigisu, S., Ibeanu, I. G. E., Adeyemo, D. J., Onoja, R. A., Bappah, I. A. and Okoh, S. (2013) 'Assessment of radiological levels in soils from Bagega artisanal gold mining exercises at Bagega Zamfara State', *Nigeria' Scholars Research Library Journal Archives of Applied Science Research*, 5(3), pp. 204-210

IAEA (1989) 'International atomic energy agency measurements of radionuclides in food and the environment', *A guide book technical report series* No. 295 Vienna, pp. 27–28

IAEA (2003) 'Extent of Environmental Contamination by Naturally Occurring Radioactive Material (NORM) and Technological Options for Mitigation', *Technical Reports Series, 66, 419*, pp. 7-10

Quinds, L. S., Fernandez, P. L., Soto, J. R., Odenas, C. and Comez, J., (1994) 'Natural radioactivity in Spanish soils' *Health Phys.*, 66, 2, pp. 194–200

Saleh, I. H., Hafez, A. F., Elanany, N. H., Motaweh, H. A. and Naim. M. A. (2007) 'Radiological Study on Soils, Foodstuff and Fertilizers in the Alexandria Region, Egypt', *Turkish Journal of Engineering and Environmental Sciences*, 31(1), pp. 9-17

Scholten, L .C. and Timmermans, C. W. M. (2005) 'Natural radioactivity in phosphate fertilizer' *Nutrient Cycling Agrecosystem* , 43(1-3), pp. 103-107

Taiwo, A. O., Adeyemo, D. J., Ibrahim Y. V. and Bappah, I. A. (2014) 'Determination of radium equivalent activity from natural occurring radionuclide around a superphosphate fertilizer factory in Nigeria', *Scholars Research Library Journal Archives of Applied Science Research*, 6(1), pp. 28-32

UNSCEAR (1988) 'Sources, effects and risks of ionizing radiation. United Nations Scientific committee on the effects of atomic radiation', Report to the general assembly. United nation sales publication E.88.IX.8. United nation. New York.

Zebracki, M. Eyrolle-Boyer, F. Evrard, O., Claval, D. and Antonelli, C. (2015) 'Tracing the origin of suspended sediment in a large Mediterranean river by combining continuous river monitoring and measurement of artificial and natural radionuclides', *Science of the Total Environment*, 502, pp. 122-132

Libyan Journal of Science & Technology 9:2 (2019) 168–175

Faculty of Science - University of Benghazi

Libyan Journal of Science & Technology

journal home page: www.sc.uob.edu.ly/pages/page/77

Nanoparticles technology promoting strategies for cancer therapy: Review

Ihssin Abdalsamed [a,*], Ibrahim Amar[a], Mohammed Ahwidi[a], Omar Abrika[b], Masood A G Ali[c]

[a]*Department of Chemistry, Faculty of Sciences, University of Sebha, Sebha-Libya*

[b] *Faculty of Pharmacy, University of Sebha, Sebha-Libya*

[c]*Department of Geology and Environment, Faculty of Sciences, University of Bani Waleed, Bani Waleed-Libya*

Highlights

- **Nano treatment is used to cure a number of cancer cases, which have shown significantly to fight cancer.**
- **Nanodevices become one of the greatest medical healthcare sittings named, as nanoparticles (NPs) are Quantum dots (QDs), Nanogold shell (AuNPs), Dendrimers, Nanopore, and Nanotubes.**
- **Nanodevices provide potential benefits for diagnosing and treating metastatic cancer such as a tumour, while the ability to deliver drugs to the major sites of metastasis and enrichment of target tumor cells without effecting noncancerous cells.**

ARTICLE INFO

Article history:

Received 01 October 2018
Revised 03 July 2019
Accepted 04 July 2019
Available online 06 July 2019

Keywords:

Quantum dots (QDs), Nanogold shell (AuNPs), Dendrimers, Nanopore, Nanotubes.

* Corresponding author:

E-mail address:
ihs.abdalsamed@sebhau.edu.ly
I. Abdalsamed

ABSTRACT

Cancer is the most serious disease in the world and has been considered as the first fatal disease to the humankind as its incidence rates continue to increase rapidly worldwide. Chemotherapy, Radiation therapy, Immunotherapy and Hyperthermia are the most common treatments for cancer in developed countries, while surgical operations are used in undeveloped countries, which have been found to cause negative side effect on human health.

Recently, Nano treatment is used to cure a number of cancer cases, which have shown significant results than surgical operations. Such success has encouraged scientists and researchers to develop Nanotechnological devices named as nanoparticles (NPs) which have become one of the greatest medical healthcare settings as they provide potential benefits for diagnosing and treating metastatic cancer, such as a tumor. On other hand, nanoparticles improved the ability to delivery drugs to the major sites of metastasis without effecting noncancerous cells. Moreover, beside reported nanoparticles (NPs) have significant to escape antibody and extravasate into the tumor cells.

In this review, we focus and outline on Nanodevice types: Quantum dots (QDs), Nanogold shell (AuNPs), Dendrimers, Nanopore, and Nanotubes for their principles, applications, operation processes and their recent highlights in cancer research area are also considered in this paper. Finally, we provide some perspectives on the future challenges and development of drug delivery systems.

1. Introduction

Cancer is defined as the uncontrolled proliferation of cells. Most human cancers arise from a single clone of cells affected by a genetic mutation. Additionally, larger proportions of cells are actively dividing with a rapid growth rate over other normal cells (Fig. 1). Globally, a huge number of people all over the world are diagnosed with various types of cancer, accounting for a yearly 8 million cancer-related deaths, and such number is apparently on the rise (Torre *et al.*, 2015, Siegel *et al.*, 2016, McGuire, 2016, Bray *et al.*, 2018). World Health Organization (WHO) demonstrated that cancer could be correlated with several risk factors such as smoking, dietary habits, age, exposure to UV-radiation and consuming vegetables treated with pesticides, in addition to work-related factors that involve hydrocarbon pollution, etc. The wider scientific community believes that those factors are responsible for growing specific categories of cancer (Parrón *et al.*, 2014; Ramírez *et al.*, 2014; Cuadras *et al.*, 2016; Stewart and Wild, 2017; Valcke *et al.*, 2017; Lee *et al.*, 2019). Presently, multimodal therapies are available against cancer, which include chemotherapy, radiation therapy, surgical operations, hyperthermia as well as immunotherapy.

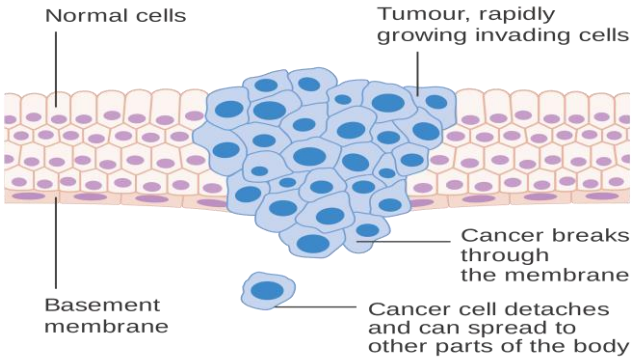

Fig. 1. Normal tissue and cancer cells (Singh *et al.*, 2015)

Chemotherapy is the main treatment used to manage cancer in different countries. Doxorubicin is a synthetic drug having a wide

 ISSN 2663-1407; National Library of Libya, Legal number: 390/2018

use to combat cancer. It is able to destroy or/and control the proliferation of cancer cells. Chemotherapy is usually given through intravenous injection, subcutaneous or orally depending on the cancer type and patient situation. Nowadays, several chemotherapy strategies have been applied to the treatment of different types of cancer. Chemotherapy can be used alone or combined with other treatments such as radiotherapy, which could be followed by surgery for controlled mass removal. Although chemotherapy is the most common treatment for cancer management it may cause undesirable side effects such as the need of the patient to be frequently hospitalized for treatment dose administration. More important, chemotherapy may have an unsuccessful outcome for many patients. Further, it could have diverse effective for different individuals (Von Minckwitz *et al*., 2012; Buch *et al*., 2019).

Radiation therapy is therapeutic treatment is applicable to many types of cancers. It uses high-energy rays emitted from instruments used specifically to target cancer cell to reduce the tumor mass. The machines emit short wavelength rays (high-energy radiation). There are different types of radiations that are suitable for cancer treatment including X-rays, gamma rays and other sources such as neutrons and protons. Although radiation therapy is an improved treatment for cancer, it has a number of drawbacks. Firstly, it is normally used for inpatients required to spend a few days in the hospital or clinic. Secondly, long rest is needed for the patients that have been exposed to high levels of radiation. Further, depending on their immune system function status they may have to see visitors for a short time only to avoid picking infections. Thirdly, once the treatment is finished, the amount of residual radiation must be checked in a patient body, and a safe level can be reached before he/she can leave the hospital. Lastly, Radiotherapy can sometimes damage organs that are closely related to the site of rays' targets such as the stomach, bowel, liver and kidneys. This drawback may result in serious side effects (Kratochwil *et al*., 2016; Chang *et al*., 2016; Lin *et al*., 2019).

Immunotherapy is an advanced strategy used against cancer. Indeed, it is a supporting method used to stimulate the immune system to enhance its ability to fight diseases such as microbial infections and cancer. Recently, immunotherapy has become more effective for the treatment of many types of cancer, since it allows the immune system to identify and target cancer cells more effectively compared to other methods, which have a deteriorating effect on the immune system itself. Immunotherapy approach has various modules including vaccines, checkpoint inhibitors, cytokines, monoclonal antibodies (MABs), and the more advanced adoptive cell transfer immunotherapy strategy. Immunotherapy is also known as biological therapy. The substances that modify the immune response or the so-called biological response are referred to as the Biological Response Modifiers (BRMs). Indeed, the body naturally produces small amounts of (BRMs) in response to infection and disease. Therefore, large amounts of BRMs can be made in the laboratory and used for the treatment of a wide range of diseases such as rheumatoid arthritis and cancer. In comparison to chemotherapy and radiotherapy, other cancer treatment methods, immunotherapy appears to improve the strength of the patient's own immune system, with fewer side effects. Furthermore, several investigations showed that combining immunotherapy with chemotherapy treatment decreased the side effect risks. In addition, it improves long-term survival. However, there are some drawbacks of immunotherapy treatment as it sometimes causes unfavorable symptoms, which include fever, chills, nausea, diarrhea and vomiting, besides generalized pain particularly in the bones joints and legs, weakness or fatigue, headaches and rashes in some patients (Smith *et al.,* 2014; Frankel *et al*., 2017; Riley *et al*., 2019).

Hyperthermia is the first clinical method improved for the goals of regional cancerous- directed therapies. In addition, to stopping bleeding, early, it has been used for a long time as the process of raising the patient's body temperature either locally or in general for medicinal purposes. Currently, hyperthermia has the potential to eliminate cancer from the body. The goals of hyperthermia technique include the significant increase in apoptosis of cancer cells or/ and the inhibition cancer cells division. Notably, this is accomplished neither through using medicine (Chemotherapy) nor through using high-energy rays (Radiotherapy) in treating the affected area, but rather by localized high temperature in the tumor area. The mechanism used to achieve hyperthermia is by means of burring or cauterizing the cancerous area with a hot metal such iron. Currently, more sophisticated Hyperthermia treatments have appeared as a new system for cancer treatment such as using a hot liquid including water. By this method, the affected area will cure faster, hence decreasing the side effects (Cabuy, 2011, Bedge *et al*., 2019).

Surgical Operation is the preliminary method for fighting cancer diseases. It involves the surgical operation to remove the primary solid tumor disease from the patient. The ancient physicians used a surgical operation to inhibit the spread of metastatic cancer cells. (Van Gijn *et al*., 2010; Tohme *et al*., 2017; Tsagozis *et al*., 2019). Although several treatment strategies have been applied for cancer treatment, these traditional strategies have various drawbacks through local or systemic effect. In addition, the low specificity of some treatments leads to similar effects in both rapidly dividing normal cells and tumor cells. Additionally to diagnostic strategies problems they are time-consuming with low sensitivity to a specific area and may cause kidney complications while suffering senior people and children practically on surgery operations. Nowadays, several researchers have become interested in further related investigations, which have a new or improved treatment method to treat large panels of cancer disease.

2. The significance of nanoparticles in cancer therapy?

Scientist found that most animal cells are 10000 nm to 20000 nm in diameter while nanoparticles have dimensions that equal 100 nm or less (Fig. 2). This enables nanoparticles to enter animal cells (Fig. 3). Moreover, nanoparticles have a greater surface area per weight than conventionally made material, which causes them to be more reactive to some other molecules. The difference between the surface atoms to total atoms of the molecule increases with the decrease in molecular size. This, in fact, can be an important property when NPs interact with biological systems. This, in addition, represents an important property for many biomedical applications (Soliman *et al*., 2012; Douba *et al*., 2017). For instance, zinc oxide has been found in Nano size to have superior UV blocking properties compared to its bulk substitute, silicon has been found at approximately the size 1nm can emit blue color and at approximately 3 nm size can emit red color with no color on material size (Zong *et al*., 2011; Chen and Ma, 2019). The properties of materials change in their size in nanoscale leading the surface of materials to become significant for nanotechnology. Over the past decade, several Nanomaterials were designed based on differences, such as: Quantum dots (QDs), Nanogold shell (AuNPs), Dendrimers, Nanopore, and Nanotubes.

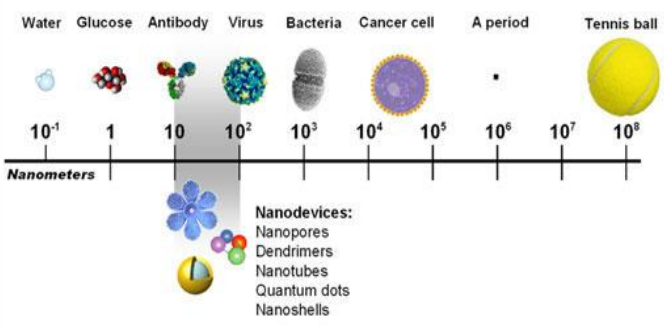

Fig. 2. Nanodevices scale (Mewara and Rathore, 2016)

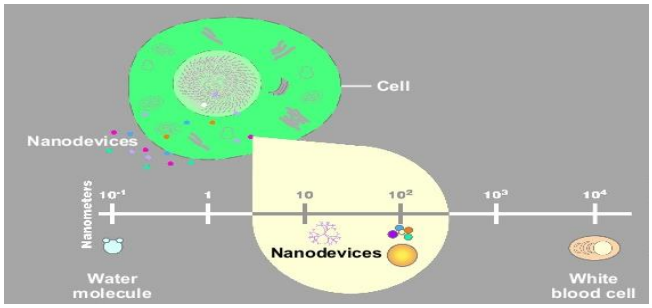

Fig. 3. Nanodevices are small enough to enter the cell (Ahmed, 2006)

Nanoparticles have multifunctional systems for cancer disease such as tumor targeting, drug delivery, diagnostics and imaging. Targeting tumor cells by nanoparticles depending on mechanism reaction upon external motivation through the functionality of tumor cells, peptides, polymers and antibodies that can be used to improve NPs circulation, effectiveness and selectivity. This exploration has opened the relatively a new field of Nanomedicine dealing with the detection, control, construction, repair, defence and improvement of all human biological systems. Nanoparticles (NPs) can be synthesised to a size compatible with biological molecules such as proteins, nucleic acids and can appropriately develop for use as potential probes, delivery platforms, carriers and devices giving unique opportunities for improvements in disease detection, therapy and prevention. For all that depending to their Nanoscale size and unique properties allowing nanoparticles to cross and interact with biomolecules in the blood, organs, tissues and cells (Fig. 4) (Conde *et al.*, 2012, Oh and Park, 2014; Wang *et al.*, 2019).

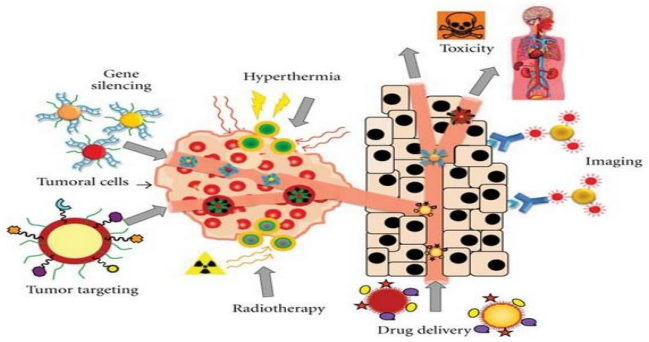

Fig. 4. Schematic illustration of potential applications of nanoparticles in cancer cells (Conde *et al.*, 2012; Mercado *et al.*, 2019)

Nanoparticles (NPs) may be organic or inorganic in nature and there are many methods for synthesis and development nanoparticles (Wang and Wang, 2014; Badi'ah *et al.*, 2019) for example synthesis citrate gold nanoparticles and silica-gold nanoparticles(Fig. 5). Recently a new method for the synthesis of eco-friendly nanoparticles have been introduced (Divakaran *et al.*, 2019; Kooshki *et al.*, 2019).

3. Quantum dots (QDs)

Quantum dots are inorganic nanoparticles of semiconductors, which had been theorized in the 1970s and were initially created in the early 1980s. Quantum dots are semiconductor nanoparticles that can glow a specific color after absorbing light. The glow of color depends on the size of the nanoparticle. Many semicon-ductor substances on Nano size can use as quantum dots. Semi-conductor substances nanoparticles or other semiconductor substances have high properties of a quantum dot. Quantum dots (QDs) can be great values fluorescent given good photochemical stability and high photoluminescent quantum yields (Chinen *et al.*, 2015; Lu *et al.*, 2019).

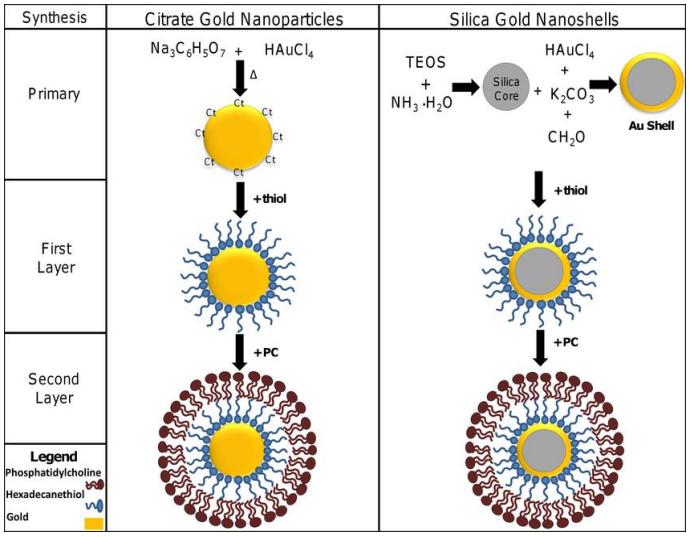

Fig. 5. Synthesis of gold nanoparticles (England *et al.*, 2015; Kumar *et al.*, 2019)

Quantum dots (QDs) with properties absorb and emits different wavelengths are becoming a useful tool in many biological applications (Igweh *et al.*, 2018). QDs consist of a core made of heavy metal responsible for fluorescence properties surrounded by an external coating generally an amphiphilic polymer that to increase solubility in a biologically compatible medium. The core/shell QDs usually have a layer (or "shell") of zinc sulphide (ZnS) between the core and the coating that can reduce the leaching of metals from the core and improving photo-stability (Fig. 6A). Nanoscientist found that many types of the quantum dot would emit light when applied UV light and those lights can be different in color due the QDs size, shape and material. For example, larger QDs at radius from 5 nm to 6 nm can emit longer wavelengths resulting in emission colors like orange or red while smaller QDs at radius from 2 nm to 3 nm can emit shorter wavelengths resulting in colors such as green or blue, although the specific colors and sizes vary depending on the exact composition of the QDs. Semiconductor quantum dots (QDs) have attracted the attention of many research groups because of their scientific and technological significance in microelectronics, optoelectronics and cellular imaging several groups have reported that with biocompatible surface coatings, such as PEG-silica, QDs can be well tolerated by cells in vitro as they can be conjugated to a legends by coating a polymeric layer onto it. For further QDs is a critical issue application as diagnostic and imaging tools for the human body. Moreover the applications of QDs for imaging are inside the cell are in the cytoplasm, endosomes and lysosome this can make QDs have got unique properties which make them ideal for detecting specific tumor cells (Fig. 6B) (Di Corato *et al.*, 2011; Yanover *et al.*, 2014; Lim *et al.*, 2015; Cai *et al.*, 2016; Lee *et al.*, 2017).

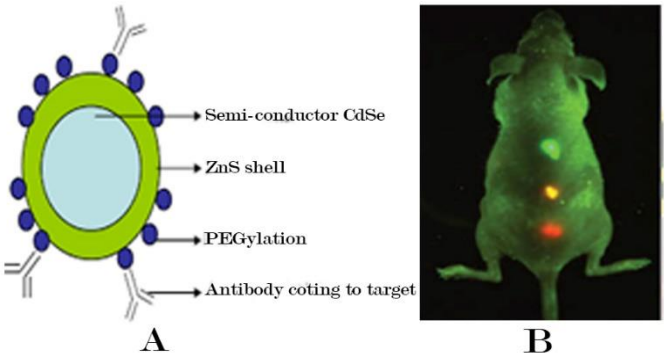

Fig. 6. (A) Quantum dots, (B) Quantum dots significant to glow by UV light targeting tumor cells

4. Gold nanoparticles (GNPs) drug delivery

Doxorubicin (Dox) is a popular anticancer drug commonly used in chemotherapy. In recent years, gold nanoparticles have been investigated for using them as drug or gene delivery carriers and as diagnostic agents. Having such delivery ability of various payloads into their specific targets they can extravasate (escape) into the tumor tissues. The surfaces of GNPs can be further functionalized to allow for increasing biocompatibility, targeting and uptake by cell (Fig. 7). The gold nanoparticles (Au NPs) have an advantage compared to other agents as they provide nontoxic carriers for drug and gene delivery applications. Furthermore, they can be used to deliver medicine explicitly to cancer cells without affecting normal cells. Gold nanoparticles are shaped so that the gold core imparts stability to the assembly while the monolayer allows tuning of surface properties such as charge and hydrophobicity (Kanapathipillai *et al*., 2014; Muddineti *et al*., 2015; Daraee *et al*., 2016; Mugaka *et al*., 2019). Significant studies have revealed that Gold Nanoparticles (GNPs) exhibit unique physicochemical properties including Surface Plasmon Resonance (SPR) and the ability to bind amine and thiol groups allowing surface modification and use in biomedical applications. Lately, the synthesis of Gold Nanoparticles (AuNPs) became possible in the laboratory (Guo *et al*., 2016; Chen *et al*., 2019).

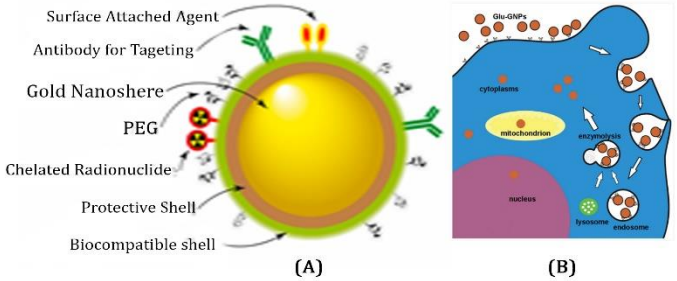

Fig. 7. (A) Gold nanoparticles, (B) Gold nanoparticles attached in and out of a cancer cell (Song *et al*., 2013; Singh and Mitragotri, 2019)

5. Gold nanoparticles (GNPs) thermal therapy

Generally, cancer cells die at 47°C and this can be through apoptotic pathways. In fact, hyperthermia method typically involves an external heating source that generates temperature gradients from the external source to the tumor with the maximum heat dissipated on the body's surface, which may affect normal cells. Gold NPs can improve thermal therapy efficiency through absorption of infrared (IR) light, this will exhibit low toxicity, ease of functionalization, suitable biocompatibility and uptake into cells with less exposure of light. Moreover, gold NPs can transform absorbed light into heat giving lower temperature and thus have the high potential for infrared phototherapy (Dorsey *et al*., 2013; Wang and Wang, 2014; Hainfeld *et al*., 2014; Baffou, 2018). Extensive studies strongly support the notion that gold nanoparticles at lower wavelength produce heat that can kill cancer cells (Fig. 8). GNP tunable optical properties have propelled them to the forefront of cancer hyperthermia as photothermal agents. Photothermal therapy is a method of killing off cancer cells carried out by changing optical energy to thermal energy upon irradiation with light (Chithrani *et al*., 2010; Yuan *et al*., 2012; Yu *et al*., 2012; Zhang *et al*., 2019).

GNPs are efficient converters of light energy into heat, making them promising agents for targeted photothermal effects. They have also been investigated for cancer hyperthermia due to their unique optical properties when exposed to visible-near infrared (NIR) wavelengths where they are capable of efficient conversion of light energy into heat, which is quickly dissipated into the environment. Over the past decade, researchers have concentrated on improving GNPs design for hyperthermic treatments focusing on varying particle shapes such as rods, cubes, stars, and prisms to promote GNPs light absorption and thus heat generation (Khlebtsov and Dykman, 2011; Joseph *et al*., 2019).

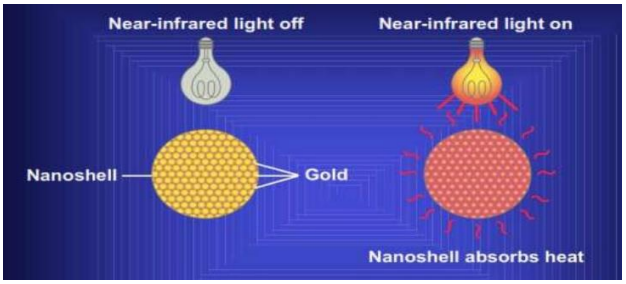

Fig. 8. Effective IR light to melt nanogold particles (Ahmed, 2006)

6. Dendrimers

Dendrimers are an organic nano type repetitively branched molecules. The name of dendrimers comes from the Greek word (Dendron) which translates to "tree". They have wider uses in a biological system. Dendrimers chemically is typically symmetric around the core and often adopts a spherical three-dimensional morphology; this is means that dendrimers consist of a series of chemicals. They are a branch of the dendritic family as illustrated in (Fig. 9). Applications of dendrimers typically involve conjugating other chemical species to the surface of dendrimers that can function as detecting agents (Zhou *et al*., 2014; Wei *et al*., 2015; Caminade, 2019).

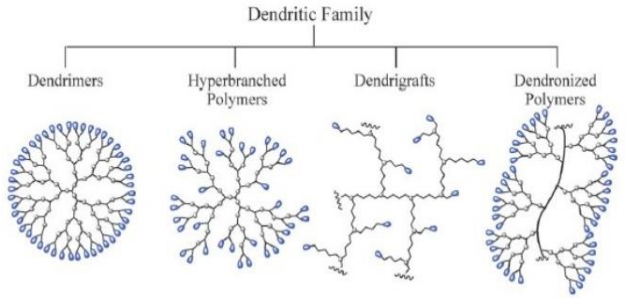

Fig. 9. Schematic of dendritic family

In recent years, the application of dendrimers has successfully proved themselves as useful in advanced technology and medicine due to their small size, which is not more than 15 nm, and has very high molecular weight. With this size, dendrimers are easy uptake by the cell through endocytosis. Notably, Dendrimers have advantages over other applications, as they have become an ideal carrier for drug delivery and chemical catalysts.

Dendrimers grow from core to periphery. The core molecular reacts with monomer molecular having two dormant and one reactive group. The small molecular comes together and the reaction proceeds inward and eventually the molecular become attached to the core (Fig. 10). Therefore, the structure of dendrimers from a simple mono molecule compound of the more complex molecule compounds is the key to dendrimers plays multifunction, especially in biosystem. In spite that dendrimers are advantageous for highly specialized applications such as drug delivery along with molecular carrier for chemical catalysts (Fig. 11), they have several disadvantages such as positively charged surface groups prone to destabilize cell membranes and cause cell lysis. Secondly, the degree of substitution, type of amine functionality is important as primary amines being more toxic than secondary or tertiary amines while the fourth generation is the most toxic (Somani and Dufès, 2014; Hughes, 2017; Ho *et al*., 2019).

Recently, Nanoscientist developed dendrimers that can conjugation with DNA/RNA and have become a new revolution in manipulating cancer cells (Kalomiraki *et al*., 2016; Gorzkiewicz *et al*., 2019).

There are several types of dendrimers, which involve Pamam dendrimers, Pamamosdendrirners, Tecto dendrimers, PPI dendrimers, Chiral dendrimers, Hybrid dendrimers Linear Polymers, Amphiphilic dendrimers, and also Micellar dendrimers.

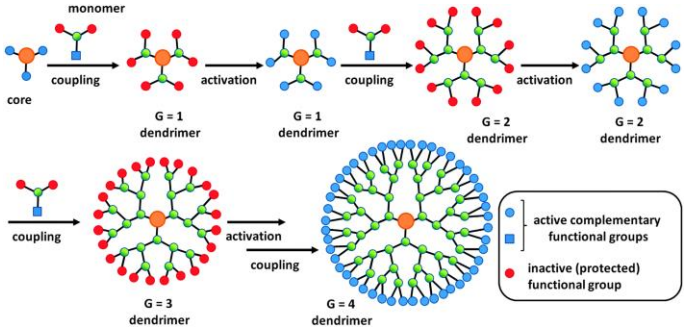

Fig. 10. Synthesis of dendrimers according to the divergent method (Sowinska and Urbanczyk-Lipkowska, 2014).

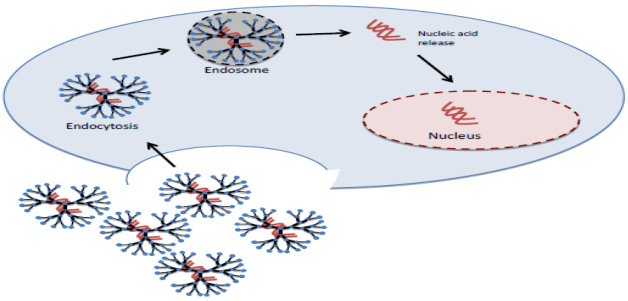

Fig. 11. Dendrimers mediated gene delivery to a cancer cell (Ahmed *et al.*, 2016)

7. Nanopore

Previously published studies have defined the Nanopore as a very small hole on the instruction of 1 nanometer in internal diameter; hence, electrical current can pass flow through this hole. Nowadays, diverse types of nanopore are available such as Alpha-Hemolysin nanopore, MspA nanopore and Graphene nanopore (Deamer *et al.*, 2016; Jain *et al.*, 2016; Jeck *et al.*, 2019). DNA sequencing is the process of determining the precise order of nucleotides within a DNA molecule. DNA molecules consist of four nitrogen bases. Cytosine (C), Guanine (G), Adenine (A), and Thymine (T). Nanopore can electrically thread DNA electrically through nanometer-sized pores. The pore is submerged in a salt solution while an electrical current is applied. Eventually, the DNA molecule through the pore has detecting and sequencing DNA. In the same time, a low potential (voltage) is applied across the membrane with an ion flux through the pore (Fig. 12). The ion flux is measured by an application specific integrated circuit. The ion flux is partially blocked by the Trans locating DNA strand. Scientific works established the DNA sequencing method has been classified in four generations; first Sanger sequencing, second amplification based massively parallel sequencing, third single molecule sequencing, and fourth nanopore sequencing, it is advantages inexpensive, reliable and high throughput sequencing (Ozsolak and Milos, 2011; Norris *et al.*, 2016). A graphene Nanopore platform using electric fields is improved to tiny DNA strands will pushed through Nanoscale sized, atomically thin pores in a that ultimately may be important for fast electronic sequencing of the four chemical bases of DNA based on their unique electrical (Tian *et al.*, 2013; Craig *et al.*, 2019).

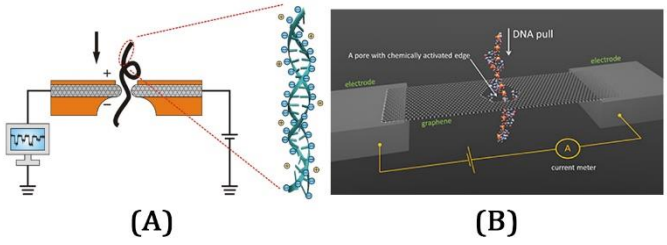

Fig. 12. (A) Nanopore sequencing of DNA, (B) DNA sequencing by graphing nanopore platform (Yang and Jiang, 2017).

8. Nanotubes

Several lines of investigation detail that nanotubes found as two types; single-walled nanotubes and multi-walled nanotubes. For instance, carbon nanotubes (CNTs) are hexagonally shaped arrangements of carbon atoms that roll into tubes. In this regard, Mittal and his colleagues demonstrated that the (CNTs) are a tubular form of carbon with small diameters; it has a nanometer scale with a hollow tubular structure and atomic arrangement that differ from other carbon allotropes as graphite (Mittal *et al.*, 2015; Kaur *et al.*, 2019). Accumulating data of published studies has identified that carbon nanotubes are cylindrical carbon molecules having novel properties. Their unique surface area with stiffness matrix, strength and resilience has led to much excitement in the field of pharmacy. In addition, CNTs have distinctive electronic and chemical features, which make them suitable for a wide variety of applications, including drug transporters, delivery systems, and diagnostics. Extensive research conducted on anticancer drugs described doxorubicin (Dox) as one of the most efficient anticancer drugs improved for cancer control. However, it can cause the death of non-cancer cells too. In this regard, the nanotubes can successfully deliver Doxorubicin (Dox) only to cancer cells fallow cancer cell marker signatures. Moreover, they are able to enter cells by themselves without obvious toxicity. The cellular uptake mechanism differs depending on the properties and the size of the CNTs (Fig. 13). Recently carbon nanotubes (CNTs) were revealed to have unique advantages over other nano delivery systems such as biological drug delivery and protein delivery (Elhissi *et al.*, 2012; Yu *et al.*, 2012; Yu-Cheng *et al.*, 2013; Sanginario *et al.*, 2017; Kaur *et al.*, 2019; Hosnedlova et al., 2019).

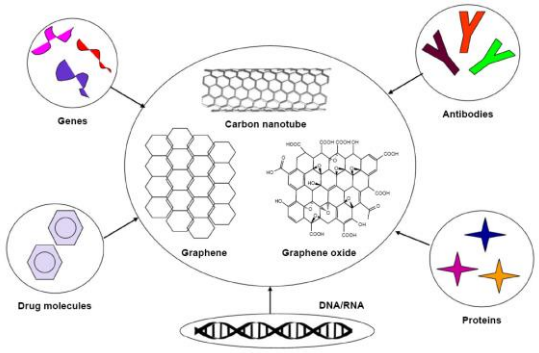

Fig. 13. Schematic of carbon nanotubes delivery system (Yu-Cheng *et al.*, 2013; John *et al.*, 2015; Hosnedlova *et al.*, 2019; Sharma *et al.*, 2019).

9. Conclusion

Recently, a mounting body of evidence confirming that nanotechnology has interesting applications in biological and medical sciences. Several publications concerning nanotechnology revealed that devices have many benefits over other modules of nanoparticles. Devices characterized by the simplicity of design in shapes and sizes. Due to the chemistry of their surface, they have the ability to allow more use of properties of matter when used with various biologically useful molecules. The multi-modules of treatment such as chemotherapy, radiotherapy, immunotherapy, hyperthermia and surgical operations techniques are the major treatments for cancer management. However, most of these techniques have various drawbacks. Therefore, the development of Nanodevices has offered a great opportunity to combat cancer, at the same time minimizing the side effect risk in both cancer diagnostic and therapy. More importantly, such devices can control cancer cells without affecting non-cancerous cells. Moreover, Nano devices could prevent or/and regulate cancer from recurrence besides destroying any cancer cells following other treatments. The Quantum dots are described as tiny particles of semiconductor nanocrystal with the size range from 2-10 nm with fluorescent lighting ability. Further, Quantum dots Nanodevices are the perfect devices to reach a good diagnosis compared to rays methods. On this basis, Quantum dots Nanodevices have the potential to be used

to diagnose specific areas of the tumor mass. Additionally, Quantum dots also can glow when stimulated by ultraviolet light, which has less energy than X-rays. Gold nanoparticle can be an effective delivery system for regional cancer-directed therapies. The gold nanoparticles containing drugs coated with targeting agents conjugated antibodies. Therefore, gold nanoparticles circulate through the blood vessels could reach the target cells and thus drugs will be released directly into the cancer cells. Hence, the gold nanoparticles module could be more beneficial than Chemotherapy treatment. Moreover, gold nanoparticle by using IR light, which has less energy than UV and X-ray, is considered a promising method with selective property to fighting cancer cell.

Dendrimers have many properties including macromolecules, high solubility, and miscibility, molecular mass increases, viscosity increase up to a 4th generation, interior layer encapsulates drug molecule, low compressibility. Dendrimers with hydrophilic groups are soluble in polar solvents whilst those with hydrophobic groups are soluble in non-polar solvents. It is important to note that the major advantages of dendrimers are drug delivery and they have the ability to conjugate with DNA/RNA.

Nanopore refers to as a nanoscale hole. Biologically, it is a pore-forming protein in a membrane such as a lipid two layers, while solid-state is formed from synthetic materials such as silicon nitride or graphene. On the other hand, the hybrid type is formed by a pore-forming protein set in synthetic material. Significant research showed that Nanopore allows single-stranded DNA to pass through them, which may help to manipulate defect DNA. Recently, published studies stated that carbon nanotubes are formed by having axis's graphite sheets (<100 nm) rolling into cylinders demonstrating excellent strength with electrical properties, In addition to efficient heat conduction due to carbon nanotubes, which allows carbon conjugation with other molecules, thus could be used in drug delivery. Although efficient, applications of nanotechnology in biology specifically in the biomedical field, it has various disadvantages. Firstly, the safety of nanotechnology has not been well approved. In addition, few investigations have been done *in vivo* to address their safety. Secondly, based on several studies the toxicity of nanodevices remains to be a big problem. Lastly, the Nanodevices functions rely on a targeting agent.

10. Future work

The scientists related to nanotechnology are trying developing and regulating the process in Nanochips that can be injected into the human body to control blood pressure. Furthermore, they are trying to invent the Nanorobot machine that could be used in medical applications such as controlling blood sugar, killing bacteria as well as repairing damaged tissues.

Acknowledgement

We would like to express our special thanks and gratitude to Dr. Abdolhadi Benhmid, Dr. Faraj Alshaire from Benghazi University and Dr. Abdalhafith Abukilsh from Sebha University for their cooperation to complete this manuscript.

References

Ahmed, M. (2006) An Overview of Nanomedicine, *Journal of Medical Research Institute*, 27, 4, pp. 248-254

Ahmed, S., Vepuri, S. B., Kalhapure, R. S. & Govender, T. (2016) 'Interactions of dendrimers with biological drug targets: reality or mystery - a gap in drug delivery and development research', *Biomaterials Science*, 4, pp. 1032-1050.

Badi'ah, H., Seedeh, F., Supriyanto, G. Zaidan, A. (2019) Synthesis of Silver Nanoparticles and the Development in Analysis Method. In: IOP Conference Series: *Earth and Environmental Science*, 27, 1, pp. 1-8. IOP Publishing, 012005.

Baffou, G. (2018)'Gold nanoparticles as nanosources of heat', *Photoniques*, pp. 42-47.

Bedge, P. A., Bohara, R. A., Patil, P. M., Joshi, M. G., Bohara, D. A. (2019) 'Current Cancer Therapies: Focus on Hyperthermia and Immunotherapy', Hybrid Nanostructures for Cancer Theranostics, Elsevier.

Bray, F., Ferlay, J., Soerjmataram, I., Siege, R. L., Torre, L. A., Jemal, A. (2018) 'Global cancer statistics 2018: Globocan estimates of incidence and mortality worldwide for 36 cancers in 185 countries. CA: a cancer', *Journal for clinicians*, 68, pp. 394-424

Buch, K., Gunmalam, V., Andersson, M., Schwarz, P., Brons, C. (2019) 'Effect of chemotherapy and aromatase inhibitors in the adjuvant treatment of breast cancer on glucose and insulin metabolism—A systematic review', *Cancer medicine*, 8, pp. 238-245

Cabuy, E. (2011) 'Hyperthermia in Cancer Treatment', *Reliable Cancer Therapies Energy-based therapies*, 1, pp. 1-48.

Cai, X., Luo, Y., Zhang, W., DU, D., LIN, Y. (2016) 'pH-Sensitive ZnO quantum dots–doxorubicin nanoparticles for lung cancer targeted drug delivery', *ACS applied materials & interfaces*, 8, pp. 22442-22450.

Caminade, A. M. (2019) 'Inorganic Dendrimers and Their Applications', *Smart Inorganic Polymers: Synthesis, Properties, and Emerging Applications in Materials and Life Sciences*, pp. 277-315.

Chang, J. Y., Jabbour, S. K., De Ruysscher, D., Schild, S. E., Simone II, C. B., Rengan, R., Feigenberg, S., Khan, A. J., Choi, N. C.,Bradley, J. D. (2016) 'Consensus statement on proton therapy in early-stage and locally advanced non–small cell lung cancer', *International Journal of Radiation Oncology, Biology, Physics*, 95, pp. 505-516.

Chen, W., Ma, L. (2019) Nanophosphors for visible light enhancement. Google Patents.

Chen, X., Zhu, L., Huang, M., Yang, C. (2019) Synthesis of gold nanoparticles and functionalization with DNA for bioanalytical applications, *Novel Nanomaterials for Biomedical, Environmental and Energy Applications*. Elsevier.

Chinen, A. B., Guan, C. M., Ferrer, J. R., Barnaby, S. N., Merkel, T. J., Mirkin, C. A. (2015) 'Nanoparticle probes for the detection of cancer biomarkers, cells, and tissues by fluorescence', *Chemical reviews*, 115, pp. 10530-10574.

Chithrani, D. B., Jelveh, S., Jalali, F., Van Proijeno, M., Allen, C., Bristow, R. G., Hill, R. P., Jaffray, D. A. (2010) 'Gold nanoparticles as radiation sensitizers in cancer therapy', *Radiation research*, 173, pp. 719-728.

Conde, J., Doria, G., Baptista, P. (2012) 'Noble metal nanoparticles applications in cancer', *Journal of drug delivery*, pp. 1-12. doi:10.1155/2012/751075, Craig, J. M., Laszlo, A. H., Nova, I. C., Brinkerhoff, H., Noakes, M. T., Baker, K. S., Bowman, J. L., Higinbotham, H. R., Mount, J. W., Gundlach, J. H. (2019) 'Determining the effects of DNA sequence on Hel308 helicase translocation along single-stranded DNA using nanopore tweezers', *Nucleic acids research*,95, 1, pp. 505-516.

Cuadras, A., Rovira, E., Marce, R. M., Borrull, F. (2016) 'Lung cancer risk by polycyclic aromatic hydrocarbons in a Mediterranean industrialized area', *Environmental Science and Pollution Research*, 23, pp. 23215-23227.

Daraee, H., Eatemadi, A., Abbasi, E., Fekri Aval, S., Kouhi, M., Akbarzadeh, A. (2016) 'Application of gold nanoparticles in biomedical and drug delivery', *Artificial cells, nanomedicine, and biotechnology*, 44, pp. 410-422.

Deamer, D., Akeson, M., Branton, D. (2016) 'Three decades of nanopore sequencing', *Nature biotechnology*, 34, pp. 518-524.

Di Corato, R., BigallI, N. C., Ragusa, A., Dorfs, D., Genovese, A., Marottaa, R., Manna, L., Pellegrino, T. (2011) 'Multifunctional Nanobeads Based on Quantum Dots and Magnetic Nanoparticles: Synthesis and Cancer Cell Targeting and Sorting', *ACS Nano*, 5, pp. 1109-1121.

Divakaran, D., Lakkakula, J. R., Thakur, M., Kumawat, M. K., Srivastava, R. (2019) 'Dragon fruit extract capped gold nanoparticles: Synthesis and their differential cytotoxicity effect on breast cancer cells', *Materials Letters*, 236, pp. 498-502

Dorsey, J. F., Sun, L., Joh, D. Y., Witztum, A., Zaki, A. A., Kao, G. D., Alonso-Basanta, M., Avery, S., Tsourkas, A., Hahn, S. M. (2013) 'Gold nanoparticles in radiation research: potential applications for imaging and radiosensitization', *Translational Cancer Research*, 2, pp. 280-291.

Douba, A., Genedy, M., Matteo, E., Kandil, U., Stormont, J., Taha, M. R. (2017) 'The significance of nanoparticles on bond strength of polymer concrete to steel', *International Journal of Adhesion and Adhesives*, 74, pp. 77-85.

Elhissi, A., Ahmed, W., Dhanak, V., Subramani, K. (2012) Carbon nanotubes in cancer therapy and drug delivery, Emerging Nanotechnologies in Dentistry. Elsevier.

England, C., S Huang, J., James, K., Zhang, G., Gobin, A., Frieboes, H. (2015) Detection of Phosphatidylcholine-Coated Gold Nanoparticles in Orthotopic Pancreatic Adenocarcinoma using Hyperspectral Imagin', *PLoS ONE*, 10, 6, e0129172. https://doi.org/10.1371/

Frankel, T., Lanfranca, M. P., ZOU, W. (2017) The Role of Tumor Microenvironment in Cancer Immunotherapy. Tumor Immune Microenvironment in Cancer Progression and Cancer Therapy. Springer.

Gorzkiewicz, M., Deriu, M. A., Studzian, M., Janaszewska, A., Grasso, G., Pulaski, Ł., Appelhans, D., Danani, A. & Klajnert-Maculewicz, B. (2019) 'Fludarabine-Specific Molecular Interactions with Maltose-Modified Poly(propyleneimine) Dendrimer Enable Effective Cell Entry of the Active Drug Form: Comparison with Clofarabine', *Biomacromolecules*, 20, pp. pp. 1429-1442.

Guo, M., He, J., Li, Y., Ma, S., Sun, X. (2016) 'One-step synthesis of hollow porous gold nanoparticles with tunable particle size for the reduction of 4-nitrophenol', *Journal of hazardous materials*, 310, pp. 89-97.

Hainfeld, J. F., Lin, L., Slatkin, D. N., Avraham Dilmanian, F., Vadas, T. M., Smilowitz, H. M. (2014) 'Gold nanoparticle hyperthermia reduces radiotherapy dose', *Nanomedicine: Nanotechnology, Biology and Medicine*, 10, pp. 1609-1617.

Ho, M. N., Bach, L. G., Nguyen, T. H., Ho, M. H., Nguyen, D. H., Nguyen, C. K., Nguyen, C. H., Nguyen, N. V., Thi, T. T. H. (2019) 'PEGylated poly (amidoamine) dendrimers-based drug loading vehicles for delivering carboplatin in treatment of various cancerous cells', *Journal of Nanoparticle Research*, 9, 214, pp. 2-17

Hosnedlova, B., Kepinska, M., Fernandez, C., Peng, Q., Ruttkay-Nedecky, B., Milnerowicz, H., Kizek, R. (2019) 'Carbon nanomaterials for targeted cancer therapy drugs: A critical review', *The Chemical Record*, 19, pp. 502-522.

Hughes, G. A. (2017) 'Nanostructure-mediated drug delivery', *Nanomedicine in Cancer*, 1, Pan Stanford.

Jain, M., Olsen, H. E., Paten, B., Akeson, M. (2016) The Oxford Nanopore MinION: delivery of nanopore sequencing to the genomics community. *Genome biology*, 17, 1, pp. 239-250

Jeck, W. R., Lee, J., Robinson, H., Le, L. P., Iafrate, A. J., Naradi, V. (2019) 'A Nanopore Sequencing–Based Assay for Rapid Detection of Gene Fusions', *The Journal of Molecular Diagnostics*, 21, pp. 58-69.

John, A. A., Subramanian, A. P., Vellayappan, M. V., Balajl, A., Mohandas, H., Jaganathan, S. K. (2015) 'Carbon nanotubes and graphene as emerging candidates in neuroregeneration and neurodrug delivery', *International journal of nanomedicine*, 10, 4267-4277.

Joseph, D., Baskaran, R., Yang, S. G., Huh, Y. S., Han, Y.-K. (2019) 'Multifunctional spiky branched gold-silver nanostars with near-infrared and short-wavelength infrared localized surface plasmon resonances', *Journal of Colloid and Interface Science*, 542, pp. 308-316

Kalomiraki, M., Theros, K., Chaniotakis, N. A. (2016) 'Dendrimers as tunable vectors of drug delivery systems and biomedical and ocular applications', *International journal of nanomedicine*, 11, pp. 1-12.

Kalluri, A., Debnath, D., Dharmadhikari, B. & Patra, P. (2018) 'Graphene Quantum Dots: Synthesis and Applications', *Methods in enzymology*, 609, pp. 335-354

Kanapathipillai, M., Brock, A., Ingeber, D. E. (2014) 'Nanoparticle targeting of anti-cancer drugs that alter intracellular signaling or influence the tumor microenvironment', *Advanced drug delivery reviews*, 79, pp. 107-118.

Kaur, J., Gill, G. S., Jeet, K. (2019) Applications of Carbon Nanotubes in Drug Delivery: A Comprehensive Review. Characterization and Biology of Nanomaterials for Drug Delivery. Elsevier.

Khlebtsov, N., Dykman, L. (2011) 'Bio distribution and toxicity of engineered gold nanoparticles: a review of in vitro and in vivo studies', *Chemical Society Reviews*, 40, pp. 1647-1671.

Kooshki, H., Sobhani-Nasab, A., Eghbali-Arani, M., Ahmadi, F., Ameri, V., Rahimi-Nasrabadi, M. (2019) 'Eco-friendly synthesis of PbTiO3 nanoparticles and PbTiO3/carbon quantum dots binary nano-hybrids for enhanced photocatalytic performance under visible light', *Separation and Purification Technology*, 211, pp. 873-881.

Kratochwil, C., Bruchertseifer, F., Giesel, F. L., Weis, M., Verburg, F. A., Mottaghy, F., Kopka, K., Apostolidis, C., Haberkorn, U., Morgenstern, A. (2016) '225Ac-PSMA-617 for PSMA-targeted a-radiation therapy of metastatic castration-resistant prostate cancer', *J Nucl Med*, 57, pp. 1941-1944.

Kumar, P. V., Kala, S. M. J., Prakash, K. (2019) 'Green synthesis of gold nanoparticles using Croton Caudatus Geisel leaf extract and their biological studies', *Materials Letters*, 236, pp. 19-22.

Lee, H., Kim, C., Lee, D., Park, J. H., Searson, P. C., Lee, K. H. (2017) 'Optical coding of fusion genes using multicolor quantum dots for prostate cancer diagnosis', *International journal of nanomedicine*, 12, pp. 4397-4407.

Lee, Y. C. A., LI, S., Chen, Y., LI, Q., Chen, C. J., Hsu, W. L., Lou, P. J., Zhu, C., Pan, J., Shen, H. (2019) 'Tobacco smoking, alcohol drinking, betel quid chewing, and the risk of head and neck cancer in an East Asian population', *Head & neck*, 41, pp. 92-102.

Lim, S. Y., Shen, W., GAO, Z. (2015) 'Carbon quantum dots and their applications', *Chemical Society Reviews*, 44, pp. 362-381.

Lin, A. J., Kidd, E., Dehdashti, F., Siegel, B. A., Mutic, S., Thaker, P. H., Massad, L. S., Powell, M. A., Mutch, D. G., Markovina, S. (2019) 'Intensity modulated radiation therapy and image-guided adapted brachytherapy for cervix cancer', *International Journal of Radiation Oncology, Biology, Physics*, 103, pp. 1088-1097.

Lu, J., Tang, M., Zhang, T. (2019) 'Review of toxicological effect of quantum dots on the liver', *Journal of Applied Toxicology*, 39, pp. 72-86.

Mcguire, S. (2016) World cancer report 2014. Geneva, Switzerland: World Health Organization, international agency for research on cancer, WHO Press, 2015. Oxford University Press.

Mercado, N., Bhatt, P., Sutariya, V., Florez, F. L. E., Pathak, Y. V. (2019) Application of Nanoparticles in Treating Periodontitis: Preclinical and Clinical Overview. Surface Modification of Nanoparticles for Targeted Drug Delivery. Springer.

Mewara, D., Rathore, B. P. S. (2016) 'A Study of Appoaches of Nanotechnology in Biomedical Nanotechnology', *International Journal Of Applied Research In Science And Engineering* (International Conference on Emerging Technologies in Engineering, Biomedical, Medical and Science (ETEBMS-November 2016)), pp. 53-5.

Mittal, G., Dhand, V., Rhee, K. Y., Park, S.-J., Lee, W. R. (2015) 'A review on carbon nanotubes and graphene as fillers in reinforced polymer nanocomposites', *Journal of Industrial and Engineering Chemistry*, 21, pp. 11-25.

Muddineti, O. S., Ghosh, B., Biswas, S. (2015) 'Current trends in using polymer coated gold nanoparticles for cancer therapy', *International journal of pharmaceutics*, 484, pp. 252-267.

Mugaka, B. P., Hu, Y., Ma, Y. & Ding, Y. (2019) Surface Modification of Gold Nanoparticles for Targeted Drug Delivery. Surface Modification of Nanoparticles for Targeted Drug Delivery. Springer.

Norris, A. L., Workman, R. E., Fan, Y., Eshleman, J. R., Timp, W. (2016) 'Nanopore sequencing detects structural variants in cancer', *Cancer biology & therapy*, 17, pp. 246-253.

Oh, N., Park, J.-H. (2014) 'Endocytosis and exocytosis of nanoparticles in mammalian cells', *International journal of nanomedicine*, 9, 1, pp. 51-63.

Ozsolak, F., Milos, P. M. (2011) 'RNA sequencing: advances, challenges and opportunities', *Nature reviews genetics*, 12, 87-98.

Parro'n, T., Requena, M., Herna'ndez, A. F., Alarco'n, R. (2014) 'Environmental exposure to pesticides and cancer risk in multiple human organ systems', *Toxicology Letters*, 230, pp. 157-165.

Rami'rez, N., Özel, M. Z., Lewis, A. C., Marce', R. M., Borruli, F., Hamilton, J. F. (2014) 'Exposure to nitrosamines in third hand tobacco smoke increases cancer risk in non-smokers', *Environment international*, 71, pp. 139-147.

Riley, R. S., June, C. H., Langer, R., Mitchell, M. J. (2019) 'Delivery technologies for cancer immunotherapy', *Nature Reviews Drug Discovery*, 18, pp. 175-196.

Sanginario, A., Miccoli, B., Demarchi, D. (2017) 'Carbon Nanotubes as an Effective Opportunity for Cancer Diagnosis and Treatment', *Biosensors*, 7, 1, pp. 9-32.

Sharma, S., Naskar, S., Kuotsu, K. (2019) 'A review on carbon nanotubes: Influencing toxicity and emerging carrier for platinum based cytotoxic drug application', *Journal of Drug Delivery Science and Technology*, 51, pp. 708-720

Siegel, R. L., Mille, K. D., Jemal, A. (2016) 'Cancer statistics', *CA: a cancer journal for clinicians*, 66, 1, 7-30.

Singh, B., Mitragotri, S. (2019) 'Harnessing cells to deliver nanoparticle drugs to treat cancer', *Biotechnology advances*, In press. doi:10.1016/j.biotechadv.2019.01.006

Singh, S. D Rai, Praveen, A. (2015) 'DNA Methylation in Cancer: Review', *Indo Global Journal of Pharmaceutical Sciences*, 5(2), pp. 138-148

Smith, A. J., Oertle, J., PRATO, D. (2014) 'Immunotherapy in cancer treatment', *Open Journal of Medical Microbiology*, 4, 178-191.

Soliman, E. M., Kandil, U. F., Taha, M. M. R. (2012) 'The significance of carbon nanotubes on styrene butadiene rubber (SBR) and SBR modified mortar', *Materials and structures*, 45, pp. 803-816.

Somani, S. & Dufe's, C. (2014) 'Applications of dendrimers for brain delivery and cancer therapy', Nanomedicine, 9, pp. 2403-2414.

Song, K., XU, P., Meng, Y., Geng, F., Li, J., Li, Z., Xing, J., Chen, J., Kong, B. (2013) 'Smart gold nanoparticles enhance killing effect on cancer cells', *International journal of oncology*, 42, pp. 597-608.

Sowinska, M., Urbanczyk-Lipkowska, Z. (2014) 'Advances in the chemistry of dendrimers', *New Journal of Chemistry*, 38, pp. 2168-2203.

Stewart, B. & Wild, C. P. (2017) World cancer report 2014. Word Health Organization.

Tian, K., He, Z., Wang, Y., Chen, S.-J., Gu, L.-Q. (2013) 'Designing a Polycationic Probe for Simultaneous Enrichment and Detection of MicroRNAs in a Nanopore', *ACS Nano*, 7, pp. 3962-3969.

Tohme, S., Simmons, R. L., Tsung, A. (2017) 'Surgery for cancer: a trigger for metastases', *Cancer research*, 77, pp. 1548-1552.

Torre, L. A., Bray, F., Siegel, R. L., Ferlay, J., Lortet-Tieulent, J., Jemal, A. (2015) 'Global cancer statistics, 2012', *CA: a cancer journal for clinicians*, 65, pp. 87-108.

Tsagozis, P., Forsberg, J., Bauer, H. C., Wedin, R. (2019) How Expected Survival Influences the Choice of Surgical Procedure in Metastatic Bone Disease. *Management of Bone Metastases*. Springer.

Valcke, M., Bourgault, M.-H., Rochette, L., Normandin, L., Samuel, O., Belleville, D., Blanchet, C., Phaneuf, D. (2017) 'Human health risk assessment on the consumption of fruits and vegetables containing residual pesticides: a cancer and non-cancer risk/benefit perspective', *Environment international*, 108, pp. 63-74.

Vangijn, W., Gooiker, G., Wouters, M., Post, P., Tollenaar, R., Van De VeldeEL, C. (2010) 'Volume and outcome in colorectal cancer surgery', *European Journal of Surgical Oncology (EJSO)*, 36, pp. S55-S63.

Von Minckwitz, G., Untch, M., Blohmer , J.-U., Costa, S. D., Eidtmann, H., Fasching, P. A., Gerber, B., Eiermann, W., Hilfrich, J., Huober, J. (2012) 'Definition and impact of pathologic complete response on prognosis after neoadjuvant chemotherapy in various intrinsic breast cancer subtypes', *Journal of clinical oncology*, 30, pp. 1796-1804.

Wang, E. C. & Wang, A. Z. (2014) 'Nanoparticles and their applications in cell and molecular biology', *Integrative Biology*, 6, pp. 9-26.

Wang, Y., Wang, Z., Xu, C., Tian, H., Chen, X. (2019) 'A disassembling strategy overcomes the EPR effect and renal clearance dilemma of the multifunctional theranostic nanoparticles for cancer therapy', Biomaterials, 197, pp. 284-293

Wei, T., Chen, C., Liu, J., Liu, C., Posoco, P., Liu, X., Cheng, Q., Huo, S., Liang, Z., Fermeglia, M., Pricl, S., Liang, X.-J., Rocchi, P., Peng, L. (2015) Anticancer drug nanomicelles formed by self-assembling amphiphilic dendrimer to combat cancer drug resistance. Proceedings of the National Academy of Sciences.

Yang, N., Jiang, X. (2017) 'Nanocarbons for DNA sequencing: A review', *Carbon*, 115, pp. 293-311.

Yanover, D., Vaxenburg, R., TilchinIL, J., Rubin-Brusilovski, A., Zalats, G., Čapek, R. K., Sashchiuk, A., LIFSHITZ, E. (2014) 'Significance of Small-Sized PbSe/PbS Core/Shell Colloidal Quantum Dots for Optoelectronic Applications', *The Journal of Physical Chemistry* C, 118, pp. 17001-17009.

Yu-Cheng, C., Xin-Chun, H., Yun-Ling, L., Yung-Chen, C., You-Zung, H., Hsin-Yun, H. (2013) 'Non-metallic nanomaterials in cancer theranostics: a review of silica- and carbon-based drug delivery systems', *Science and Technology of Advanced Materials*, 14, 4, 044407. doi: 10.1088/1468-6996/14/4/044407

Yu, J.-G., Jiao, F.-P., Chen, X.-Q., Jiang, X.-Y., Peng, Z.-G., Zeng, D.-M., Huang, D.-S. (2012) 'Irradiation-mediated carbon nanotubes' use in cancer therapy', *Journal of Cancer Research and Therapeutics*, 8, pp. 348-354.

Yuan, H., Khoury, C. G., Hwang, H., Wilson, C. M., Grant, G. A., Vo-Dinh, T. (2012) 'Gold nanostars: surfactant-free synthesis, 3D modelling, and two-photon photoluminescence imaging', *Nanotechnology*, 23, 7, 075102. doi: 10.1088/0957-4484/23/7/075102.

Zhang, Z., Wang, F., Xu, G., Liu, X., Cao, Y., Min, W. (2019) 'Design and simulation of optical drive tunable grating based on GNP and PDMS', *Materials Research Express*, 6, 5, 055704. https://doi.org/10.1088/2053-1591/ab0575

Zhou, Z., Ma, X., Murphy, C. J., Jin, E., Sun, Q., Shen, Y., Van Kirk, E. A., Murdoch, W. J. (2014) 'Molecularly precise dendrimer–drug conjugates with tunable drug release for cancer therapy', *Angewandte Chemie International Edition*, 53, pp. 10949-10955.

Zong, C., Ai, K., Zhang, G., Li, H., Lu, L. (2011) 'Dual-Emission Fluorescent Silica Nanoparticle-Based Probe for Ultrasensitive Detection of Cu2+', *Analytical Chemistry*, 83, pp. 3126-3131

Libyan Journal of Science & Technology 9:2 (2019) 176–183

Faculty of Science - University of Benghazi

Libyan Journal of Science & Technology

journal home page: www.sc.uob.edu.ly/pages/page/77

Hydro-geochemical review of groundwater and rain waters from Al Jabal Al Akhdar, Northeast Libya

Mohamed S. E. Al Faitouri, Fathi M. Salloum*, Ahmed M. Muftah

Department of Earth Sciences, Faculty of Science, University of Benghazi, Benghazi- Libya.

Highlights

- **Tritium and Carbon radioisotopes used in estimating the groundwater, surface water, springs and rain recharge rates, and origin of the water. Shallow and deep aquifers and the karstic systems are used extensively for environmental studies.**
- **Values of δ^2H and $\delta^{18}O$ indicate increase in aridity, as deuterium excess is reduced due to evaporation effects.**
- **Mixing of fresh water with the seawater indicates that the stable isotopes are enriched due to evaporation.**
- **High contents of bicarbonate ions suggesting most carbon in solution derives from the reservoir limestone.**

ARTICLE INFO

Article history:
Received 22 June 2019
Revised 05 July 2019
Accepted 08 July 2019
Available online 11 July 2019

Keywords:
Al Jabal Al Akhdar, Stable isotopes, Hydro-geochemical evaluation, Tritium, Groundwater, Libya.

*Corresponding Author:
E-mail address: fathi.salloum@uob.edu.ly
F. M. Salloum

ABSTRACT

Groundwater recharge and age dating using stable and carbon isotopes in northern Cyrenaica have been performed during the seventies of the last century. Twenty-eight groundwater samples (springs and wells), as well as sixty rain water samples, were collected from four hydrogeological units in Al Jabal Al Akhdar that have been analyzed in order to determine the composition of the stable isotopes (δ^2H, $\delta^{18}O$, ^{14}C, and ^{13}C). Tritium is used herein to determine if there is any direct infiltration of modern water to the existed aquifers in the study area. The range of compositions for each rainwater sample is: δ^2H (–28.3‰ to 0.3‰) and $\delta^{18}O$ (–5.32‰ to 0.33‰) for Benghazi rain samples whereas δ^2H (–35‰ to –22.6‰) and $\delta^{18}O$ (–6.5‰ to –4.43‰) for Al Marj rain samples which show apparently oceanic and continental effects on the studied samples to the Global Meteoric Water Line (GMWL). The Miocene water samples have δ^2H and $\delta^{18}O$ values indicated an increasing in aridity as the deuterium excess is reduced due to evaporation effects. Given this result, the isotopic values indicate that the groundwater pumped from wells in Benghazi – Al Marj region resulted from the mixing of at least two groundwater systems. Seawater intrusion should be considered in the Ayn Zayanah-Al Coeffiah karstic system. Additionally, the δ^2H /$\delta^{18}O$ ratios show that most of the Ayn Zayanah spring discharges contain evaporated waters due to enrichment in isotopic values.

1. Introduction

Libya has very low precipitation values due to its location in an arid climate. However, Al Jabal Al Akhdar is located in northeast Libya (Fig. 1), which is receiving the largest annual precipitation. In particular, the coastal plain of the eastern part of Libya receives about 250 to 650 mm of annual precipitation. On the other hand, evaporation rates are likewise high, ranging from 1530 to 1710 mm/year in the north, and significantly increases towards the south. The potential evapotranspiration is minimum at the center of the northern slope of Al Jabal Al Akhdar reaching values of 1200 mm in Shahhat area and 1600 mm in the central south of Cyrenaica (Group Etude' de France en Libya, 1972). According to Ar-Lab (1978 and 1982), the evaporation at Al Makhili was recorded as 2871 to 3174 mm/yr, whereas in Msus area ranging between 3535 to 4050 mm/yr.

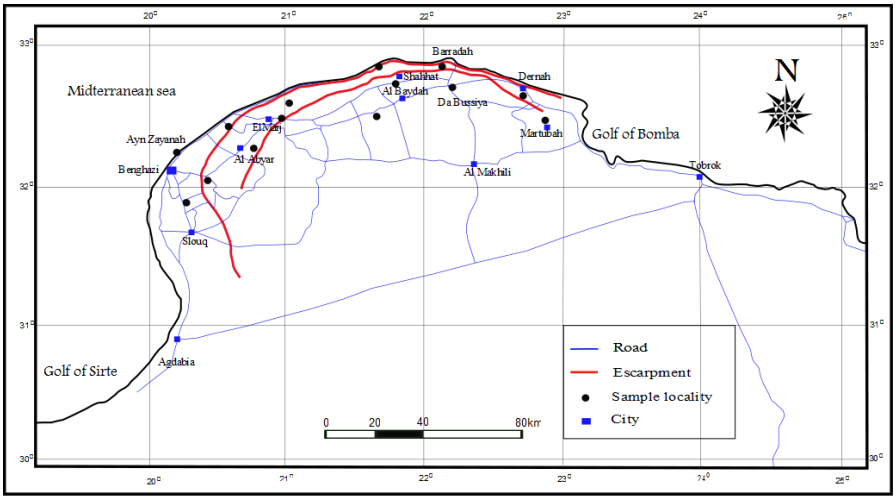

Fig.1. Location map of the study area, Al Jabal Al Akhdar, NE Libya

1ISSN 2663-1407; National Library of Libya, Legal number: 390/2018

Because of low precipitation fall over all the country and increase in population, the main source for water is the groundwater. In addition, as a result of excessive pumping, seawater intrusion has taken place in the Ayn Zayanah-Al Coeffiah aquifers. The purpose of this work is to re-evaluate the interaction between the precipitation and the recharge, as well as proving whether the groundwater receives modern water or not. Several unpublished studies and reports have been performed by some researchers, such as Group Etude' de France en Libya (Group Etude' de France en Libya 1971, 1972; Pallas, 1978; Franlab, 1976; Italconsult, 1977) on groundwater concerns. However, Anonymous (1975-76), Gonfintianii (1977) and Bahadur (1978) are the only works dealt with isotopic analyses of groundwater in Al Jabal Al Akhdar.

2. Geological settings

Al Jabal Al Akhdar anticlinorium is a part of the northern African-Arabian active margin that had been evolved following the opening of the Neotethys. This area is classified into the mobile province in the north (referred as Al Jabal Al Akhdar) and more stable Cyrenaica Platform province in the south by some workers (e.g. El Werfalli *et al*., 2000; El Hawat and Abdulsamad, 2004). Anketell (1996) delineated the Cyrenaica Fault System (CFS) that forms the boundary between Al Jabal Al Akhdar and Cyrenaica Platform into the North Cyrenaica Fault System (NCFS), which runs parallel to the coast of Cyrenaica offshore, and the South Cyrenaica Fault System (SCFS), which forms the southern limit of Cyrenaica Platform. The mobile area upfaulted at some regions in form of Cretaceous inliers including Jardas al Abid; Uwaliyah; Jardas al Jarari; Marawa; and the recently discovered Ras al Hilal anticline (El Amawy *et al*., 2011) with major SWS–ENE trending anticlines, where the older Cretaceous rocks are cropping out (Fig. 2). The exposed Upper Cretaceous rocks are strongly folded and faulted as indicated by the angular unconformity in Jardas area, whereas, the Paleocene, Eocene, Oligocene and the Miocene rocks are slightly folded. The rare exposures of Al Uwayliah Formation were the result of this tectonic event as reflected in unconformities (Faraj *et al*., 2016) (Fig. 2). The successions of the Al Jabal Al Akhdar are summarized in Fig. 3.

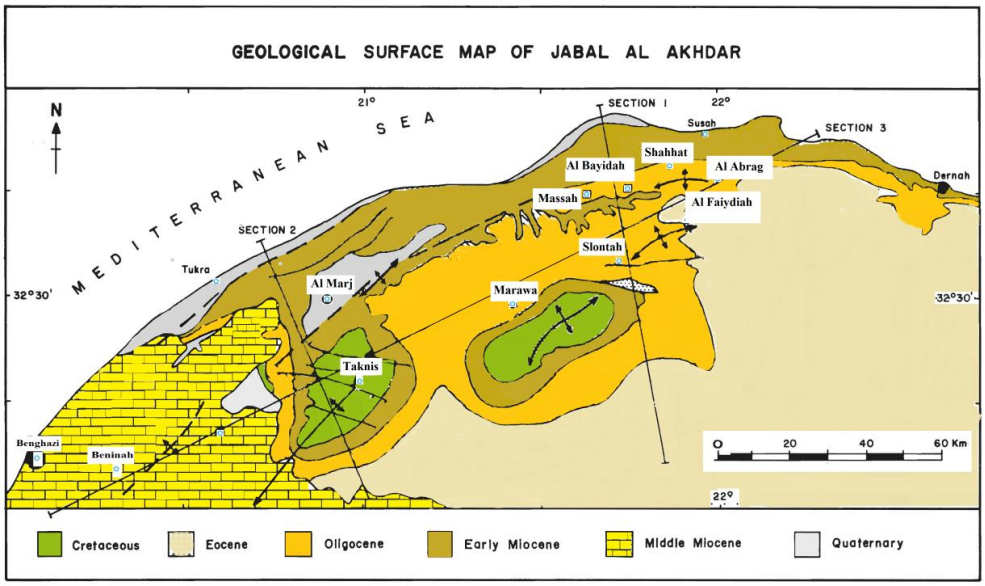

Fig. 2. The tectonic map shows the exposed rock units with Upper Cretaceous inliers (modified from El Werfalli *et al*., 2000).

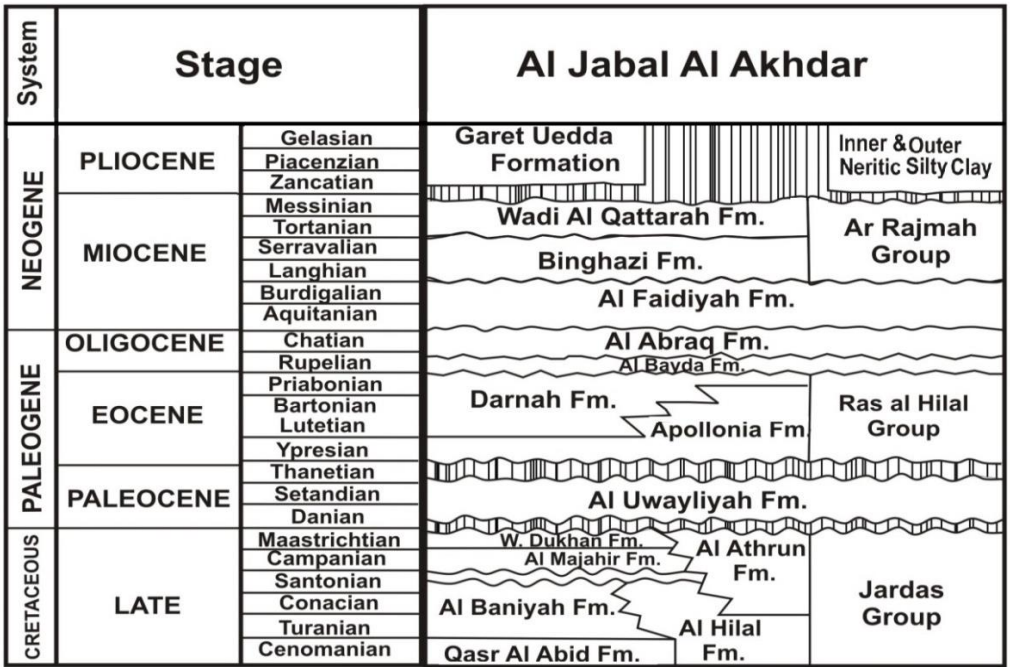

Fig. 3. Stratigraphic chart of the exposed rock units at Al Jabal Al Akhdar area (after El Hawat and Abdulsamad, 2004).

3. Methodology

Since 1972, General Water Authority (GWA) or their consultants collected groundwater, surface water, and rain samples from different regions in Al Jabal Al Akhdar. Samples were analysed to determine the composition of the stable isotopes (δ2H and δ18O, tritium and carbon) that are used to estimate the groundwater recharge rates and the origin of the water. Chemical measurements of pH, water temperature (°C), and Specific Conductance (SC) have been measured in the field.

4. Isotopic analyses and recharge

4.1 Stable Isotopes

One of the important application of isotopic is studying the groundwater recharge. A number of researchers have used environmental ^{3}H, ^{14}C, D and ^{18}O, while others have used artificial isotopic tracers to magnitude the moisture movement in unsaturated soils. Recently, Mass spectrometry (MS) is used to measure the ratio of the rare isotope to the common isotope ($^{2}H/^{1}H$ and $^{18}O/^{16}O$) instead of measuring the concentration of ^{2}H and ^{18}O individually. The variations in many isotopic abundances are relatively small, therefore, stable isotope ratios are reported relative to a standard as δ values in units of parts per thousand (per mil, and written as ‰) (Craig, 1961). Moreover, the values for water are reported relative to VSMOW (Vienna Standard Mean Ocean Water). A stable isotope has a general expression:

$$\delta_s = \left(\frac{R_s}{R_{std}} - 1\right) \times 1000 \quad (1)$$

where Rs (s=sample) and Rstd (std=standard) are $^{2}H/^{1}H$ or $^{18}O/^{16}O$ of the sample and standard, respectively. When δ has a negative value means, the sample is depleted in the heavy and it is isotopically light relative to the standard isotope (Al Faitouri and William, 2015). The relationship between $\delta^{2}H$ and $\delta^{18}O$ in precipitation worldwide is called the Global Meteoric Water Line (GMWL) Craig (1961) and is represented by the following equation

$$\delta^{2}H = 8\delta^{18}O + 10 \quad (2)$$

4.2 Stable Isotopes Results

The stable isotope results are presented in Tables (1&2) and the location of these samples is indicated in Fig. 1. Role of stable isotopes of the water molecule has been reviewed for the solution of the problem connected with the arid zones Bahadur (1978). A number of isotopic studies were performed by different consultants at different times in different areas in northern Cyrenaica (Bahadur *et al.*, 1980). The results are summarized below. Group Etude' de France en Libya (1972) has established that there is an altitude effect for ^{2}H and ^{18}O from the mean annual stable isotopic concentrations for precipitations at Benghazi.

Table 1

Stable Isotope compositions of groundwater samples in per mil (GWA, 1982).

Sample No	Location		^{18}O ‰ SMOW	D ‰ SMOW	d	$\delta D/\delta^{18}O$	^{3}H (T.U.)	^{14}C % NBS	^{13}C‰ PDB
1	Dabusiah	Springs in Miocene limestone aquifer	−5.8	−26.4	20.0	4.6	<1		
2			−5.8	−26.6	19.8	4.8	<1		
3			−5.3	−23.7	18.7	4.5	2±1		
4			−5.5	−26.2	17.8	4.8	2±1		
5			−5.3	−26.4	16.0	5.0	4±2		
6								62.2±1.2	−9.68
7			−5.1				10±2		
8			−3.1	−16	8.8	5.2	5±2		
9	Ayn Zayanah		−2.8	−13	9.4	4.65	5±2		
10			−1.5	−12.8	−0.8	8.5	2±1		
11			−2.3	−13	5.4	5.7	<1		
12			−2.4	−12.4	6.8	5.2	7±2		
13			−2.5		20.0		6±2		
14					0.0			38.8±2.1	−8.25
15	Baradah		−5.0	−22.8	17.2	4.6		94.3±1.5	−28
16	Shahat	Wells in Miocene limestone aquifer	−5.7	−27.4	18.2	4.8	14±2		
17	Marawa				0.0			9.7±0.7	−6.79
18	Salanta		−5.8	−28.1	18.3	4.8	6±2	35.5±1	6.97
19			−5.4		43.2		<1		
20	Al haniah				0.0			62.2±1	−9.64
21	Militaniah				0.0			4.6±0.9	−0.99
22	Abyar				0.0			4±0.6	−5.92
26			−4.9	−24.6	14.6		2±1		
27			−5.0	−24.3	15.7				
28	Beninah		−4.5	−23.3	12.7	5.2	<1		
29			−4.7	−24.5	13.1				−7.04
30			−4.4	−14.9	20.3	3.4	2±1		
31			−4.7	−24.5	13.1	5.2	5±2		
32			−4-4		35.2		3±2		
33	Al Marj				0.0			43.21±1.1	−8.06
34			−4.6	−23.6	13.2	5.21	5±2		

The range of compositions for each of the sampled unit are: $\delta^{2}H$ from −28.3‰ to 9.9‰ and $\delta^{18}O$ from −5.32‰ to 2.12‰ for Benghazi rain samples; $\delta^{2}H$ from −35‰ to −22.6‰ and $\delta^{18}O$ from −6.5‰ to −4.43 ‰ for Al Marj rain samples. The water samples collected from springs, wells in the Miocene limestone aquifer and Benghazi region, have values of $\delta^{2}H$ and $\delta^{18}O$ as shown in Tables (1 & 2). Fig. 4 to 7 indicate the effect of an increase in aridity as the deuterium excess is reduced due to evaporation.

Table 2

Stable isotope compositions of rain water samples in per mil (GWA, 1982)

S .No.	Location	$\delta^{18}O^{0}/_{00}$ SMOW	$\delta D^{0}/_{00}$ SMOW	d	$\delta D/\delta^{18}O$	^{3}H(T.U.)	^{14}C % NBS	^{13}C % PBD
1	Ayn Zayanah	2.12	−9.90	−26.86	-4.670			
2		−2.64	−12.60	8.52	4.773			
3		−2.87	−14.10	8.86	4.913	2.7±2		
4		−2.92	−13.4	9.96	4.589			
5		−2.54	−12.3	8.02	4.843			
6		−2.90	−13.1	10.10	4.517			
7		−4.98	−23.3	16.54	4.679	0.47±0.15	17.4±1	−7.59
8		−518	−25.4	16.04	4.903	0.36±0.15	17.7±0.9	−8.17
9		−3.82	−19.00	11.56	4.974			
10		−4.89	−22.1	17.02	4.519	0.36±0.2		
11		−0.33	−0.30	2.34	0.909			
12		−2.88	−12.00	11.04	4.167	2.4±0.3	26.9±3.2	−4.91
13	Beninah & Hawari	−4.96	−25.3	14.38	5.101	0.38±0.19	15.7±0.9	−7.95
14		−5.06	−25.2	15.28	4.980			
15		−4.54	−25.1	11.22	5.529			
16		−4.70	−25.2	12.40	5.362			
17		−5.26	−26.2	15.88	4.981	0.37±0.26		
18		−4.08	−22.8	9.84	5.588		4.4±0.6	−3.25
19		−4.83	−25.3	13.34	5.238			
20		−4.99	−28.3	11.62	5.671			
21		−4.93	−26.5	12.94	5.375			
22		−4.99	−26.5	12.94	5.375			
23		−4.66	−26.0	11.28	5.579		8.4±0.7	−5.43
24		−4.36	−23.1	11.78	5.298		11.6±0.8	−6.06
25		−4.53	−24.4	11.84	5.386			
26		−4.88	−27.6	11.44	5.656		6.2±0.6	−3.98
27		−4.94	−27.2	12.32	5.506		8.2±0.6	−5.78
28	Al Marj & Abyar	−4.63	−21.8	15.24	4.708		41.7±1.2	0.54
29		−4.96	−25.3	14.38	5.101		6.3±0.7	−4.38
30		−5.63	−29.4	15.64	5.222		10.8±0.8	−5.52
31		−4.56	−24.8	11.68	5.439		16.2±3.5	−7.45
32		−4.58	−23.6	13.04	5.153			
33	Beninah & Hawari	−4.81	−26.5	11.98	5.509			
34		−5.24	−28.6	13.32	5.458			
35		−4.68	−25.8	11.64	5.513			
36		−4.88	−27.8	11.24	5.697			
37	Al Marj & Abyar	−4.65	−26.1	11.10	5.613		12. 2±0.8	−6.59
38	Beninah & Hawari	−5.32	−26.4	16.16	4.962			
39		−4.46	−23.8	11.88	5.336			
40		−4.32	−25.8	8.76	5.972			
41		−4.44	−25.9	9.62	5.833			
42	Al Marj & Abyar	−5.44	−28.9	14.62	5.313			
43		−4.67	−25.4	11.96	5.439			
44		−5.06	−26.4	14.08	5.217			
45		−5.18	−26.8	14.64	5.174			
46		−4.77	−24.5	13.66	5.136			
47		−6.50	−35.00	17.00	5.385			
50		−5.28	−28.10	14.14	5.322			
51		−5.52	−28.40	15.76	5.145			
52		−5.21	−28.10	13.58	5.393			
53		−5.26	−27.30	14.78	5.190			
54		−5.20	−28.10	13.50	5.404			
55		−4.64	−25.80	11.32	5.560			
56		−4.43	−23.80	11.64	5.372			
57		−4.43	−23.80	11.64	5.372			
58	Ayn Zayanah	−5.05	−22.60	17.80	4.475			
59		−4.75	−22.70	15.30	4.779			
60	Beninah & Hawari	−4.86	−24.30	14.58	5.000			

4.3 Stable Isotopic Interpretation and Discussion

The precipitation samples at Benghazi and Al Marj- Al Abyar show that δD varied from -9.9 to -35‰ and $\delta^{18}O$ from 2.12 to -6.5 ‰ (Table 2). Fig. 4 shows apparently oceanic and continental effects of the sample from the Global Meteoric Water Line (GMWL), which inferred from Eq. 2 or may be due to the origin of moistures that releases from clouds at different elevations. Also, dominant air temperatures at these locations could affect the water. The changes in the isotopic concentrations with time for discharge at Ayn Zayanah water samples show that the water comes from precipitation under altitude and temperature conditions similar to those dominant in Benghazi area (Bahadour *et al.*, 1980). Spring waters show some occurrence of recent precipitation due to changes observed in the stable isotopic concentrations in the direction of changes observed in precipitation collected from the nearby hydrometer logical stations (Fig. 5). The isotopic concentrations of water well data show that the groundwater in the Miocene limestone aquifer of Cyrenaica is a mixed water system (Fig. 6). In addition, Guerre (1984) reported that the contents of δD and $\delta^{18}O$ in different water samples from the Ayn Zayanah karstic network indicate that these are mixed of seawater and fresh water.

Overall, the results of the analyses of 60 samples collected from eastern Libya (from Benghazi region to Al Marj) have been divided into three groups according to the geographical location. The first group includes samples collected from Al Coeffiah area closed to Ayn Zayanah, and related to the study of the spring (sample Nos. 1-12 & 58-59) (Fig. 1). The second group of samples includes those collected from Benghazi plain, mainly from the water wells in the area of Baninah and Hawari (sample Nos. 13-27, 33-36, 38-41, 60) (Fig. 1). The third group includes samples collected from Al Marj Al Abyar area (sample Nos. 28-32, 37, 42-56). Most of these samples plotted just above and on the GMWL, indicating less oceanic and continental effects (Figs. 6 & 7). Particularly, sample (No. 1) does not follow the GMWL and shows the mixing of fresh water with the seawater and indicates that the stable isotopes are enriched due to evaporation. However, the sample (No. 47) shows highly negative δ values of GMWL. The salt presence is most probably due to seawater encroachment as a consequence of intensive exploitation.

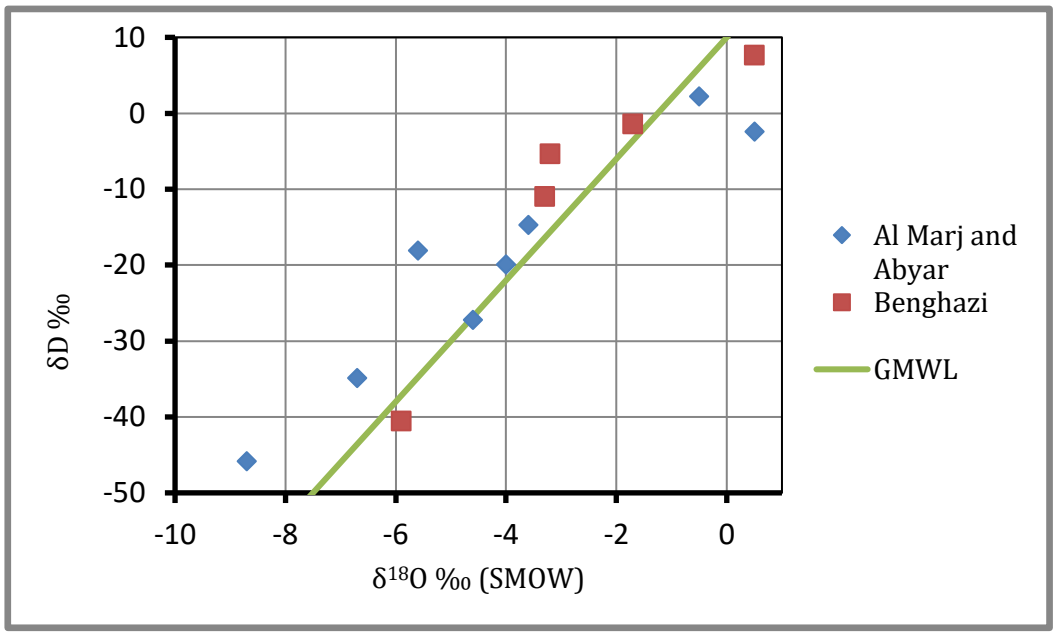

Fig. 4. Compositions of δD vs. $\delta^{18}O$ against the Global Meteoric Water Line (GMWL) from Al Marj, Al Abyar, and Benghazi areas.

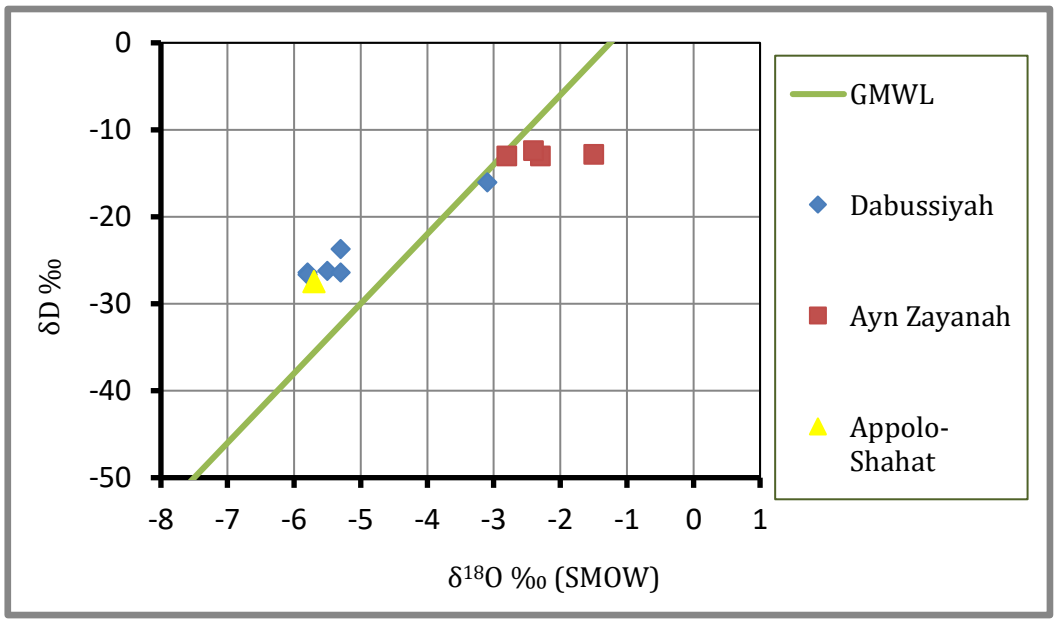

Fig. 5. Compositions δD vs. $\delta^{18}O$ against the Global Meteoric Water Line (GMWL) from Dabussiyah, Ayn Zayanah, and Appolo-Shahhat areas.

The δD and $\delta^{18}O$ relationship between all samples excluding those which contain a high seawater fraction (sample Nos. 2-6, 9, 11 & 12) are affected by evaporation (Fig. 7). The lack of homogeneity of the isotope composition is most surprising within small heavily exploited subsystem as in Baninah well field. The fraction of seawater existing at each site can also be evaluated from the isotopic composition of the three sites in Al Coeffiah area with low conductivity (sample Nos. 7, 8, 58). δD=–23.8‰ and $\delta^{18}O$=–5.07‰ representative of the fresh groundwater component. The δ values given by the seawater sample (No. 11) collected from the Ayn Zayanah indicating that the sample should contain an appreciable fraction of fresh water coming from the Blue Lagoon. Therefore, on the basis of other measurements existing in the literature available, we assume the values of δD= +8‰ and $\delta^{18}O$= +1.5‰ as representative of the seawater component. Moreover, from all the figures above, we can conclude that the groundwater consists of at least two different types of fresh waters that do not mix or only partially mix in somehow. This means that there are two or more fresh water systems present where relative contribution might change from one well to another according to the karstic fissures encountered in drilled wells. Seawater is another component that makes the picture more complicated. Several processes cause water to deviate from local meteoric water lines, e.g. evaporation from surface-water bodies, humidity, temperature, and salt concentration (Gat, 1981). Figs. 4 to 7 also show the intercept and the trends of the meteoric lines that indicate these waters were more or less isotopically light. Some samples will not follow these two groups because they could be mixtures of different types of water. It is clearly seen that the compositions of all samples are quite depleted relative to that of modern precipitation. According to Group Etude' de France en Libya (1976), most of the groundwater in Benghazi Plain are ancient and signified very slow circulation of underground waters. This appears to be contrary to the transmission characteristics of the aquifer systems of the region. The isotope geochemistry of the Miocene limestone aquifer in Al Jabal Al Akhdar for the study of regional recharge and discharge characteristics of the system has been performed by Castany *et al*. (1974). They demonstrated that the isotope geochemistry is helpful for determining the homogeneity or heterogeneity of a groundwater reservoir, and also possible to explore large scale groundwater movement. GWA (1982) had described the results of the analyzed groundwater samples from Al Coeffiah and Benghazi region, using ^{3}H, ^{2}H, $^{18}0$ and ^{34}S analysis. It was concluded that the samples are having some fraction of recent recharge.

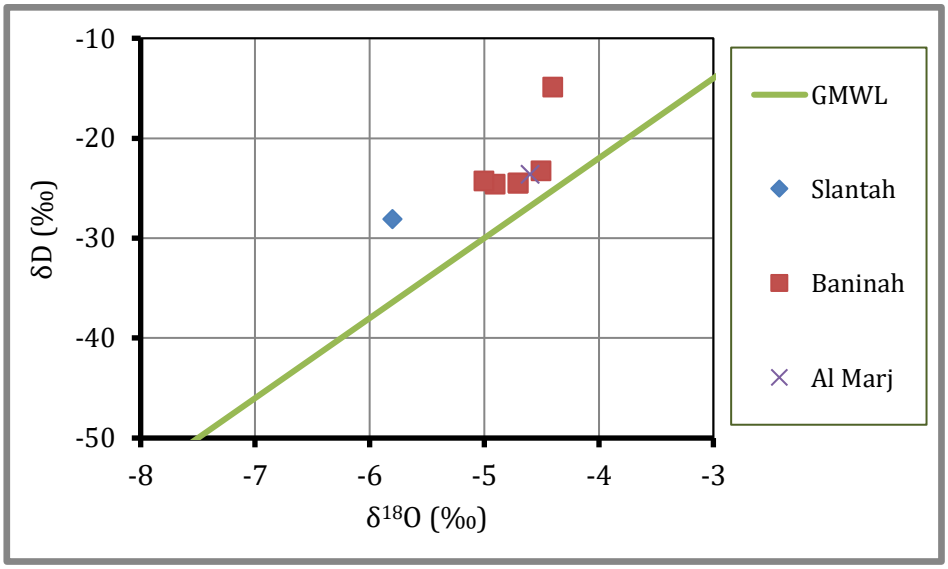

Fig. 6. Compositions of δD vs. $\delta^{18}O$ against the Global Meteoric Water Line (GMWL) from Salantah, Baninah, and Al Marj areas.

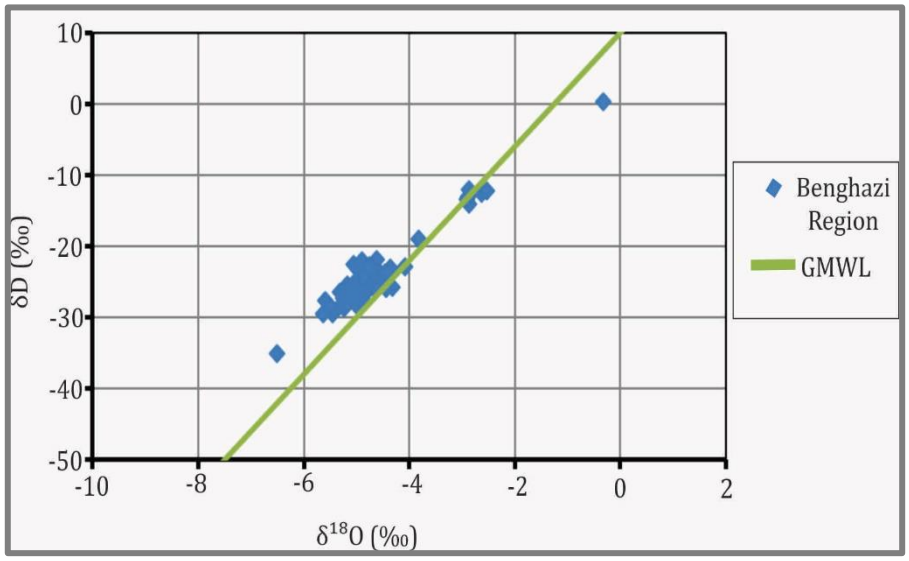

Fig 7. Compositions of δD vs. $\delta^{18}O$ against the Global Meteoric Water Line (GMWL) from Benghazi region.

Fossil groundwater at wells in Miocene aquifers (Fig. 6) are of marine origin and not terrestrial. The water at Baninah had a greater fraction of recent recharge from the precipitation. Investigation of water resources in Benghazi Plain in the area between Sidi Khalifa and Tulmaythah, shown that the groundwater samples collected during the spring season are depleted in $\delta^{18}O$ values by 0.5–0.6‰ from those collected during autumn at the same location thereby indicating that the recharge is occurring in the present environmental conditions. The maximum pollution reported in observed so far in the study area corresponded to an addition of ~20% of seawater to the contemporary fresh groundwater.

5. Tritium Samples Results

The analytical accuracy, as well as the detection limit of the tritium measurements, was approximately ± 0.1 TU (tritium units, 1 TU is equivalent to a $^3H/^1H$ ratio of 10^{-18}, which represents one atom of tritium in 101 atoms of hydrogen) (Bahadour, 1978). Tritium, which is reported in tritium units (TU), was measured by ^3He accumulation method where the samples were vacuum degassed and shelved for 60 days to allow for the growth of ^3He from tritium decay. Tritium content of the groundwater, precipitation, and springs in Cyrenaica region are high ranging from <1 T.U. to 70+4 T.U. This high content of tritium indicates that these waters have recent recharge.

The precipitation samples show that the tritium content varied from 32 to 70 TU for Shahhat area and 27 to 59 TU for Benghazi (Bahadour *et al*., 1980). The corresponding changes in emerging springs in Miocene limestone are less than 1 to 14 TU. Table 1 shows changes in concentration depending on the location as well as the time of sampling. The wells tapping the same aquifer show a variation from less than 1 to 65 TU (Table1), thus demonstration the absence or presence of contemporary recharge respectively. It was recommended that the sampling for ^3H at different locations to be monitored at regular intervals of time to determine whether the concentrations are constant and to confirm the presence of more than one groundwater body on a regional scale for delineation of areas and aquifer depths for preferential exploitation of groundwater resources of the area (Bahadour *et al*., 1980).

The tritium concentrations varied from <1 to 10±1 for Al Dabusiah spring. However, the water samples which have not been mixed with seawater show little content of tritium. On the other hand, Ayn Zayanah with about 1/3 of seawater has an average of 5 TU (Table 1). Thus, one can evaluate a tritium content of 6 to 7 TU for the seawater component. Such a concentration may have been attained by the surface Mediterranean water and therefore the seawater component of Ayn Zayanah should not be older than a few years. The amount of tritium in water from deep aquifers at Baninah wellfield indicates little of modern water but does not necessarily mean the absence of recharge. Analyses of sample collected from a well at Baninah have tritium up to 5±2 TU that is very high and may be due to the limitation of analytical system utilized.

6. Carbon Isotopes

Recently, the ^{14}C radioisotope has extensively been used for environmental studies. The main sources of the dissolved carbon in groundwater are (1) *active carbon from the soil zone, from carbon dioxide of soil gases and solid carbonate from the soil*, and (2) *less active carbon of inorganic origin, formed during the production of the bicarbonate*. Moreover, dissolved CO_2 or carbonate is depending on the pH (Fontes and Garnier, 1979).

6.1 Carbon Isotope Results

The ^{14}C activities and $\delta^{13}C$ values were determined on a different type of water: groundwater and springs samples from different sites in Cyrenaica as in Fig. 1, and the results are presented in Tables 1 and 2. ^{13}C analyses are reported as δ values relative to the PDB (Belemite of the PeeDee Formation) standard and ^{14}C abundances are reported as Percent Modern Carbon (PMC).

Carbon isotope analysis shows that the differences in the ages of groundwater samples could not be related to chemical or ^{18}O composition of the samples. In addition, ^{13}C contents of bicarbonate ions are very high, suggesting that most of the carbon in solution derives from the reservoir limestone, which does not contain C. Therefore, it is concluded, that the available data do not confirm the existence of paleo waters in the coastal plain.

In Fig. 7, plots of the $\delta^{18}O$ values against the percent of modern carbon for the wells in which there are both sets of data. It can be seen that the lighter and heavy values of $\delta^{18}O$ are associated with all age of water as shown by Percent Modern Carbon (PMC) – lower PMC, which indicates older water. This comparison suggests that the waters were recently recharged.

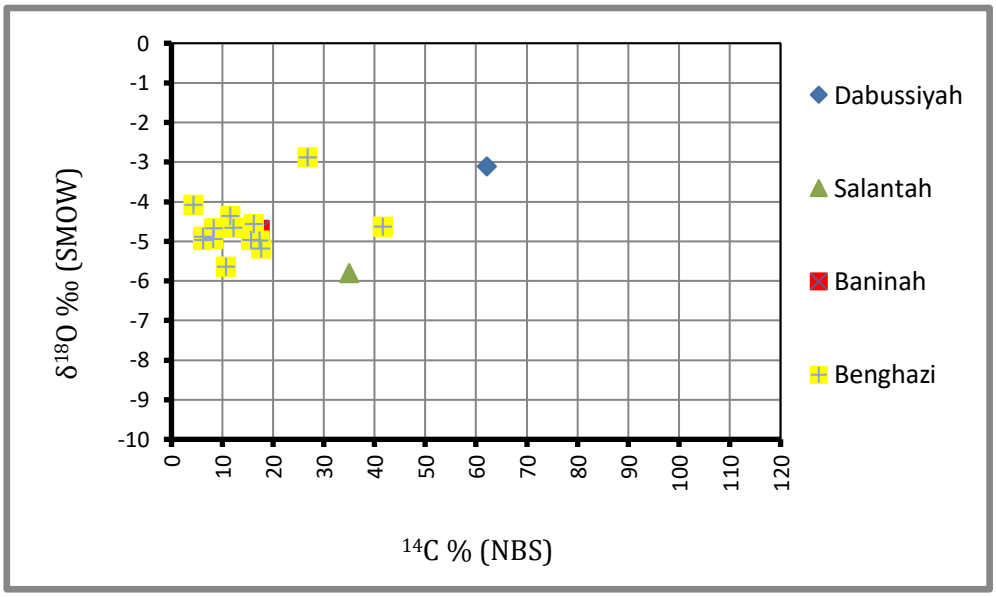

Fig. 8. Comparison of $\delta^{18}O$ vs. ^{14}C from Dabussiyah, Salantah, Beninah, and Benghazi areas. The lighter and heavy values of $\delta^{18}O$ have almost the same values but with different age.

7. Conclusions

- The stable isotopes data from the precipitated samples collected from coastal stations confirmed that the rainfall at these stations is affected by both humid and arid climates.
- Stable isotope composition of this charging water from natural springs show variations with time could be utilized to study the mixing characteristic of different aquifers by time sampling.
- The isotopic values indicate that the groundwater pumped from wells in the Benghazi-Al Marj region results from the interaction and mixing of at least two groundwater systems, to which seawater intruded in the Ayn Zayanah-Al Coeffiah area.
- The changes in stable isotopic concentrations for the spring sample show that they receive the recent recharge. The δD/δ^{18}O ratios show that most of the spring discharges contain evaporated waters due to enrichment in isotopic values, as well as, isotopic data of groundwater, show that they contain waters, which have been differential evaporated.
- The high values of tritium in most of the analyzed samples are linked to the nuclear bomb onwards. The ^{14}C values are not representatives in groundwater from karstified limestone aquifers, due to the influence of carbonate exchange of deeper layers of soil formation. It is the complexity of carbonate chemistry, which has denied the development of single unified criteria ^{14}C dating for all type of groundwater therefore individual aquifer systems should be studied using Carbon isotopes in close corporation with other disciplines as discussed before.
- Tritium results show that there is minor direct infiltration of rainwater. Small tritium content of these waters in Benghazi region, as well as Salantah and Dabussiyah regions, concluded that the contribution of local recent recharge to the karstic system is negligible.

Acknowledgments

The authors are grateful to the General Water Authority in Tripoli and Benghazi for offering the data used in this paper. Special thanks go to Dr. I. Bahadour from General Water Authority in Tripoli. Likewise, thanks extend to Dr. Raju and Dr. Alan Guerre from the General Water Authority in Benghazi Branch for their valuable help. We would also like to thank Dr. W. Samford from Colorado State University for his valuable comments and manuscript reviewing. Many thanks go to the Editor-In-Chief and the Editors of the Libyan Journal of Science and Technology (LJS&T), Faculty of Science, University of Benghazi. We also extend our thanks to the paper reviewers who made important comments, which improved the quality of this paper.

References

Al Faitouri, Mohamed, William E. Sanford (2015) 'Stable and radioisotope analysis to determine recharge timing and paleoclimate of sandstone aquifers in central and southeast Libya', *Hydrogeology Journal*, 23(4), pp. 707-717. doi: 10.1007/s10040-015-1232-7.

Anketell J. M. (1996) Structural history of Sirt Basin and its relationship to the Sabratah basin and Cyrenaica Platform, northern Libya. In: Geology of Sirt Basin, M. J. Salem, M. T. Bisrewil, A. A. Misalati and M. A. Sola (eds.) Elsevier, Amsterdam, vol. 3, pp. 57-89.

Anonymous 1975-76. Ana1ys d' Eau- Datãtion: Determination do la teneur en tritum et analyse isotopique do l'oxygen du deuterium et du sufro dans differents echantillons d'eau preleves dans Jo socteur do couefiah et do Benghazi.

Ar-Lab (1983) Complementary investigation of surface, groundwater and climatology survey preparation of tender documents for drilling and testing production and observation wells, Final Report. The Agricultural Development Council, The Executive Authority of Al Jabal Al Akhdar, The southern flank of Al Jabal Al Akhdar Project. Al Marj, NE Libya

Bahadur, J. (1978) Role of stable isotopic investigations in arid zone hydrology. Proc. Symp on Study and Management of Water Resources in Arid and Semiarid Regions', Ahmedabad, India.

Bahadur. J. Gueer, A., Salloum, F., Fadel, M. (1980) On Groundwater Recharge Evaluation. In North Cyrenaica, Unpublished Report, Secretariat of Dams and Water Resources, Tripoli. Libya.

Castany, G. (1974) An environmental isotope study of the groundwater regime in large aquifers. Proc. Inter. Symp. On isotopic techniques in groundwater hydrology, Vienna, IAEA, Vol. 1, 244p.

Craig, H. (1961) 'Standard for reporting concentrations of deuterium and oxygen-18 in natural waters', *Science*, 133 (3467), pp. 1833-1834.

Elamawy M. A., Muftah A. M., Abd-El-Wahid M., Nassar, A. (2011) Wrench structural deformation in Ras Al Hilal-Al Athrun area, NE Libya: a new contribution in Northern Al Jabal Al Akhdar belt. Arab. G. Geosci, vol. 4, pp. 1967-1985.

El-Hawat A. S., Abdulsamad E. O. (2004) The geology of Cyrenaica: A field seminar. Sedimentary basins of Libya. Earth Science Society of Libya. Tripoli.

Elwerfalli A., Muftah A. M., El-Hawat A. S. and Shelmani M. (2000) A guidebook on the geology of Al Jabal al Akhdar, Cyrenaica NE Libya. ESSL, Tripoli.

Faraj, H. F., Salloum, F. M., Muftah, A. M. and Bilal, A. A. (2016) Unique Dolines field in the area between Soluq and Msus, NE Libya: Origin and distribution. 4th International Symposium on Karst Evolution in the Mediterranean area: Karst Geosites. Sicily, Itali.

Fontes, J. and Garnier, J., (1979) 'Determination of the initial ^{14}c activity of the total dissolved carbon: A review of the existing models and a new approach', *Water Resources Research*, 15 (2), pp. 399–413.

Franlab. (1974-1976) Water Resources Study of the Southern Flank of Jabal Akhdar' Phase I final report (1974), Phase II final report (1976), Al Jabal Al Akhdar Authority, Ministry of Agriculture, Tripoli, Libya.

Gat, J. R. (1981) Lakes. In Stable Isotope Hydrology-Deuterium and Oxygen-18 in the Water Cycle, Gat JR & Gonfintianii R (eds.). IAEA Technical Report Series No. 210. IAEA: Vienna; 203–221.

Group Etude' de France en Libya (1971 and 1972) Soil and Water Resources Survey for Hydro Agricultural Development Eastern Zone'. Interim Report, General Water Authority. Tripoli, Libya

Group Etude' de France en Libya (1976) Soil and Water Resources Survey for Hydro Agricultural Development Eastern Zone'. Final Report, General Water Authority. Tripoli, Libya.

General Water Authority, (1982) Hydrogeological aspects of east Libya, unpublished internal Report, Benghazi Branch, Benghazi, Libya.

Gonfintianii, R. (1977) Progress Report on the Application of Isotope Techniques to Hydz1ogy in the Libyan Arab Republic, IAEA, Vienna.

Guerre, A. (1984) Hydrological Study of the Coastal Karstic Spring of Ayn Zayanah (Eastern Libya). Internal Mission Report. General Water Authority, Benghazi, Libya.

Italconsult. (1977) Preliminary Water-Resources Investigations in Bombah, Ayn Ghazala Tobruk Area. Report for Secretariat of Dams and Water Resources.

Pallas, P. (1978) Water Resources of Socialist People's Libyan Arab Jamahiriya, second symposium on the geology of Libya-Vol.2, Editors M .J. Salem and M.T. Busrewil 1980. Al Fateh University, Tripoli, Libya.

Libyan Journal of Science & Technology 9:2 (2019) 184–193

Faculty of Science - University of Benghazi

Libyan Journal of Science & Technology

journal home page: www.sc.uob.edu.ly/pages/page/77

Insight into the soil seedbank characteristics of the arid rangelands in Libya: A case study in Marmarica Plateau, Cyrenaica (Northeastern part of Libya)

Manam W. B. Saaed[a,*], Yacoub M. El-Barasi[b], Nazeeha A. Elhashani[b]

[a] *The Higher Institute of Agricultural Techniques, El-Marj, Libya.*

[b] *Botany Department, Faculty of Science, Benghazi University, Benghazi, Libya.*

Highlights

- **This study was conducted in Daphna, an arid rangeland area lies in the far northeastern part of Cyrenaica. This area was used as a case study to investigate the soil seedbank characteristics in the arid rangelands of Libya.**
- **Using the floatation in a salt solution method, the seeds were extracted from the soil then counted and identified.**
- **The results illustrated that the area still retained an adequate density of soil seedbank, however, the majority were for therophytes. The depressions and dykes in valleys retained higher seed density than the open flat areas..**

ARTICLE INFO

Article history:
Received 19 February 2019
Revised 31 July 2019
Accepted 02 August 2019
Available online 05 August 2019

Keywords:
anthropogenic factors, arid climate, landforms, rangeland degradation, rehabilitation..

*Corresponding Author:
E-mail address: muniem1965@gmail.com
Manam. W. B. Saaed

ABSTRACT

The current study was conducted in Daphna area, an arid region in Cyrenaica located at the northeastern part of Libyan Sea Coast at the Libyan-Egyptian Border. The soil was sampled in 40 different sampling sites along five different sectors through scraping the soil from 0-10 cm layer (25×25 cm) in the Platea and from 0–10 cm and 10–30 cm layers in the depressions and valleys. Using the floatation in a salt solution method, the seeds were extracted from the soil, counted and identified. The majority of the extracted seed were tinny (< 5 mm) and mainly belonged to annual species. Seeds density in the plateau ranged between 0 and 25400 seed m^{-2} with an overall mean of 4110 seed m^{-2} (±949.30 SE), which is adequate density when compared to similar arid ecosystems. The low-lying lands in depressions (Sakifas) and valleys (Wadis) retained higher seed density than the higher-lying lands on the plateau, and the northern areas retained higher density than the southern areas. The higher top soil layer (0–10 cm) in both Sakifas and behind the Dykes in valleys retained higher mean density than the layer (10–30 cm). The homogeneity of seed characteristics across the plateau and the dominance of annual and short-lived species could be a sign of degradation, and the absence of many perennial species in the soil seedbank may hamper any conservation or rehabilitation effort to improve these rangelands..

1. Introduction

Dryland ecosystems occupy about 45% of the Earth's land surface, store about 20% of the global soil carbon pool and contribute up to 30–35% of terrestrial net primary production (Ochoa-Hueso *et al*., 2018). Therefore, understanding ecosystem components and dynamics of these arid areas is a key role in any conservation, rehabilitation, and sustainable management programs. Particularly, the studies of the soil seedbanks (SSBs) improve our understanding of ecosystem dynamics and the effects of disturbance on ecosystem characteristics (van Etten *et al*., 2014).

Usually, SSBs survive disturbances including climate-related disturbances, diseases, and herbivory suffered by the plants (Ma *et al*., 2012), confer resilience to the plant community in response to changing ambient conditions (Ge *et al*., 2013). Furthermore, detailed information about the SSB is crucial for interpreting the consequences of disturbance related to ecological processes and ecosystem rehabilitation (Ge *et al*., 2013). Several degraded ecosystems have been rehabilitated successfully through SSBs (Braz *et al*., 2014; Saaed *et al*., 2018), but rarely so in Africa, where studies are few and, thus, debilitate decision-making in rangeland management (Saaed *et al*., 2018).

Seeds enter the SSB via seed-rains or through physical and animal-mediated dispersion (Louda, 1989; Roberts, 1981) and leave it via germination, secondary dispersal, seeds consumption by granivores, seeds decay, and parasite attack (Fenner, 1985; Shaukat and Siddiqui, 2004; Traba *et al*., 2006). Seeds in soils play prominent ecological and evolutionary roles (Zaghloul, 2008) linking past, present, and future plant population and community structure and dynamics (Leck *et al*., 1989; Thompson and Grime, 1979). Seed banks are especially important in desert ecosystems where annual plants account for a large part of the flora and their seeds may remain viable in the soil for many years (Inouye, 1991; Kemp, 1989; Rundel and Gibson, 2005) avoiding dry seasons and extended drought periods (Kinloch and Friedel, 2005a).

Although, SSB investigation in arid rangeland areas is an essential key to understand ecosystem state and dynamic, very few SSB studies have been conducted in North Africa, especially in the arid rangelands of Libya (El-Barasi and Saaed, 2013, 2015; El-Jetlawi, 2004; El-mograby *et al*., 2018; Nafea, 2015). Rangeland ecosystems in Libya still poorly understood and little is known about how decades of mismanagement and degradation affect the SSBs in these areas. Therefore, rehabilitation and sustainable utilisation of the landscape in these areas might be hampered by the lack of SSBs information (Saaed *et al*., 2018). This is particularly important in degraded arid ecosystems such as the study area, where plants mostly propagate via seeds (Saaed *et al*., 2018).

The present study is an attempt to cover the apparent gap in the available information on the rangeland ecosystem in Libya, particularly in the northeastern part of Cyrenaica, through investigating the SSB density, composition, spatial distribution, and the main factors influencing its characteristics. The study aimed to answer these questions:

 ISSN 2663-1407; National Library of Libya, Legal number: 390/2018

(1) *What is the density of SSB in the study area?*
(2) *Is there any variation in seed density amongst the different landforms across the landscape?*
(3) *What is the composition of the SSB in the area?*

Understanding of SSB characteristics could explain the ecosystem state, degradation dynamics, the influence of site features, and the future ecological responses of the rangelands in the study area and similar rangelands in the region.

2. Materials and methods

2.1 Study area

The study area is considered as an important rangeland area in Libya, lies in the northeastern part of Cyrenaica at the Mediterranean sea by the Libyan-Egyptian border (El-Barasi and Saaed, 2015). It is extending in an east-west rectangular shape, about of 130 km long and 25-35 km wide between longitudes 23° 54'–25° 09' east and latitudes 31° 36'–32° 06' north (Fig. 1). The study area is about 2 866 km² in size, comprises the western half of Marmarica Plateau (Libyan part of Marmarica Plateau). Locally the area is known as "Daphna area".

At the far north of the study area, there is a narrow strip of plains, while the southern high plateau covers most of the area and is divided by many valleys (dry rivers), which run with water in rainy season northwardly to end at the sea. Dykes (hampering rocky dams) are present along the valleys in different places as old practices to harvest runoff water and prevent soil erosion. There are many topographical depressions "locally named Sakifas" which distributed on the plateau as narrow ribbons in an east-west direction (Annexure A). Sakifas are sites of agricultural activities; relatively, they have more soil fertility and deeper strata, which offer good root penetrability. The different landscape features in the area provide different habitat types; therefore, the area is heterogeneous in soil properties and vegetation structure. The valleys shelter many wild biotas (flora and fauna) especially endemic and rare species that disappeared from the open areas. In some places, the elevation of the plateau reaches 220 m above sea level.

In general, Marmarica Plateau is characterized by an arid climate, with fluctuated and irregular monomodal winter rainfall regime (El-Barasi and Saaed, 2015). The annual mean maximum temperature is 24°C and the mean minimum temperature is 16°C. The annual rainfall rate is of 184 mm y^{-1} at Tobruk area in the north, while at EL-Bardia area in the Far East by the Egyptian border is of 117 mm y^{-1}, and southwardly at Tobruk airport (Al-A'daam area) 25 km south the coast is of 89 mm y^{-1}. The average relative humidity is of 71%, which increases during summer and reaches its minimum value during spring. The area is distinguished with high rates of evaporation, which exceeds 2000 mm y^{-1}. Based on the UNCCD aridity index obtained from the ratio between the values of mean annual precipitation (MAP) and potential evapotranspiration (PET), the study area classified as an arid land (MAP: PET ranged between 0.05 and 0.09).

The soil in the area is typical for arid areas. It is dry soil sediment over parent calcareous rocks characterized by shallow skeletal profile, low organic matter %, high calcium carbonate%, mainly loam or sandy loam texture, and tends to be alkaline (pH ≥ 8) (El-Barasi and Saaed, 2015). As a consequence of the harsh environmental conditions, the vegetation in the area is thermo-xerophilic vegetation dominated by sparse shrubs and dwarf-shrubs constituting the permanent vegetation cover. A mass display of flowering annuals occurs after rainfall in winter and early spring, often on degraded or fallow lands (El-Barasi and Saaed, 2015).

In addition to the accumulation of anthropogenic impacts over decades (over-grazing, dry farming, gathering wood, uprooting medical and economic species, soil trampling through off-road driving), the distribution and characteristics of vegetation in the area is influenced by natural factors (position on landscape, topography, climate, and soil properties) (El-Barasi *et al.*, 2013). Generally, the vegetation in the area is very heterogeneous and lowlands and watercourses characterised by relatively denser vegetation and some tall shrubs because they received more moisture through runoff after rainfall.

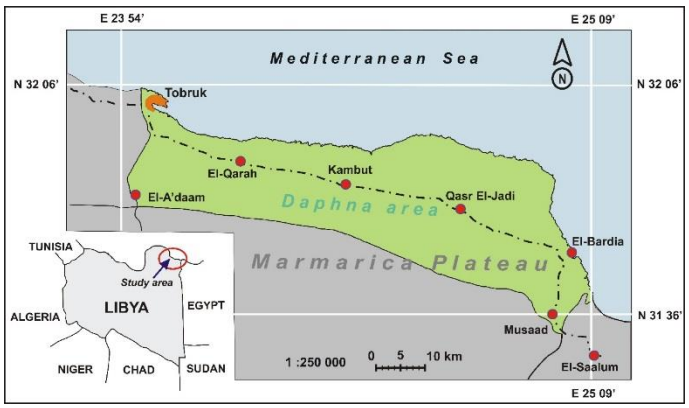

Fig. 1. The geographic location of the study area (Daphna) at the northeastern part of Cyrenaica

2.2 Soil seedbank survey

As a baseline, the SSB in this study is defined as all the seeds found in the soil or on the ground surface (Moles and Drake, 1999; Thompson and Grime, 1979). First, the area was divided into five sectors ranged between 25 and 35 km in length, each initiated from the coast and ended at the southern boundary of the study area. These sectors were at the localities, Ras-Biad (east Tobruk), El-Qarah, Kambut, Qasr EL-Gadi and Musaad respectively from the west to the east (Fig. 1). Along with each sector, the sampling sites were located systematically at five km intervals in north-southward direction. There were additional five sampling sites located at the depressions (Sakifas) and other five sampling sites collected from the sedimentary of five different Dykes.

Samples were collected by scraping the soil from the uppermost 10 cm layer in an area of 25×25 cm², and for the Dykes and Sakifas were at two different depths (0–10 cm and 10–30 cm) to know the different SSB density in the different soil layers (soil strata). There were 30-sampling sites along the different sectors and extra five-sampling sites in the depressions and other five-sampling sites behind the Dykes, the total was 40 sampling sites. Samples were weighed and packed in sealed plastic bags, labeled, and transported to the laboratory, and then they were allowed to air dry for 72 hours before processing. Then each soil sample was pooled and thoroughly homogenized, and soil seeds were extracted by flotation in a salt solution using the modified method of Malone (1967) by Buhler and Maxwell (1993) and Price *et al.* (2010).

The floating solution was prepared by combining 20 g of sodium hexametaphosphate, 10 g of $NaHCO_3$, and 500 g of K_2CO_3. The three chemical compounds were dissolved in tap water to make one liter. The experiment was conducted using three replications per each soil sample, each weighing 100 g. Initially, each sample was immersed in one liter of the prepared solution; then the solution was thoroughly agitated using a spatula for 30 seconds and left for 60 minutes to allow the organic matter to be floated on the salt solution. The floated organic debris was separated by filtration through filter paper (15 cm in diameter). The organic materials extracted were dried, and seeds were separated from the organic materials using binocular stereomicroscope and forceps. Then seeds were counted, and the seed numbers were estimated as the average of the three replications for each sample and recalculated as a number of seeds per square meter (seed m^{-2}). Seeds were identified based on the morphological feature, although most of these seeds could not be identified to species level, we were able to identify most of them to the family level.

2.3 Data analysis

The acquired data were first verified and tabulated and then entered into a Microsoft Office Excel spreadsheet (version 2016).

Initially, the data sets were inspected using descriptive statistical analysis and then checked for normal distribution using the Shapiro-Wilk W test. Significant differences for all of the examined parameters were explored using ANOVA (one-way) followed by the Tukey HSD post hoc test. In cases where the distribution of the data was not normal, Kruskal-Wallis one-way ANOVA test and T-test were used.

3. Results and discussion

3.1 Climate

In arid areas, the climate is one of the most important factors having a direct impact on wildlife, particularly the distribution and density of plant species, in addition to its impact on the soil properties (El-Barasi and Saaed, 2015). In the Libyan context, rangelands have fragile ecosystems, as they are located within the arid and semi-arid region, about half of the rangelands is under the 100-mm isohyet (Al-bukhari *et al*., 2018). This arid climate manifested as a poor composition and dynamic of the rangeland ecosystem components above ground (i.e. vegetation) and below ground (i.e. soil and SSB). Arid climatic factors play an important role in SSB's characteristics in these zones, which are mainly composed of ephemeral and annual seeds (therophytes). These species can complete their life cycle and producing considerable quantities of seeds in just a few weeks during the rainy and wet season. The annual therophytes growth in the study area comprised about 55% of the life-form spectra (El-Barasi and Saaed, 2013).

3.2 Seed size

Most of the seeds extracted from the soil were small in size (<5 mm) (Annexure B). The prevalence of small seed size in the study area is a typical feature of SSBs in arid and overgrazed, degraded rangelands (Baskin and Baskin, 2014; Dreber and Esler, 2011; Dreber *et al*., 2011). In such ecosystems, most plants are r-strategists producing many small seeds to survive prolonged dry periods (Grombone-Guaratini and Rodrigues 2002). Seeds of small-seeded species can be either highly abundant or rare whereas large seeds are always rare (Guo *et al*., 1999).

These small (tinny) seeds are primarily from annuals and can survive in the SSB until conditions are conducive for germination (Fenner and Thompson 2005). Usually, annual and short-lived plants produced small seeds in copious quantities, as a response to aridity, and accumulate persistent seedbanks that last more than a year in the soil (Bakker *et al*., 1996). While perennials, on the other hand, produce larger but fewer seeds that normally last less than a year, i.e. they have transient SSB of K-strategists (Esler 1999; Milton and Dean 1993). Larger seeds germinate less, are less viable, eaten more, and more prone to fungal infection (Guo *et al*., 1999). Perennials depend more on their long life-span and vegetative propagation than seeds for regeneration (Amiaud and Touzard 2004).

3.3 Seed density

At the scale of the entire study area, the results revealed that the area retained an adequate density of seeds in the soil compared to other similar arid areas. Seeds density in the study area ranged between 0 and 25 400 seed m^{-2} with an overall mean of 4 110 seed m^{-2} (±949.30 SE). This seed density was less equivalent to that in northern areas of Al-Jabal Al-Akhdar which was ranged between 2 400 and 60 000 seed m^{-2} (El-Barasi and Saaed 2013), and was more or less equivalent to that in the rangeland areas south Al-Jabal Al-Akhdar which ranged between 1 200 and 20 520 seed m^{-2} (El-Barasi and Saaed 2013), and to desert areas west Al-Jabal Al-Akhdar (Ajdabya region) which ranged between 676 and 15 101 seed m^{-2} (El-mograby *et al*. 2018). However, it was more equivalent than the seed density in the Arid Mesus Area far south of Al-Jabal Al-Akhdar at the fringe of the Sahara Desert, which was ranged between 228 and 2 568 seed m^{-2} (El-Jetlawi, 2004) and to the density identified by Zaghloul (2008) in the arid Sinai in Egypt which ranged between 0 and 1 350 seed m^{-2}, and also more equivalent to the density identified by Yang and Evans (1975) who stated that the seed density in certain arid zones worldwide varies between 2450 and 8431 seed m^{-2}.

The density of SSBs is governed by many factors that include seed production, the extent of the area covered by seed-rain, the rate of seed mortality, predator's behaviour, and the density of seedling (Saaed *et al*., 2018). However, these factors vary widely in arid environments (Roberts, 1981) such as in the arid rangelands of Cyrenaica. The comparatively high density of SSB in the area most likely due to the dominance of xerophilous species which composed mainly of annual and short-lived species that produce a large number of seeds (El-Barasi and Saaed, 2013). The relatively high density of SSB in the area can provide a potential for regeneration under suitable environmental conditions such as good rainy seasons.

Amongst the different sectors in the study area, there was no distinct variation in SSBs density (p-value = 0.804), which mean that all sectors follow the same pattern in seed density (Table 1 and Fig. 2). This is in contrast to many other studies in a similar arid environment (Guo *et al*., 1998; Saaed *et al*., 2018; Zaghloul, 2008) who stated that the SSBs in arid areas characterized by high variation across the landscape. The highest mean value of SSB density was recorded in Al-Qarah sector (2760 seed m^{-2}±818.29 SE) and the lowest mean value was in Kambut sector (1 600 m^{-2}±912.14 SE). The SSBs homogeneity across the landscape in such arid ecosystems reflect the homogeneity in the above vegetation as well, which increases with rangeland degradation (Kassahun *et al*. 2009; Saaed *et al*., 2018). Stresses such as high stocking density and prolonged arid conditions act as a filter, and few species can cope with and survive these harsh conditions (El-Sheikh *et al*., 2006) resulted in a homogeneity across the landscape. This is most likely related to a breakdown of the hierarchical dominance and competitive structures of the vegetation resulting from vegetation alteration (Rutherford and Powrie 2010).

In general, the SSB densities in the northern regions of the study area were the highest, and it gradually declined in the southward direction as we approach the desert except for Musaad sector (Fig. 3), which is most likely due to the decline in vegetation cover in the southern areas. This coincides with the results of (El-Barasi and Buhwarish, 2005; Pugnaire and Lázaro, 2000) who stated that the seed density declines as we move away from the canopy of what trees surf, which however may be at the expense of seed density and diversity.

Table 1

Soil seedbank density in the different sectors according to the different soil depths.

Locality	Depth (cm)	Min. seed (m^{-2})	Max. seed (m^{-2})	Mean seed (m^{-2})	SE
Ras-Biad sector	0-10	600	3000	1800	±424.26
El-Qarah sector	0-10	600	4800	2760	±818.29
Kambut sector	0-10	0	6000	1600	± 912.14
Qasr EL-Gadi sector	0-10	0	3000	1800	±434.25
Musaad sector	0-10	600	5400	1971.42	±624.00
Depressions (Sakifas)	0-10	1800	21000	10300	±3324.15
	10-30	0	27000	8550	±6327.91
Dykes	0-10	3000	25200	12480	±4974.58
	10-30	1800	21600	10080	±352624

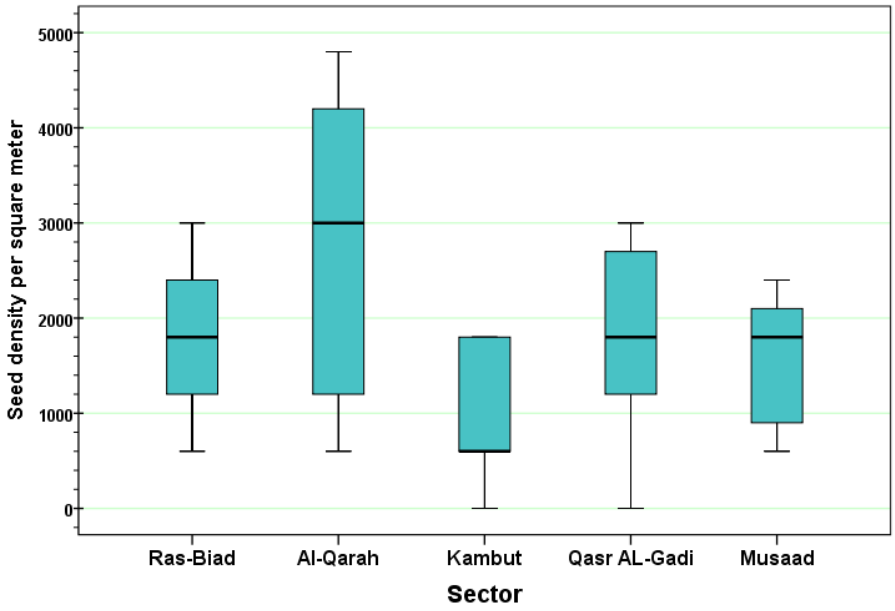

Fig. 2. Box and Whiskers plots showing the median (midline in box) and the first and third quartiles of the data for soil seedbank density at the different sectors in the study area. Bars indicate 95% confidence intervals level.

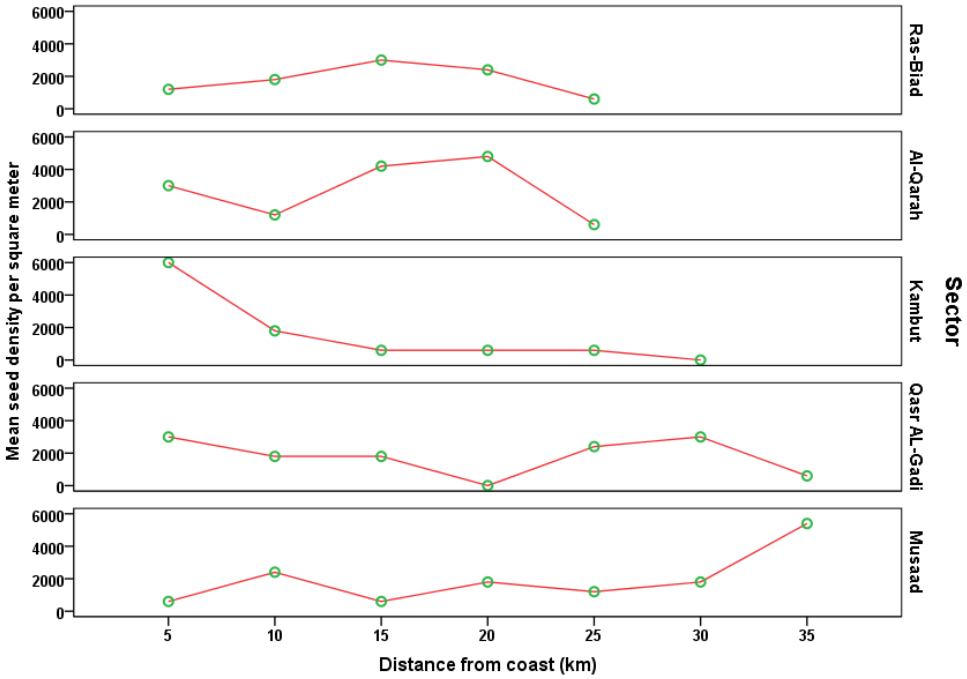

Fig. 3. Lines representing soil seedbank density in the different sectors based on the distance in kilometers from the seacoast southwardly.

The Sakifas and Dykes showed significant differences in seed density when compared to the open areas, the *p*-value were 0.003 and 0.000 respectively. The SSB density in Sakifas ranged between 0 and 27000 seed m^{-2} and behind Dykes ranged between 1800 and 25200 m^{-2} (Table 1). The higher seed density in Sakifas might be ascribed to the clustered seed-rain of some plants species as *Peganum harmala* which dominated these depressions. These such species produce a big quantity of seeds, which is also reported previously by Nelson and Chew (1977). The high seed density in the Sakifas and behind Dykes could be also attributed to the accumulation of soil particles and organic matter including seeds in these low-lying areas from the surrounding higher catchment areas via wind and runoff water. The results illustrated that the seed density in the soil behind Dykes increased with time (Fig. 4). This illuminates the importance and influence of these Dykes overtime on the enrichment of SSB as well as in preserving soil from erosion.

The disparity in landform of the study area plays a major role in the spatial variation of soil, vegetation, and SSB across the landscape. Due to the hydrological system that consists of many depressions and drainage courses, the runoff water after rains is redistributed across the area and the low lands receive a higher quantity of water. Overall, the study area, the Sakifas and valleys retained higher SSB density than the higher-lying areas on the plateau. The highest SSB density was behind Dykes, and the lowest density was in the open land on the plateau (Fig. 5). This is may be attributed to the poorer vegetation cover on the plateau in addition to the impact of soil erosion when compared to the depressions and valleys, which is compatible with the finding of (Peco *et al.*, 1998). Obviously, shrubby areas, depressions, and litter-covered patches retain seeds more effectively than smooth bare areas (Kinloch and Friedel, 2005a). This phenomenon in these zones is considered as an effective factor in increasing vegetation cover and species diversity and enriching SSB density.

When compare the SSB density between the different layers of soil strata, the mean values in the upper layer (0–10 cm) of the Sakifas and Dykes were higher than the lower layer (10–30 cm) (Fig. 6). The higher density of SSB in the upper layer than the lower layer in these low lands (Sakifas and Dykes) may be attributed to the accumulation of soil particles and new seeds with time, as most of the seeds are present in the 0-10 cm soil layer (Bernhardt *et al*., 2008; Edwards and Crawley, 1999).

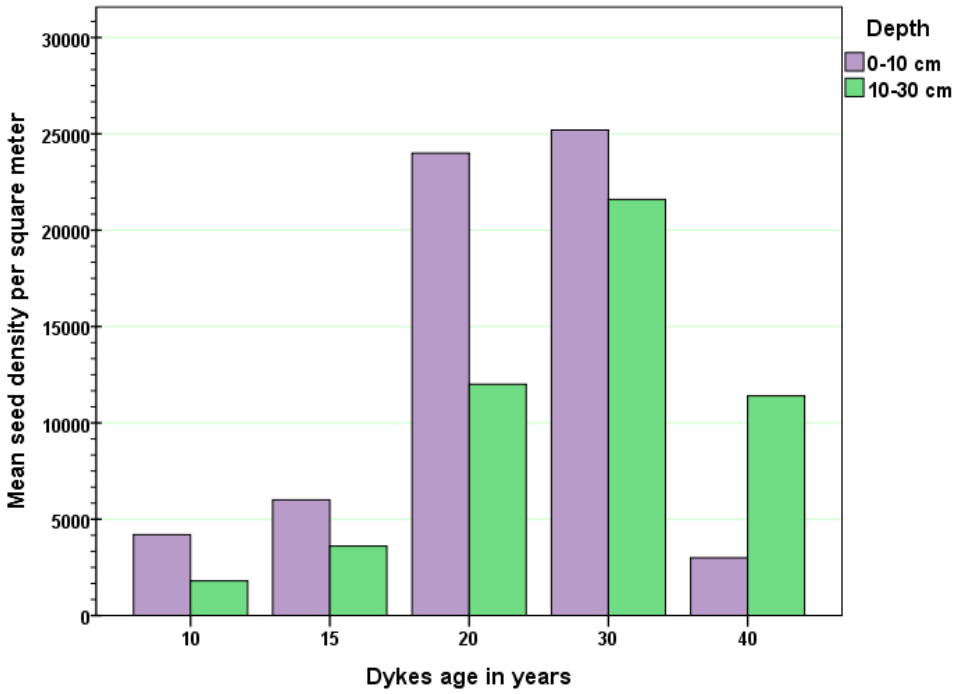

Fig. 4. Bars representing mean soil seedbank density in the soil behind Dykes of different ages (years) showing the importance of these Dykes in retaining and increasing soil seedbank with time.

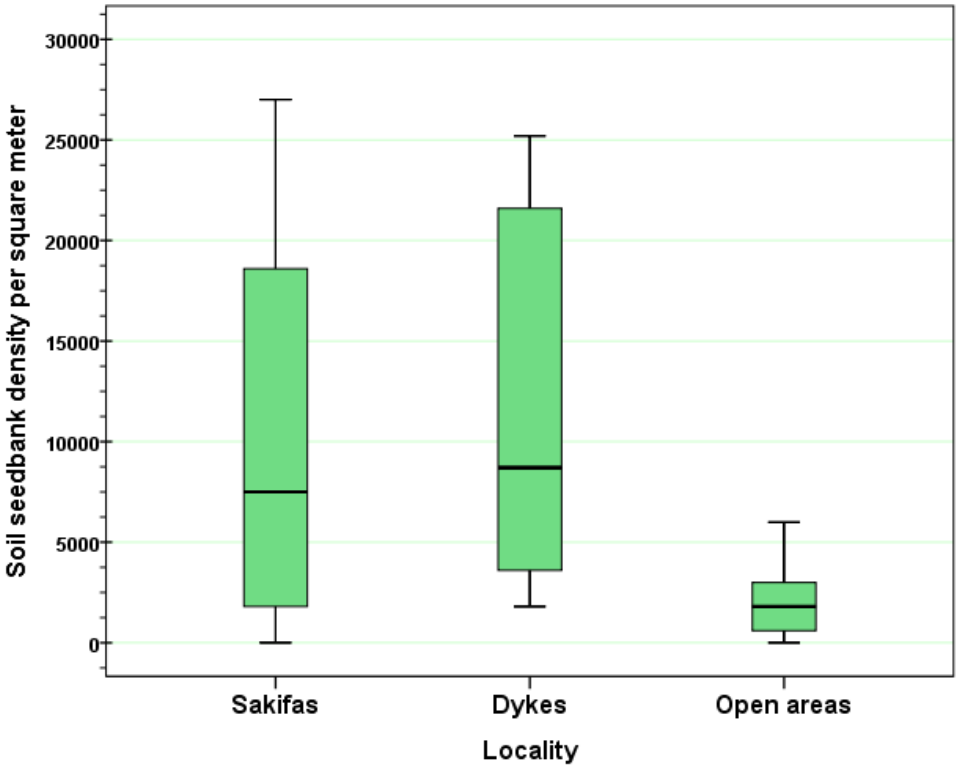

Fig. 5. Box and Whiskers plots showing the median (midline in box) and the first and third quartiles of the data for soil seedbank density in different localities in the study area. Bars indicate 95% confidence intervals level.

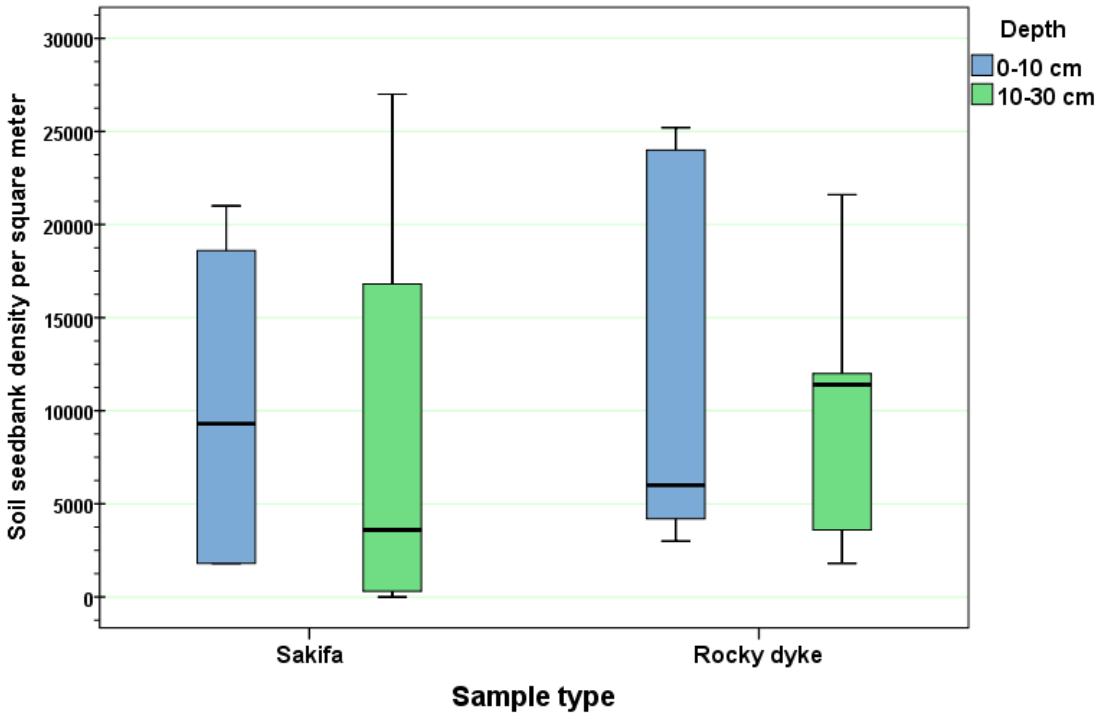

Fig 6. Box and Whiskers plots showing the median (midline in box) and the first and third quartiles of the data for soil seedbank density in different soil depths (0–10 and 10–30 cm) at Sakifas and behind Dykes. Bars indicate 95% confidence intervals level.

3.4 Seed composition

The SSB in any area is an important part of the vegetation (Major and Pyott, 1966). Therefore, the composition of SSB reflects the ground layer vegetation composition, both as a seedling in the field and as mature vegetation (Nafea, 2015). On the other hand, the SSB reveals clues to past vegetation (Leck and Simpson, 1987). New seeds are continuously added by seed-rain; representing a record of the past and present state of vegetation in the area and nearby vicinity (Batanouny *et al*., 1991). The present and future floristic composition and other main characteristics of vegetation are controlled by the ability of seeds present in the soil to germinate and establish as seedlings (Batanouny *et al*., 1991).

In arid rangelands, the SSB is of vital importance as the short-lived and ephemeral plants that dominate the ground layer vegetation in extreme and variable climates exist for the majority of the time as stored seeds only (Inouye, 1991). Some perennial plants also rely on SSBs to enable populations to re-establish after long periods of drought (Kinloch and Friedel, 2005b). This is more so in arid zones as the study area.

Flowering plants in the area constituted of 71 families, 395 species mostly shrubs, dwarf shrubs, and annual herbs (Saaed, 2008) constituted 31% of eastern Libyan species and 23% of Libyan flora. In the SSB, most seeds belonged to Brassicaceae (43.3 %), Chenopodiaceae (10 %), Fabaceae (10 %), and the remainder (36.7 %) (Table 2 and Fig. 7). This is similar to many other arid areas in Libya (El-Mograby *et al*., 2018) and worldwide (Esler 1999, De Villiers *et al*., 2003). These families possess drought-resistance and/or drought-avoidance features in response to the ambient dry conditions of the area. They are also common in areas currently suffering long periods of disturbance, i.e. overgrazing (Hoffmann *et al*. 2015). The scarcity of grasses and legumes seeds in the SSB of the area is unlike similar environments elsewhere (Figueroa *et al*., 2004; Peco *et al*., 1998). This phenomenon can be attributed to a low proportion of grasses and legumes in the above-ground vegetation due to the long history of overgrazing, as they are often very palatable and preferred by livestock (Samuels *et al*., 2016). Although, the seed coat characteristics of legumes are hard and of good quality and enable the seeds to persist for a longer time in the soil, their scarce is mainly due to early grazing before reaching the flowering stage. It may also be attributed to the effect of predators and/or secondary seed dispersal by wind or runoff after the rain. Seed harvesting insects and rodents are very selective and can affect the composition of SSBs in such arid environments as well (DeFalco *et al*., 2009).

In line with other studies in arid region (Dean and Milton, 1991; Saaed *et al*., 2018; Van Rooyen and Grobbelaar, 1982), annual species were well represented in the SSB, similar to the above-ground vegetation. The annuals are active only during the rainy season, their appearance and abundance change from one year to another depending on the amount and frequency of rain. Annuals are comprised mostly of winter-growing species and are abundant after good rains. Their abundance indicates the desert nature of the climate (Raunkiær 1934; Rossa and Willert 1999). Which, supposed to be more resistant to long summer drought as they pass summer in the form of seeds (Van der Merwe and Van Rooyen, 2011).The perennials, on the other hand, form more or less the permanent framework of the vegetation and do not suffer such drastic temporal changes in presence or abundance.

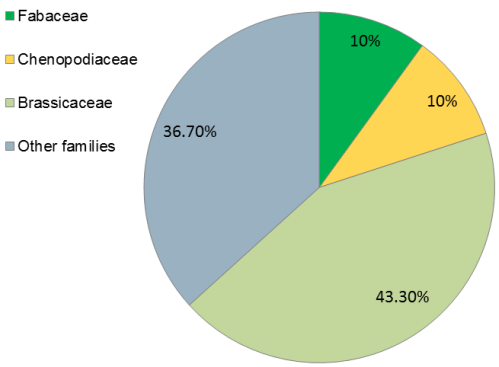

Fig. 7. Percentage of seed families based on the number of species in the entire study area.

Table 2

Species of isolated soil seeds.

Families	Species	Family (%)
Zygophyllaceae	*Peganum harmala*	3.33
Fabaceae	*Onobrychis crista-galli* *Medicago orbicularis* *Medicago truncatula*	10
Leonticaceae	*Leontice leontopetalum*	3.33
Thymelaeaceae	*Thymelaea hirsuta*	3.33
Primulaceae	*Anagallis arvensis*	3.33
Santalaceae	*Thesium humile*	3.33
Resedaceae	*Reseda lutea*	3.33
Papaveraceae	*Papaver rhoeas*	3.33
Brassicaceae	*Diplotaxis harra* *Diplotaxis muralis* *Enarthrocarpus pterocarpus* *Rapistrum rugosum* *Didesmus bipinnatus* *Erucaria microcarpa* *Cakile aegyptiaca* *Carrichtera annua* *Moricandia arvensis* *Biscutella didyma* *Lobularia libyca* *Matthiola tricuspidata* *Sisymbrium irio*	43.33
Polygonaceae	*Emex spinosus*	3.33
Hypecoaceae	*Hypecoum geslini*	3.33
Asteraceae	*Carthamus lanatus*	3.33
Poaceae	*Avena fatua*	3.33
Chenopodiaceae	*Haloxylon scoparia* *Atriplex halimus* *Suaeda vera*	10
14	**30**	**100**

4. Conclusion

Although the study area has suffered long mismanagement and land degradation, it is still retained adequate seed density in the soil. However, the majority of the seeds belonged to annual species. In the open plateau areas, there was no distinct variation in SSB density, which might be a sign of degraded rangelands. The seed density showed a general decline trend from north to southward direction as we approach the desert at the south. Due to the topographical features and big drainage system, which redistribute runoff water after rainfall, the depressions and valleys significantly retained higher seed density when compared to the higher-lying lands on the plateau. This can be noticed as a higher vegetation cover in these low-lying lands. Besides the important role of the Dykes (small hampering dams) in harvesting runoff water and conserve soil, this study demonstrated their importance in increasing SSB density and diversity, which improves with time (Dyke age). Although the study showed adequate seed density in the soil, the dominance of annual and short-lived species in the SSB and the absence of many perennial species may hamper the rehabilitation effort that depends only on the SSB in the area, which may necessitate active interventions for any successful management effort. A conservation program and reseeding of the area with indigenous perennial shrubby species in rainy seasons and in selected areas specially designed for rehabilitation is urgently needed.

References

Al-bukhari, A., Hallett, S. and Brewer, T. (2018) 'A review of potential methods for monitoring rangeland degradation in Libya', *Pastoralism*, 8(13), pp. 1-14

Amiaud, B. and Touzard, B. (2004) 'The relationships between soil seed bank, aboveground vegetation and disturbances in old embanked marshlands of Western France', *Flora*m, 199(1), pp. 25–35.

Bakker, J. P., Poschlod, P., Strykstra, R. J., Bekker, R. M. and Thompson, K. (1996) 'Seed banks and seed dispersal: Important topics in restoration ecology', *Acta Botanica Neerlandica*, 45(4), pp. 461–490.

Baskin, C. C. and Baskin, J. M. (2014) *Seeds: Ecology, Biogeography, and, Evolution of Dormancy and Germination*. 2nd ed. New York, USA: Academic Press.

Batanouny, A. K. H., Zayed, K. M., Marei, F. A. and Gilel, S. A. (1991) 'The seed bank of arable lands in Egypt The seed bank of arable lands in Egypt', *Abstracta Botanica*, 15(1), pp. 19–24.

Bernhardt, K.G., Koch, M., Kropf, M., Ulbel, E. and Webhofer, J. (2008) 'Comparison of two methods characterising the seed bank of amphibious plants in submerged sediments', *Aquatic Botany*, 88(2), pp. 171–177.

Braz, M. I. G., Rodin, P. and de Mattos, E. A. (2014) 'Soil seed bank in a patchy vegetation of coastal sandy plains in southeastern Brazil', *Plant Species Biology*, 29(3), pp. 40–47.

Buhler, D. D. and Maxwell, B. D. (1993) 'Seed Separation and Enumeration from Soil Using K2CO3-Centrifugation and Image Analysis', *Weed Science*, 41(2), pp. 298–302.

Dean, W. R. J. and Milton, S. J. (1991) 'Disturbances in semi-arid shrubland and arid grassland in the Karoo, South Africa: mammal diggings as germination sites', *African Journal of Ecology*, 29(1), pp. 11–16.

DeFalco, L. A., Esque, T. C., Kane, J. M. and Nicklas, M. B. (2009) 'Seed banks in a degraded desert shrubland: Influence of soil surface condition and harvester ant activity on seed abundance', *Journal of Arid Environments*, 73(10), pp. 885–893.

De Villiers, A. J., Van Rooyen, M. W. and Theron, G. K. (2003) 'Similarity between the soil seed bank and the standing vegetation in the Strandveld Succulent Karoo, South Africa', *Land Degradation and Development*, 14(6), pp. 527–540.

Dreber, N. and Esler, K. J. (2011) 'Spatio-temporal variation in soil seed banks under contrasting grazing regimes following low and high seasonal rainfall in arid Namibia', *Journal of Arid Environments*, 75(2), pp. 174–184.

Dreber, N., Oldeland, J. and Van Rooyen, M. W. (2011) 'Impact of severe grazing on soil seed bank composition and its implications for rangeland regeneration in arid Namibia', *Agriculture, Ecosystems and Environment*, 141, pp. 399–409.

Edwards, G. R. and Crawley, M. J. (1999) 'Herbivores, seed banks and seedling recruitment in mesic grassland', *Journal of Ecology*, 87(3), pp. 423–435.

El-Barasi, Y. M. and Saaed, M. W. B. (2013) 'Threats to plant diversity in the Northeastern part of Libya (El-Jabal El-Akhdar and Marmarica Plateau)', *Journal of Environmental Science and Engineering*, 2, pp. 41–58.

El-Barasi, Y. M. and Saaed, M. W .B. (2015) 'Land use and disturbance effects on the natural vegetation of Daphna range zone (North Eastern part of Libyan coast)', *International Journal of Environment and Water*, 4(2), pp. 89–103.

El-Barasi, Y. M., Saaed, M. W. B. and Al Tajoury, O. R. (2013) 'Land Deterioration of a Semi-desert Grazing Area in the North-Eastern Zone of Libya (Cyrenaica)', *Journal of Environmental Science and Engineering*, B2, 2, pp. 357–373.

El-Jetlawi, A. O. (2004) *Study of vegetation and soil seed bank of a range desert zone (Msus-Al Ajramia)*. Msc. Thesis, Department of Botany, Faculty of Science, Benghazi University, Benghazi, Libya. pp. 1-210.

El-Mograby, A. S., Saaed, M. W. B., El-Barasi, Y. M. and Rahil, R. O. M. (2018) 'Characteristics of vegetation and Soil seedbank of a transect in the coastal strip of the arid rangelands in Solouq Plain, Cyrenaica, Eastern Libya', *The fifth Scientific Conference of Environment and Sustainable Development in the Arid and Semi- Arid Regions (ICESD)* In Ajdabya, Libya. pp. 132–143.

El-Sheikh, M. A. E., El-Ghareeb, R. M. and Testi, A. (2006) 'Diversity of plant communities in coastal salt marshes habitat in Kuwait', *Rendiconti Fisiche Accademia Lincei*, 17(3), pp. 311–331.

Esler, K. J. (1999) *Plant reproductive ecology*. In W. R. J. Dean and S. J. Milton (eds.). Cambridge: Cambridge University Press *The Karoo, Ecological Patterns and Process*, p. 123–144.

Fenner, M. (1985) *Seed Ecology*. London, England: Chapman and Hall.

Fenner, M. and Thompson, K. (2005) *The ecology of seeds*. Cambridge, UK: Cambridge University Press.

Figueroa, J. A., Teillier, S. and Jaksic, F. M. (2004) 'Composition, size and dynamics of the seed bank in a Mediterranean Shrubland of Chile', *Austral Ecology*, 29(5), pp. 574–584.

Ge, X., Wang, R., Zhang, Y., Song, B. and Liu, J. (2013) 'The soil seed banks of typical communities in wetlands converted from farmlands by different restoration methods in Nansi Lake, China', *Ecological Engineering*, 60, pp. 108–115.

Grombone-Guaratini, M. T. and Rodrigues, R. R. (2002) 'Seed bank and seed rain in a seasonal semi-deciduous forest in south-eastern Brazil', *Journal of Tropical Ecology*, 18(5), pp. 759–774.

Guo, Q., Rundel, P. W. and Goodall, D. W. (1998) 'Horizontal and vertical distribution of desert seed banks: patterns, causes, and implications', *Journal of Arid Environments*, 38, pp. 465–478.

Guo, Q., Rundel, P. W. and Goodall, D. W. (1999) 'Structure of desert seed banks: comparisons across four North American desert sites', *Journal of Arid Environments*, 42(1), pp. 1–14.

Hoffmann, V., Verboom, G. A. and Cotterill, F. P. D. (2015) 'Dated plant phylogenies resolve Neogene climate and landscape evolution in the Cape Floristic Region', *PLoS ONE*. 10(9), pp. 1–25.

Inouye, R. S. (1991) *Population biology of desert annual plants*. In G.A. Polis (ed.). University of Arizona Press, Tucson, USA *The Ecology of Desert Communities*, pp. 27–54.

Kassahun, A., Snyman, H. A. and Smit, G. N. (2009) 'Soil seed bank evaluation along a degradation gradient in arid rangelands of the Somali region, eastern Ethiopia', *Agriculture, Ecosystems and Environment*. 129(4), pp. 428–436.

Kemp, P. R. (1989) *Seed banks and vegetation processes in deserts*. In M.A. Leck, V.T. Parker, and R.L. Simpson (eds.). San Diego, California, USA: Academic Press *Ecology of Soil Seed Banks*, p. 257–281.

Kinloch, J. E. and Friedel, M. H. (2005a) 'Soil seed reserves in arid grazing lands of central Australia. Part 2: Availability of "safe sites" ', *Journal of Arid Environments*, 60(1), pp. 163–185.

Kinloch, J. E. and Friedel, M. H. (2005b) 'Soil seed reserves in arid grazing lands of central Australia. Part 1: Seed bank and vegetation dynamics', *Journal of Arid Environments*, 60(1), pp. 133–161.

Leck, M. and Simpson, R. L. (1987) 'Seed bank of a freshwater tidal wetland: turnover and relationship to vegetation change', *American Journal of Botany*, 74(3), pp. 360–370.

Leck, M. A., Parker, V. T. and Simpson, R. L. (1989) *Ecology of Soil Seed Banks*. London: Academic Press.

Louda, S. M. (1989) *Predation in the dynamics of seed regeneration*. In M.A. Leck, V.T. Parker, and R.L. Simpon (eds.). New York: Academic Press. *Ecology of soil seed banks*, pp. 25–51.

Ma, M., Zhou, X., Ma, Z. and Du, G. (2012) 'Composition of the soil seed bank and vegetation changes after wetland drying and soil salinization on the Tibetan Plateau', *Ecological Engineering*, 44, pp. 18–24.

Major, J. and Pyott, W. T. (1966) 'Buried, viable seeds in two California bunchgrass sites and their bearing on the definition of a flora', *Vegetatio Acta Geobotanica*, 13(5), pp. 253–282.

Malone, C. R. (1967) 'A rapid method for enumeration of viable seeds in soil', *Weeds*, 15(4), pp. 381–382.

Milton, S. J. and Dean, W. R. J. (1993) 'Selection of seeds by harvester ants (*Messor capensis*) in relation to condition of arid rangeland.', *Journal of Arid Environments*, 24, pp. 63–74.

Moles, A. T. and Drake, D. R. (1999) 'Potential contributions of the seed rain and seed bank to regeneration of native forest under plantation pine in New Zealand', *New Zealand Journal of Botany*, 37(1), pp. 83–93.

Nafea, E. (2015) 'Relationship between Vegetation and Soil Seed Bank at Protected Versus Unprotected Sites at Coastal Habitats in Libya', *CATRINA*, 15(1), pp. 77–87.

Nelson, J. F. and Chew, R. M. (1977) 'Factors affecting seed reserves in the soil of a Mojave Desert ecosystem, Rock Valley, Nye County, Nevada', *American Midland Naturalist*, 97(2), pp. 300–320.

Ochoa-Hueso, R., Eldridge, D. J., Delgado-Baquerizo, M., Soliveres, S., Bowker, M. A., Gross, N., Le Bagousse-Pinguet, Y., Quero, J. L., et al. (2018) 'Soil fungal abundance and plant functional traits drive fertile island formation in global drylands. *Journal of Ecology*.', 106(1), pp. 242–253.

Peco, B., Ortega, M. and Levassor, C. (1998) 'Similarity between seed bank and vegetation in Mediterranean grassland: a predictive model', *Journal of Vegetation Science*, 9(6), pp. 815–828.

Price, J. N., Wright, B. R., Gross, C. L. and Whalley, W. R. D. B. (2010) 'Comparison of seedling emergence and seed extraction techniques for estimating the composition of soil seed banks', *Methods in Ecology and Evolution*, 1(2), pp. 151–157.

Pugnaire, F. I. and Lázaro, R. (2000) 'Seed bank and understorey species composition in a semi-arid environment: the effect of shrub age and rainfall', *Annals of Botany*, 86, pp. 807–813.

Raunkiær, C. C. (1934) *The life forms of plants and statistical plant geography*: being the collected papers of C. Raunkiær, translated by H. Gilbert-Carter, A. Fausbøll, and A. G. Tansley. Introduction by A.G. Tansley. Oxford, UK: Oxford University Press.

Roberts, H. A. (1981) 'Seedbanks in soils', *Advances in Applied Biology*, 6, pp. 1–55.

Rossa, B. and Willert, D. J. Von. (1999) 'Physiological characteristics of geophytes in semi-arid Namaqualand, South Africa', *Plant Ecology*, 142(1), pp. 121–132.

Rundel, P. W. and Gibson, A. C. (2005) *Ecological communities and processes in a Mojave Desert ecosystem*. Cambridge, UK: Cambridge University Press.

Rutherford, M. C. and Powrie, L. W. (2010) 'Severely degraded rangeland: Implications for plant diversity from a case study in Succulent Karoo, South Africa', *Journal of Arid Environments*, 74(6), pp. 692–701.

Saaed, M. W. B. (2008) *Studying factors causing vegetation degradation in the semi-arid Daphna area, Cyrenaica (Northeastern part of Libya)*. MSc. Thesis, Department of Engineering and Environmental Science, Academy of Graduate Studies, Benghazi, Libya, pp. 103-111.

Saaed, M. W. B., Jacobs, S. M., Masubelele, M. L., Samuels, I., Khomo, L. and El-Barasi, Y. M. (2018) 'The composition of the soil seed-bank and its role in ecosystem dynamics and rehabilitation potential in the arid Tankwa Karoo Region, South Africa', *African Journal of Range and Forage Science*, 35(3 and 4), pp. 351–361.

Samuels, I., Cupido, C., Swarts, M. B., Palmer, A. R. and Paulse, J. W. (2016) 'Feeding ecology of four livestock species under different management in a semi-arid pastoral system in South Africa', *African Journal of Range and Forage Science*, 33(1), pp. 1–9.

Shaukat, S. S. and Siddiqui, I. A. (2004) 'Spatial pattern analysis of seeds of an arable soil seed bank and its relationship with above-ground vegetation in an arid region', *Journal of Arid Environments*, 57(3), pp. 311–327.

Thompson, K. and Grime, J. P. (1979) 'Seasonal variation in the seed banks of herbaceous species in ten contrasting habitats', *Journal of Ecology*, 67(3), pp. 893–921.

Traba, J., Azcárate, F. M. and Peco, B. (2006) 'The fate of seeds in Mediterranean soil seed banks in relation to their traits', *Journal of Vegetation Science*, 17(1), pp. 5–10.

Van der Merwe, H. and Van Rooyen, M. W. (2011) 'Life form spectra in the Hantam-Tanqua-Roggeveld, South Africa', *South African Journal of Botany*, 77(2), pp. 371–380.

Van Etten, E. J. B., Neasham, B. and Dalgleish, S. (2014) 'Soil seed banks of fringing Salt Lake vegetation in arid Western Australia: density, composition and implications for post mine restoration using topsoil', *Ecological Management and Restoration*, 15(3), pp. 239–242.

Van Rooyen, M. W. and Grobbelaar, N. (1982) 'Saadbevolkings in die grond van die Hester Malan-natuurreservaat in die Namakwalandse Gebrokeveld, *South African Journal of Botany*, 1, pp. 41–50.

Yang, J. A. and Evans, R. A. (1975) 'Germinability of seed reserves in a big sage-brush community', *Weed Science*, 23, pp. 358–364.

Zaghloul, M. S. (2008) 'Diversity in soil seed bank of Sinai and implications for conservation and restoration', *African Journal of Environmental Science and Technology*, 2(7), pp. 172–184.

Annexure A: Photos of the different landforms and vegetation framework in the study area.

Topographical depression
(Hafalaze Sakifa) south Kambut village).

The southern parts of the study area retained the least soil seedbank density due to the low vegetation cover and sever erosion effect.

The natural vegetation on Marmarica Plateau which is the main source of soil seedbank. The species which appear in the photo are: *Thymelaea hirsuta, Atriplex halimus and Haloxylon scoparium.*

The Dykes, which have been built in the flat area, play a significant role in increasing soil seedbank and conserving the soil.

Annexure B: Samples from the isolated soil seedbank in the study area showing size, shape, and the identification of some of the seeds.

Vicia monantha

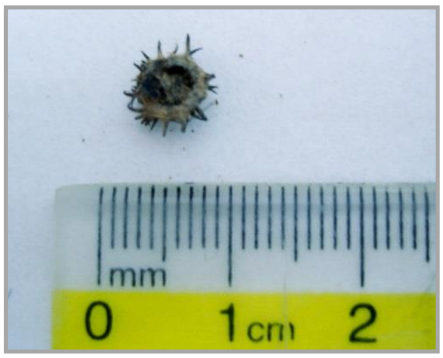

Medicago orbicularis

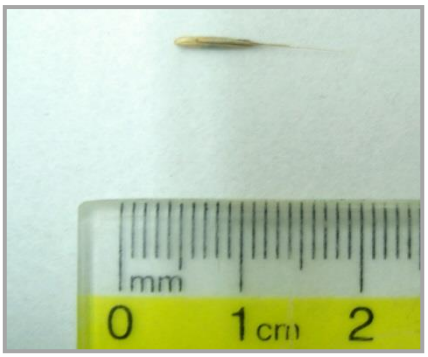

Avena fatua

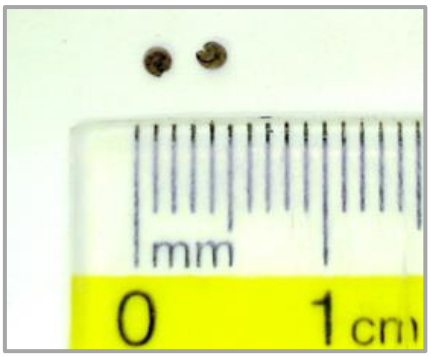

Malva reflexa

Vicia abgustifoia

Peganum harmala

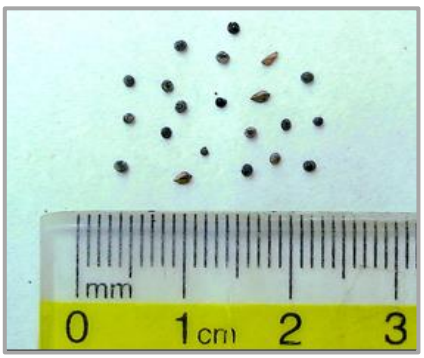

Different seeds for various plant species

Leontice leontopetalum

Libyan Journal of Science & Technology 9:2 (2019) 194–197

Faculty of Science - University of Benghazi

Libyan Journal of Science & Technology

journal home page: www.sc.uob.edu.ly/pages/page/77

Sterilization versus disinfection of the dental handpieces (pilot study)

Khadiga. A. H. Mohamed

Fixed Prosthodontics Department, Faculty of Dentistry, Benghazi University, Libya

E-mail address: khadgih.mohamed@uob.edu.ly

Highlights

- **The dentists are responsible for the protection of their patients from cross-infection risk.**
- **The cross-infection policy guidelines should be followed in the correct manner**
- **The autoclaving sterilization is a mandatory procedure to get handpieces free from contamination**

ARTICLE INFO

Article history:
Received 17 February 2019
Revised 13 August 2019
Accepted 15 August 2019
Available online 18 August 2019

Keywords:
Handpiece (HP), Culture growth (Cg).

ABSTRACT

Improperly following the cross-infection policy can transfer infection from infected patients to others. The Handpieces are the most important workhorse devices properly in all dental procedures. A retro-contamination may occur through their use of a septic environment. Unaware dentists could reuse a contaminated dental handpiece only after wiping with disinfectant.

Objectives: To evaluate the infection control status of the wiped handpiece. Moreover, to increase the awareness of dentists toward this issue.

Methods: Ten contaminated Handpieces were collected from the dental clinic. They swabbed from their external and internal surfaces and cultured in two types of growth culture media. Next, they were wiped (with InstruPlusForte Sol), swabbed and cultured again. In the last step, the handpieces were sterilized and swabbed for culturing in the same manner.

The results: The wiped Handpieces showed that only three (30%) had no bacterial growth from their external surfaces, While 100% revealed the bacterial growth from their internal surfaces. No growth with sterilized Handpieces was demonstrated.

Conclusion: Wiping the outside of the handpiece with disinfectant does not eliminate the potential cross-infection risk.

1. Introduction

The mouth contains bacteria and viruses from the nose, throat and respiratory tract. The saliva is of particular concern during dental treatment because frequently is contaminated with the blood. Methicillin-resistant Staphylococcus aureus (MRSA) is resistant to common antibiotics. As a result, the infections caused by these organisms are difficult to treat. MRSA colony was found in the nose, axillae and perineum, and abnormal skin as well as in the oral cavity. Therefore, any dental procedure that has the potential to cause contamination with organisms from some or all of these sources. Moreover, failure to adequately clean, disinfect and/or sterilize dental instruments "contaminated with pathogenic organisms from a previous patient will endanger the subsequent patient. This route of pathogenic microorganisms transfer is known as cross-contamination and the resulting infection is referred to as cross-infection (Carmenelena *et al*., 2002; Australian Dental Association 2012). In addition to that, one study confirmed that a cluster of 5 cases of acute hepatitis B virus infections was reported among patients of a two-day, receiving dental in West Virginia clinic. However, through the virus molecular sequencing from those acutely infected patients are identified. None of these cases were reported behavioral risk factors for hepatitis B (Jennifer *et al*., 2016).

2. Retro-contamination of handpieces

The Handpieces are the most important workhorse systems in the dental work representing a significantly vital role in any dental practice procedures. Since the head of the HP is running in an aseptic environment, a retrocontamination and internal soiling of the HP occurs, This contamination takes place at the different levels of their internal and external parts (Offne *et al*., 2016). However, the contamination of the internal handpiece surface can spread through the engine to the air/water pipes reaching the entire unit waterline were subsequently can then constitute a secondary reservoir of microorganisms aggregating in biofilms. These biofilms could potentially grow from microorganisms that come from the mouth of patients to the general water supply network. Furthermore. This contamination can lead to serious infection forms. So that, flushing for 2 minutes in the morning and for 20-30 seconds between patients should be considered the daily dental procedures, and longer flushing is suggested after weekends. In the case of using storage tanks, they should be frequently washed and disinfected, filled with distilled sterile water (Sagar & Ramesh., 2013).

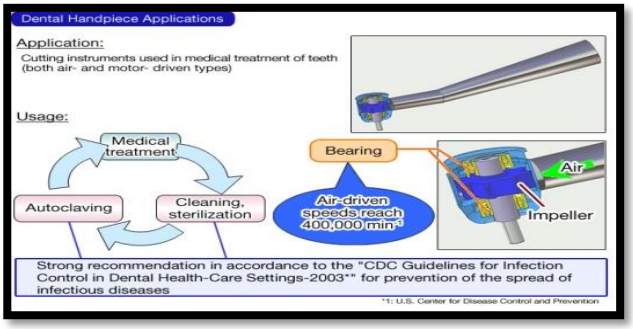

Fig 1. (CDC) in its Guidelines for Disinfection

1ISSN 2663-1407; National Library of Libya, Legal number: 390/2018

3. Objectives of the study

Up to now some of the dentists could be re-using contaminated dental handpieces only after wiping them with a disinfectant, for that this study was done to see the contamination of the external and internal surfaces of disinfected (an autoclaved) dental handpiece through swab culture procedure.

1-*To evaluate the culture growth from the external and internal surfaces of (unautoclaved) wiped handpiece through a swab.*

2-*To increase the dentists' awareness of the cross-infection policy.*

4. Material and method

A collection of ten contaminated Handpieces (used for only one patient) from the private clinic was done in the present study. Each handpiece was swabbed from the external and the internal surface with a suitable sterile cotton swab. A sterile cotton swab was used to touch the external surface of the handpiece shank through several strokes to collect any bacteria for a microbiological culturing.

Fig. 2. Swabbing the external surface of the handpiece

Then, with another suitable size sterile swab the same procedure was done, but from the internal surface (bur opening presents in the hopes head and the connecting end of the dental unit.

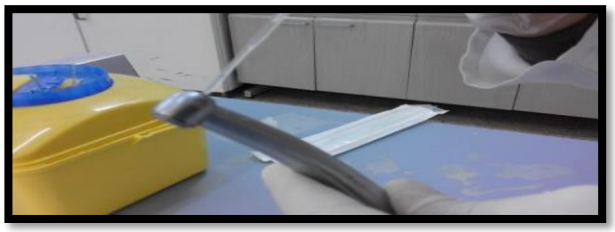

Fig. 3. Swabbing the internal surface of the handpiece

The swabbed material was implanted into two cells-culture dishes containing (chocolate and blood) culture ager media. The cell-culture dishes providing with two halves (one used to culture from the external surface of the handpiece. While, the second used for the internal surface). All Petri dishes containing the collected swabs were incubated into the incubator for 24 hours.

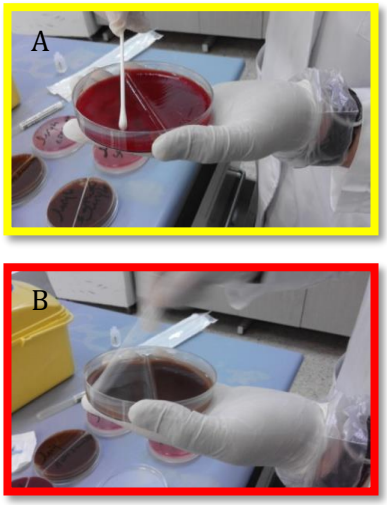

Fig.4. (A, B) culture dishes implantation (chocolate and blood) culture ager media.

Fig. 5. The samples in the incubator

Next, the ten contaminated Handpieces were wiped with Instru-PlusForte Sol as usual as done in some dental clinics. Then the previously mentioned procedure of the external and the internal surface swabbing was performed.

5. Instru plus forte disinfectant

It is a highly effective instrument disinfectant based on acetals and aldehydes (but without formaldehyde) can be used for dental instruments, Active ingredients 100 grams: contain 5,75 form acetate, 8,00 g glutardialdehyde (pentlandite). Surfactants, corrosion inhibitors, preservatives, PH-value regulator. It is Bactericidal, fungicidal, tuberculocidal (3% 5 min), Virus-inactivating (incl. HBV/HIV, 3% 5 min), against all covered viruses: HCV (1% 15 min) and Vaccinia (1% 15 min) effective against all uncovered viruses: Polio (3 %30 min), Adeno (1% 15 min). Herpes Simplex Virus, SV40 (2% 15 min), Instru plus forte is tested according to the standard methods of the (German Society of Microbiology and Hygiene), (www.schumacher-online.com). In the last step, the handpieces were sterilized, in an autoclave in the right way following the stranded procedure. Each sterilized handpieces was swabbed from the external and from the internal surface and cultured in a similar manner.

6. Results

First of all, there was no difference in the cultural growth either on the blood agar media or on the chocolate one. However, it was almost the same. The bacterial culture growth was evaluated semi-quantitatively.

(-): No bacterial growth.

(+): **Low** the bacterial growth less than 50% of the experimental Petri ditch whole area.

(++): **Medium** the bacterial growth from 50% and less than 75% of the experimental Petri ditch whole area.

(+++): Heavy the bacterial growth by more than 75%.

The results of the study were:

1. The bacterial culture growth from the contaminated handpieces (before wiping) revealed that the samples of the external surface were too heavy (+++), too low (+) and six medium (++) growth. While from the internal surface the culture growth was as four heavy (+++) and six medium (++).
2. The bacterial culture growth from the contaminated handpieces (after wiping) showed that the samples of external surface three-nil (-), six low (+) and one medium (++) growth.

Moreover, there was no sample free from culture growth (-) from the internal surface of the handpieces one (+++), four (+), five (++).

3. No culture growth was found from the external and internal surfaces of headpieces after the sterilization step.

Table 1

The growth culture before wiping **the handpices**:

Sample №	1	2	3	4	5	6	7	8	9	10
External surface	++	+++	++	+++	+	++	++	+	++	++
Internal surface	+++	++	++	++	++	++	+++	++	+++	+++

Table 2

The growth culture after **wiping the handpices** with Instru Plus Forte So

Sample №	1	2	3	4	5	6	7	8	9	10
External surface	+	++	+	+	-	+	+	-	-	+
Internal surface	++	+++	++	++	+	++	+	+	+	++

Table 3

The growth culture after the handpices sterilization

Sample №	1	2	3	4	5	6	7	8	9	10
External surface	-	-	-	-	-	-	-	-	-	-
Internal surface	-	-	-	-	-	-	-	-	-	-

The data were analyzed using a nonparametric test that is (Wilcoxon signed-rank test). This test is similar to the paired Student's t-test, the signed-rank test takes into account that the two treatments are being assigned to the same subject. The test is based on the difference in the measurements within each subject. Since the P-value is (0.046, 0.003) ≦ 0.05, i.e., that is a significant difference.

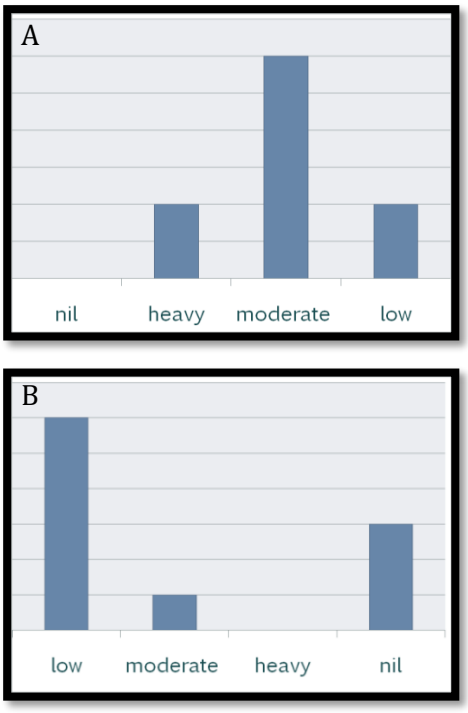

Fig. 6. A before, B after the Graphic representation of the External surface swab culture before and after wiping

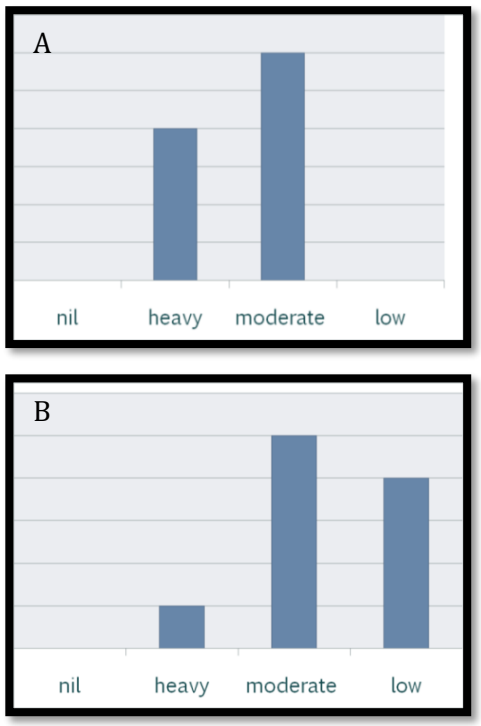

Fig. 7. A_before, B after the Graphic representation of the Internal surface swab culture before and after wiping

7. Discussion

The results of the present study found out that the external surface of the handpiece culture growth from the swabbed wiped could be nil 30%. While, the results from the internal surface could be nil unless they **were autoclaved which** agreed with previous studies (Hauman, 1993; Judith & Chin, 2006). Furthermore, emphasizing on that the cold sterilization." For practical purposes, there they have no place in dentistry (Redd *et al*., 2007; Smith & Smith., 2014).

In this study, the explanation of free external surface contamination of swabbing wiped handpiece may be due to the variation in the number of microbes from one patient to another which could be disappearing with using the high-level disinfectant. In addition to that, the wiping method plays an important role. As it is supposed to be using several wipes and not one for all parts of the surface. A wipe is used to clean any blood or debris from the surfaces. After this, a new wipe is used to reapply the disinfectant to the same surfaces in order to clean, and then disinfect. The use of one wipe on multiple surfaces may result in the cross-contamination of surfaces (Offne *et al*., 2016). Other factors that should be considered include contact time. Moreover, the direction of the wiping is assumed to be in one-direction from up to down. Otherwise, the microbes are transported from one side to another and reintroduced in another way on the surface. Most importantly, the wiping material is a disinfectant and not sterilant. But, with high-level disinfectant, we still found heavy and medium swab culture growth from the internal surface of the handpiece (Michael., 2008). The decrease of bacterial growth from the internal surface could be attributed to that the ability of a disinfectant to penetrate the accessible paths of the internal surface and lack of accessbility to the narrow and twisted one. For the complexity installation and the lack of access of disinfectant to the inner parts of the handpiece there was no internal sample (after wiping with disinfectant) had nil swab culture growth which as it's known for us that the handpieces are coupled with narrow pipes bringing air and water during the drilling. So that logically any contaminate materials could be pushed from the outward to inward working surfaces and we can never immerse the handpieces in disinfectant solutions, which will cause their corrosion.

What is the correct method to sterilize dental Handpieces?

1. *The handpiece should be clean from the outside with detergent and water never immerse it in disinfectant solutions or the ultrasonic cleaner.*
2. *The lubrication with pressurized oil for the recommended period and the excess oil should be clean off for maintaining goal must be performed.*
3. *The sterilizing in an autoclave and run the handpiece briefly before use to clear excess lubricant. After sterilizing, Handpieces must be stored in* a way to prevent their contamination. They should not be fitted to the **dental unit until the time of use in a patient's mouth.**

Is Disposable *Handpiece* an alternative solution?

A single-use device also called a disposable device, is designed to be used on one patient and then discarded.

Advantages:

1. *They do not need sterilization.*
2. *They are maintenance-free, one-time use.*
3. *More predictable performance than age handpiece, new hand-pick every time.*
4. *The dentist feels nice tactile sensation, lightweight construction.*

Disadvantages:

1. *More cost, new hand-picked for every patient.*
2. *Increased waste generation.*

This is to notify you that the Food and Drug Administration (FDA) recommends that reusable dental Handpieces must be sterilized after use. The chemical disinfection is not recommended fact sheet entitled HIV Transmission in Dental Settings. The American Dental Association and CDC have always recommended that dental Handpieces be autoclaved between each patient use (William *et al*., 2003; Radcliffe *et al*., 2013).

8. Conclusion

Integrity is doing the right thing even when no one is looking. While the conscience is the ability of a person to distinguish between what is right and what is wrong. However, which leads to a sense of regret when the things that an individual does are contrary to his moral values and to the sense of integrity. Furthermore, ethics are the rules for deciding correct conduct based on the available information. There are times in our lives when we have to take a stand. Other times the everyday little things make an impact on someone's life. Therefore, using the integrity and ethics in our decision-making in infection control is how each of us can decrease the disaster infection risks in dental care. For many years until now we have known that the number of dentists inadvertently or unconsciously reusing the dental Handpieces without autoclaving them, which leads to a negative impact on their patients' lives. The wiping the outside of the handpiece with disinfectant does not eliminate the potential cross-infection risk. The dentist should not care about the infections on economics ground alone and forget the loss of patient confidence and individual suffering.

Acknowledgement

I would like to thank Professor, **Ali El merit** (Faculty of Dentistry, Benghazi University, Libya) for his valuable tips. **Dr. Wafa. Elamari, Dr. Niglia Elhasi** (Lab of the pediatric hospital, Benghazi, Libya,) where the all-experimental steps have performed. Most sincerely, for all of their help, diligence, hard work, efforts and their time spent with me to make this study to go well**.**

References

Carmenelena, G. Skaug, N. Patrascu, I. (2002) 'Cross Infection in Dentistry', *Roum. Biotechnol. Lett*, 7(4), pp. 861-868.

Australian Dental Association (2012) 'ADA Guidelines for Infection Control, Second Edition', Published by the Australian Dental Association Inc. Email: adainc@ada.org.au, Available at Web: http://www.ada.org.au. ISBN 978-0-909961-41-1

Jennifer, L. Shellie, K. Jennifer, A. Valerie, A. (2016) 'Transmission of blood-borne pathogens in US dental health care settings', Update Published by Elsevier Inc. on behalf of the American Dental Association http://dx.doi.org/10.1016/j.adaj.2016.03.020

Offline, D. Lucien. Anne, M. (2016) 'Cleaning of Dental Handpieces: A Method to Test its Efficiency, and its Evaluation With a Washer-Disinfector- Lubricator-Dryer', *Dent Open J.*; 3 (1), pp.10-16.

Sagar, Ji. Ramesh, N. (2013) 'Cross-contamination in dentistry: A comprehensive overview. Comprehensive overview', *Chronicles of Young Scientists*, 4(1), pp. 51-58. **DOI:** 10.4103/2229-5186.108807

Hauman, C. (1993)' Cross-infection risks associated with high-speed dental Handpieces', *J Dent Assoc, S Afr., Jul*, 48(7), pp. 389-391.

Judith, R., and Chin. (2006) 'Internal contamination of air-driven low-speed Handpieces, and attached prophy angles', *American Dental Association*, 137(9), pp. 1275–1280.

Redd, J. Baumbach, J. Kohn, W. Nainan, O. Khristova, M. Williams, I. (2007) 'Patient-to-patient transmission of hepatitis B virus-associated with oral surgery', *J Infect Dis*, 195(9), pp. 1311-1314.

Smith, G., Smith, A. (2014) 'Microbial contamination of used dental Handpieces', *Am J Infect Control*, 42(9), pp. 1019-1021. Cross-infection: 10.1016/j. ages. 2014.06.008

Michael, k. (2008) 'Cardiff University Antibacterial Wipes Can Spread Bacteria Around', *ScienceDaily*, June. Available at Web: http://www.sciencedaily.com/releases/2008/06/080603133410.htm

William, G. Kohn, D. Amy, S. Collins, M. Jennifer, L.(2003) 'Centers for Disease Control and Prevention. Guidelines for infection control in dental healthcare settings', MMWR Recomm Rep; 52 (RR-17): 1 –61. Available at: www.cdc.gov/mmwr/PDF/rr/rr5217.pdf

Radcliffe. Bixler, D. Moorman, A. (2013) 'Hepatitis B Virus Transmissions Associated with a Portable Dental Clinic, West Virginia', *Journal of the American Dental Association*, 144(10), pp. 1110–1118.

Libyan Journal of Science & Technology 9:2 (2019) 198–201

Faculty of Science - University of Benghazi

Libyan Journal of Science & Technology

journal home page: www.sc.uob.edu.ly/pages/page/77

Malnutrition-Inflammation complex syndrome in Libyan patients with end-Stage renal disease at Hun-Aljufrah

Mohammed Siddig Mulah[a,*], **Hana A. Zaed**[b]

[a] *College of Medical Technology, University of ALjufra–Libya*

[b] *Faculty of Health Science, University of Sirte– Libya*

Highlights

- **Diabetes and Hypertension are the leading cause of ESRD.**
- **Serum Albumin, BMI and hs-CRP are sensitive markers for MIA Syndrome**
- **Serum Albumin and hs-CRP are negatively correlated in ESRD patients**

ARTICLE INFO

Article history:
Received 11 February 2019
Revised 01 September 2019
Accepted 05 September 2019
Available online 29 September 2019

Keywords:
CKD Chronic Kidney Disease, **HD** hemodialysis, **PEM** protein-energy malnutrition, **BMI** Body mass index, **MIA Syndrome** Malnutrition-Inflammation-atherosclerosis Syndrome, **ESRD** End-Stage Renal Disease

*Corresponding author:
E mail address: mulah77@gmail.com
M. S. Mullah

ABSTRACT

Malnutrition and inflammation complex syndrome in ESRD Patients on maintenance Hemodialysis therapy remains the most common cause of morbidity and mortality characterized by alteration in the structural and functional ability of plasma proteins. The aim of this study was to assess the serum level of albumin, BMI and hs-CRP as a marker of Malnutrition-Inflammation Complex Syndrome. This is a case-control study conducted at Alafia Hospital Hun-Aljufrah from December 2014 to December 2015. Libyan patients with ESRD who routinely attend to dialysis center at the above-mentioned hospital during the period of the study were randomly recruited for this study. The study included one hundred ESRD and one hundred age and sex-matched healthy controls. The patients' information such as age, sex, height, weight, and clinical history were recorded. Blood samples (6 ml) were collected from patients in plain and EDTA containers from which EDTA and Serum samples were separated. The results of our study showed that there were significant decrease in the mean serum level of albumin (3.12±0.39) (p. value=0.000) and BMI (20.3±5.5) (p. value=0.000) as well as significant increase in the mean serum level of serum C-reactive protein (20.13±5.704) (p. value=0.000) in case group when compared to the control group. The DOT Blot Correlation test showed that there was a significant negative correlation between hs-CRP with albumin (r= –0.812, p=0.02). In conclusion, the significant decreased in the mean level of serum albumin and BMI, as well as the significant increase in the mean level of serum C-reactive protein among hemodialysis ESRD patients, might place them at risk of developing Malnutrition-Inflammation Complex Syndrome in the future. The significant negative correlation between serum albumin with hs-CRP support the facts systemic inflammation is the main cause of malnutrition and cardiovascular disease in ESRD patient.

1. Introduction

Patients undergoing hemodialysis have a high prevalence of protein-energy malnutrition and inflammation. Those conditions often occur together in ESRD patients on maintenance hemodialysis therapy, they have been referred to the malnutrition-inflammation-atherosclerosis syndrome (MIA syndrome) to confirm their important association with atherosclerotic cardiovascular disease. Chronic kidney disease is an effective disease command by multiple factors that affect its progression and prognosis. The prevalence of dialysis-treated ESRD was 624 per million populations.

2. Protein Energy Malnutrition (PEM)

Known as protein-calorie malnutrition it refers to a form of malnutrition where there is an inadequate supply of protein that is not enough to meet the body's metabolic demands due to either an inadequate dietary intake of protein or increased demands due to disease, or increased protein losses.

2.1 Epidemiology

Recent studies report that 20–50% of ESRD Patients on maintenance haemodialysis therapy suffer from PEM. In most of the hemodialysis patients, malnutrition extends from mild to moderate and only 10% of the haemodialysis ESRD have severe Protein Energy Malnutrition (PEM). In spite of the high prevalence of malnutrition, it was rarely listed as a cause of death in CKD patients on maintenance haemodialysis therapy because malnourished patients die from cardiovascular disease. The strong relationship between malnutrition, inflammation, and arteriosclerosis (MIA-syndrome) in CKD patients on maintenance hemodialysis therapy, suggesting that systemic inflammation participates in the acceleration of the incident of atherosclerosis and malnutrition on hemodialysis ESRD patients (Stenvinkel *et al.*, 2005).

2.2 Malnutrition in patients with MIA Syndrome

It has been recently reported that a systemic inflammatory response may take part in developing hypoalbuminemia in CKD patients on maintenance hemodialysis (Lim VS, 2001). The systemic inflammatory process stimulated by many factors as a uremic state, dialysis membranes, dialysis solution, and infection, causing down-regulation of the cellular metabolism and reduction of the protein synthesis causing acceleration in the negative balance and protein degradation (Stenvinkel *et al.*, 2000).

Malnutrition in CKD patients on maintenance hemodialysis caused by uremic syndrome, comorbid conditions, and inflammation (Chung *et al.*, 2000). Malnutrition is often present in early

1ISSN 2663-1407; National Library of Libya, Legal number: 390/2018

stages of chronic renal failure which characterised by a loss of skeletal muscle mass but a preservation of fat mass (O' Sullivan *et al.*, 2002), This loss result from uraemia, or from inflammation, metabolic acidosis and nutritional deficiency and supposedly hyperleptinemia (Bárány *et al.*, 1997). During the evaluation of chronic renal failure, malnutrition can appear when glomerular filtration assessed by creatinine clearance becomes lower than 40 ml/min/1.73m and there was different mechanism can explain this state of malnutrition as reduction in protein and caloric intakes, deterioration of the renal function, disorders in metabolism of the main nutrients and increased protein catabolism due to acidosis, infections, and inflammations (Aparico *et al.*, 1997). The various aspects of the pathophysiology of malnutrition in HD patients are (schematically presented in Fig. 1 (Alfonso, 2001).

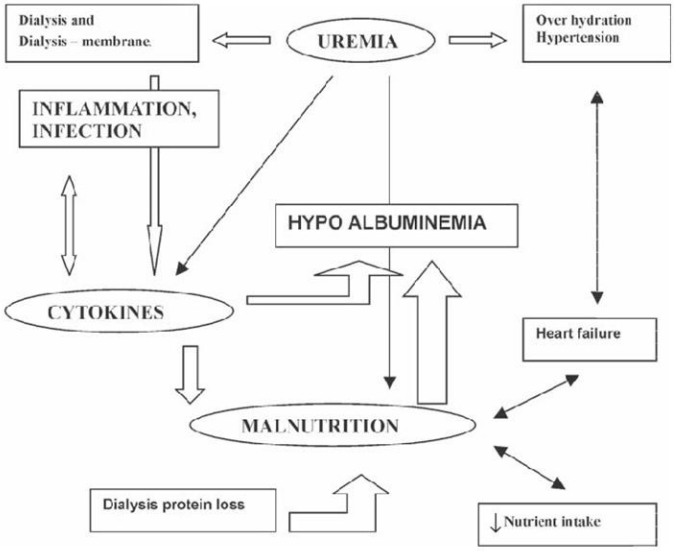

Fig. 1. Pathophysiology of malnutrition in patients with MIA syndrome (Alfonso, 2001).

2.3 Laboratory parameters

Laboratory techniques depend on the determination of the plasma protein levels mainly the negative acute phase reactant. The evaluation of nutritional status depends on an assessment of biochemical laboratory parameters combined with biophysical markers; both will help to find the onset of nutritional disorders and rapid assessment of ongoing treatments.

2.3.1 Serum albumin (half-life 20 days)

Serum albumin levels have been used to assess malnutrition in an individual with and without chronic renal failure (CRF). Serum albumin level is a long-term blood marker of nutritional status (half-life 3 weeks), Malnutrition and hypoalbuminemia were common in hemodialysis CKD patients due to a group of pathological conditions such as hypertension, cardiovascular disease, inflammation, infection, low nutrient intake, protein loss through dialysis and systemic inflammatory response (Kaysen *et al.*, 1995). Albumin has been considered as a negative acute-phase protein because it is level fall actually with inflammation, thus it can be used as an indicator of chronic inflammation.

Hypoalbuminemia in CKD patients on maintenance hemodialysis therapy patients can be a consequence of a combination of malnutrition and inflammatory reactions (Lowrie *et al.*, 1995). Serum albumin and pre-albumin levels were negatively correlated with mortality in patients on maintenance dialysis (Bossola *et al.*, 2005). Many studies have classified the diverse levels of malnutrition by using serum albumin the shows that serum albumin levels of 3.5g/dL or greater are considered normal, serum albumin levels of 2.7g/dL indicate moderate malnutrition, and levels serum albumin level of less than 2.1g/dl indicate severely depleted levels (Storker *et al.*, 1982).

2.3.2 C-reactive protein (CRP)

Is a positive acute-phase reactant whose levels are elevated with both acute and chronic inflammation? It has a short half-life of 19 hours (Vigushin *et al.*, 1993). CRP is not an indicator of malnutrition but many studies reported that serum albumin and pre-albumin were correlated negatively with hs-CRP during an acute phase response, thus hs-CRP was helpful in determining the levels of other visceral proteins (Kushner *et al.*, 2006).

2.3.3 Anthropometry

Anthropometry is a semi-quantitative quantification of body compartments such as bone, fat, and muscle. Anthropometric assessment includes the measurement of skeletal frame size, skinfold thickness (fat mass), body weight, height and mid-arm muscle circumference (muscle mass) (Woodrow *et al.*, 1996). Body mass index (BMI) is calculated from patients height and weight. BMI is used for assessment of obesity and malnutrition. BMI less than 18 kg/m^2 was considered as malnutrition, but should not be used alone as an indicator of nutritional status (Woodrow *et al.*, 1996).

Problem: Increasing risk of malnutrition-inflammation complex syndrome in ESRD patients on hemodialysis maintenance therapy.

Objective: The study aimed to:

1- *Measure and compare serum albumin, pre-albumin, and transferrin as markers for malnutrition in cases versus control groups.*

2- *Measure and compare serum hs-CRP, fibrinogen, albumin, and transferrin to assess acute inflammatory response in cases versus control groups.*

3- *Correlate study parameters with BMI, duration of dialysis, Age and hs-CRP in CKD group.*

4- *Determine the prevalence of chronic renal failure related to age, gender, and causative disease.*

3. Materials and Methods

This is a case-control study conducted at Alafia Hospital Hun-Aljufrah from December 2014 to December 2015. Libyan patients with ESRD who routinely attend to dialysis center at the above-mentioned hospital during the period of the study were randomly recruited for this study. The study included one hundred ESRD patients on regular hemodialysis maintenance therapy and one hundred age and sex-matched healthy controls, the sample size was derived by using the Fleiss formula for cross-sectional study using the following information (Fleiss, 1981)

Confidence interval = 95%, power of study = 80%, the ratio of cases to control of 1:1, the percentage of control exposed: 8.7% and percentage of cases exposed: 26%, this formula gave a minimum sample size of 75 for cases and 75 for control .

None of the participants suffered from any symptoms of infections or presented with clinical signs of infection (Hepatitis B, Hepatitis C, and HIV), malignancy, congestive heart failure, and active immunological disorders and they did not receive any medications known to affect immune functions and Overhydrated patients or patient with ascites or eclampsia were excluded from the study. The patients' information such as age, sex, height, weight, and clinical history were recorded. Blood samples (6ml) were collected from patients in plain containers from which serum is separated for various measurements. Serum albumin was measured by Bromo-cresol green method using spectrophotometer (Germany).CRP was measured by sandwich Enzyme-Linked Immunosorbent Assay using Stat Fax Microstrip Reader (Awareness Technology, USA). BMI calculated from a subject's height and weight.

4. Statistical analysis

The student's t-test was employed to compare differences between the mean concentration of study parameters and Pearson's

correlation for the association between study variables. P-value=0.05 indicating the difference was statistically significant. Data were analysed by SPSS (Version 16.0; SPSS Inc).

5. Result

This is a case-control study, included 100 patients with ESRD, 54% of them were males and 46% were females, their ages ranged between 16-81 years and the mean age was 43 years (Fig. 2). The results obtained revealed that hypertension was the primary cause of CKD (35.0% of respondents) while diabetes mellitus accounted for 30.0% of cases. However, UTI and glomerulonephritis were identified to be the primary cause in 8.0% and 7.0% of cases, respectively. Other identified causes, were Lupus Nephritis (4.0%), Polycystic Kidney Disease (3.0%), Gout (4.0%), Renal Stone (5.0%) and Obstructive Uropathy (4.0%) (Fig. 3).

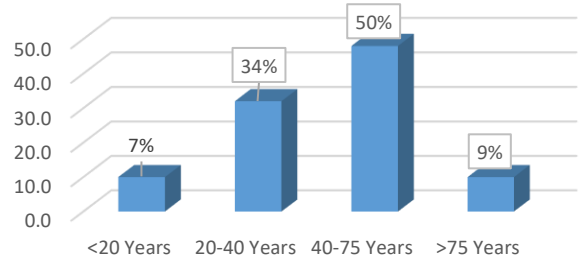

Fig. 2. Age distributions among patients with End-Stage Renal Disease.

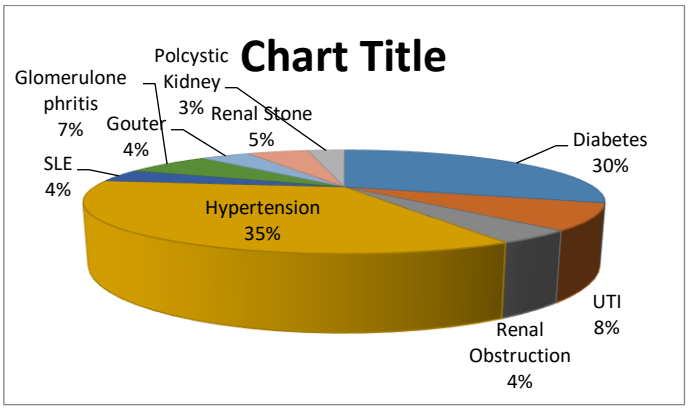

Fig. 3. Causes of End-Stage Renal Disease.

The result in Table 1 showed that the mean of albumin level (3.116 g/dl) was lower in a case group when compared to the control group (4.70 g/dl) with a significant difference between the two groups (p. value=0.000). The result in Table 1 also showed that the mean level of the CRP level (20.13 mg/dl) was higher among CKD patients when compared to the control group (3.22 mg/dl) with a significant difference between the two groups (p. value=0.000). Furthermore, the result in Table 1 showed that the mean level of BMI 20.3 Kg/m^2 was lower among CKD patients when compared to the healthy control group 26.1 Kg/m^2 with a significant difference between the two groups (p. value =0.049).

Table 1

Levels of albumin, BMI and CRP in CKD patients group and control group.

Study group / Parameters	CKD patients (Case group)		**Healthy Individuals (Control group)**		
	Mean	SD	Mean	SD	P. value
Albumin g/dl	3.116	0.3897	4.703	0.3883	0.000
CRP mg/dl	20.13	5.704	3.22	1.277	0.000

6. Discussion

Chronic kidney disease is a dynamic disease governed by multiple factors that affect its progression and prognosis. The prevalence of dialysis-treated ESRD was 624 per million populations (Wiam *et al.*, 2012). The principal aim of this study was to assess the association of Malnutrition-Inflammation Complex Syndrome in hemodialysis ESRD patients. The finding of this study showed that malnutrition in CKD patients on maintenance hemodialysis might be at risk of developing malnutrition which confirmed by the reduction in the mean serum level of albumin among the ESRD patients when compared to the control group and our findings were similar to those reported by Sathishbabu *et al.*, 2013 who reported that there was a reduction in serum albumin level and other biochemical protein parameters of malnutrition in hemodialysis patient. Our findings reported that the BMI levels were decreased among case group when compared to the control group and these findings were in agreement with the study done on Saudi patients conducted by Alharbi *et al.*, 2012 who showed that Malnutrition is Prevalent among Hemodialysis Patients. Furthermore, the present study correlated the level of serum with the level of the acute phase proteins CRP to link between malnutrition and systemic inflammation. The results obtained revealed that there was a significant negative correlation between albumin with hs-CRP and these findings were agreed with results published by Kelleher *et al.*, 1983 who reported that British ESRD patients had a significant negative correlation between plasma proteins markers of malnutrition and hs-CRP. Our findings support the fact that Albumin and prealbumin were negative acute-phase proteins their level tends to decrease during inflammation; also, the chronic inflammation is the main cause of malnutrition in ESRD patients. The correlation analysis showed that serum hs-CRP was correlated negatively with Albumin (r=-0.471, p-value=0.000) (Fig. 4).

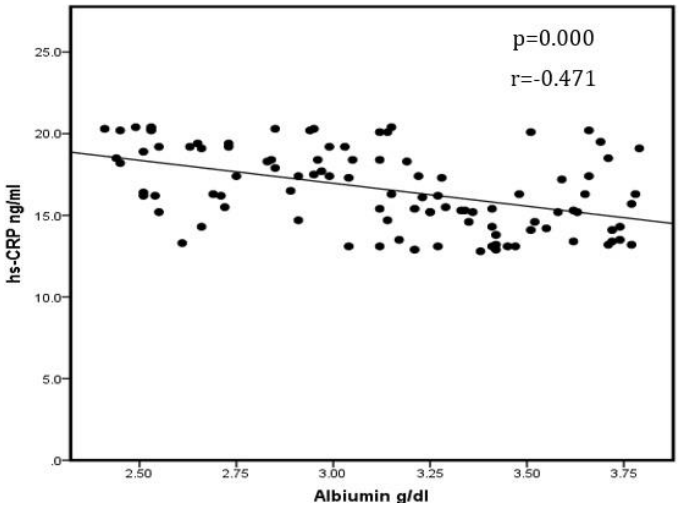

Fig. 4. Dot blot regression between hs-CRP level and Albumin among ESRD patients.

7. Conclusion

The significant decreased in the mean level of serum albumin and BMI, as well as the significant increase in the mean level of serum C-reactive protein among hemodialysis ESRD patients, might place them at risk of developing Malnutrition-Inflammation Complex Syndrome in the future. The significant negative correlation between serum albumin with hs-CRP support the facts that systemic inflammation is the main cause of malnutrition and cardiovascular disease in ESRD patient.

References

Alfonso, M. C., (2001) 'Hypoalbuminemia in Dialysis Patients: Malnutrition or an Inflammatory Marker?', *La Revista de Investigation Clinica*, 52, pp. 152-158.

Alharbi, K., Enrione, E. B., Enrione (2012) 'Malnutrition is Prevalent among Hemodialysis Patients in Jeddah, Saudi Arabia', *Saudi J Kidney Dis Transpl*, 23(3), pp. 598-608.

Aparico, M., De Pre`cegout V, Combe, C. (1997) 'Malnutrition in Renal insufficiencies', *Chronique Press Mid*., 26, pp. 389-395.

Bárány P, Eriksson L. C., Hultcrantz R., Pettersson E, Bergström J. (1997) 'Serum Ferritin and Tissue Iron in Anemic Dialysis Patients' *Miner Electrolyte Metab*, 23, pp. 273–276.

Bossola, M., Muscaritoli, M., Tazza, L. (2005) 'Malnu.trition in hemodialysis patients: what therap', *Am J Kidney Dis*', pp. 371–386.

Chung S. H., Lindholm B., Lee H. B. (2000) 'Influence of Initial Nutritional Status on Continuous Ambulatory Peritoneal Dialysis Patient Survival', *Perit Dial Int*, 20, pp. 19-26.

Fleiss, J. L., (1982) Statistical methods for rates and proportions. John Wiley& Sons .2nd ed., New York, NY.

Ikizler, T. A., Wingard, R. L., Sun, M., Harvell, J., Parker, R. A., Hakim, R. M, (1996) 'Increased Energy Expenditure in Hemodialysis Patients', *J. Am Soc Nephrol*; 7, pp. 2646-2653.

Kaysen, G. A., Rathore, V., Shearer, G. C., Depner, T. A., (1995) 'Mechanisms of hypoalbuminemia in hemodialysis patients', *Kidney Int* ., 48, pp. 510–516

Kelleher, J., Humphrey, C. S., Dana, H., Davison, A. M., (1983) 'Vitamin A and its transport proteins in patients with chronic renal failure receiving maintenance haemodialysis and after renal transplantation', *Clinical Science*, 65, pp. 619-626.

Kushner, I., Rzewnicki, D., Samols, D. (2006) 'What does minor elevation of C-reactive protein signify?', *Am J Med*. 119, 2, pp. 166 (e17-e28).

Lim, V. S. (2001) 'Thyroid Function in Patients with Chronic Renal Failure. Metabolic Dysfunction in Uremia', *Am J Kidney Dis*., 38, pp. 580-584.

Lowrie, E. G., Huang, W. H., Lew, N. L. (1995) 'Death risk predictors among peritoneal dialysis and hemodialysis patients: a preliminary comparison', *Am J. Kidney Dis.*, 26, pp. 220–228

Luger, A., Kovarik, J., Stummvoll, H. K., Urbanska, A., Luger, T. A., (1987) 'Blood Membrane Interaction in Hemodialysis Leads to Increased Cytokine Production', *Kidney Int*., 32, pp. 84-88.

Moshage, H. J., Janssen, J. A., Franssen, J. H., Hafkenscheid, J. C., Yap, S. H. (1987) 'Study of the Molecular Mechanisms of Decreased Liver Synthesis of Albumin in Inflammation', *J. Clin Invest*., 79, pp. 1635-1641.

O' Sullivan, A. J., Larson, J. A., Chan, M., Kelly, J. J. (2002) 'Body Composition and Energy Metabolism in Chronic Renal Insufficiency', *Am J Kidney Dis*., 39, pp. 369-375.

Sathishbabu, A., Suresh, S. (2012) 'A study on the correlation of serum pre-albumin with other biochemical parameters of malnutrition in a hemodialysis patient', *Int J Biol Med Res*., 3(1), pp. 1410-1412.

Stenvinkel, P., Heimbürger, O., Lindholm, B., Kaysen, G. A., Bergström, J. (2000) 'Are There Two Types of Malnutrition in Chronic Renal Failure? Evidence for Relationships between Malnutrition, Inflammation, and Atherosclerosis (MIA syndrome)', *Nephrol Dial Transplant*., 15, pp.953-960.

Stenvinkel, P., Ketteler, M., Johnson, R. J. (2005) 'IL-10, IL-6, and TNF-alpha: central factors in the altered cytokine network of uremia – the good, the bad, and the ugly', *Kidney Int*., pp. 67, pp. 1216–1233.

Storker, P. M., Gumb, F. E., Askanazi, J. (1982) 'Serum albumin levels as an index of nutritional support, surgery', *J Clin Invest*, 91, pp. 194-199.

Vigushin, D. M., Pepys, M. B, Hawkins, P. N. (1993) 'Metabolic and scintigraphic studies of radio-iodinated human C-reactive protein in health and disease', *J Clin Invest,* 91, pp. 1351-1357.

Wiam, A., Christopher, M., Maarten, T. (2012) 'Epidemiology and aetiology of dialysis-treated end-stage kidney disease in Libya', *BMC Nephrology*, 13, 33, pp. 2-7

Woodrow, G., Oldroyd, B., Smith, M. A., Turney, J. H. (1996) 'Measurement of body composition in chronic renal failure: comparison of skinfold anthropometry and bioelectrical impedance with dual-energy X-ray absorptiometry', *Eur J Clin Nutr*., 50, pp. 295–301.